DISSERTATION

SYNTHESIS OF COBALT(III) AND RUTHENIUM(II) COMPLEXES OF PYRIDINE- AND 4-SUBSTITUTED PYRIDINE-CAPPED MONO- AND BIS-DIOXOCYCLAMS

Submitted by

Angela L. Reiff

Department of Chemistry

In partial fulfillment of the requirements

for the Degree of Doctor of Philosophy

Colorado State University

Fort Collins, Colorado

Fall 2005

COLORADO STATE UNIVERSITY

September 29, 2005

WE HEREBY RECOMMEND THAT THE DISSERTATION PREPARED UNDER OUR SUPERVISION BY ANGELA LEA REIFF ENTITLED THE SYNTHESIS OF COBALT(III) AND RUTHENIUM(II) COMPLEXES OF PYRIDINE- AND 4-SUBSTITUTED PYRIDINE-CAPPED MONO AND BIS-DIOXOCYCLAMS BE ACCEPTED AS FULFILLING IN PART REQUIREMENTS FOR THE DEGREE OF DOCTOR OF PHILOSOPHY.

Committee on Graduate Work

Tomislav Rovis

Richard G. Finke

Steven H. Strauss

Julia M. Inamine

Louis S. Hegedus / Advisor

Anthony K. Rappe / Department Head / Director

ABSTRACT OF DISSERTATION

THE SYNTHESIS OF COBALT(III) AND RUTHENIUM(II) COMPLEXES OF PYRIDINE- AND 4-SUBSTITUTED PYRIDINE-CAPPED MONO- AND BIS-DIOXOCYCLAMS

A new class of 4-substituted pyridine-capped cobalt(III) dioxocyclam complexes has been synthesized. Coordination of the cobalt(III) dioxocyclams to either rhodium acetate or ruthenium phthalocyanine complexes resulted in the synthesis of polymetallic complexes that contain two or more metals. Polymetallic complexes often exhibit metal-metal interactions in the form of electrical, magnetic, and photochemical properties. However, the polymetallic cobalt(III) dioxocyclam complexes did not exhibit metal-metal interaction as assessed by cyclic voltammetry experiments.

Studies were conducted towards the synthesis of bis-capped bis-dioxocyclams and their metal derivatives. Progress was hindered by the discovery that 4-substituted bis-capped bis-dioxocyclams were difficult to synthesize. Pyridine- and pyrazine-capped bis-dioxocyclams were examined for their coordination to both copper and cobalt.

Angela L. Reiff

Department of Chemistry

Colorado State University

Fort Collins, CO 80523

Fall 2005

TABLE OF CONTENTS

LIST OF ABBREVIATIONS

AIBN	azobisisobutyronitrile
Bpy	4,4′-bipyridine
CMW	commercial microwave
m-CPBA	*meta*-chloro peroxybenzoic acid
CSA	camphorsulfonic acid
CV	cyclic voltammetry
DBU	1,8-diazabicycloundec-7-ene
DMAP	N,N-dimethyl 4-pyridinamine
DMF	N,N-dimethylformamide
DMSO	dimethylsulfoxide
DPPP	diphenylphosphino propane
ESR	electron spin resonance
Exact mass	calculations are based on the exact mass of only the most abundant isotopes for each element
FAB	Fast Atom Bombardment referring to the use of a Cs ion gun
IVCT	intervalence charge transfer
K_c	comproportionation value
LiHMDS	lithium hexamethyldisilazane
NBS	N-bromosuccinimide
NMR	Nuclear Magnetic Resonance
ORTEP	Oak Ridge Thermal Ellipsoid Programme
Py	pyridine
Pz	pyrazine

SQUID	superconducting quantum interference device
TEA	triethylamine
TsCl	4-methyl benzenesulfonyl chloride

ACKNOWLEDGEMENTS

I would like to thank Dr. Hegedus for being a highly motivating yet supportive boss. My graduate career would not have been the same without him. To Hegedus group members past and present, thank you. The family environment in the Hegedus group was a uniquely comfortable place to grow and learn. I would like to thank all of my friends and family, especially Dad, Mom, and Andrea, who have supported me in so many ways. And finally to my husband Jason, we started this program together and have finished it together. It would have been a far different journey without your hugs and constant support, I thank you from my heart.

CHAPTER ONE

SYNTHESIS OF COBALT(III) COMPLEXES OF 4-SUBSTITUTED-PYRIDINE-CAPPED MONO-DIOXOCYCLAMS

Introduction

I. Dioxocyclams

Cyclams are 14-membered tetraazamacrocycles (Figure 1). They have been attractive ligands because of their ability to coordinate to a variety of first and second row transition metals, as well as lanthanides. Complexation usually involves all four nitrogens and the coordination geometry of the cyclam-metal complex is square planar. *Trans*- or *cis*-coordination of additional ligands results from a planar or folded cyclam geometry respectively (Figure 1). The coordinated metals are mainly divalent, but cyclams can also stabilize higher, less stable oxidation states of certain metals (e.g. copper(III) and nickel(III)). Additionally, substitution on the carbon backbone or on the nitrogens of the macrocycle can introduce additional ligands for metal chelation. Substituents on both carbon and nitrogen can affect the conformation of the ring, which can in turn affect the properties of the metals coordinated by the cyclams.

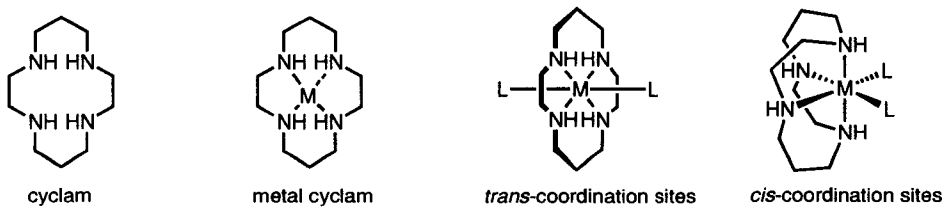

Figure 1. A cyclam and metal cyclam complex.

Dioxocyclams differ from cyclams in that they contain two amine and two amide nitrogens and are considered an intermediate between cyclic polyamines and cyclic

peptides (Figure 2). The first examples of dioxocylams were synthesized by Tabushi but remained unstudied since the amides were reduced to the fully saturated cyclam. Kimura saw their potential as a new class of coordination ligand and has extensively studied various dioxocyclams and their metal complexes. Historically, the synthesis of dioxocylams involves multiple condensation reactions giving unfunctionalized dioxocyclams in very low yields.[1-4]

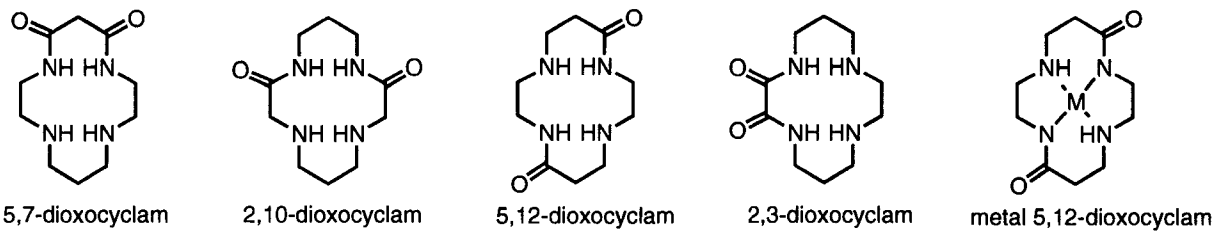

Figure 2. Dioxocyclam isomers and a metal dioxocyclam complex.

Hegedus discovered an efficient synthesis of dioxocyclams in an attempt to synthesize azapenams as penicillin analogs.[5-8] Acid-catalyzed ring opening of the azapenam formed a seven-membered imine, which underwent a dimerization to form an imine-dioxocyclam (Scheme 1). Reduction of the imine resulted in a stable saturated 5,12-dioxocyclam.

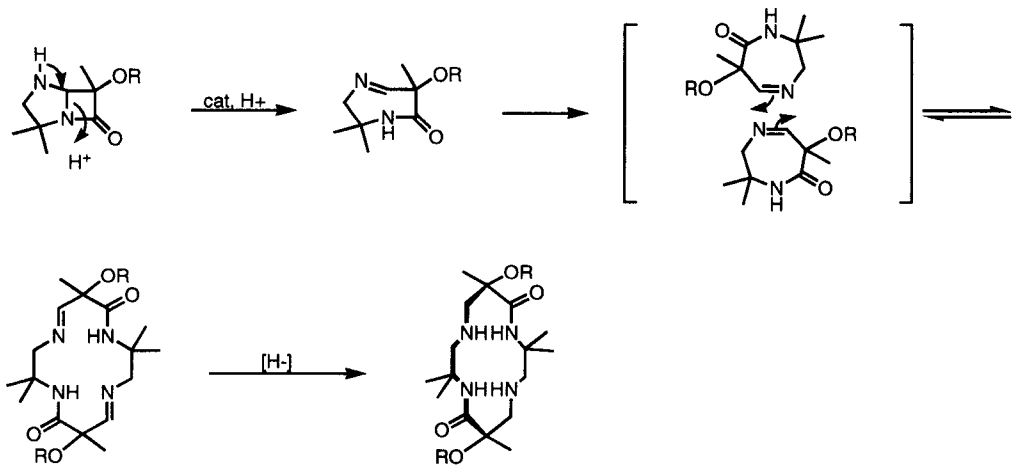

Scheme 1. Hegedus' synthesis of 5,12-dioxocyclams.

Dioxocyclams complex metals more selectively than cyclams. Copper(II), nickel(II), palladium(II),[8,9] cobalt(II),[9,10] and platinum(II)[8] form stable complexes and their complexation can be easily monitored by IR spectroscopy due to the change in the stretching frequency of the amide carbonyls, which upon complexation decrease by ≈80 cm^{-1}. Upon coordination of a metal the amide protons become acidic. The amide nitrogens can then be deprotonated forming a neutral complex (Scheme 2).

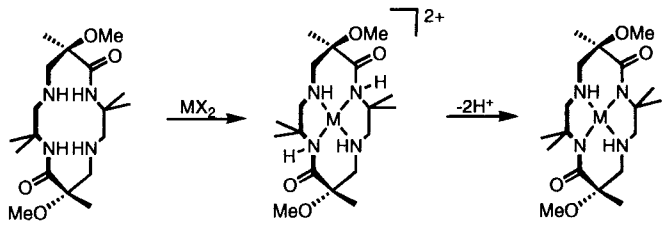

Scheme 2. Metal complexation.

Dioxocylams contain two nucleophilic amine nitrogens that can be alkylated. Williams showed that treatment of 5,12-dioxocyclam with 2-(chloromethyl)pyridine hydrochloride gave a dialkylated dioxocyclam in 75% yield (Scheme 3).[11] Further reaction with copper(II) perchlorate under basic conditions gave a paramagnetic copper(II) dioxocyclam complex. X-ray crystal structure analysis revealed weak coordination between both pyridine nitrogens and the copper, with bond lengths averaging around 2.721 Å. Typical copper-pyridine bond lengths average around 2.10 Å, indicating that coordination is weak. This distorted octahedral environment is caused by Jahn-Teller distortion, and is common among octahedral copper(II) complexes.

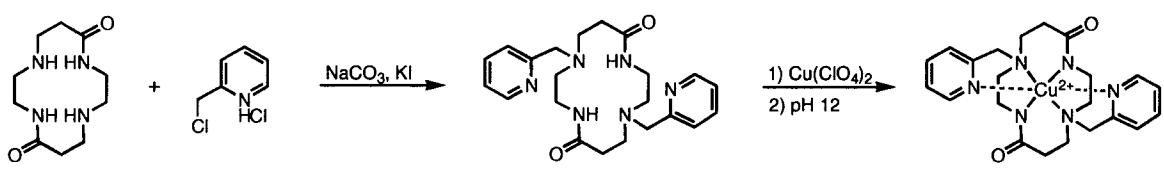

Scheme 3. Dioxocyclam alkylation and copper(II) complexation.

Guilard demonstrated that bidentate alkylating agents could be used to either "cap" one face of the dioxocyclam or to bridge two cyclams.[12,13] For capping, treatment of a 5,12-dioxocyclam with α,α′-dibromo-*m*-xylene or 2,6-bis(bromomethyl)pyridine gave capped dioxocyclams in good yields (Scheme 4).[12]

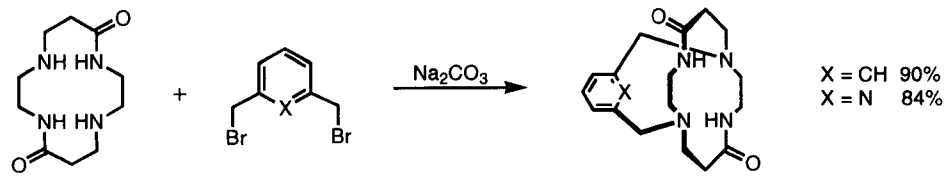

Scheme 4. Mono-capped dioxocyclam.

Coordination of the capped dioxocyclam with copper followed. Interestingly, either the tetracoordinate or pentacoordinate complex could be obtained depending on the pH of the reaction mixture. Tetracoordinate dioxocyclam was obtained from reaction of pyridine-capped dioxocyclam with copper perchlorate hexahydrate in methanol (Scheme 5).[14] These conditions were acidic enough to leave one of the amide nitrogens protonated and uncoordinated. Alternatively, treatment of pyridine-capped dioxocyclam with anhydrous copper chloride and sodium carbonate gave the pentacoordinate species (Scheme 5).

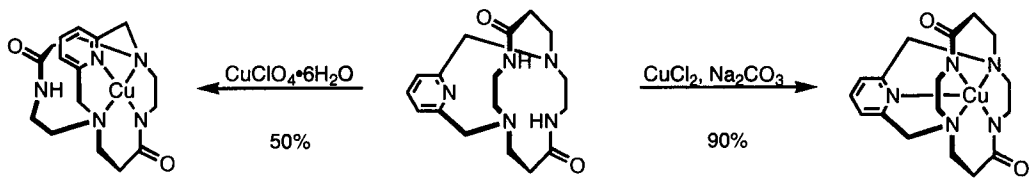

Scheme 5. Copper complexes of pyridine-capped dioxocyclam.

Bridged or bis-dioxocyclams are formed in a similar manner, although protection of one of the amine nitrogens is necessary to prevent "capping". Monoprotection with *t*-butoxycarbonyl (Boc) anhydride gave a protected dioxocyclam (Scheme 6).[13] Reaction

with α,α′-dibromo-*m*-xylene gave a mono-bridged dioxocyclam. Removal of the protecting group followed by reaction with another equivalent of α,α′-dibromo-*m*-xylene provided the bis-dioxocyclam. Unfortunately, no metal complex of this bis-dioxocyclam was synthesized. However, certain nickel(II) bis-cyclams have been synthesized and have shown high activity towards HIV-1,2.[15]

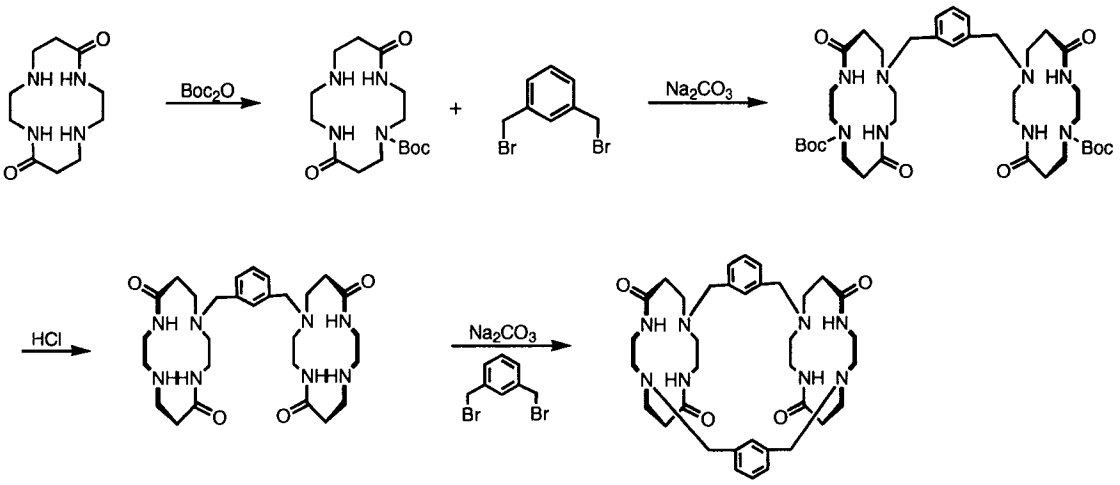

Scheme 6. Bridged dioxocyclam.

Highly functionalized capped 5,12-dioxocyclams have been synthesized in the Hegedus laboratories. Pyridine and pyrazine-capped dioxocyclams have been made. Treatment of *trans*-dioxocyclam **1** with capping reagents **2a-b** and Na_2CO_3 provides capped dioxocyclams **3a-b** in good yields (Scheme 7).[16,17]

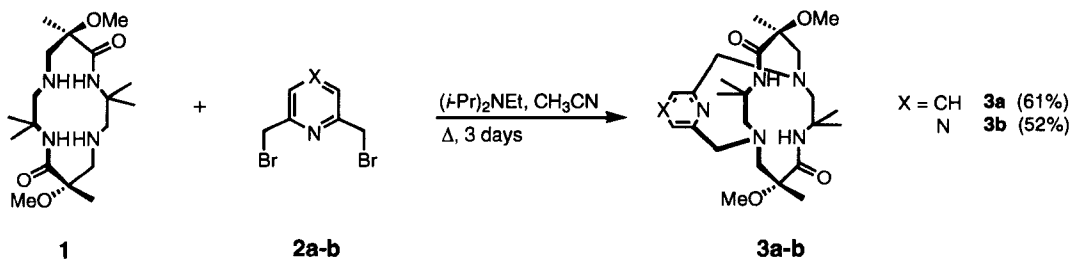

Scheme 7. 4-substituted pyridine and pyrazine capped dioxocyclams.

The capping reagent provides a fifth coordination site for metal complexation through the pyridine nitrogen making the dioxocyclam a pentadentate ligand. Capping with pyrazine provides an additional coordination site external to the cyclam through the nitrogen at the 4-position of the capper allowing for further elaboration.

Capping of the *trans*-dioxocyclam **1** results in a racemic mixture because alkylation can occur from either the front or back face of the dioxocyclam (Scheme 8).[16] Once capped, the amine nitrogens can no longer invert, and become two stereocenters. The pyridine cap eliminates the center of symmetry in the dioxocyclam producing a pair of enantiomers that differ by the absolute configuration at the amine nitrogens. The two faces of the dioxocyclam ring were differentiated as either R or S, depending on the absolute configuration of the amines (Scheme 8).

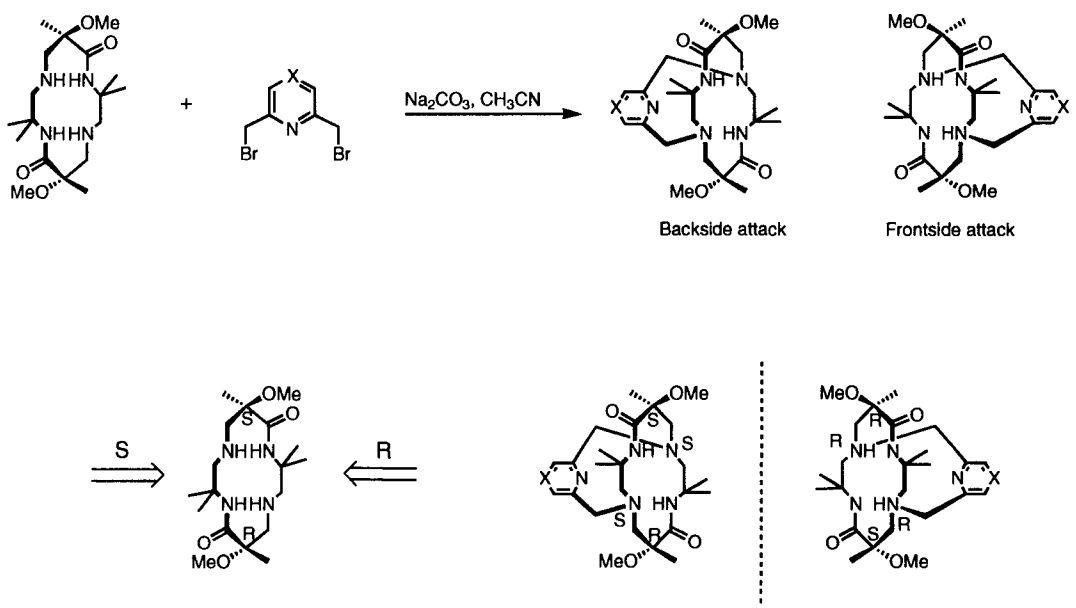

Scheme 8. A mixture of enantiomers of capped dioxocyclams.

Copper complexes of these capped dioxocyclams have been synthesized.[16,17] The general procedure involves treatment of capped dioxocyclam **3a-b** with copper

tetrafluoroborate and potassium carbonate in methanol at reflux giving **4a-b** (Scheme 9). X-ray crystal structure analysis of these compounds shows that the copper is five-coordinate, with an average bond length of 2.125 Å for the pyridine nitrogen-to-copper bond.

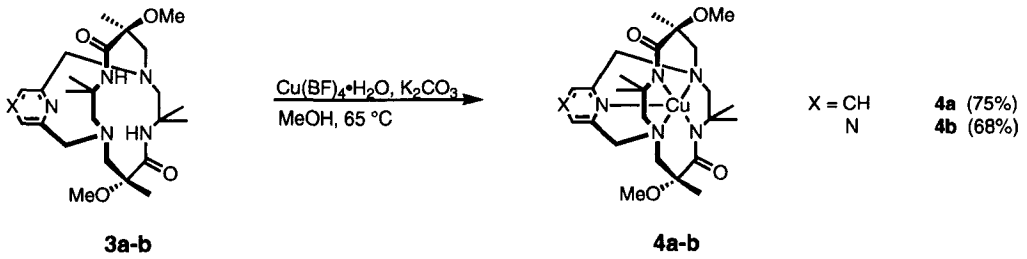

3a-b **4a-b**

Scheme 9. Copper coordination of capped 5,12-dioxocyclams.

The full potential of capped dioxocyclams has yet to be realized. Expanding the scope of metals for coordination and the synthesis of new capping reagents could led to a new series of capped dioxocyclams. Further functionalization of these monometallic dioxocyclams complexes could produce building blocks for the synthesis of new bimetallic complexes. For example, **4b** contains a coordination site external to the cyclam through the 4-position of the pyrazine capper (Figure 3). Coordination at the 4-position of the pyrazine to another metal center would provide a bimetallic complex. The synthesis of multimetallic complexes is of great interest because they often exhibit interesting optical, electronic and magnetic properties.[18] Transition metal macrocyclic compounds with extended π-chromophores, such as pyrazine, are of particular interest because of their ability to communicate electronically across the ligand array.[19]

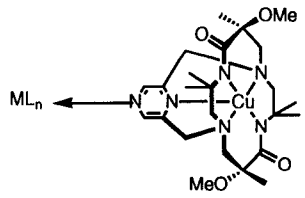

4b

Figure 3. Formation of a bimetallic complex.

II. Polymetallic Complexes – Coordination Oligomers

Coordination oligomers are polymetallic coordination complexes in which the monometallic units are connected by bridging, bi- or polydentate ligands. An important subset of this class of coordination complexes includes coordination oligomers of redox-active metals connected by π-conjugated bridging ligands capable of transmitting electronic or magnetic information across the mutimetallic array through the π–conjugated system. Polymetallic complexes such as these can have useful physical properties and specific examples have potential for the construction of molecular wires,[20] photonic wires,[21] light-harvesting systems,[22] information transfer,[23] information storage,[24] molecular switches,[25] and for the study of long range electron-transfer processes in mixed-valent complexes.[26] Although complexes of this type have been extensively studied over the past decade, progress has been hindered by difficulties in the controlled synthesis of larger arrays, and by the inability to predict physical properties from structural features. [27,28]

There are two basic classes of polymetallic complexes, isovalent and mixed valence complexes. Isovalent complexes are mutimetallic complexes in which the metals are in the same oxidation state. The metal-metal interaction in isovalent complexes occurs through space or a bridging ligand and does not involve the transfer of electrons.

Mixed valence complexes are multimetallic complexes in which the metals are in different oxidation states ($Cu^{I}Cu^{II}$, $Ru^{II}Ru^{III}$). The metal-metal interaction in mixed valence complexes result from electron-transfer through a bridging ligand. The extent of metal-metal communication in both of these systems is determined on a case by case basis by examining the electrochemical, spectroscopic, and magnetic properties of the complex. It is difficult to predict if complexes will demonstrate metal-metal interaction.[29] The only way to know for certain if a complex will exhibit metal-metal interaction for either isovalent or mixed valence complexes is to synthesize it and examine it.

A. Isovalent Complexes

Metal-metal interactions of isovalent complexes are either direct (through space) or mediated by a bridging ligand. The extent of interaction is commonly probed using electron spin resonance (ESR) and superconducting quantum interference device (SQUID) to measure magnetic coupling of a complex. Both ESR and SQUID rely on the interaction of the unpaired spins in a complex. If coupling of the unpaired spins is observed with these techniques, the metals within the complex are believed to be in communication. If no coupling is observed for a complex, the metals are not interacting with each other.

Cyclic voltammetry (CV) is also utilized for determining metal-metal interactions in complexes. If the metals are in communication with each other, the oxidation of a M^{II}—M^{II} complex to M^{II}—M^{III} will have an affect on the neighboring metal so that its oxidation (M^{II}—M^{III} to M^{III}—M^{III}) is more difficult. In this case, the CV will contain two distinct redox waves, one for each metal. If the metals are not in communication with each other, both metals will be oxidized and reduced at the same potential.

Therefore, only one redox wave will be observed for the two metal centers. Although the oxidation/reduction of isovalent complexes by cyclic voltammetry results in mixed valent complexes, the metal-metal interaction is usually a result of electrostatic (direct or ligand directed) interaction and not from electron-transfer/delocalization.

1. Examination by ESR

Lampeka examined the metal-metal interactions of a mono-bridged 14-membered pentaaza copper complex with ESR (Figure 4).[30] ESR measures the hyperfine coupling constant or spin interaction ($A_{\|}$) for a complex. Hyperfine coupling interaction is visualized by the splitting of lines in an ESR spectrum. The splitting (*a*) is measured in units of millitesla (Figure 4, ESR spectrum (c)). The relation between the hyperfine splitting and hyperfine coupling must be calculated for each system. The hyperfine coupling constant is calculated from the splitting value (Equation 1).

$$A_{\|} = g\mu_B a$$

μ_B = Bohr Magneton
g = g-factor

Equation 1

However, the hyperfine coupling constant of a polymetallic complex is meaningless without understanding how the component parts of the complex interact in the magnetic field. First the parent or monometallic species is examined as a baseline because no metal-metal interaction is possible. If the $A_{\|}$ value of a bimetallic complex remains the same as the parent molecule, no metal-metal interaction exists. Alternatively, a decrease in the $A_{\|}$ value indicates metal-metal interaction. Figure 4 illustrates the dipole-dipole interaction of three metal complexes. The parent complex **(a)** has a hyperfine coupling of 205. Bis-copper complex **(b)** has a similar coupling constant

at 200, indicating no metal-metal interaction. However, when the bridge length is shortened to two carbons for bis-copper complex (**c**), $A_{||}$ values drop to 108. This is a strong indication of metal-metal interaction. This demonstrates the importance of metal-metal distance to the degree of interaction. Also, this is an example of direct (through space) spin-spin interaction that is not mediated through a bridging ligand.

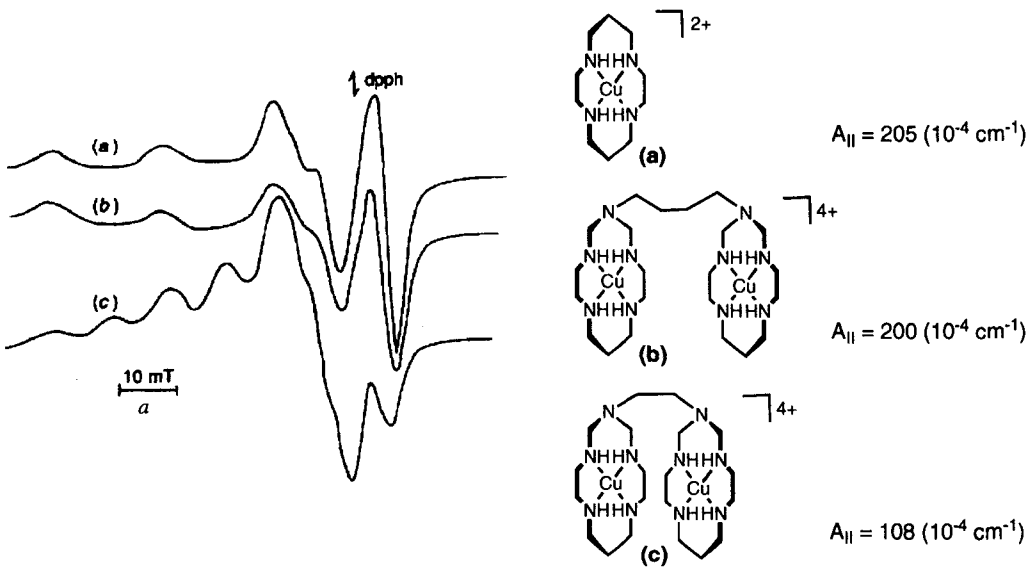

Figure 4. ESR of isovalent copper(II) complexes.

2. Examination by SQUID

Ishida examined metal-metal interactions of isovalent metal(II) complexes bridged by a pyrazine derivative using magnetic susceptibility measurements (SQUID). SQUID can detect spin-spin coupling of interacting magnetic dipoles on neighboring atoms. Ishida synthesized a series of bimetallic manganese(II), cobalt(II), nickel(II), and copper(II) complexes bridged by 2,3-di(2-pyridyl)pyrazine (Figure 5).[31] The experiment begins at temperatures of 300 K at which the metals are in a high-spin state. A decrease of $\chi_{mol}T$ values with decreasing temperature indicates that the spins of the metal ions become antiferromagnetically coupled, or that they have a low-spin ground state. A

sharp decrease in $\chi_{mol}T$ indicates that the observed magnetic interaction is due to intramolecular coupling. No drop off is seen if there is no interaction between the two metals. The spectrum in Figure 5 shows a sharp drop off for both manganese (Mn) and cobalt (Co) complexes demonstrating that the two metals are antiferromagnetically coupled. The spectrum of the copper (Cu) complex, however, is nearly straight, an indication of no interaction. This demonstrates that the choice of metal can greatly affect the metal-metal interaction of a complex.

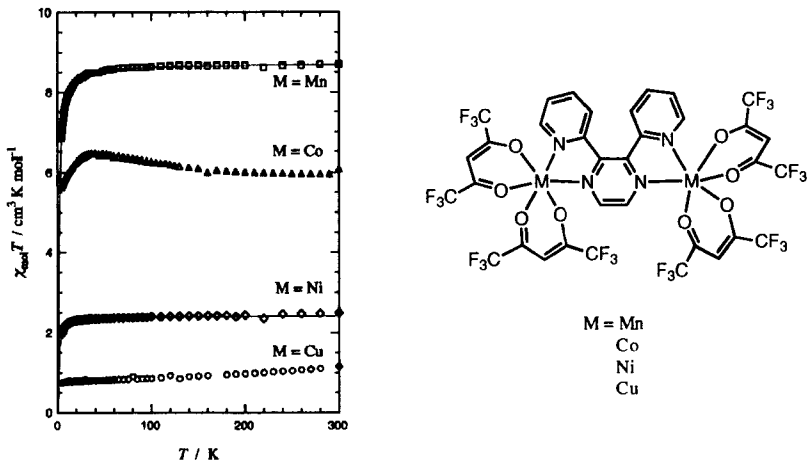

Figure 5. SQUID of isovalent Mn, Co, Ni, and Cu complexes.

3. Examination by Cyclic Voltammetry

Petersen synthesized isovalent ruthenium(II) 2,2′- bipyrimidine complexes **10a** and **10b** (Figure 6).[32] He examined the extent of metal-metal interaction of these complexes with cyclic voltammetry. Similar to ESR, the monometalic or parent complex is examined as a baseline to which the bimetallic complexes can be compared. The monometalic derivative **10a** was examined, and had a reversible one-electron 2+/3+ oxidation-reduction couple at $E_{1/2}$ = +0.756 V (Figure 6). Examination of the bimetallic system followed. If no metal-metal interaction were observed the redox potentials of the

bimetallic complex would appear to be the same as those for the monometalic system. When two identical metals in the same complex have the same redox potential, their oxidation/reduction is not affected by the neighboring metal and as a result they exhibit identical redox potentials. Alternatively, cyclic voltammetry of the bis-ruthenium ligand **10b** gave a reversible one-electron 4+/5+ redox couple at $E_{1/2}$ = +0.830 V and a second quasi-reversible oxidation peak at $E_{1/2}$ - +1.02 V for the 5+/6+ oxidation and reduction (Figure 6). Two distinctly separable $E_{1/2}$ values were observed, and were different than the CV of the starting material. This demonstrates that the metals are interacting with each other through the bridging ligand, signifying possible metal-metal communication. The separation between $E_{1/2}$ values is ΔE =190 mV for complex **10b**. The ΔE value corresponds to a comproportionation constant (K_c), which reflects the degree of metal-metal communication due to electrostatic or electron-delocalized interactions (Equation 2).[33] K_c can range from 4, the statistical value, to more than 10^{15}.[33] The K_c value of **10b** was calculated to be 1.5×10^3 which is much higher than the statistical value of 4, representing a high degree of metal-metal interaction. This is an example of metal-metal interaction mediated through a bridging ligand.

$$K_c = 10^{\Delta E/59\ mV} = [M^{(n-1)}]^2/[M^n][M^{(n-2)}]$$

$$M^n + M^{(n-2)} \leftrightarrows 2\ M^{(n-1)}$$

Equation 2

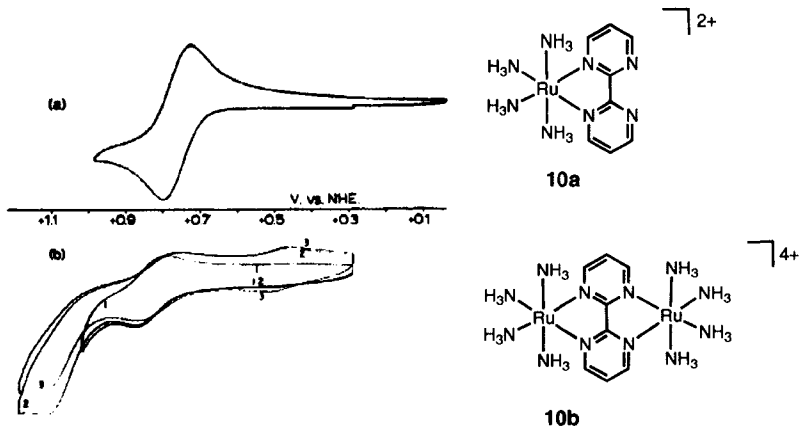

Figure 6. CV of isovalent ruthenium(II) complexes.

B. Mixed Valent Complexes

Metal-metal interactions of mixed valent complexes ($Cu^{I}Cu^{II}$, $Ru^{II}Ru^{III}$) are mediated through a bridging ligand and involve intramolecular electron transfer. These complexes often exhibit unusual spectroscopic properties and have potential applications for molecular electronics.[34] The metal-metal interaction of these complexes is often called "coupling". Coupling refers to either electrochemical, spectroscopic, or magnetic measurements that indicate metal-metal interaction.

Mixed valence systems are divided into three classes according to the extent of delocalization of the electron.[35] Class 1: The "extra" electron is completely localized on one of the metal centers. Since the electron is isolated on one of the metal centers, no metal-metal interaction is observed via CV, or UV-vis/near IR. Class 2: These complexes exhibit intermediate behavior. Delocalization of the electron is often solvent and temperature dependent. When delocalized, they exhibit an intervalence charge transfer band. Class 3: Systems where the "extra" electron is completely delocalized over both metal centers. These complexes have no solvent sensitivity and usually have large K_c values typical of strong metal-metal communication.

Classification of mixed valence systems requires substantial spectroscopic and magnetic experiments. Mixed valent metal-metal interactions are typically mediated through a bridging ligand and are most commonly observed using cyclic voltammetry and UV-vis/near IR. Metal-metal interactions in mixed valent complexes, observed by CV, can result from either electrostatic or electron delocalization interactions. However, it is difficult to determine by CV alone whether the interaction is due to electrostatic or electron delocalization interactions. Metal-metal interaction is observed when the CV contains two distinct redox waves for each metal. If the metals are not in communication with each other, both metals will be oxidized and reduced at the same potential.

Electron transfer in mixed valent complexes is observed by UV-vis/near IR spectroscopy by the appearance of an intervalence charge transfer (IVCT) band. This band only appears if the electron is delocalized across the system from the photoinduced excitation and subsequent transfer of an electron from a low oxidation state metal to a neighboring metal of higher oxidation state. The IVCT band is generally a strong sloping absorption in the range of 500-2500 nm.

1. Examination by Cyclic Voltammetry

Ito synthesized a series of mixed valent ruthenium pyrazine bridged complexes (Figure 7).[36] He examined the extent of metal-metal interaction in these complexes with cyclic voltammetry. Ito was not only interested in the metal-metal interaction in these complexes but the effect on interaction caused by changing the ancillary ligand. The ancillary pyridine ligand was made to be both electron-donating and electron-withdrawing by substitution at the 4-position. Substitution with both dimethylaminopyridine (DMAP) **11a** and pyridine (py) **11b** resulted in two distinctly

separable $E_{1/2}$ values. Substitution with cyanopyridine **11c** also gave separated $E_{1/2}$ values but not as well defined. The comproportionation values (K_c) related to **11a**, **11b** and **11c** show strong metal-metal interaction with all ligands. However, it is important to note that the K_c values decrease as the ancillary ligand becomes more electron-deficient.

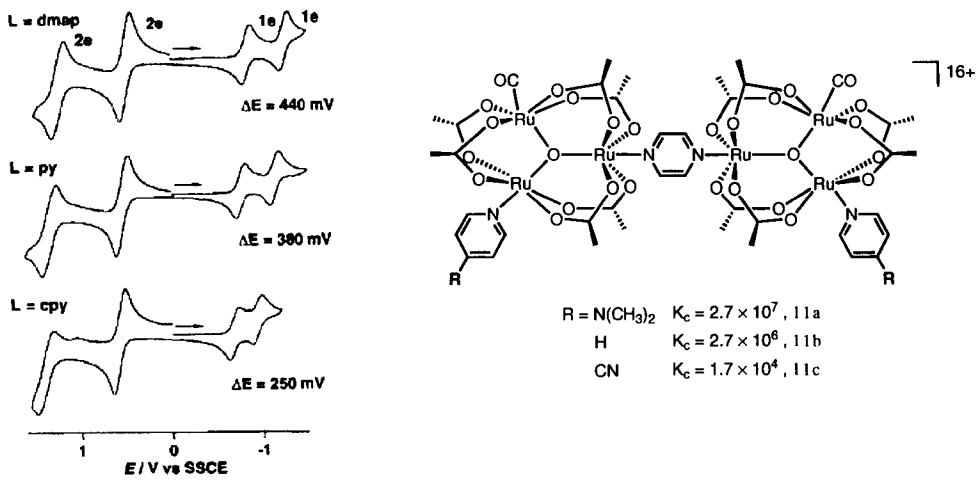

Figure 7. CV of mixed valent pyrazine bridged ruthenium complexes.

The same ruthenium complex was examined but with 4,4′-bipyridine as the bridging ligand. The electron-withdrawing and -donating substituents attached to the ancillary ligand were examined for their effect on metal-metal interaction. Similar to the pyrazine bridged complexes **11a** and **11b**, substitution with both DMAP **11d** and pyridine **11e** resulted in two separable $E_{1/2}$ values (Figure 8). The K_c values for **11d** and **11e** are much smaller than the corresponding pyrazine complex, but still indicate metal-metal interaction. However, in the case of **11f**, no metal-metal interaction was observed since the splitting between the two states was too small ($\Delta E < 50$ mV) to be resolved by CV indicating that their redox potential was close to equivalent.

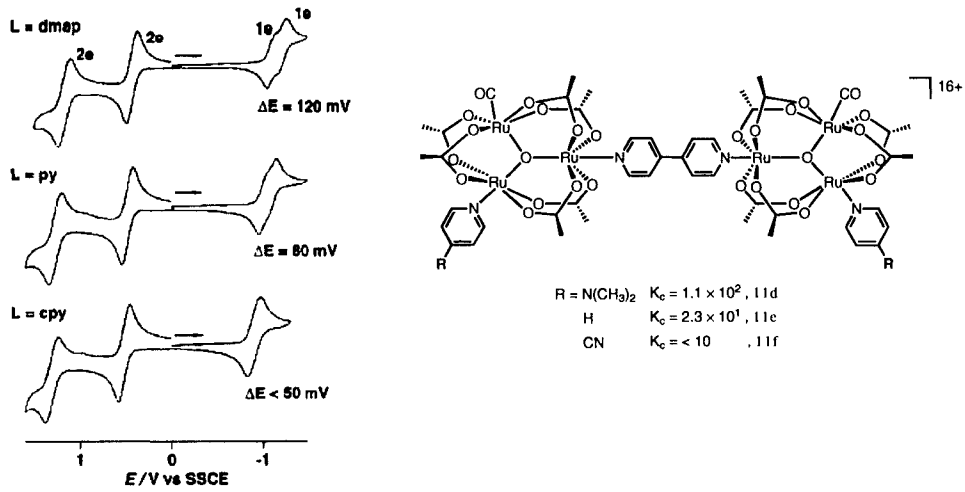

Figure 8. CV of mixed valent bpy bridged ruthenium complexes.

2. Examination by UV-vis/near IR

The extent of mixed valent interaction can be determined with UV-vis/near IR to see if an intervalence charge transfer band is present. The IVCT band appears in the near-IR region only when electron delocalization exists (mixed valence classes 2 &3). This phenomenon is seen with the Creutz-Taube ion **12b**. The isovalent 4+ complex **12a** is made by coordination of pentaamminepyrazineruthenium(II) and pentaammine-aquoruthenium(II) (Figure 9).[33,37] One-electron oxidation with Ce(IV) provides the Creutz-Taube mixed valent 5+ complex **12b**. Upon oxidation of **12a** to **12b**, the visible region is only slightly shifted from the 4+ to the 5+ species. However, extending the investigation to the near IR for **12b** reveales an intervalence charge transfer band at λ_{max} 1570 mμ (1570 nm) (Figure 9). This IVCT band has been attributed to an electron-transfer transition and exists only in mixed valent complexes whose electron is delocalized. Further one-electron oxidation of **12b** with Ce(IV) provides the isovalent 6+ species **12c**, which no longer exhibits an IVCT band as expected.

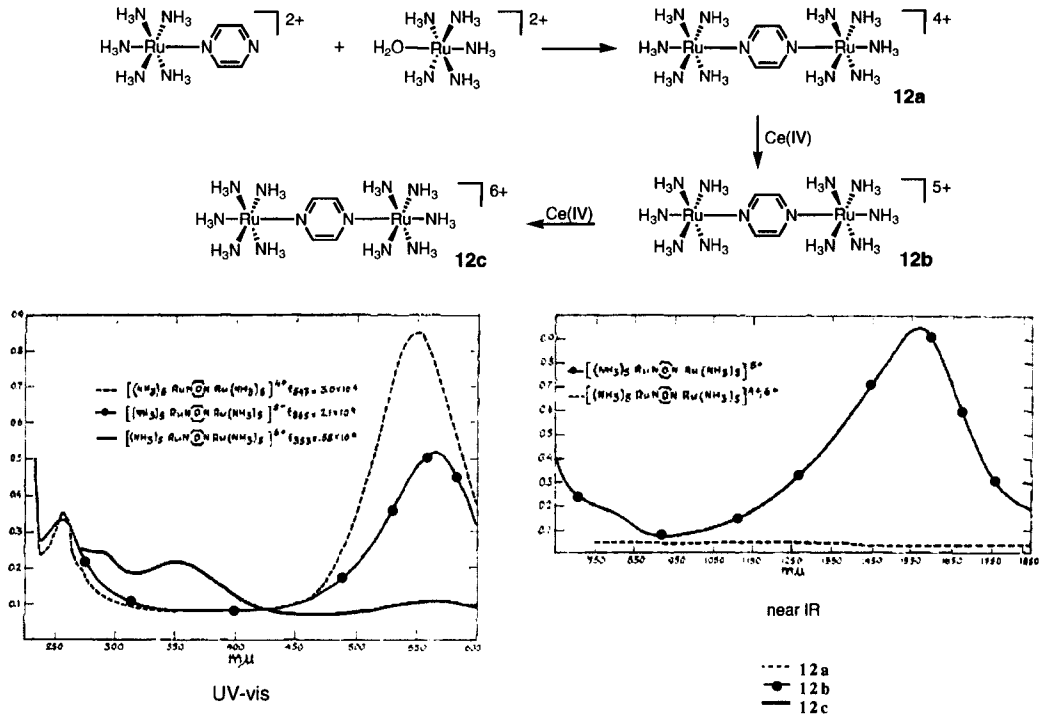

Figure 9. UV-vis/near IR of the Creutz-Taube ion.

C. Synthesis of Polymetallic Complexes

Although the polymetallic complexes above may seem structurally unrelated, there are some important characteristics common to all. These characteristics not only play an important role in the synthesis of polymetallic complexes, but in their ability to exhibit metal-metal interactions. The above polymetallic complexes contain 1) A redox active metal that is in an organized environment. 2) Bridging ligands that promote electronic interaction between metal centers. 3) Incorporation of bridging metals for the formation of bimetallic complexes containing two different metals. 4) Manipulation of the metal ligands by attaching either electron-donating or electron-withdrawing substituents.

1. Metals and Environment

The most commonly used metals in complexes that exhibit metal-metal interaction include iron, ruthenium, osmium, copper, nickel and cobalt. These metals are used because they are all redox active. The ligand determines coordination environment, i.e. square planar, squate pyramidal, tetragonal, octahedral. The appropriate redox active metal is then chosen to best suit the ligand.

2. Bridging Ligands

The role of the bridging ligand is very important because it helps to determine the overall structure of the polymetallic complex. Also, the chemical nature of the bridging ligand controls electronic communication between the metals. Numerous bridging ligands have been useful in coordinating two metal centers together to function as a conductor of electronic information between the metals. Pyrazine and bipyrimidine were used as bridging agents for several isovalent and mixed valent complexes mentioned above. Other common ligands for bridging include cyanide[39-42], acetylide[38], and 4,4′-bipyridine[33,36]. These bridging agents are both neutral (pyrazine, bipyrimidine, and 4,4′-bipyridine) and anionic (cyanide, and acetylide) to accommodate the coordination necessities of the metal.

Bridging cyanide ligands have been very useful in the assembly of multimetallic systems. The cyanide ligand is capable of promoting electronic coupling between different metal centers because of the availability of both σ-donating and π-back-bonding interactions of the cyanide with the metal centers.[39] In addition, cyanide ions possess good donor qualities at both the carbon and the nitrogen terminus making them excellent bridging ligands.[40] Hence, complexes containing terminal cyanides are particularly

attractive because of the possibility for using them in the synthesis of larger and more complex systems. Coordination of metal cyanides to other metal complexes has afforded both isovalent and mixed valent complexes (Figure 10).[39,41] These compounds and others have exhibited metal-metal interactions which were observed by cyclic voltammetry.[39-42]

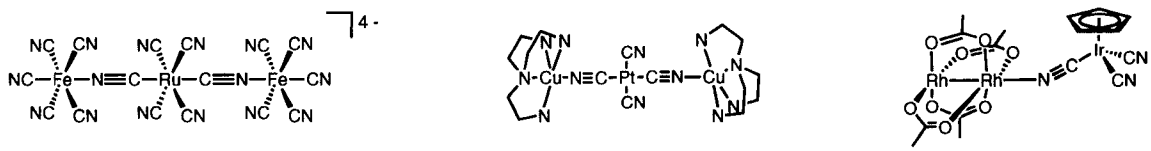

Figure 10. Cyanide bridged multi metallic complexes.

The geometry of these cyanide complexes is also important. When examining the structures in Figure 10, one could imagine that either a *cis*- or *trans*-configuration could be obtained in the trimetallic systems (Figure 11). Both regioisomers have been examined and *trans*-configuration around the central metal promotes better interaction between the terminal copper units.[41]

Figure 11. *Cis*- versus *trans*-isomers of trimetallic complex.

Pyrazine and 4,4′-bipyridine (bpy) are neutral coordination ligands that are rigidly linear and provide varied intermetallic separations with pyrazine at 6.8-7.8 Å and bpy at 11.5 Å (Figure 12).[43] Pyrazine and bpy have donor qualities through ring nitrogens as well as a delocalized π-system to transmit electronic information. Both pyrazine and bpy have been used as bridging agents in many different complexes. In some cases however, metal-metal communication is slightly lower with the bpy ligand when compared to the

identical pyrazine system.[36] This difference is probably due to metal-metal separation, which is much larger in the case of 4,4′-bipyridine.

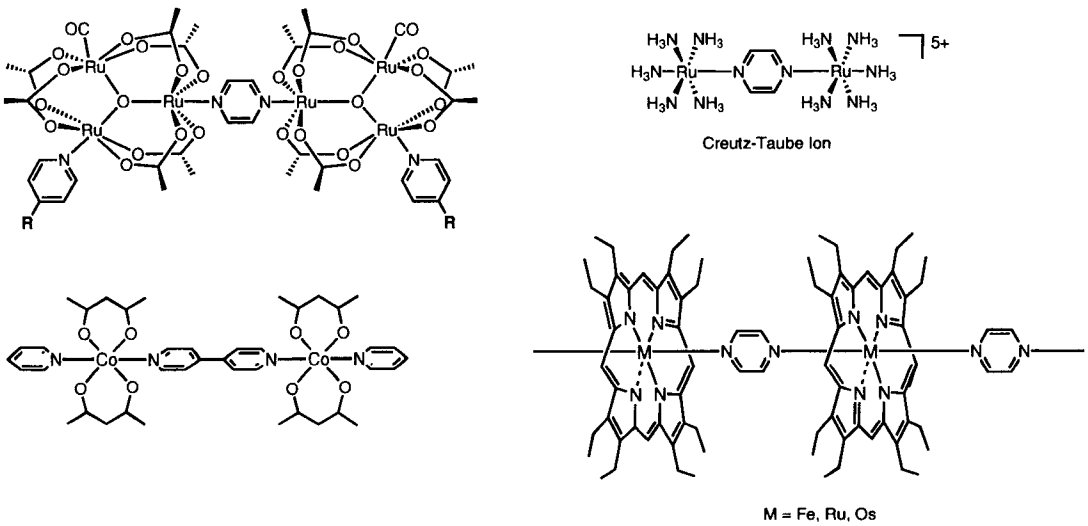

Figure 12. Pyrazine and Bpy bridged complexes.

3. Multimetallic Complexes

Multimetallic complexes that contain two or more different metals also exhibit metal-metal interaction. As seen above in Figures 9 and 11, rhodium acetate and metal octaethyl porphyrins have been used as bridging metals between two identical metal complexes. They readily coordinate to the ligands of a metal complex in a *trans*-orientation for facile construction of polymetallic complexes. Other bridging metal complexes capable of this type of coordination include ruthenium acetate[44] and metal phthalocyanines[45] (Figure 13). These bridging metal complexes allow access to complexes containing two or more different metals. If the metals are in two different oxidation states mixed valent systems will also be obtained.

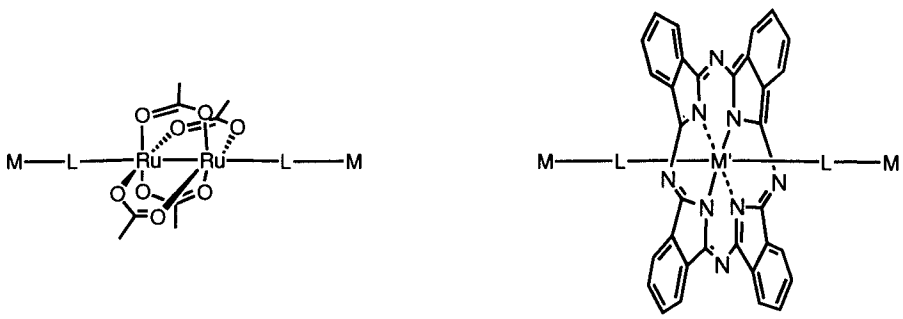

Figure 13. Ruthenium acetate and metal phthalocyanine bridging agents.

4. Metal Ligand Manipulation

Electron-donating and electron-withdrawing substituents are often connected to the metal ligand to see how they will effect the metal-metal communication of the metal system. Metal-metal interaction can sometimes be increased or decreased depending on the nature of the ligand. It was previously shown that changing the ancillary ligand of **11a-b** can have large effects on the electronic communication of a system (Figure 7).[36] Similar reactivity was seen when an electron-withdrawing substituent was affixed to the Creutz-Taube ion **12b**. Attaching chlorine to each ruthenium decreased the comproportionation constant by a factor of 3, $K_c = 10^{2.0}$. Both ancillary ligands as well as ligands directly coordinated to the metal in question can have a substantial effect on the metal-metal interactions of a given complex.

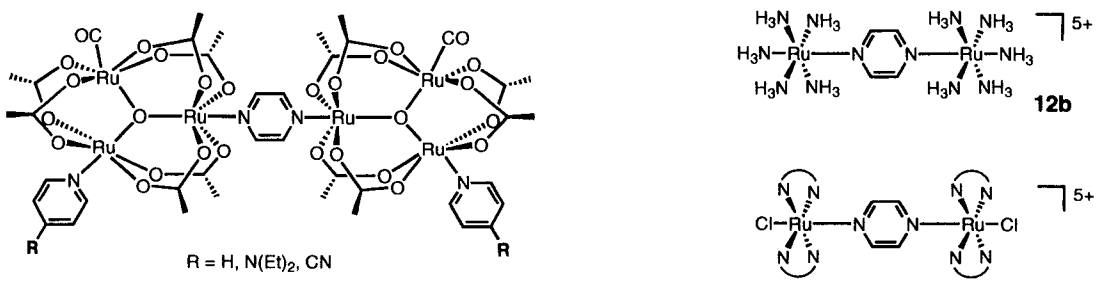

Figure 14. Ligand effects on electronic communication.

Rationale

I. Dioxocyclam Incorporation into Polymetallic Complexes.

The research presented below is based upon the idea of synthesizing capped dioxocyclam complexes coordinated to redox active metals for use as building blocks in the synthesis of polymetallic complexes capable of metal-metal communication. Functionalization of the dioxocyclam and coordination to other metal systems could give rise to polymetallic complexes such as **13** and **14** (Figure 15). These dioxocyclam complexes (**13** & **14**) would provide a new class of coordination oligomer that may exhibit interesting properties.

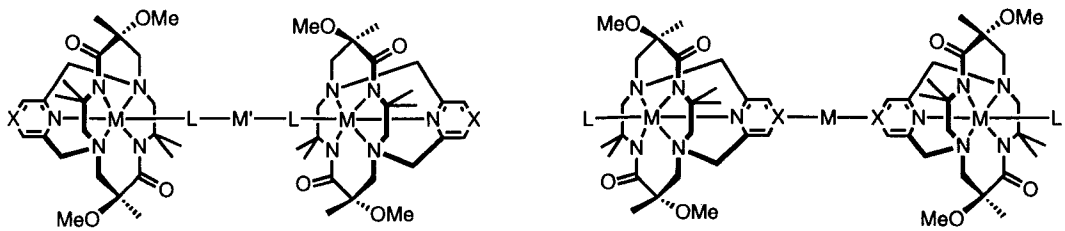

13 **14**

Figure 15. Potential multi metallic dioxocyclam complexes.

Dioxocyclam complexes are appropriate building blocks for the synthesis of polymetallic complexes. They have the potential to coordinate to a variety of transition metals and form both covalent (capping reagent) and coordination (axial metal-ligand) π-chromophores, which is rare among polymetallic complexes. Furthermore, development of 4-substituted pyridine capping reagents would provide access to electron-rich and electron-poor capped dioxocyclams whose metal complexes could also be examined. The long-term goal is to develop complexes having useful physical properties based upon electronic communication between metals through a bridging ligand. However, since the physical properties of polymetallic complexes cannot be predicted from structural

features, the development of new classes of these complexes relies on the evolution of new synthetic approaches, followed by the measurement of physical properties. For this reason, the focus of the dissertation is on the synthesis of novel capped dioxocyclams and their metal derivatives for use as building blocks for the synthesis of polymetallic complexes such as **13** and **14** (Figure 15).

The synthesis of dinuclear complexes with dioxocyclams was recently demonstrated in the Hegedus labs. Treatment of pyrazine-capped dioxocyclam copper complex **4b** with $Rh_2(OAc)_4$ produced tetrametallic complex **15**, which was characterized by X-ray crystallography (Scheme 10).[17] Characterization of complex **15** with cyclic voltammetry revealed irreversible oxidation of the complex. Copper (III) tends to adopt a square-planar coordination rather than a penta-coordinate one.[46] Oxidation of Cu(II) to Cu(III) in **15** would have to involve the decomplexation of the pyrazine capper to form a stable, square-planar Cu(III) which is not possible since the capping reagent is attached to the dioxocyclam ring. Interestingly, magnetic susceptibility experiments showed antiferromagnetic coupling between the two coppers, either through the rhodium dimer or through space, a clear sign of metal-metal interaction. Complex **15** demonstrated that multimetallic dioxocyclam complexes can be readily synthesized, and exhibit magnetic coupling across the metal ligand array. Further functionalization, however, is limited. Copper prefers a square planar or square pyramidal coordination environment. Additional coordination of ligands to the copper has been unsuccessful. Since capped dioxocyclams are pentadentate the introduction of metals capable of coordinating in an octahedral fashion is desired. They would provide an additional coordination site for further functionalization/coordination at the metal center of the dioxocyclam.

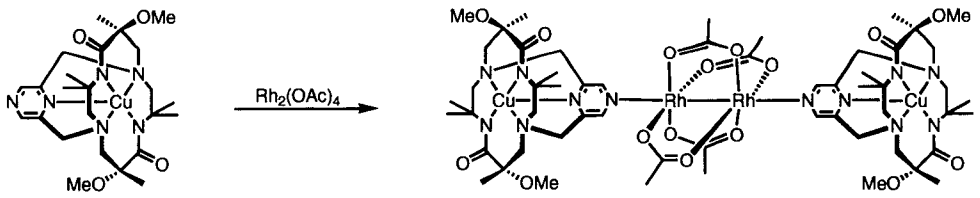

Scheme 10. Formation of a tetrametallic dioxocyclam complex.

To prepare 5,12-capped dioxocyclams for use in polymetallic complexes, five items must be addressed (Figure 16). 1) Incorporation of electron-donating and electron-withdrawing substituents for their effects on metal-metal interaction. 2) Introduction of new redox active metals into the dioxocyclam core. 3) Examination of new bridging ligands. 4) Coordination of metals to the 4-position of the capping reagent. 5) Coordination to other metals complexes such as bridging metals.

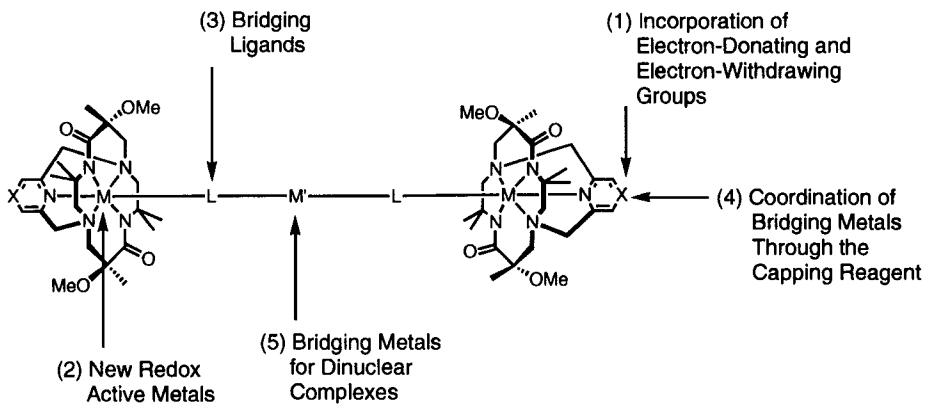

Figure 16. Dioxocyclam modifications.

A. Ligand Manipulation

To incorporate electron-donating and electron-withdrawing substituents into the dioxocyclam, manipulation of the 4-position of the capping reagent was envisioned. The synthesis of 4-substituted pyridine-capped dioxocyclams would provide a way to introduce donating and withdrawing groups. A variety of new capping reagents from 4-aminopyridine to 4-nitropyridine-capped dioxocyclams would be ideal for the series

(Figure 17). The pyridine-capped dioxocyclam would be used as the parent compound to which the other capped dioxocyclams would be compared.

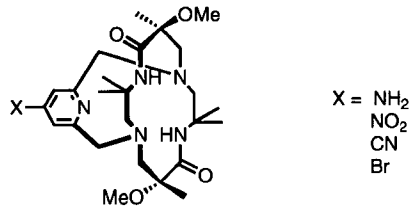

Figure 17. Incorporation of electron-donating and -withdrawing substituents.

B. Metal coordination

Capped dioxocyclams are pentacoordinate ligands. To synthesize the extended ligand arrays pictured in Figure 15, metals capable of octahedral coordination were desired. They would allow for further functionalization or coordination to metals through the axial ligand (L), which is *trans* to the pyridyl capper (Figure 18). There is precedence for cobalt and more recently ruthenium coordination in uncapped dioxocyclams.[10b,47] Coordination of these metals with the dioxocyclam should provide a redox active dioxocyclam complex that could be coordinated to other metal system either through the 4-position (X) of the pyridine capper or through the ligand (L) attached to the metal center (Figure 18). It is uncertain what effect the capped dioxocyclam will have on the coordination of cobalt or ruthenium.

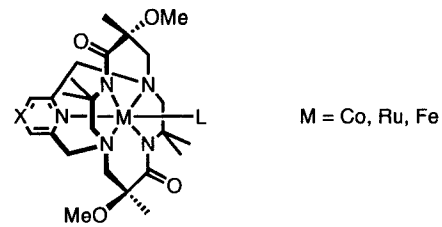

Figure 18. Metal coordination.

Capped dioxocyclams are more rigid than uncapped dioxocyclams. The capper links the two amine nitrogens which decreases the flexibility of the ring, making

coordination to metals more difficult. Increasing the rigidity of ligand has been found to decrease the rate constant for solvent exchange, making coordination slow.[48] This was observed when copper coordination of uncapped and pyridine-capped dioxocyclam was compared. An additional 4 days was required for coordination to the pyridine-capped compared to the uncapped bis-dioxocyclam. Copper coordination to 5,12-dioxocyclam **1** was accomplished in 36 hours at room temperature while the corresponding pyridine-capped 5,12-dioxocyclam **3a** required reflux conditions and increased the reaction time to 5 days. Slow coordination is anticipated for cobalt, ruthenium and iron. However, the ease of introduction of metals into dioxocyclams is both a function of the metal and the ligand and must be examined on a case by case basis.

C. Incorporation of Bridging Ligands

The ligand initially attached to the metal after coordination to the dioxocyclam will result from the metal source used, i.e. chlorine, acetate. Therefore, ligand exchange conditions will be examined because ligands that can function as a conductor of electronic information between the metallic groups are desired. Anionic cyanide and acetylide or neutral pyrazine and 4,4′-bipyrimidine will be used according to the needs of the metal (Figure 19).

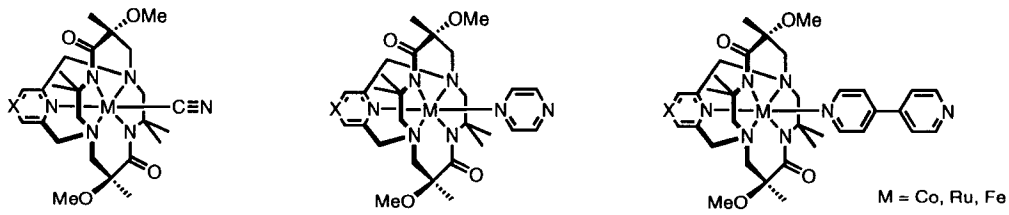

Figure 19. Ligand exchange.

D. Incorporation of Bridging Metal

The Hegedus labs have recently demonstrated that rhodium acetate can be used as a bridging metal between two pyrazine-capped dioxocyclam copper complexes (Scheme 10). Ruthenium acetate and metal phthalocyanines will also be examined for their bridging ability. Ligand coordination versus capper coordination to the bridging metal will be inspected (Figure 20). Preference for ligand coordination over capper coordination will be affected by the presence of a coordination site. If ligand coordination is desired, a capper lacking a coordination site at the 4-position will be used. If capper coordination is desired, a non-bridging ligand that lacks an external coordination site can be used.

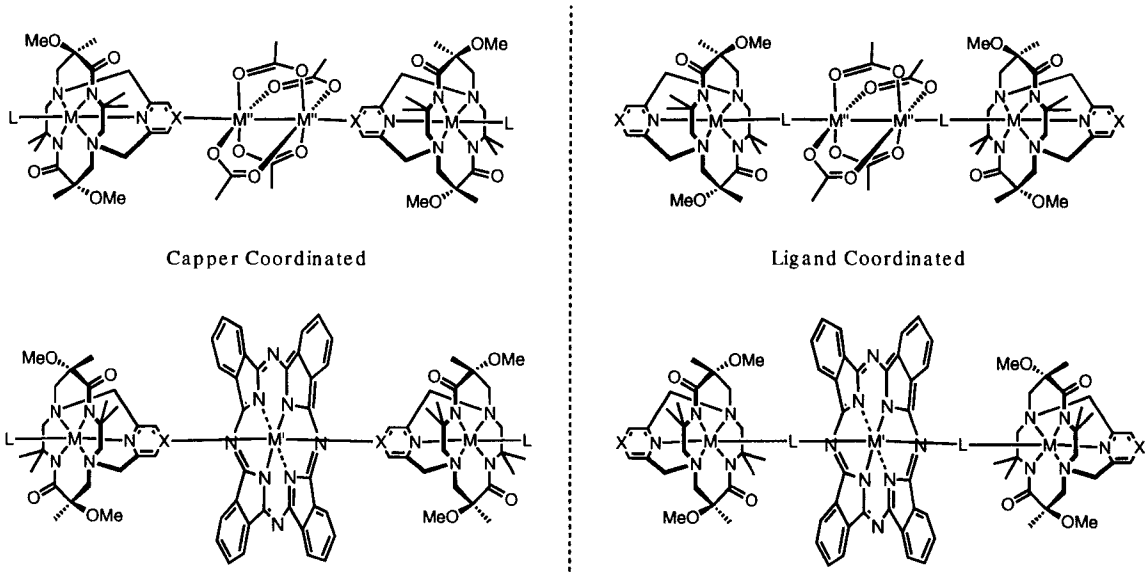

Figure 20. Metal bridging agents for dinuclear complexes.

The presence of two coordination sites at both the ligand and the capper could lead to the formation of extended coordination oligomers and polymers (Figure 21). The challenge of synthesizing these complexes lies in controlling their coordination specificity.

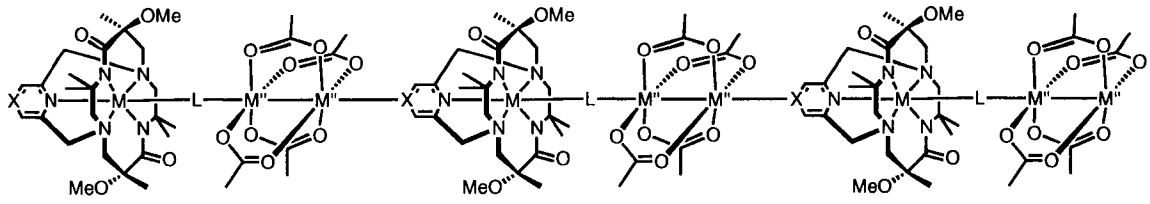

Figure 21

Results and Discussion

(Methyl)(methoxy)cyclam **1** was synthesized following methodology previously established in the Hegedus group. Photolysis of (methyl)(methoxy)chromium carbene **16** in the presence of benzyloxycarbonyl (Cbz) protected imidazoline **17** gave protected azapenam **18** in 74% yield. Removal of the protecting group with Pd/C hydrogenation gave azapenam **19**. Treatment with CSA opens the azapenam to a seven-membered ring imine, which undergoes an unusual cycloaddition giving imines **20** and **21** in a 1:1 mixture of *cis*- (C_2) and *trans*-isomers (C_i), respectively. Acid-catalyzed isomerization results in nearly quantitative yields of the more stable *trans*-isomer **21**, which is isolated by recrystallization. Reduction of *trans*-imine **21** with sodium cyanoborohydride in the presence of benzoic acid affords *trans*-5,12-dioxocyclam **1** (Scheme 11).

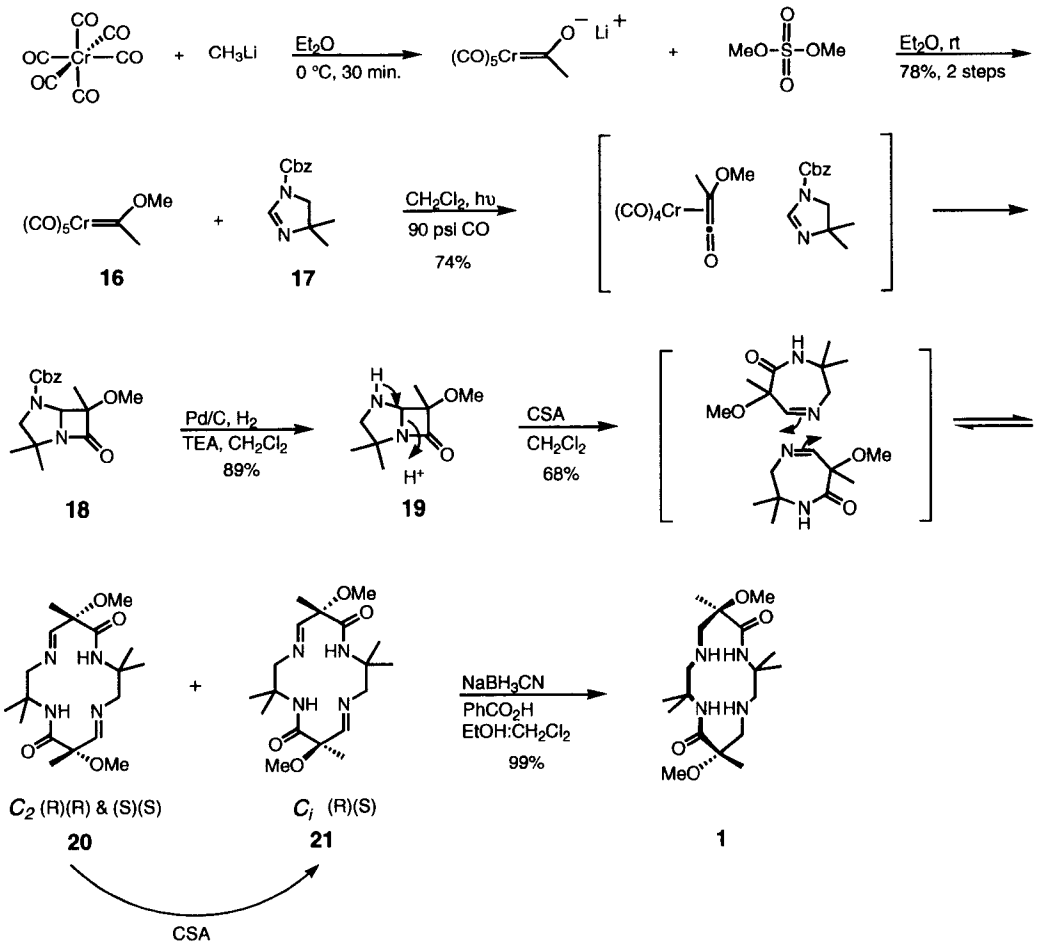

Scheme 11. 5,12-dioxocyclam synthesis.

I. Preparation of Capping Reagents

A series of capping reagents was prepared in order to obtain both electron-donating and -withdrawing capped dioxocyclams (Figure 22). The series included 2,6-bis(bromomethyl)pyridine **2a**, 2,6-bis(bromomethyl)pyrazine **2b**, 4-amino-2,6-bis(bromomethyl)pyridine **2c**, 4-bromo-2,6-bis(tosylmethyl)pyridine **2d**, 4-nitro-2,6-bis(bromomethyl)pyridine **2e**, and 4-cyano-2,6-bis(bromomethyl)pyridine **2f**. There is a fundamental electronic difference between the pyridine and pyrazine capping reagents. Pyridine is a moderate base (pKa ≈5), and acts primarily as a good σ-donor. In contrast, pyrazine is not at all basic (pKa ≈0.37) and coordinates mainly as a strong π-acceptor.

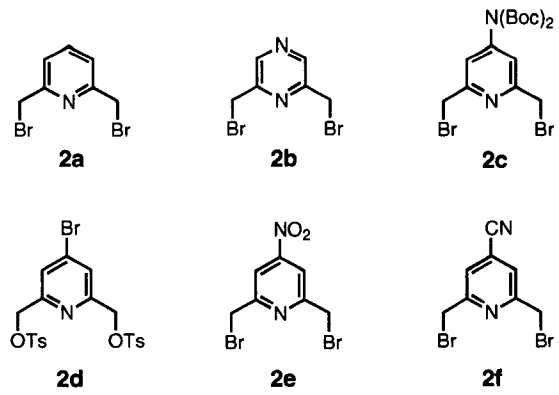

Figure 22. Capping reagents.

Bis-(bromomethyl)pyridine **2a** can be synthesized from benzylic bromination of 2,6-lutidine. However, benzylic brominations are often unreliable, affording a mixture of products including monobrominated, dibrominated, and multibrominated materials. This was avoided when 2,6-bis(hydroxymethyl)pyridine was activated with tosylchloride to provide the pyridine capping reagent **2a′** (Scheme 12).

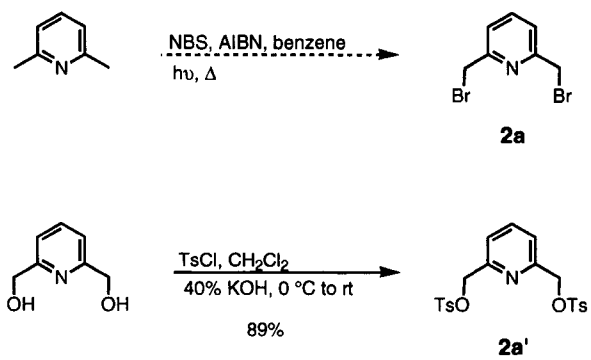

Scheme 12. Pyridine capper synthesis.

Preparation of 4-substituted pyridine and pyrazine capping reagents follow. 4-substituted 2,6-dimethylpyridines, although simple in appearance, are oddly substituted making their syntheses nontrivial and not widely examined in the literature. Ochiai accomplished pioneering work on the substitution of unsubstituted pyridines.[49] Utilizing this methodology, oxidation of 2,6-lutidine **22** with *m*-CPBA followed by nitration with

nitric and sulfuric acids afforded 4-nitro-2,6-dimethylpyridine *N*-oxide **24** in good yield (Scheme 13).[50] Reduction of the *N*-oxide followed by conversion of **25** to an electrophilic capping reagent was accomplished by taking advantage of benzylic bromination. Classical bromination conditions afforded 4-nitro-2,6-bis(bromomethyl)pyridine **2e** albeit in poor yields. The poor yields of the reaction were due to the uncontrollable nature of benzylic bromination reactions, which favor polybrominated products. Although only 2.5 equivalents of NBS were used for the reaction, a mixture of mono-bromo, bis-bromo, and poly-brominated products were obtained.

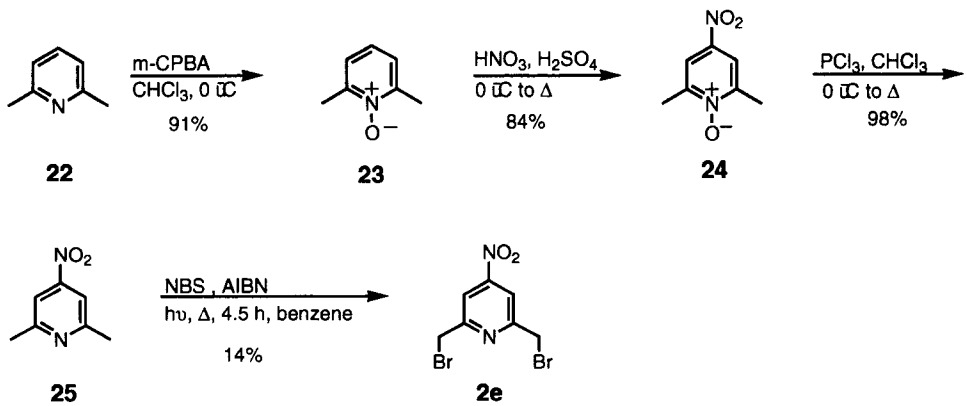

Scheme 13. Synthesis of 4-nitro bis-(bromomethyl)pyridine.

Diethyl phosphite and triethylamine have been found useful for debromination of α,α-dibromomethyl arylketones, *gem*-dibromoalkenes and *gem*-dibromocyclopropanes to the corresponding monobromo compound.[51] For the debromination of benzylic bromides it is necessary to use *N,N*-diisopropylethylamine (*i*-Pr_2NEt) in place of triethylamine to avoid nucleophilic substitution side reactions.[52] Overbromination conditions allowed us to take advantage of the propensity for polybromination at the benzylic position. Reduction of polybrominated pyridine **26** with diethyl phosphite and $(i\text{-Pr})_2NEt$ afforded **2e** in much improved yields.

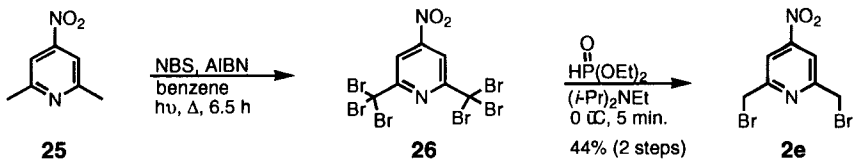

Scheme 14. Optimized bromination conditions.

Lutidine *N*-oxide intermediate **23** was not only useful for the synthesis of **2e** but also for the syntheses of 4-aminopyridine **2c** and 4-cyanopyridine **2f**. Nitration of lutidine *N*-oxide with nitric and sulfuric acids afforded **24**. Next, Ti(0) was prepared in situ by refluxing titanium tetrachloride with magnesium (Scheme 15).[53] Upon Ti(0) formation, **24** was added which simultaneously reduced both the *N*-oxide and the 4-nitro to the 4-amino **27** in excellent yields. Protection of the amine proved to be quite difficult, with recovery of starting material under numerous conditions.[54] Sonication conditions were finally examined. Fortuitously, an unseen star crack in the flask allowed slow addition of water into the reaction mixture resulting in bis-Boc protected amine **28**. Slow addition of water proved to be necessary for the formation of **28** (Schotten-Baumen conditions). Optimized bromination conditions were used to give the 4-amino capping reagent **2c** in good yields.

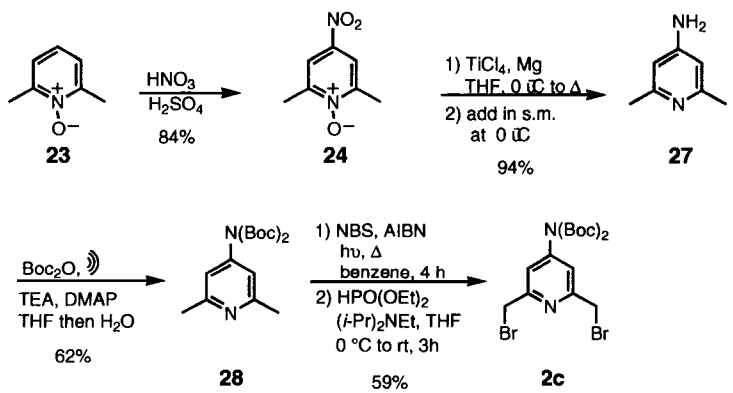

Scheme 15. 4-amino capping reagent.

For the preparation of 4-cyanopyridine, *o*-methylation of lutidine *N*-oxide **23** followed by treatment with aqueous potassium cyanide gave **29** in modest yields.[59] Overbromination followed by diethyl phosphite reduction gave 4-cyano-bis-(bromomethyl)pyridine capping reagent **2f** (Scheme 16).

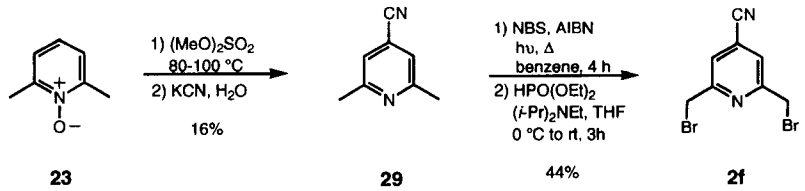

Scheme 16. Synthesis of 4-cyano-2,6-bis(bromomethyl)pyridine.

The 4-bromopyridine capping reagent was prepared not from a pyridine precursor but from chelidamic acid **30**. Chelidamic acid is commercially available but can be easily prepared by condensation of diethyl oxalate with acetone and ammonia. Treatment of chelidamic acid with PBr_5 followed by methanol provided **31** (Scheme 17). Reduction of the ester with $NaBH_4$ provided the alcohol, which was then tosylated[55], giving **2d** in good yields.

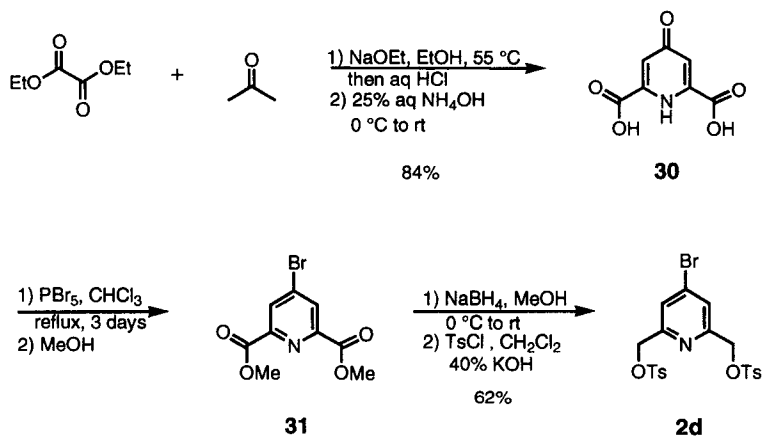

Scheme 17. Synthesis of 4-cyano-2,6-bis(tosylmethyl)pyridine.

Pyrazine proved to be much more difficult to work with. Classical bromination conditions were used with 2,6-dimethylpyrazine. As expected, poor yields of the bis-brominated material were obtained (Scheme 18). Overbromination conditions were examined, but failed because the multibrominated material proved to be unstable and seemed to decompose upon its formation. Examination of alternative bromination conditions allowed us to increase the yields slightly. Benzylic bromination with bromine in ethyl acetate afforded the bis-brominated pyrazine in 25% yield (Scheme 18). However, even with an increase in yield, the bis(bromomethyl)pyrazine was unstable. It would decompose immediately when out of solution, or slowly upon standing in a solution of CH_2Cl_2 or ethyl acetate. During capping reactions, the capping reagent would decompose continuously throughout the reaction and would have to be repeatedly synthesized and added portion-wise. To avoid these tedious problems, alternative pyrazine capping reagents were desired.

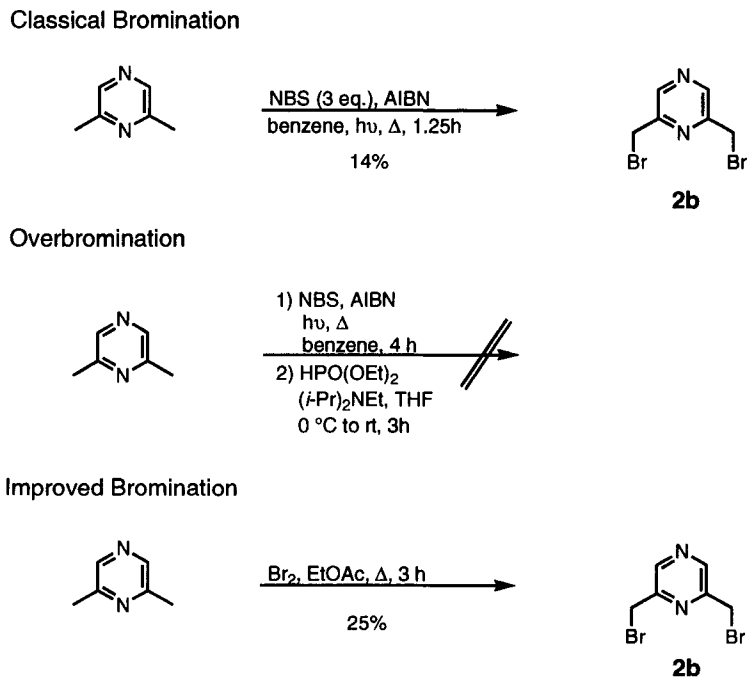

Scheme 18. Benzylic brominations of 2,6-dimethylpyrazine.

Pyrazine 2,6-dicarboxylic acid can be synthesized from glucose. Heating glucose **32** and *p*-toluidine in acid gave **33** (Scheme 19).[56] Further reaction with hydrazine hydrate and *o*-phenylenediamine gave quinoxaline intermediate **34**. Oxidation with excess $KMnO_4$ afforded pyrazine 2,3,6-tricarboxylic acid **35**. Decarboxylation afforded a mixture of pyrazine 2,5- and pyrazine 2,6-dicarboxylic acids **36** and **37**, favoring the desired 2,6-pyrazine. The two regioisomers were easily separated by recrystallization.

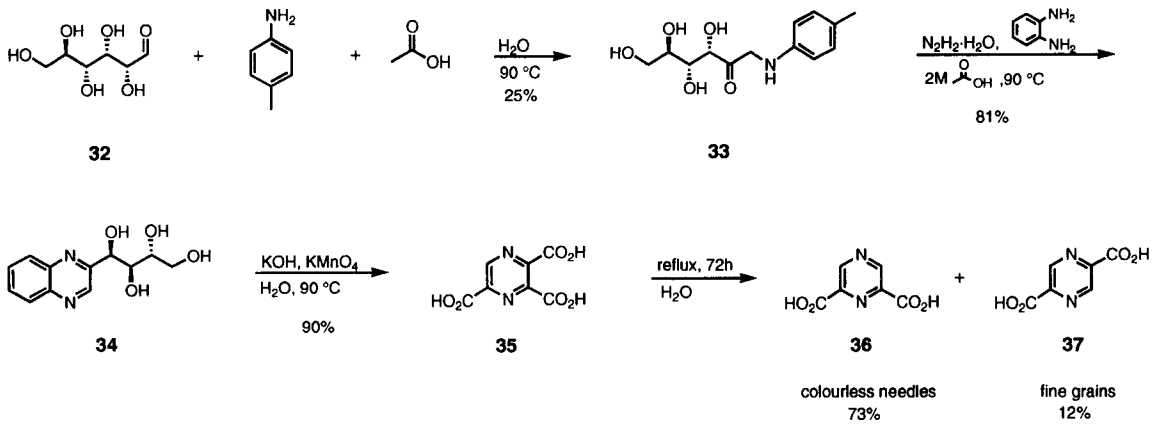

Scheme 19. Synthesis of pyrazine 2,6-dicarboxylic acid.

Esterification of pyrazine 2,6-dicarboxylic acid was planned. It was hoped, similar to 4-bromo-2,6-pyridinedicarboxylate **31**, the pyrazine ester could be reduced to the alcohol followed by tosylation potentially forming a more stable capping reagent. However, **36** proved to be insoluble in organic solvents resulting in only mild reactivity under several esterification conditions (Table 1). The poor and irreproducible yields of pyrazine 2,6-dimethylester made this route unattractive.

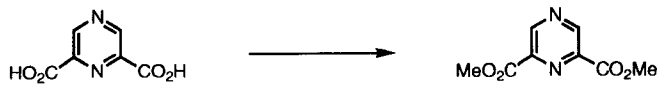

	Conditions	Yield
1	MeOH, H_2SO_4, Δ, 48h	12%
2	MeOH, HCl, Δ, 3 days	8%
3	MeOH·HCl (1.39M), Δ, 7days	s.m.

Table 1. Esterification conditions.

Pyrazine acid chloride intermediates were then examined in lieu of pyrazine esters. Reaction of pyrazine 2,6-dicarboxylic acid and oxalyl chloride lead to complete recovery of starting materials (Scheme 20). Synthesis of 2,6-bis(hydroxymethyl)pyrazine was then approached more straightforwardly by reducing the acid directly to the alcohol. Reduction of the acid to the alcohol with BH_3 to obtain 2,6-bis(hydroxymethyl)pyrazine resulted in complete decomposition of starting materials (Scheme 20). The extreme insolubility of pyrazine 2,6-dicarboxylic acid in any solvent except for water may have played a role in its poor reactivity. Alternative pathways for obtaining a suitable pyrazine capping reagent followed.

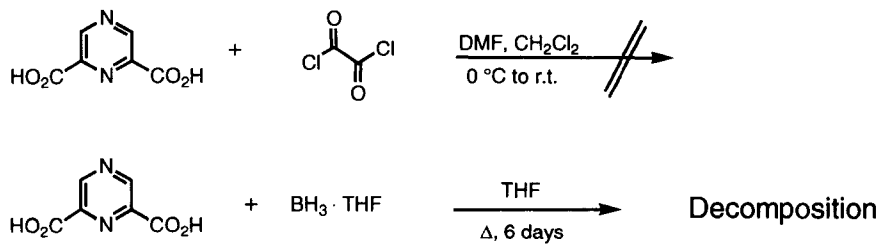

Scheme 20. Alternative pyrazine reactions.

Palladium catalyzed carbonylation was found to be successful for the carbonylation of pyridine polychlorides.[57] Treatment of 2,6-dichloropyrazine **38** with

palladium(II) acetate, DPPP, and Na_2CO_3 at 20 psi CO afforded pyrazine 2,6-dibutylester **39** in good yields (Scheme 21). Transesterification of **39** to **40** occurred smoothly under acidic conditions.

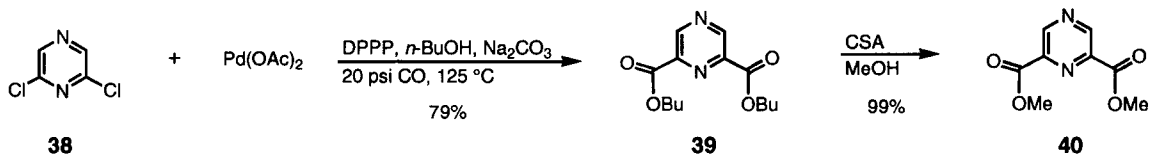

38 **39** **40**

Scheme 21. Synthesis of pyrazine 2,6-dimethylester.

With the pyrazine dimethylester in hand, reduction conditions to obtain the bis-alcohol ensued. Reduction of **40** with $NaBH_4$ seemed to give the diol **41** by TLC (Table 2). However, like the 2,6-bis(bromomethyl) pyrazine, the product was unstable and precipitated as a black solid upon removal of solvent. Examination of the black solid by NMR and IR spectroscopy was inconclusive. The pyrazine diol seemed to be more sensitive than the 2,6-bis(bromomethyl)pyrazine **2b**, making its isolation difficult. Alternative reducing conditions using aprotic solvents were examined for in situ alcohol protection. However, reduction of **40** with either DIBAL or $Zn(BH_4)_2bpy$[58] (bpy = 2,2′-bipyridine) lead to decomposition or recovery of a small portion of starting material (Table 2). It was unclear if the pyrazine diol decomposed in solution prior to protection or if the reducing conditions were too harsh for the substrates.

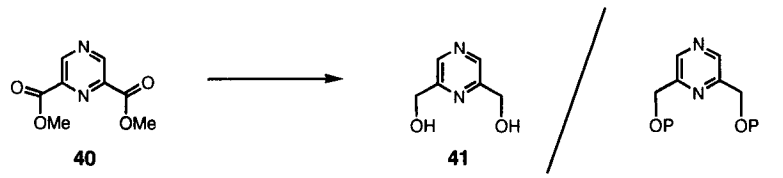

	Reagents	Conditions	Yield
1	$NaBH_4$	0 °C EtOH	Decomposition upon isolation
2	1) DIBAL 2) py, TsCl	0 °C to rt THF	Decomposition
3	1) DIBAL 2) py, DMAP, acetic anhydride	-78 °C to rt THF	Decomposition
4	1) $Zn(BH_4)_2$bby 2) TsCl	0 °C to rt CH_2Cl_2	S.M. / Decomposition

Table 2. Reduction of pyrazine 2,6-dimethylester.

Currently, effort is being focused on solvent exchange conditions for entry 1, after $NaBH_4$ reduction (Table 2). If 2,6-bis(hydroxymethyl)pyrazine **41** is formed after $NaBH_4$ reduction of the ester, solvent exchange of methanol for an aprotic solvent would provide conditions under which the alcohol could be protected. Once protected, it is hoped that the pyrazine capper will be stable, or at least more stable than the 2,6-bis(bromomethyl)-pyrazine capping reagent.

Although synthesis of the pyrazine capping reagent has not yet been optimized, all of the desired capping reagents were synthesized. Capping conditions were next examined to obtain capped 5,12-dioxocyclams.

II. Dioxocyclam Capping Conditions

Capped 5,12-dioxocyclams were prepared according to methodology previously developed in the Hegedus laboratories. Similar to the pyridine- and pyrazine-capped dioxocyclams, 4-substituted pyridine capping reactions proceeded smoothly. Capped dioxocyclams **3a-f** were obtained as white crystalline solids in good yields from

treatment of 5,12-dioxocyclam **1** with capping reagents **2a'** and **2b-f** with $(i\text{-Pr})_2$NEt in CH_3CN at ≈95 °C (Table 3). However, reaction time is a big drawback in these capping reactions. The reaction time span can range between 4 to 8 days. In an attempt to decrease reaction time, microwave conditions were examined.

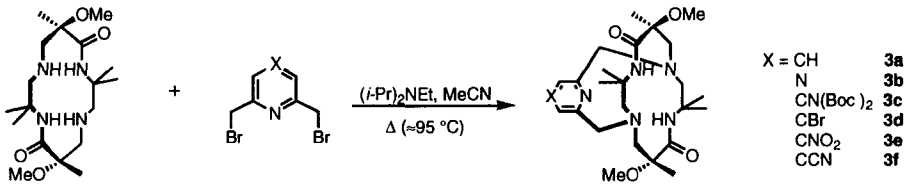

1 **2a', 2b-f** **3a-f**

	Capper	% Yield	Time
1	X=H	61%	3 days
2	pyrazine	52%	4 days
3	X=CN(Boc)$_2$	43%	8 days
4	X=CBr	72%	3 days
5	X=CNO$_2$	65%	4 days
6	X=CCN	62%	4 days

Table 3. Heat assisted capping reactions.

Microwave conditions decreased capping times from days to minutes (Table 4). Treatment of 5,12-dioxocyclam with capping reagents **2a'**,**2b-f** and $(i\text{-Pr})_2$NEt in CH_3CN under microwave radiation for periods of 2 minutes at a power level of 2 afforded the corresponding capped dioxocyclams **3a-f**. Only two capping reagents led to lower yields of capped dioxocyclam with microwave radiation. The pyrazine and 4-nitropyridine capping reagents did not respond well to these conditions. The harsher reaction conditions of the microwave may be too extreme for the sensitive pyrazine capping reagent. Also, the 4-nitropyridine capping reagent failed to react well, giving only 6% yield of **3e**.

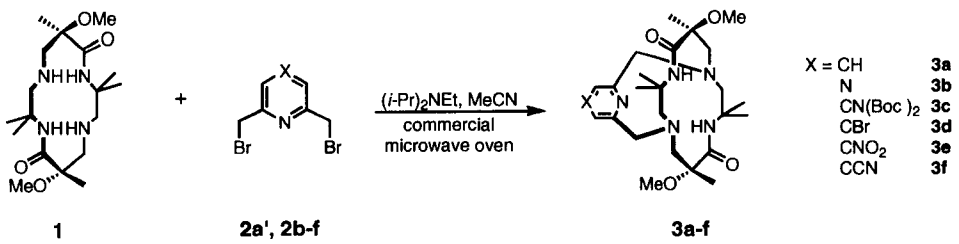

	Capper	% Yield	Time
1	X=CH	69%	20 min.
2	pyrazine	23%	20 min.
3	X=CN(Boc)$_2$		
4	X=CBr	71%	20 min
5	X=CNO$_2$	6%	30 min
6	X=CCN	64%	15 min.

Table 4. Microwave assisted capping reactions.

Related research from these labs has shown that 4-bromopyridyl-capped dioxocyclam **3d** allows further functionalization. Palladium-catalyzed coupling reactions including Stille (**42a**), Sonagashira (**42b**), Suzuki (**42c**), and Buchwald-Hartwig amination (**42d**) have afforded capped dioxocyclams that would be difficult to obtain by traditional capping methods (Scheme 22).[59]

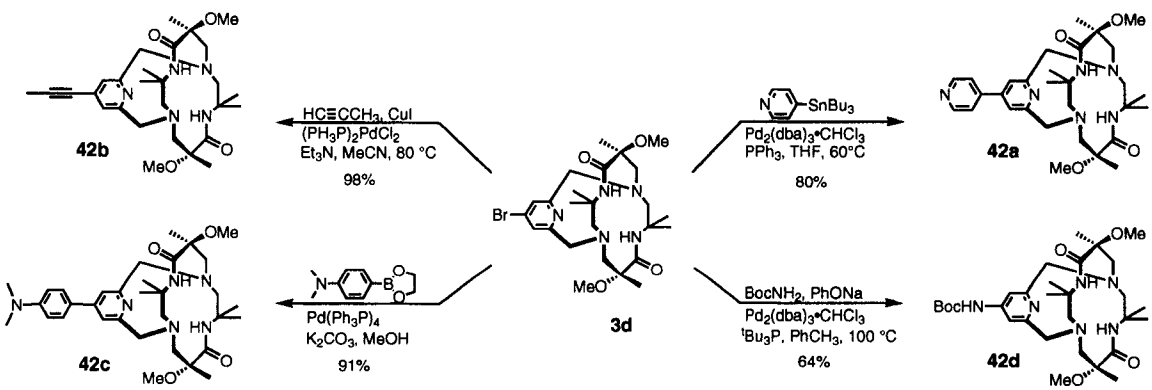

Scheme 22. Palladium-catalyzed coupling reactions of 4-Bromo pyridine capped dioxocyclam.

III. Metal Coordination

With a series of electron-donating and electron-withdrawing capped 5,12-dioxocyclams in hand, metal coordination followed. As mentioned earlier, both nickel and copper complexes of 5,12-dioxocyclams are well known. Metal complexes of capped 5,12-dioxocyclams are less common, with copper being the only known complex.[14,16] As discussed earlier, capped dioxocyclams are more rigid than uncapped dioxocyclams making their coordination to metals more difficult. For example, it takes an additional 4 days to insert copper into a capped dioxocyclam versus the uncapped dioxocyclam. Coordination of nickel into the capped dioxocyclam has been unsuccessful under a number of conditions.

The coordination of cobalt, ruthenium and iron within the dioxocyclam was desired because of their anticipated redox activity, and their preference to form octahedral complexes. Coordination complexes of both cobalt and ruthenium uncapped 5,12-dioxocyclam complexes have been synthesized. [10b,47] However, it is unknown what effect the capped dioxocyclams will have on metal coordination of cobalt, ruthenium and iron.

A. Cobalt Coordination

Cobalt was examined first for its coordination potential. Since cobalt(III) is relatively substitution inert, coordination with a cobalt(II) precursor followed by oxidation was the planned approach. Treatment of pyridine-capped dioxocyclam **3a** with cobalt(II) chloride with an insoluble base, similar to reaction conditions for the coordination of copper, resulted in no reaction. Different cobalt complexes, bases and solvent were examined, yet only starting material was recovered in all cases (Table 5).

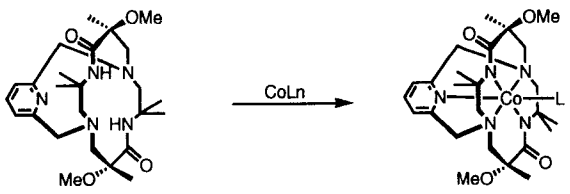

3a

	Metal	Base	Solvent	Reaction Conditions	Color Change	IR (cm^{-1})	Product
1	$CoCl_2 \cdot 6\ H_2O$	K_2CO_3	abs. EtOH	room temp. to 50 °C	blue to purple	1660	startingmaterial
2	$CoCl_3$	$(i\text{-Pr})_2NEt$	abs. EtOH	room temp. to 65 °C	dk. blue to lt. blue upon base	1660	starting material
3	$CoCl_2 \cdot 6\ H_2O$	$(i\text{-Pr})_2NEt$	abs. EtOH	room temp. to 50 °C	blue to grey upon base	1660	starting material
4	$Co(CH_3CO_2)_2 \cdot 4\ H_2O$	Na_2CO_3	abs. EtOH	85 °C	pink to purple upon base	1660	starting material
5	$Co(CH_3CO_2)_2 \cdot 4\ H_2O$	$(i\text{-Pr})_2NEt$	MeOH	90 °C, 10 days	pink to dark pink	1660	starting material

Table 5. Cobalt coordination attempts.

Microwave radiation of pyridine-capped dioxocyclam **3a** with cobalt(II) acetate and $(i\text{-Pr})_2NEt$ for two minutes at a power level of 2 caused the dark pink solution to turn purple then fade back to pink upon cooling. After a total of 20 minutes of microwave sets, IR spectroscopy showed the presence of starting material (1660 cm^{-1}) and a new carbonyl stretch at 1564 cm^{-1}. Additional microwave radiation of the solution, for a total of two hours, afforded pyridine-capped cobalt(III) complex **5a** as a pink solid in 78% yield (Scheme 23). During the reaction process cobalt was oxidized by air to the cobalt(III) complex. Mass spectrometry of purified **5a** confirmed its constitution, with a parent ion at 590.20 m/z. IR carbonyl stretches were seen at 1564 cm^{-1} and 1613 cm^{-1} for the amide and acetate groups respectively.

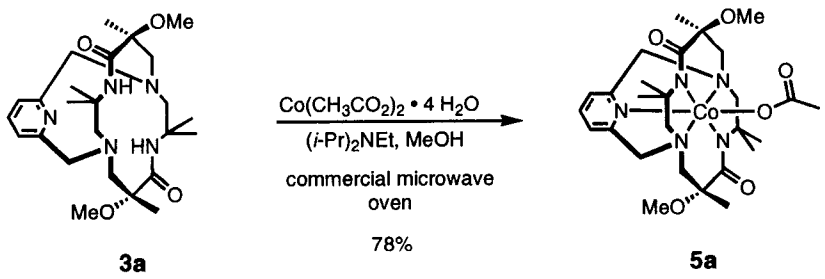

Scheme 23. Cobalt coordination with pyridine-capped dioxocyclam.

The pyridine-capped cobalt acetate complex **5a** was quite crystalline providing good quality single crystals suitable for X-ray diffraction (Figure 23). Figure 22 shows the dioxocyclam ring vertical with the pyridine capping reagent to the left and the acetate ligand to the right.

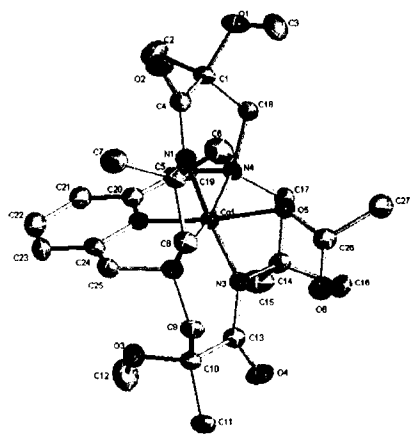

Figure 23. ORTEP drawing of pyridine-capped cobalt acetate.

These cobalt coordination conditions were applied to the rest of the capped dioxocyclams **3b-f**. Cobalt coordination of **3b** and **3c** afforded pyrazine and 4-aminopyridine-capped cobalt complexes **5b** and **5c** as bright pink solids in good yields (Table 6). Again, the pyrazine-capped cobalt acetate **5b** was crystalline, providing good quality single crystals for X-ray diffraction (Figure 24). Unfortunately, poor yields were obtained for dioxocyclams capped with electron-withdrawing substituents.

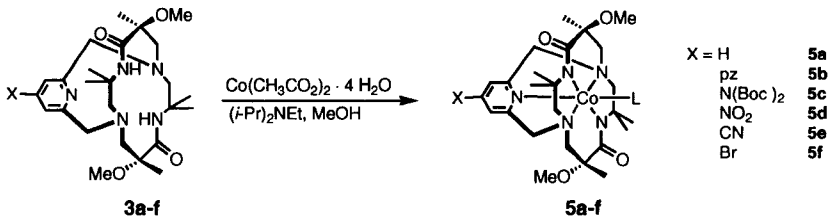

	Capped Cyclam	Ligand	Conditions cmw, 2 min @ p 2	Yield
1	X = H	L = OAc	1 hour	78%
2	pyrazine	L=OAc	1 hour	51%
3	X = N(Boc)$_2$	L = OAc	6 minutes	81%
4	X = NO_2	L = OAc, OMe, OH	40 minutes	10%
5	X = CN		1 hour	0%
6	X = Br	L = OAc, OMe, OH	1 hour	20%

Table 6. Cobalt coordination for all 4-substituted capped dioxocyclams.

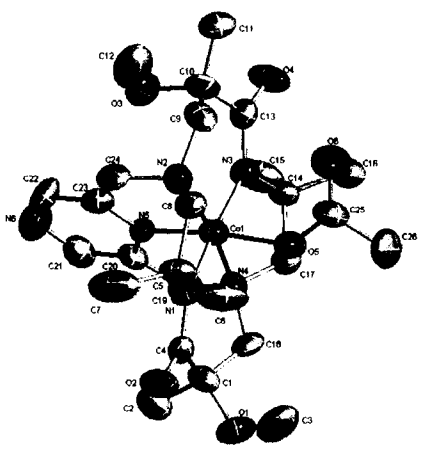

Figure 24. ORTEP drawing of pyrazine-capped cobalt acetate.

Dioxocyclams capped with electron-withdrawing substituents proved to be challenging. The most surprising result was a 0% yield for the introduction of cobalt into the 4-cyanopyridine-capped dioxocyclam (Table 6, entry 5). Instead of cobalt coordination, cobalt catalyzed hydrolysis of the cyanide to the corresponding amide was observed under these reaction conditions (Scheme 24). Similar reactivity was observed

by Michal Achmatowicz on related work of copper coordination with 4-cyanopyridine-capped dioxocyclam. Hydrolysis was prevented when CH_2Cl_2 was substituted for methanol as the solvent.[59] Unfortunately, this approach cannot be used in this case for two reasons. Cobalt(II) acetate is not soluble in CH_2Cl_2 and it has a low dielectric constant, which is not desirable in microwave reactions. The energy from microwaves is transferred to the substance being heated through either dipole or ionic interactions.[60] Microwave energy is transferred to solvents with high dielectric constants more readily because of their dipole rotation.

Alternatively, anhydrous cobalt acetate was prepared. However, reaction of 4-cyanopyridine dioxocyclam and anhydrous cobalt acetate in methanol resulted in no reaction. The solvent was exchanged for acetonitrile, which has a similar dielectric constant to methanol. However, introduction of both cobalt acetate and anhydrous cobalt acetate in the 4-cyanopyridine dioxocyclam only resulted in recovery of starting material **3f**.

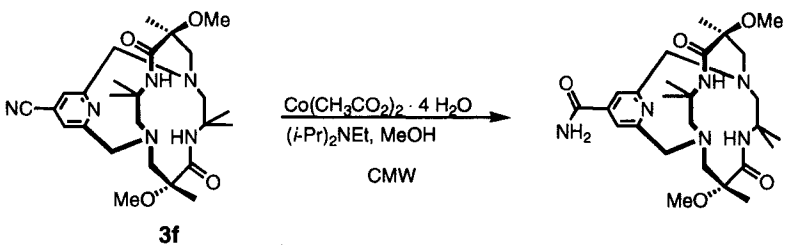

3f

Scheme 24. Hydrolysis of 4-cyanopyridine-capped dioxocyclam.

Introduction of cobalt into 4-nitropyridine-capped dioxocyclam **3e** resulted in a mixture of products resulting in low yields of coordinated product (Table 6, entry 4). Mass spectrum analysis of the crude mixture indicated the presence of the 4-nitropyridine cobalt acetate complex **5e**, the 4-nitropyridine cobalt methoxide complex **5e′**, and the 4-

nitrosopyridine cobalt complex **5e″** lacking a sixth ligand (Scheme 25). The reducing agent for the formation of 4-nitrosopyridine **5e″** is not obvious but methanol is the most likely candidate. There are examples of 4-nitrosopyridine N-oxides[61] in the literature, although 4-nitrosopyridine[62] itself is unstable. The 4-nitropyridine cobalt methoxide product **5e′** was isolated in 10% yield by chromatographic purification of the mixture. Characterization by mass spectrometry confirmed its constitution with a parent ion at 607.07 m/z. IR carbonyl stretch was observed at 1570 cm^{-1} with characteristic NO_2 stretching at 1379 cm^{-1} and 1323 cm^{-1}.

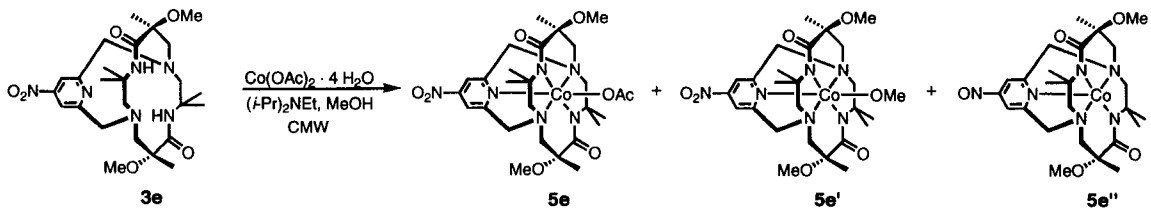

Scheme 25. Coordination products for 4-nitropyridine-capped dioxocyclam.

Introduction of cobalt into 4-bromopyridine-capped dioxocyclam also resulted in a mixture of products (Table 6, entry 6). Mass spectrum analysis of the crude mixture showed the 4-bromopyridine cobalt acetate complex **5d**, and the 4-methoxypridine cobalt hydroxide complex **5d′** (Scheme 26). Chromatographic separation of the mixture on silica gel separated the mixture of **5d** and **5d′** away from uncomplexed capped dioxocyclam. A second separation on neutral alumina separated the two products but also resulted in hydrolysis of the 4-bromopyridine cobalt acetate **5d** to 4-bromopyridine cobalt hydroxide **5d″**. A second neutral alumina column gave pure 4-bromopyridine cobalt hydroxide complex in 20% yield.

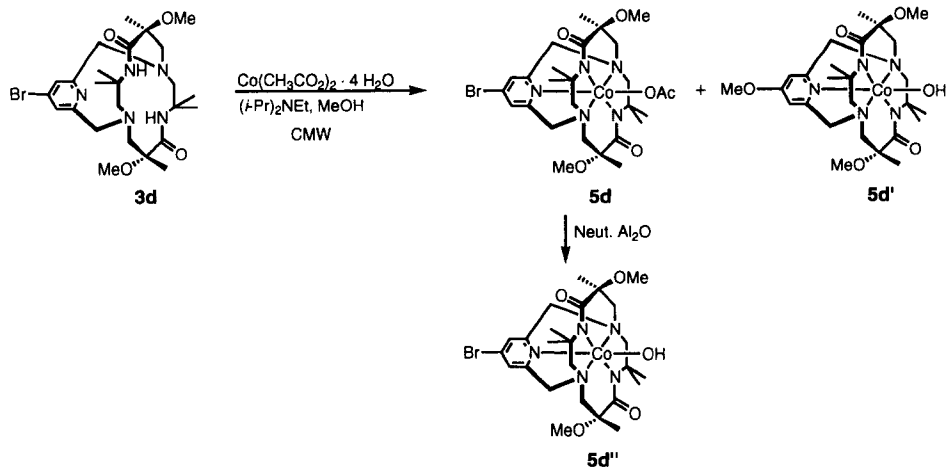

Scheme 26. Coordination products of 4-bromopyridine-capped dioxocyclam.

Cobalt complexes of dioxocyclams capped with electron-donating substituents were easily synthesized in good yields. Dioxocyclams capped with electron-withdrawing substituents proved problematic during coordination experiments. Only low yields of the desired cobalt coordinated products could be isolated.

1. Ligand Exchange for Cobalt Complexes

The acetate ligand is anionic and must be replaced with another anionic ligand that provides an additional coordination site. The cyanide or acetylide ligand would be appropriate in this case because it is anionic and provides a π-coordination motif. Treatment of pyridine-capped and 4-substituted pyridine-capped cobalt dioxocyclams **5a-e** with sodium cyanide in methanol afforded the corresponding cyanide complexes **6a-e** in good yields (Table 7). Treatment of **5a-e** with sodium cyanide in methanol resulted in a slow color change from pink to orange. Examination of **5a** by IR spectroscopy during the reaction showed the acetate carbonyl stretch at 1613 cm^{-1} had been replaced by a cyanide stretch at 2123 cm^{-1}. Mass spectrometry of purified **6a** confirmed its constitution, with a parent ion at 557.18 m/z. In addition, x-ray quality crystals of both

the pyridine **6a** and pyrazine **6b** cobalt cyanide complexes were obtained that confirmed their structure (Figure 25).

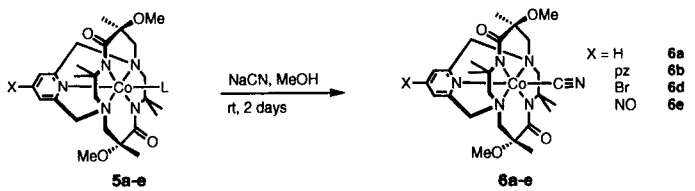

	Capped Cyclam	5a-e Ligand	Yield
1	X=H	L=OAc	76%
2	pyrazine	L=OAc	75%
3	X=NO_2, NO	L=OAc, OMe, OH	6%
4	X=Br	L=OMe	60%

Table 7. Cyanide ligand exchange.

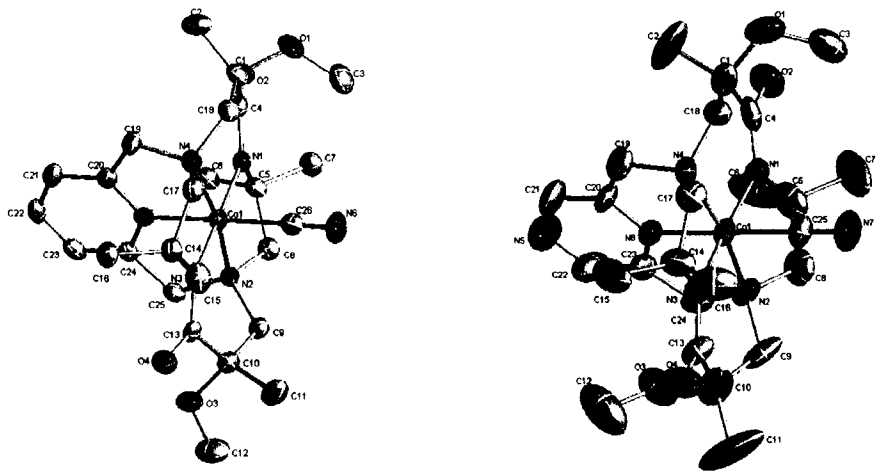

Figure 25. ORTEP drawings of pyridine and pyrazine-capped cobalt cyanide.

In the case of 4-nitropyridine dioxocyclam, the crude mixture was carried on since its separation was difficult and low yielding. Treatment of the crude reaction mixture with sodium cyanide in methanol allowed isolation of a low yield of the 4-nitrosopyridine cobalt cyanide product **6e**. Mass spectrometry of purified **6e** confirmed its constitution, with a parent ion at 587.3 m/z. IR carbonyl stretches were seen at 1560 cm^{-1} for the amide and NO stretching frequencies were observed at 1448 cm^{-1}, 1360 cm^{-1}

and differed substantially from the characteristic NO_2 frequencies of **5e′** which were observed at 1379 cm^{-1} and 1323 cm^{-1}.

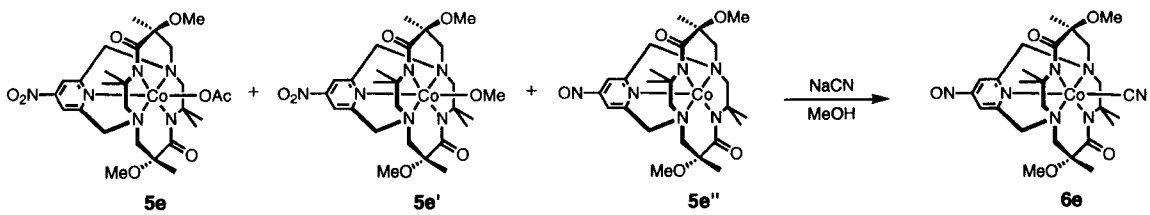

Scheme 27. Cyanation of the crude mixture of **5e**, **5e′**, and **5e″**.

Conversion of the 4-bromopyridine-capped cobalt methoxide **5d″** to the corresponding cyanide complex with sodium cyanide and methanol unexpectedly produced the 4-methoxypyridine cobalt cyanide complex **6d′**. This product was a result from nucleophilic substitution of the complexed 4-bromopyridine. Fortunately, cyanation in acetonitrile with 18-crown-6 afforded the desired complex **6d** in good yield.

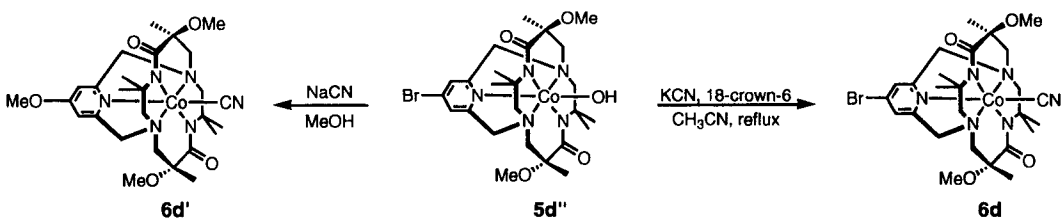

Scheme 28. Cyanide products from 4-bromopyridine cobalt hydroxide.

Acetylene was also examined as an axial ligand. However, its coordination did not prove to be as facile as cyanide. The pyridine substrate was examined first by treatment of pyridine-capped cobalt acetate with TMS-acetylide, prepared from the reaction of *n*-butyllithium and TMS-acetylene.[63] Surprisingly, the product isolated after chromatographic purification was found to be the pyridine-capped cobalt hydroxide by mass spectrometry (Scheme 29). Instead of ligand exchange, the TMS-acetylide preferentially reacted with the carbonyl carbon of the acetate group.

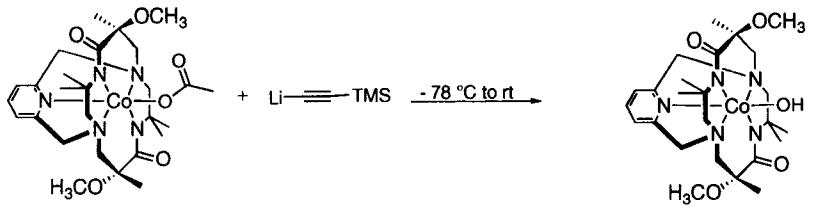

Scheme 29. Acetylene ligand exchange.

Ligand exchange with TMS-acetylide under milder conditions was inspected. However, both triethylamine (TEA) and copper iodide[64] coupling conditions resulted in recovery of the starting material **5a** (Table 8). Alternative ligand exchange was examined. Perhaps exchanging the acetate group for a more labile ligand, i.e. iodide or bromide, would provide access to the acetylene product. Acetate ligand exchange for iodide did not provide any isolable product so further ligand exchange was not examined.

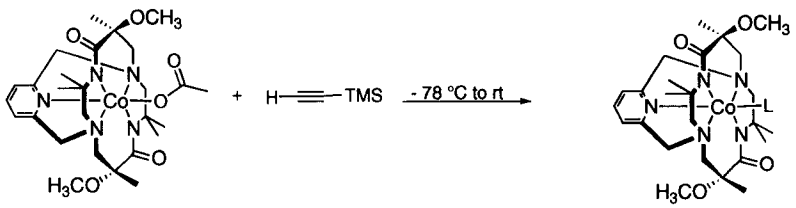

	Reagents	Conditions	Product
1	TEA	rt 24 h	Starting Material
2	TEA, CuI	rt 24 h then D 4 h	Starting Material

Table 8. Acetylene ligand exchange.

2. Synthesis of Polymetallic Complexes Containing Cobalt Dioxocyclams.

The cyanide complexes of pyridine, pyrazine, and 4-bromopyridine dioxocyclams were prepared in good yields. One of the goals of this research project was the synthesis of polymetallic complexes through the coordination of bridging ligands. Metal acetates and metal phthalocyanines were examined for their ability to bridge two cobalt dioxocyclam complexes.

Reaction of pyridine-capped cobalt cyanide complex **6a** with rhodium(II) acetate afforded a tetrametallic, mixed valent complex **7** as a greenish-brown solid in excellent yield (Scheme 30). The infrared spectrum of the greenish-brown solid showed the 1566 cm^{-1} amide band as well as the 1595 cm^{-1} band for the rhodium bridging acetates. The bridging cyanides absorbed at 2228 cm^{-1}, 2200 cm^{-1}, and 2142 cm^{-1} where the terminal cyanide of **6a** absorbs at 2123 cm^{-1}. This increase in ν is likely due to the "kinematic" effect which is the constraint of the C–N vibration due to metal attachment at both C and N which is not compensated for by π*-backdonation from the metal. Mass spectrometry showed a parent ion at 1559.4 m/z for **7**. IR carbonyl stretches were observed at 1593 cm^{-1} for rhodium acetate and 1566 cm^{-1} for the amide carbonyls. Dark red X-ray quality crystals, that supported its constitution, were obtained (Figure 26).

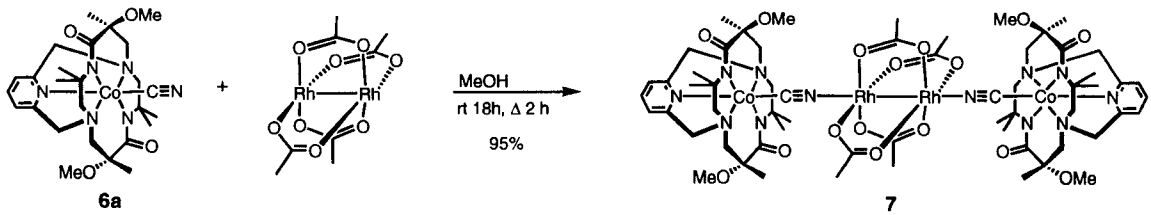

Scheme 30. Tetrametallic cobalt dioxocyclam complex.

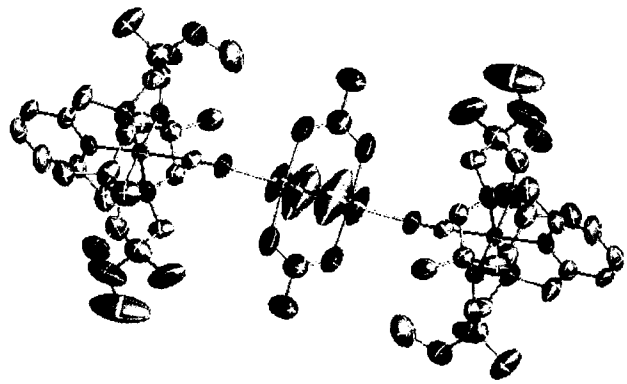

Figure 26. ORTEP drawing of rhodium acetate bridged pyridine cobalt cyanide complex.

Ruthenium acetates were also examined. The ruthenium acetate complex could be synthesized in both isovalent ($Ru^{2+}Ru^{2+}$)[65] or mixed valent ($Ru^{2+}Ru^{3+}$)[66] forms. Reaction of ruthenium(II) acetate and pyridine-capped cobalt cyanide **6a** resulted in no coordination (Scheme 31). Mixed valent ruthenium acetate was prepared from $RuCl_3 \cdot 3H_2O$ and acetylacetonate in acetic acid.[66] Treatment of pyridine-capped cobalt cyanide **6a** with ruthenium(II/III) acetate again resulted in no coordination.

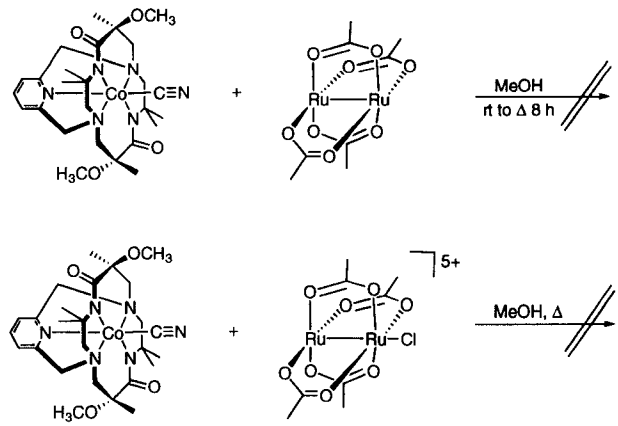

Scheme 31. Coordination with ruthenium acetate

Recently in the Hegedus labs, Mike Sundermann synthesized trimetallic complexes by using $RuCl_2(DMSO)_4$ to bridge two pyrazine-capped copper dioxocyclam complexes.[17] Similar reaction of $RuCl_2(DMSO)_4$ with pyridine-capped cobalt cyanide **6a** afforded an inseparable mixture of products. $RuCl_2(DMSO)_4$[67] is synthesized as a mixture of *cis*- and *trans*-isomers regarding the orientation of the two chlorine atoms which could be the source of the product mixture in this case.

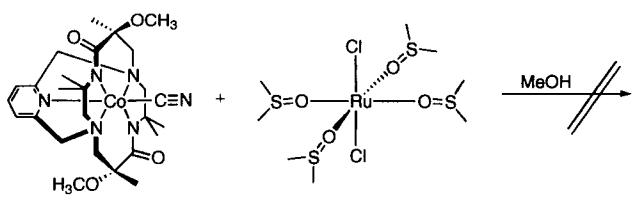

Scheme 32. Coordination with $RuCl_2(DMSO)_4$.

Treatment of pyridine-capped cobalt cyanide complex **6a** with ruthenium(II) phthalocyanine gave the trimetallic, mixed valent complex **8** as a red solid (Scheme 33). Mass spectrum confirmed the constitution, having a parent peak at 1729 m/z. In contrast to **7**, the cyanide absorption in IR appeared as a single weak stretch at 2125 cm^{-1}. This stretching frequency was virtually unchanged from the uncoordinated pyridine cobalt cyanide complex **6a**. Unlike the rhodium complex **7**, the lack of CN shift must be due to the cyanide nitrogen π^*-backdonation from the metal to the cyanide group. Ruthenium phthalocyanine complex **8** was crystalline and provided good single crystals for characterization by X-ray crystallography (Figure 27).

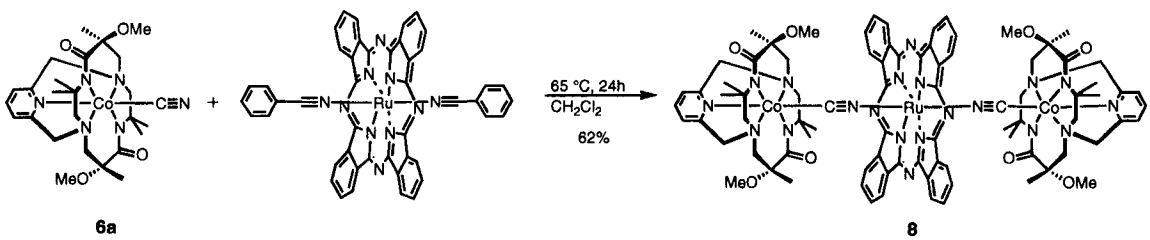

Scheme 33. Trimetallic cobalt dioxocyclam complex.

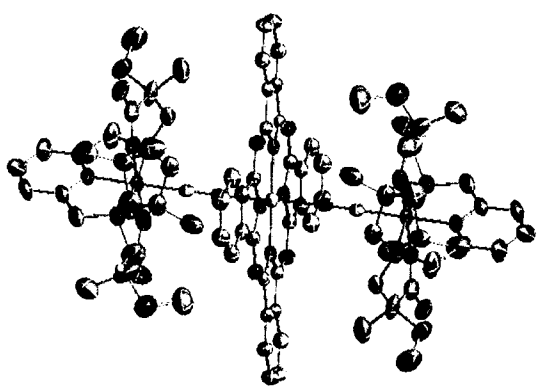

Figure 27. ORTEP drawing of ruthenium phthalocyanine bridged pyridine cobalt cyanide complex.

Treatment of pyrazine-capped cobalt cyanide complex **6b** with ruthenium(II) phthalocyanine gave a mixture of products (Scheme 34). Unlike the pyridine-capped cobalt cyanide complex, pyrazine contains an additional coordination site through the nitrogen at the 4-position. Indeed, a separable mixture of products was obtained corresponding to the bis-cyanide bridged **9a**, the bis-pyrazine bridged **9b**, and the cyanide-pyrazine bridged ruthenium phthalocyanine **9c**. The ^{1}H NMR spectrum of uncomplexed pyrazine-capped cobalt cyanide **6b** showed the two pyrazine proton peaks as singlets at δ 8.62 ppm and 8.60 ppm. Complex **9a** also showed the pyrazine hydrogens as singlets at δ 8.07 ppm and 8.04 ppm while **9b** differed having the hydrogens as a singlet at δ 8.77 ppm. As expected **9c** had pyrazine peaks at δ 8.75 ppm, 8.07 ppm, and 7.99 ppm for the pyrazine- and cyanide-linked complex respectively. Currently, equilibrating conditions are being examined to obtain one regioisomer preferentially over the others.

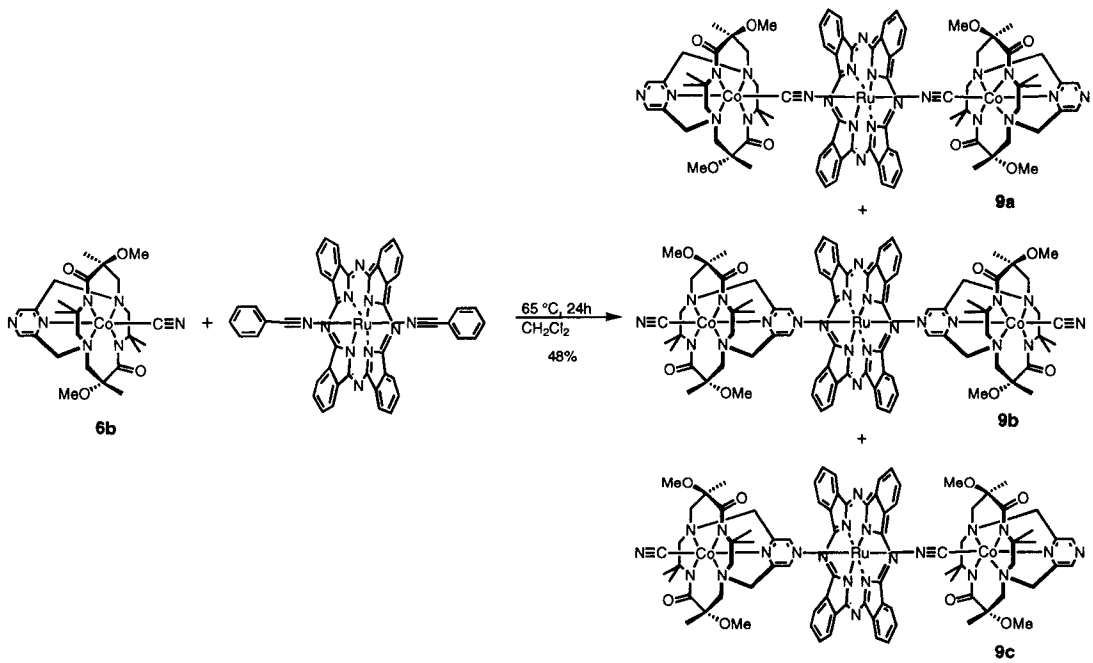

Scheme 34. Ruthenium phthalocyanine coordination to pyrazine-capped cobalt cyanide.

Pyridine cobalt cyanide coordination to iron phthalocyanine was also examined. After heating **6a** and iron phthalocyanine at 65 °C for 24 hours, TLC showed formation of a new green product (Scheme 35). Chromatographic purification resulted in recovery of starting material and isolation of a new green product in 46% yield. However, upon isolation of the green material it began to revert to starting material. Because the green complex could not be separated from **6a**, it could not be fully characterized.

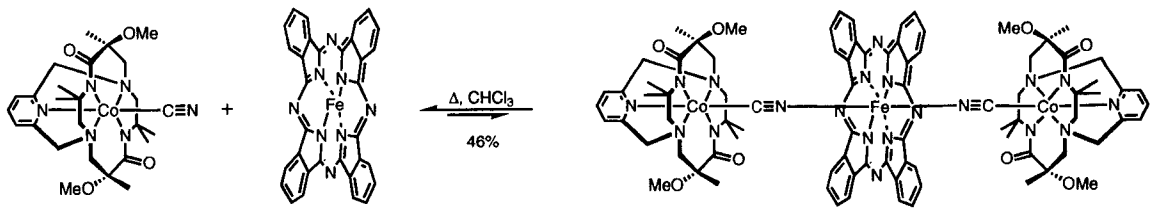

6a

Scheme 35. Iron Phthalocyanine bridged pyridine-capped cobalt cyanide complex.

3. Cobalt Coordination in Uncapped Dioxocyclams

Coordination of cobalt into uncapped dioxocyclams would provide an addition bridging metal similar to the metal acetate and metal phthalocyanins. Dr. Eva Garcia-Frutos found that treatment of 5,12-dioxocyclam **1** with cobalt(II) acetate either under microwave radiation or heat gave a surprising result (Scheme 36).[68] Under these reaction conditions, hydrolysis of one of the amide bonds formed a ring-opened dioxocyclam cobalt acetate complex **43**. The structure of **43** was determined by single crystal X-ray diffraction (Figure 28).

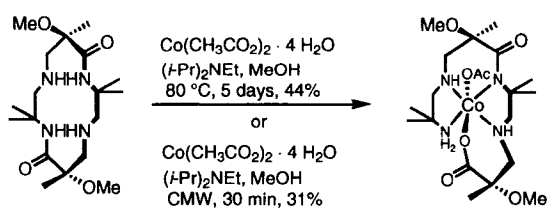

1 **43**

Scheme 36. Cobalt acetate coordination of uncapped dioxocyclam.

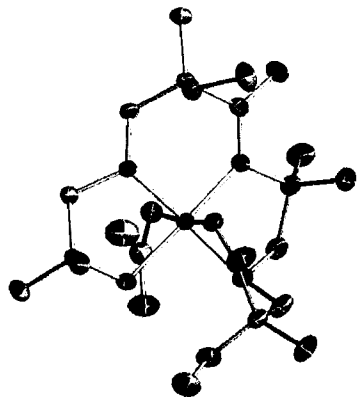

Figure 28. ORTEP diagram of ring-opened cobalt acetate dioxocyclam.

The coordination of dioxocyclam **1** with Co(II) acetylacetonate has been successful without hydrolysis of the amide bond.[10b] Treatment of 5,12-dioxocyclam **1** with $Co(acac)_3$ in ethanol at 100 °C for 24 h produced neutral cobalt(III) complex **44** in which both amide protons and one amine proton has been lost (Scheme 37). Although unstudied in the Hegedus laboratories as a bridging agent, **44** could be useful for the synthesis of polymetallic complexes. The structural assignment for **44** is based on spectroscopic data. Mass spectrometry of purified **44** confirmed its constitution, with a parent ion at 427.17 m/z rather than at 428 for the protonated amine complex. IR spectroscopy showed that both amide nitrogens were coordinated with a single band at 1552 cm^{-1}. Additionally, the ^1H NMR spectrum was more complex than previously synthesized nickel(II) and copper(II) complexes of uncapped 5,12-dioxocyclams, a sign of asymmetry in complex **44**. The ^1H NMR spectrum revealed a pair of two proton apparent triplets at δ 5.11 (J = 13.8 Hz) and δ 5.46 (J = 11.7 Hz). These are assigned to the two methylene groups flanking the deprotonated amine, their downfield shift being attributed to the deshielding effect of the deprotonated amine.

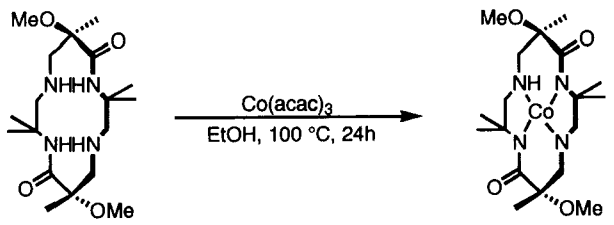

1 44

Scheme 37. Cobalt coordination with uncapped dioxocyclam.

4. Properties of Polymetallic Complexes Containing Cobalt Dioxocyclams.

a. Spectroscopic and Electrochemical Properties

The spectroscopic and electrochemical properties of complexes **1**, **5a-b**, **6a-e**, **7** and **8** are displayed in Table 9. Similar to Ni(II) and Cu(II) dioxocyclams synthesized in these laboratories, complexation of the capped dioxocyclams to Co(III) resulted in a shift of the IR band for the amide carbonyl group from ≈1660 cm^{-1} in the free ligand to 1560-1570 cm^{-1} in the complex. Little variation was observed between complexes with electron-donating and electron-withdrawing capping groups. The acetate and cyanide group absorptions also appear insensitive to the nature of the capping group appearing ≈1615 cm^{-1} and 2120-2130 cm^{-1} respectively.

	IR, νcm^{-1}	UV λmax, nm	δ ^{13}C	CV CH_2Cl_2 vs SCE
1 dioxocyclam	1659, amide		173.7 amide 173.3 amide	
5a py-Co-OAc	1613, acetate 1564, amide	MeOH ε[526] = 156	173.8 amide 173.0 amide 178.5 acetate	Ep. –1.24V (-1.28)
5b pz-Co-OAc	1616, acetate 1559, amide	CH_2Cl_2 ε[530] = 160	174.2 amide 172.5 amide 178.7 acetate	Ep. –0.95V
5d″ 4-Br-Co-OH	1561, amide	CH_2Cl_2 ε[556] = 160	174.1 amide 172.7 amide	
5e′ 4-NO_2-Co-OMe	1570, amide 1379, NO_2 1323, NO_2		173.4 amide 172.8 amide	

6a py-Co-CN	2123, CN 1566, amide	MeOH ε[463] = 313	173.0 amide 172.5 amide 129.6 CN	Ep. –1.36V
6b pz-Co-CN	2128, CN 1558, amide	CH_2Cl_2 ε[454] = 475	172.9 amide 172.5 amide 139.8 CN	Ep. –1.17V
6d 4-Br-Co-CN	1560, amide	MeOH ε[462] = 238	173.1 amide 172.6 amide 136.7 CN	
6d' 4-OMe-Co-CN	2123, CN 1560, amide	MeOH ε[462] = 317	173.3 amide 172.4 amide	
6e 4-NO-Co-CN	1560, amide 1448, NO 1360, NO		174.2 amide 172.3 amide 132.2 CN	
7 py-Co-CN-Rh-Rh-NC-Co-	2228, CN 2200, CN 2142, CN 1595, acetate 1566, amide	MeOH ε[455] = 744 ε[574] = 246	191.1 acetate 173.1 amide 172.8 amide don't see CN	Ep. –1.39V (2e-) Ep. +1.07V
8 py-Co-CN-RuPc-NC-Co-py	2125, CN 1562, amide	CH_2Cl_2 ε[320] = 4220 [372 (sh)] ε[412] = 2500 [571 (sh)] ε[628] = 26900	171.5 amide 171.1 amide don't see CN	

Table 9. Spectroscopic and electrochemical data.

Uniformity was also seen in the ^{13}C chemical shifts between the free ligand and all of the cobalt(III) complexes. The amide carbonyl ^{13}C peaks for all complexes appeared between δ 172-174 ppm, identical to previously reported nickel(II) complexes. No change in the chemical shift was observed upon complexation to a metal, regardless of the metal, its oxidation state (Ni(II), Co(III)) or its ancillary ligands (OAc, CN, OMe, OH, electron-rich, electron-poor capping groups). The signals for the cobalt-bound acetate groups appear at ≈ δ 178 ppm, for both the electron-donating pyridine and electron-accepting pyrazine-capped complexes **5a** and **5b**. The ^{13}C chemical shift of the cyanide group showed slightly more sensitivity to the nature of the capping agent,

ranging from δ 129.2 ppm for the electron-rich pyridine group **6a** to δ 139.7 ppm for the electron-poor pyrazine group **6b**.

The visible spectra are also relatively consistent throughout the series. Complexes with acetate or hydroxides as the sixth ligand absorb weakly (ε = 160) between 526-556 nm, while the cyanide complexes absorb at ≈460 nm, with slightly greater intensity (ε = 200-475). The spectrum of tetrametallic complex **7** showed an absorption of λmax 455 nm (ε = 744) and 574 nm (ε = 246). This was comparable to the component parts of **7** with absorptions at 463 nm (ε = 313) for the cyclam portion and 446 nm and 588 nm for $Rh_2(OAc)_4$.

Cyclic voltammetry experiments of the monometallic cobalt complexes all exhibited irreversible reduction and reoxidation of the complexes, demonstrating an insensitivity to the 4-substituent on the capping pyridine. The pyridine-capped acetate complex **5a** was slightly easier to reduce (-1.24 V) while both the pyrazine-capped cyanide complex **6b** and the corresponding pyrazine-capped acetate complex **5b** underwent irreversible reduction at –1.17 V and –0.95 V respectively, perhaps a reflection of the strong π-accepting nature of the pyrazine group contrasting to the σ-donor nature of the pyridine.

The cyclic voltammograms of the polymetallic complexes **7** and **8** resembled those of their component parts. Tetrametallic complex **7** underwent irreversible cobalt(III) to cobalt(II) reduction at Ep –1.39 V/SCE (compared to Ep –1.36V/SCE for **6a**) and an irreversible oxidation due to the rhodium acetate group at Ep +1.07 V/SCE. This data indicates that there is little interaction between the cobalt moieties and the dirhodium tetraacetate. Trimetallic complex **8** underwent an apparent two electron

irreversible cobalt(III) to cobalt(II) reduction at Ep –1.40 V/SCE, a reversible phthalocyanine based reduction at $E_{1/2}$ –1.67 V/SCE, a reversible oxidation at $E_{1/2}$ 0.41 V/SCE, and an irreversible oxidation at Ep +1.25 V/SCE. In contrast, the bis-(benzonitrile)ruthenium(II) phthalocyanine precursor under went an irreversible reduction at Ep –1.48 V/SCE, a reversible oxidation at $E_{1/2}$ +0.51 V/SCE and an irreversible oxidation at Ep +1.4 V/SCE. Cyclic voltammetric measurements indicate no detectable metal interaction of trimetallic complex **8**.

Cobalt(III) complexes are kinetically inert while the cobalt(II) complexes are very labile because of the presence of electrons in the $\sigma^*_M(e_g)$ antibonding orbitals.[69] As a consequence, reduction of CoL_n(III) results in irreversible reductions caused by the dissociation of ligands or decomposition of the complex. Kinetically inert metals that remain stable throughout the reduction/oxidation cycle may allow us to see if metal-metal interaction exists in these systems.

b. Structural Properties

X-ray crystal structures of **5a**, **5b**, **6a**, **6b**, **7**, **8** and **43** were obtained. Selected bond lengths and bond angles are listed in Table 10 and the ORTEP diagrams are displayed in Figure 29. A table of crystallographic data are assembled in Table 1 and located in Supplemental Data. Obtaining good data for X-ray crystal structures **5a-8** was not a facile process. Although the complexes crystallized readily, the crystals themselves were often poor, suffering from powdering and low reflection. For all of these complexes, a variety of recrystallization conditions were examined in order to obtain crystals that exhibited optimal reflection. Once a suitable data set was obtained, much time was spent trying to optimize that data due to poor data to parameter ratios.

Disordered solvent molecules and poor data to parameter ratios contributed to the high R values observed for almost all data sets. The data often showed signs of twinning, and unfortunately, all twin laws applied were unsuccessful at detwinning the data. Twinning occurs when two or more crystals of the same material are intergrown so that the unit cell of the first is related to the unit cell of the second by a symmetry element. Twin laws can be used to transform the *hkl* indices of one cell into the other. Even with these hurdles, we were fortunate to obtain data sets for a range of the complexes synthesized in the cobalt series.

The most surprising structural feature of complexes **5a-6b** is their similarity in bond lengths and bond angles. Regardless of the σ-donating/π-accepting nature of the capping reagent, bond lengths remain relatively unchanged. For example, the Co-acetate bond lengths for pyridine and pyrazine-capped cobalt acetate complexes are 1.935 Å and 1.928 Å respectively. The acetate is slightly displaced from linearity with the capping nitrogen-cobalt bond for both complexes. The Co-cyanide bond lengths for pyridine- and pyrazine-capped cobalt cyanide complexes are similar with bond lengths at 1.891 Å and 1.889 Å respectively. The geometry of the cobalt atom approximates octahedral, with a slight out-of-plane displacement of the amine nitrogens.

Complexes **7** and **8** present two rather different structural types for cyanide-bridged polymetallics because the bridging metals are bound quite differently as can be seen in Figure 29. In complex **7**, the cyanide N–to–Rh bond is relatively long, 2.190 Å, supporting the infrared data that suggests little π*-back donation.[41a,42a] The C≡N–Rh bond angle is 157.8° which is strongly distorted from linear while the Co–C≡N bond angle almost linear at 175.4°. The Rh–Rh bond length is 2.388 Å, virtually identical to

that in the bis-acetonitrile adduct of $Rh_2(OAc)_4$. These structural features of **7** are very similar to those found in the related rhodium acetate $Cp^*Ir(CN)_2$ complex mentioned in Figure 10.[39] The Ir/Rh complex displayed CN–Rh bond length 2.232 Å and C≡N–Rh bond angle 151.9°, also distorted form a linear arrangement. Its Rh–Rh bond length is 2.402 Å and Ir–C≡N bond angle 175.8°, also close to linear.[39]

In contrast, complex **8** has a considerably shortened cyanide N–to–Ru bond length at 2.017 Å, supporting infrared data that suggests at least modest π*-back donation.[41a,42b] Also, **8** has an almost linear arrangement along the entire bridging axis of the molecule. These structural features are very similar to those founds in $[(NC)_5Fe–C≡N–Ru(Py)_4–N≡C–Fe(CN)_5]^{4-}$, having a short C≡N–Ru bond length of 2.02 Å and an almost linear arrangement along the bridging axis of the molecule.[41a]

Bond Lengths, Å	**5a**	**5b**	**6a**	**6b**	**7**	**8**
$Co-N_5$	1.868(3)	1.845(6)	1.888(3)	1.869(6)	1.896(7)	1.893(6)
$Co-O_5$ / $(Co-C_{26})^a$	1.935(2)	1.930(6)	1.892(4)	1.879(8)	1.887(9)	1.895(7)
$Co-N_3$	1.963(2)	1.951(6)	1.958(3)	1.964(6)	1.980(8)	1.930(7)
$Co-N_1$	1.974(2)	1.980(7)	1.971(3)	1.971(6)	1.960(8)	1.986(8)
$Co-N_2$	1.973(3)	1.965(6)	1.967(3)	1.959(6)	1.958(8)	1.957(7)
$Co-N_4$	1.978(2)	1.981(6)	1.963(3)	1.975(6)	1.962(7)	1.961(7)
O_2-C_4	1.257(4)	1.232(9)	1.264(4)	1.263(9)	1.287(12)	1.221(11)
O_4-C_{13}	1.248(4)	1.224(8)	1.257(4)	1.222(9)	1.246(12)	1.271(12)
O_6-C_{26} [a] / (N_6-C_{26}) [a]	1.233(4)	1.215(9)	1.150(5)	1.147(10)	1.140(10)	1.178(8)
N_1-C_4	1.318(4)	1.331(9)	1.328(5)	1.326(10)	1.234(13)	1.246(12)
N_3-C_{13}	1.331(4)	1.339(9)	1.329(5)	1.354(10)	1.265(13)	1.261(12)
$-CN_6-M$					2.192(8)	2.017(5)

M-M					2.3879(15)	
Bond Angles,°						
N_5-Co-N_3	93.10(1)	92.9(2)	90.09(12)	92.9(3)	90.1(3)	92.1(3)
N_5-Co-N_1	91.95(11)	92.3(3)	90.09(12)	91.5(2)	92.0(3)	90.1(3)
N_5-Co-N_4	84.19(I1)	83.8(3)	84.56(13)	83.9(3)	84.9(3)	85.1(3)
N_5-Co-N_2	84.65(I1)	84.4(3)	84.29(12)	83.7(3)	84.8(3)	83.6(3)
O_5-Co-N_3	90.09 (10)	89.8(2)				
C_{26}-Co-N_3 [a]			88.47(14)	88.2(3)	89.5(3)	86.4(3)
O_5-Co-N_1	84.98(10)	85.1(2)				
C_{26} Co-N_1 [a]			91.35(14)	87.4(3)	88.3(4)	91.4(3)
O_5-Co-N_2	102.49(1)	102.5(2)				
C_{26}-Co-N_2 [a]			95.41(13)	95.2(3)	97.0(3)	97.1(3)
O_5-Co-N_4	88.66(10)	89.3(2)				
C_{26}-Co-N_4 [a]			95.73(14)	97.2(3)	93.4(3)	94.3(3)
O_5 Co-N_5	171.80(10)	172.3(3)				
C_{26} Co-N_5 [a]			178.51(15)	178.3(3)	178.2(3)	178.4(3)
N_3-Co-N_2	96.63(10)	96.7(3)	92.86(12)	95.9(2)	93.7(4)	95.2(3)
N_3-Co-N_4	83.82(10)	83.6(3)	87.05(13)	84.8(2)	86.7(3)	86.3(4)
N_3-Co-N_1	174.92(11)	174.8(3)	179.61(14)	175.6(3)	177.6(3)	177.7(3)
N_4-Co-N_1	97.27(10)	97.2(2)	92.62(12)	95.4(2)	92.5(4)	93.6(4)
N_2-Co-N_1	83.27(10)	83.6(3)	87.50(12)	84.8(3)	87.5(4)	85.4(3)
N_2-Co-N_4	168.83(11)	168.2(3)	168.85(12)	167.6(2)	169.7(3)	168.6(3)
C_{26}-N_6-M [a]					157.6(7)	176.3(6)
N_6-Ru-N_6'						180.00(3)
N_6-C_{26}-Co [a]			178.0(4)	177.1(8)	175.3(8)	176.4(6)

[a] $C_{25}N_7$ in compounds **5b** and **6b**

Table 10. Selected bond lengths and bond angles.

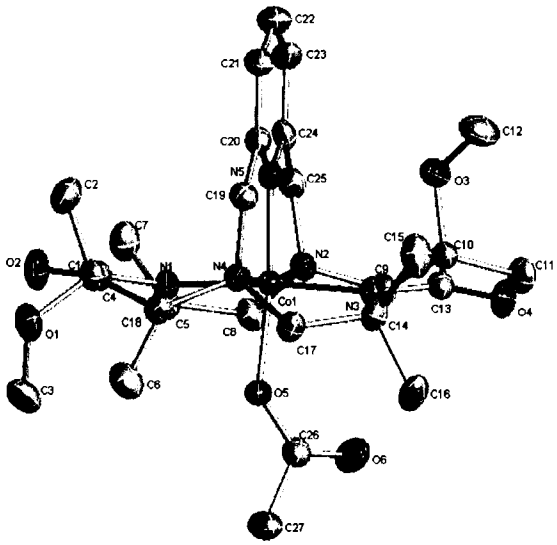

5a

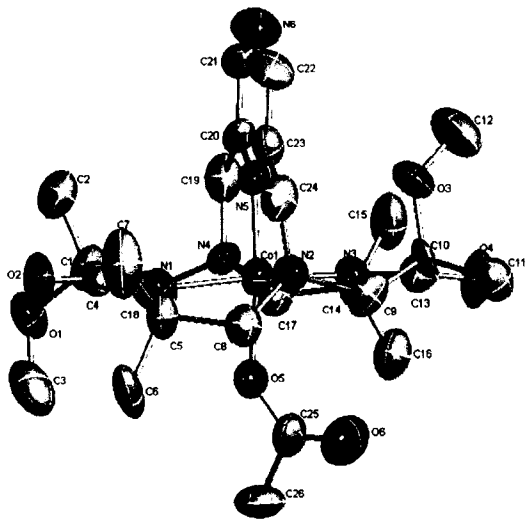

5b

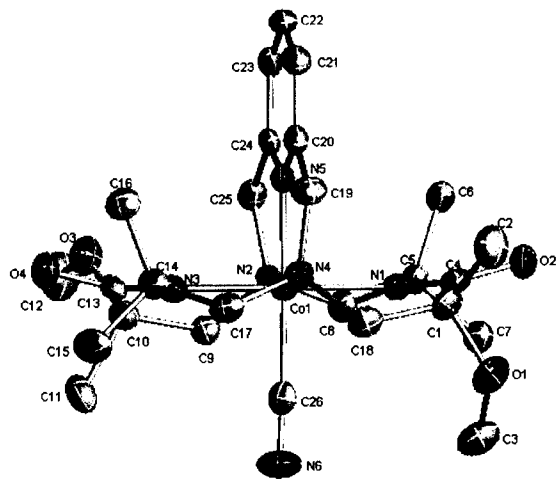

6a

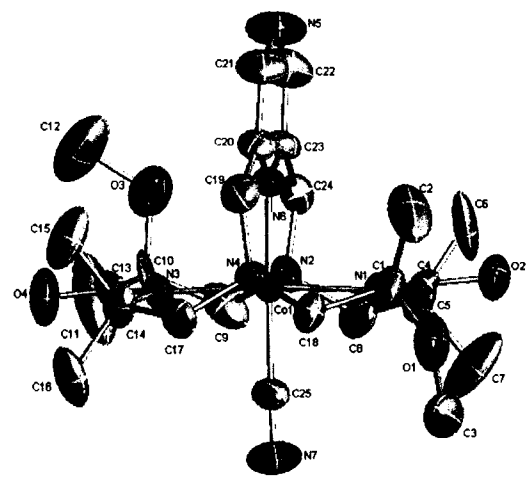

6b

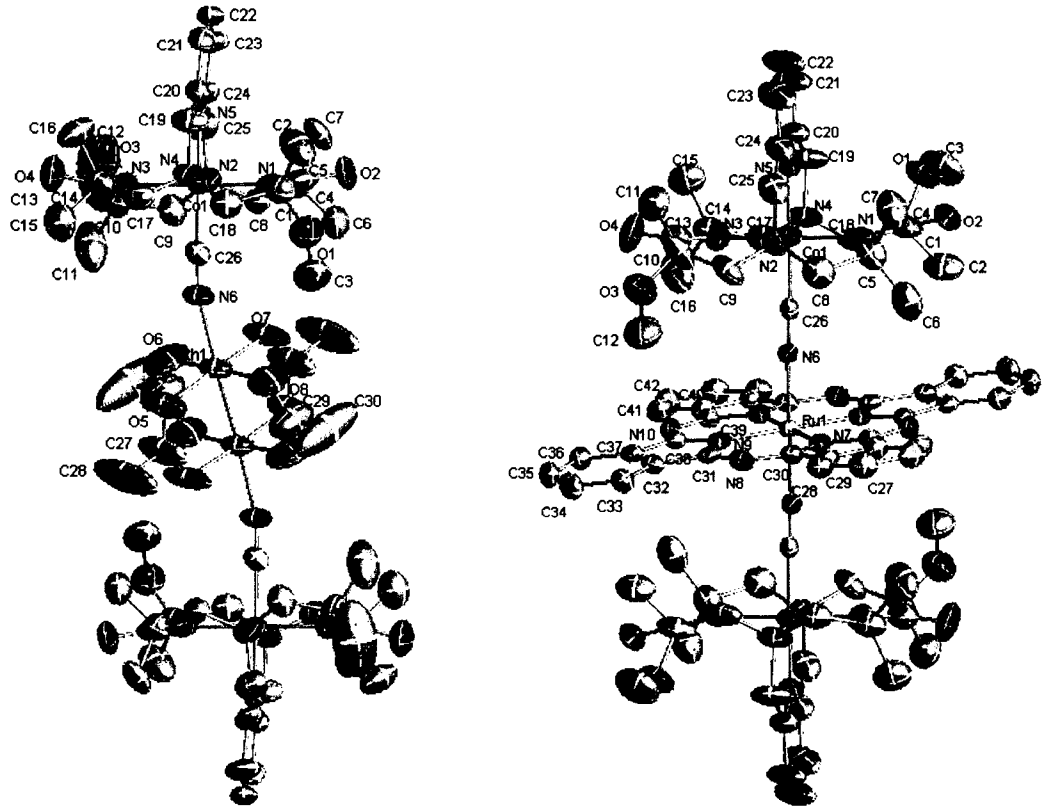

7 8

Figure 29. ORTEP diagrams of cobalt complexes.

B. Ruthenium Coordination

Ruthenium is well known for the stability of its metal complexes, the ease of obtaining oxidation states II and III, and for the kinetic inertness of these oxidation states.[26] These characteristics make ruthenium an ideal metal for incorporation into polymetallic complexes. Keeping in mind the difficulty encountered during cobalt coordination with capped dioxocyclams, almost no stone was left unturned when examining ruthenium coordination. Treatment of pyridine-capped dioxocyclam **3a** with ruthenium(II) and ruthenium(III) complexes and various bases resulted in recovery of starting material in all but one reaction (Table 11). Microwave radiation of **3a** and $Ru_3(CO)_{12}$ afforded an unusual coordination product (Table 11, Entry 2).

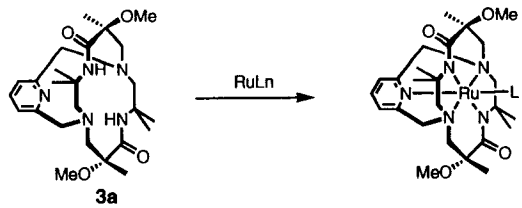

3a

	Metal	Conditions	Base	Solvent	Yield
1	$RuCl_3 \cdot 3\ H_2O$	Reflux	-----	2-ethoxyethanol	Starting Material
			K_2CO_3	wet MeOH	Starting Material, Ru decomposition
			$(i\text{-}Pr)_2NEt$	MeOH	Starting Material, Ru decomposition
			DBU	CH_3CN	Starting Material
			TEA	MeOH	Starting Material
		cmw	$(i\text{-}Pr)_2NEt$	MeOH	Starting Material, Ru decomposition
			DBU	MeOH	Starting Material
2	$Ru_3(CO)_{12}$	Reflux	-----	benzonitrile	Starting Material
		cmw	-----	MeOH	Red Material, not Starting Material
3	$Ru(CHCN)_4Cl_2$	Reflux	$(i\text{-}Pr)_2NEt$	MeOH	Starting Material
			$(i\text{-}Pr)_2NEt$	MeOH	Starting Material, Ru decomposition
			TEA	CH_3CN	Starting Material
4	$RuCl_3NO \cdot 5\ H_2O$	cmw	-----	MeOH	Starting Material
			$(i\text{-}Pr)_2NEt$	MeOH	Starting Material, Ru decomposition
5	$Ru(acac)_3$	cmw	-----	MeOH	Starting Material
			$(i\text{-}Pr)_2NEt$	MeOH	Starting Material

Table 11. Ruthenium coordination attempts.

Treatment of pyridine-capped dioxocyclam with $Ru_3(CO)_{12}$ under microwave conditions afforded a pyridine-capped triruthenium pentacarbonyl complex **45** (Scheme 38).[70] Mass spectrometry of purified **45** confirmed its constitution with a parent ion at 918.33 m/z (calcd 918.99) and the calculated isotopic distribution for a complex containing three ruthenium atoms. IR carbonyl stretches were observed at 2000 cm^{-1} for the ruthenium-bound carbonyls and at 1683 cm^{-1}, 1660 cm^{-1}, and 1618 cm^{-1} in the amide region. Ruthenium complexes of phthalocyanines have shown that ruthenium readily coordinates to cyano-aromatics including benzonitrile, which may be used in displacing the "extra" ruthenium atoms.[71]

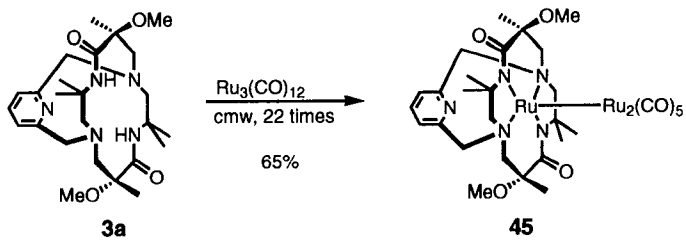

Scheme 38. Ruthenium coordination product.

Treatment of **45** with benzonitrile under microwave radiation afforded pyridine-capped ruthenium benzonitrile complex **46** (Scheme 39). Mass spectral analysis of crude **46** supported its constitution with a parent ion at 678.80 m/z (calc 678.24). IR carbonyl stretches were observed at 2030 cm^{-1} and 1955 cm^{-1} for residual ruthenium carbonyl and at 1658 cm^{-1} and 1578 cm^{-1} in the amide region. Purification of the complex with either silica or neutral alumina chromatography unfortunately resulted in the recovery of uncoordinated pyridine-capped dioxocyclam.

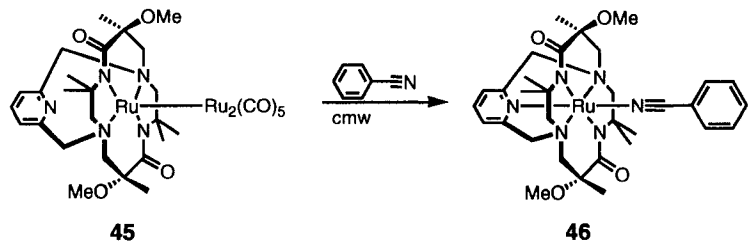

Scheme 39. Ligand exchange for pyridine-capped ruthenium benzonitrile.

Reexamination of the IR data for complexes **45** and **46** revealed a carbonyl stretch at 1660 cm^{-1}, the frequency for amide carbonyls not coordinated to a metal. The amide carbonyls must not be completely deprotonated as portrayed in Scheme 38 and 39, leaving the ruthenium coordinated only to the amine nitrogens or loosely to the face of the dioxocyclam. To verify this, oxidation conditions for the removal of the "extra" ruthenium atoms of **45** were investigated.

Removal of the carbon monoxide ligands attached to ruthenium would allow the extra ruthenium atoms to disassociate to be replaced by a bridging ligand. Tertiary amine *N*-oxides are mild reagents that irreversibly oxidize metal-bound carbon monoxide to carbon dioxide. The carbon dioxide then readily dissociates from the metal leaving it bare to dissociate from the pyridine-capped ruthenium complex. Oxidation of pyridine-capped triruthenium pentacarbonyl **45** with pyridine *N*-oxide resulted in recovery of pyridine-capped dioxocyclam with no coordinated ruthenium (Scheme 40).

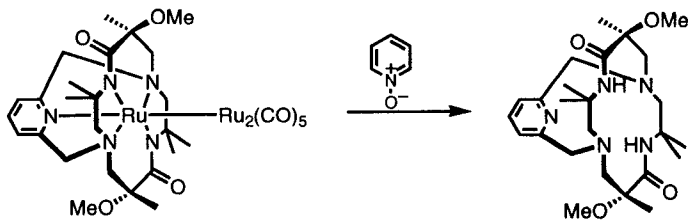

Scheme 40. Pyridine *N*-oxide oxidation conditions.

Air oxidation was also examined by bubbling air through the reaction solution either prior to microwave radiation or after the formation of the triruthenium pentacarbonyl complex **45** (Scheme 41). Again however, uncoordinated pyridine capped dioxocyclam was recovered. As anticipated, ruthenium complex **45** must be coordinated loosely to the face of the dioxocyclam resulting in recovery of starting materials under all conditions.

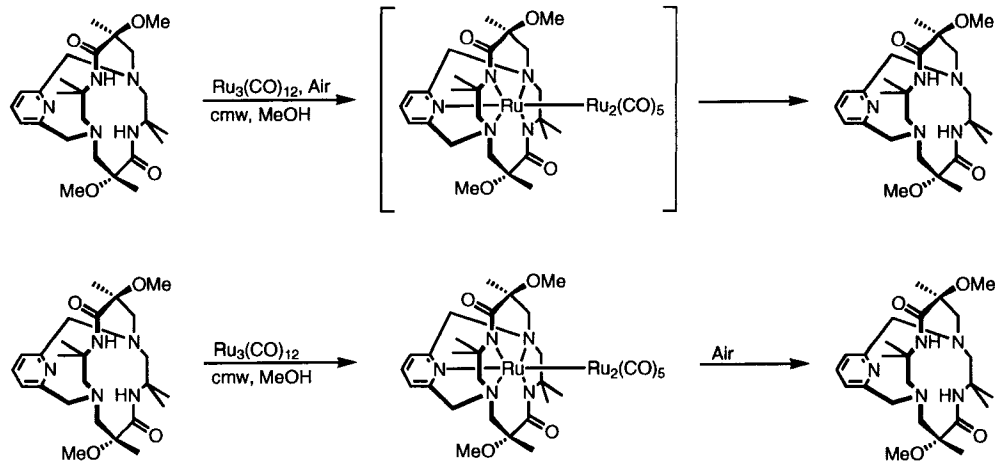

Scheme 41. Air oxidation conditions.

Alternative approaches for ruthenium coordination were needed. Deprotonation of the dioxocyclam amine nitrogens prior to coordination would form a highly reactive dioxocyclam, which may coordinate more easily with ruthenium. Treatment of pyridine-capped dioxocyclam with *n*-butyllithium afforded the dianion as a bright orange solution (Table 12). Addition of different ruthenium sources however led to no coordinated product.

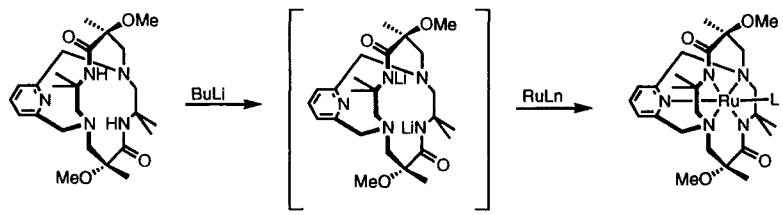

	Metal	Conditions	Yield
1	$Ru(CH_3CN)_4Cl_2$	THF, -78 °C to rt	Starting Material
2	$Ru(acac)_3$	THF, -78 °C to rt	Starting Material
3	$RuCl_3$	THF, -78 °C to rt	Starting Material

Table 12. Anionic ruthenium coordination.

Another approach is being examined that involves coordination of the metal to the dioxocyclam first, followed by capping to yield the metal coordinated capped dioxocyclam. When complexed to a metal, the coordinated amines become relatively acidic compared to the corresponding free amine with pKa's on the order of 14-18.[72] Alkylation of nickel-coordinated dioxocyclams have been reported in the literature. Alkylation reactions of nickel(II) cyclams with methyl iodide, *o*-bis(bromomethyl)-xylene, and benzyl bromide occur in good yields.[72] Currently, experiments are being preformed on both nickel and copper dioxocyclam complexes.

Treatment of nickel(II) dioxocyclam **47** with base to deprotonate the amine nitrogens of the dioxocyclams followed by slow addition of the capping reagent did not yield capped nickel dioxocyclam (Table 13). However, nickel dioxocyclam was recovered after workup. Since nickel preferentially coordinates to square planar ligands, perhaps alkylation with a compound providing a fifth coordination site towards the metal prevents alkylation in this case. It is possible that copper would eliminate this issue since we have already shown that copper easily forms square pyramidal complexes with the capped dioxocyclam.

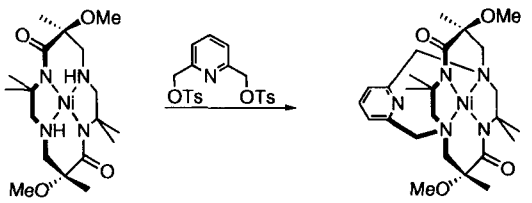

47

	Conditions	Base	Solvent	Product
1	48 h, r.t.	KOH	CH_3CN	Starting Material
2	24 h, r.t.	NaH	THF/CH_2Cl_2	Starting Material

Table 13. Nickel dioxocyclam capping reactions.

Treatment of copper dioxocyclam **48** with base to deprotonate the amine nitrogens of the dioxocyclam followed by slow addition of the capping reagent did not yield capped copper dioxocyclam (Table 14). Unfortunately, either decomposition or recovery of starting material was experienced in each reaction.

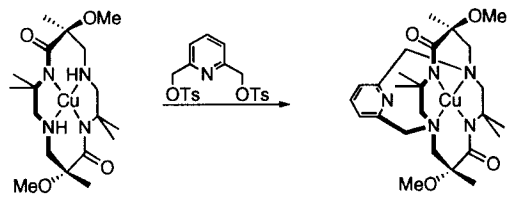

48

	Conditions	Base	Solvent	Product
1	24 h, r.t.	KOH	DMSO	Decomposition
2	r.t. to reflux	$(i\text{-Pr})_2$NEt	CH_3CN	Starting Material
3	r.t. to reflux	DBU	DBU	Starting Material
4	r.t. to reflux	DBU	DMSO	Starting Material

Table 14. Copper dioxocyclam capping reactions.

C. Iron Coordination

Under a variety of reaction conditions, treatment of pyridine capped dioxocyclam **3a** with iron(II) complexes, resulted in recovery of starting material all cases (Table 15). However, little focus was applied to the coordination of iron with dioxocyclams. The possibility for coordination in this series is intriguing and yet to be fully investigated.

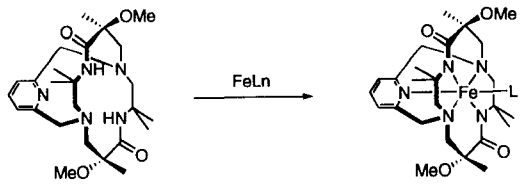

	Metal	Conditions	Base	Solvent	Yield
1	$Fe(CH_3CO_2)_2$	Reflux	-----	MeOH	Starting Material
			$(i\text{-}Pr)_2NEt$	MeOH	Starting Material
		CMW	-----	wet MeOH	Starting Material, Fe decomposition
			-----	MeOH	Starting Material
			$(i\text{-}Pr)_2NEt$	MeOH	Starting Material
2	$Fe_3(CO)_{12}$	CMW	-----	MeOH	Starting Material
3	$Fe(BF_4)_4 \cdot 6\ H_2O$	Reflux	K_2CO_3	MeOH	Starting Material
			$(i\text{-}Pr)_2NEt$	MeOH	Starting Material
		CMW	K_2CO_3	MeOH	Starting Material
			$(i\text{-}Pr)_2NEt$	MeOH	Starting Material
4	$FeCl_2$	CMW	$(i\text{-}Pr)_2NEt$	MeOH	Starting Material, Fe decomposition

Table 15. Iron coordination attempts.

Future Work

The examination of more reaction conditions for the coordination of ruthenium and iron is needed. Sonication conditions have yet to be examined. Also, new ruthenium and iron sources should be examined. The coordination of ruthenium and iron into pyridine and 4-substituted pyridine-capped dioxocyclams would provide a kinetically inert metal complex. Polymetallic complexes of these ruthenium and iron dioxocyclams could then be synthesized and examined for their potential properties.

Conclusions

A variety of 4-substituted pyridine capping reagents have been synthesized that contained both electron-donating and electron-withdrawing as well as σ-donating and π-accepting characteristics. Microwave capping conditions were developed for these new capping reagents that decreased reaction times from days to minutes. Cobalt complexes of the capped dioxocyclams were synthesized as acetate analogs and ligand exchange

conditions provided capped cobalt cyanide complexes with a ligand that supports electronic interaction across its π-system. Polymetallic complexes were synthesized from the coordination of pyridine-capped dioxocyclam cobalt cyanide with both rhodium acetate and ruthenium phthalocyanine. Although complexes **7** and **8** did not exhibit any metal-metal interaction as observed by cyclic voltammetry experiments. Further analysis of these compounds coupled with the synthesis of ruthenium and iron polymetallic dioxocyclam complexes will provide more insight into the characteristics of these complexes.

Experimental Section

General Procedures. Acetonitrile was distilled over calcium hydride. Methanol was distilled over calcium hydride and dried over molecular sieves. NMR spectra were recorded on a Varian JS-300. Infrared spectra were recorded on a Nicolet Magna-IR 760 spectrometer. UV-vis spectra were recorded on an Agilent G 1103 spectrometer. Electrochemical measurements were conducted with an EG and G, Princeton Applied Research, model 75 universal programmer, model 179 digital coulometer, and model 173 potentiostat/galvanostat. The complex was dissolved in a 0.1 M solution of tetrabutylammonium hexafluorophosphate in acetonitrile or CH_2Cl_2. The working electrode was glassy carbon and the counter electrode was a platinum wire. The reference electrode was SCE and potentials were reported versus SCE. Cyclic voltammograms were obtained at a scan rate of 100 mV/s under argon atmosphere at 23 °C. The glassy carbon electrode was cleaned before each run by hand plishing on a buffing pad with fine grit alumina using deionized water. It was then rinsed repeatedly with the solvent used and dried with a Kim wipe. Data were plotted with the *x*-axis equal to 100 mV/cm. Microwave reactions were performed in a GE countertop microwave oven, model number JES1339WC, which had a capacity of 1.3 cubic feet (1.21 L) and a watt output of 1,100W. X-ray crystallographic studies were performed on a Bruker SMART CCD diffractometer, and the intensity of the data set was integrated using Bruker SAINT software. The structures were solved using Bruker SHELXTL V6.1 software. Compounds **2a-2f** were synthesized by published procedures.[59]

Procedure for the Preparation of a Commercial Microwave Oven for Reaction Use. CAUTION! All operations involving microwave techniques were carried

out in a hood behind safety shields. To prepare a commercial microwave oven for reaction conditions the focus point of the microwave radiation must be determined. The rotation wheel was removed from under the glass plate of the microwave. The plate was then covered evenly with 4 Å mol sieves. The microwave was then operated at high power until one area of the sieves started to glow. This spot was marked on the glass plate. This determined the focus point on the horizontal plane. For the vertical plane a pressure tube was rotated 360° on the marked spot until maximum microwave radiation was found. This was determined by preparation of the cobalt(III) complex **5a**. When not in the focus point the tube would become warm but the solution would remain pink. When in the focus point the pressure tube would become warm and the solution would turn purple. The direction the tube should point was then marked on the glass plate. This setup procedure is necessary only once to find the focus point. All reactions were performed behind a blast shield starting at a power level of 10% and a time of 30 seconds. The power level and time were increased until appropriate conditions were determined and all reactions were cooled to room temperature between microwave sets. The power level and time were never increased above 20% and 3 minutes, respectively. To prevent explosions or bumping, all reactions were shaken prior to a microwave set. This is especially important if the reaction forms a precipitate. The precipitate must be suspended in solution prior to each microwave set. When all of these precautions were followed, our laboratories safely preformed several thousand cycles with no adverse side affects such as explosions.

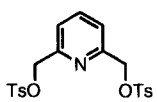

Bis-(tosylmethyl)pyridine (2a'). 2,6-pyridinedimethanol (249.5 mg, 1.793

mmol) and tosylchloride (769.1 mg, 4.034 mmol) were combined with 9 mL CH_2Cl_2 and brought to 0 °C in an ice bath. To the stirring solution was added 6 mL 40% aq. KOH. The solution was brought to room temperature slowly and left to stir until conversion to product by TLC (1:1 EtOAc:Hex). Purification by flash chromatography on silica gel (50% EtOAc:Hexane) afforded a white crystalline solid in 76% yield. ^{1}H NMR ($CDCl_3$, 300 MHz) δ 7.81 (d, *J*=8.4 Hz, 4H), 7.70 (t, 1H), 7.34 (d, *J*=8.0 Hz, 6H), 5.06 (s, 4H), 2.45 (s, 6H).

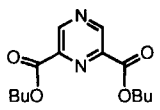

Pyrazine 2,6-butylester (39). To a small pressure tube, flame dried under argon, was added 2,6-dicholopyriazine **38** (103.2 mg, 0.6927 mmol), palladium(II) acetate (3.1 mg, 0.0138 mmol), DPPP (8.6 mg, 0.0208 mmol), sodium carbonate (88.8 mg, 0.838 mmol) and 2.1 mL *n*-BuOH. The tube was then purged with argon three times followed by attachment of the pressure head. The solution was then purged four times with carbon monoxide then filled to 20 psi with carbon monoxide and placed in an oil bath at 125 °C for exactly 2.5 h. During this time the solution turned from a clear orange solution to dark brown/orange in color. The reaction was allowed to cool to room temperature followed by release of excess CO. The solution was filtered over Celite and rinsed with MeOH. Solvent was removed in vacuo followed by addition of more MeOH and solvent removal to remove most of the *n*-BuOH then left on high vacuum line over night leaving a yellow solid in 77% yield. ^{1}H NMR ($CDCl_3$, 300 MHz) δ 9.425 (s, 2H), 4.476 (dd, *J*=6.59, 6.95 Hz, 4H), 1.83 (m, 4H), 1.50(m, 4H), 1.00 (t, 6H). ^{13}C NMR ($CDCl_3$, 75 MHz) δ 148.3, 143.4, 66.7, 30.8, 19.4, 14.0.

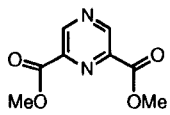

Pyrazine 2,6-methylester (40). Pyrazine 2,6-butylester **39** (70.0 mg, 0.2494 mmol) and camphor sulphonic acid (60.1 mg, 0.2494 mmol) in 4 mL abs. MeOH were combined in a 25 mL flask. The solution was left to stir at room temperature for 24 h followed by reflux for 4 h. Solution was cooled to room temperature and solvent was remove in vacuo. Purification by column chromatography (50% EtOAc:Hexane) afforded **40** as a white solid in 99% yield. ^{1}H NMR ($CDCl_3$, 300 MHz) δ 9.481 (s, 2H), 4.078 (s, 6H).

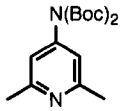

2,6-dimethyl 4-bis-Boc aminopyridine (28). 2,6-dimethyl 4-aminopyridine (137.3 mg, 1.124 mmol), Boc anhydride (564.2 mg, 2.585 mmol), triethylamine (0.2 mL, 1.349 mmol), and dimethyl aminopyridine (54.9 mg, 0.4495 mmol) in 10 mL THF were combined in a 25 mL flask. A condenser was attached and flask was placed in a sonication bath for 18 h. After 8 h, 1 mL dist. H_2O was added to solution. Water added to sonication bath continuously due to evaporation. THF layer separated from water then water layer was extracted with CH_2Cl_2. Organic layers combined, dried over Na_2SO_4 and solvent removed in vacuo. Purification by column chromatography on silica gel (10% MeOH:CH_2Cl_2) giving **28** as a white solid in 62% yield. ^{1}H NMR ($CDCl_3$, 300 MHz) δ 6.80 (s, 2H), 2.55 (s, 6H), 1.476 (s, 18H).

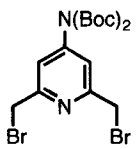

Bis-(bromomethyl)pyridine 4-bis-Boc-amine (2c). To a 10 mL flask was added bis-(tetrabromomethyl)pyridine 4-bis-Boc-amine (151.9 mg, 0.2381 mmol) and 1.6 mL THF. The solution was brought to 0 °C in an ice bath. To the stirring solution was added diethylphosphite (0.06 mL, 0.4762 mmol) followed

dropwise by $(i\text{-Pr})_2NEt$ (0.08 mL, 0.4762 mmol). The reaction was monitored by TLC and was stopped after 3 h and poured over ice water. The aqueous solution was extracted with Et_2O and then dried with $NaSO_4$. Solvent was removed in vacuo. Purification by flash chromatography on silica gel (20% EtOAc:Hexane) giving **2c** as a pale yellow solid, 59% yield. ^1H NMR ($CDCl_3$, 300 MHz) δ 7.204 (s, 2H), 4.54 (s, 4H), 1.477 (s, 18H).

Experimental Procedure for the Preparation of Capped Dioxocyclams in the Microwave. Dioxocyclam **1** (80.8 mg, 0.216 mmol), capping reagent (0.260mmol), and iPr_2NEt (0.3 mL, 1.735 mmol) were combined in a screw-cap pressure tube. The mixture was dissolved in 5 mL CH_3CN then degassed with argon for 5 minutes. The reaction vessel was sealed tightly then microwaved for periods of two minutes at a power level of 20% until no starting material detected by TLC (20-25 cycles). The tube was allowed to cool to room temperature between microwave sets. The solvent was removed in vacuo then brought up in CH_2Cl_2 and washed 2 x 10 mL sat. $NaHCO_3$. The organic layer was isolated and dried over Na_2SO_4. The solvent was removed in vacuo. Purification by flash chromatography on silica gel (5% $MeOH/CH_2Cl_2$) afforded the product as a white solid.

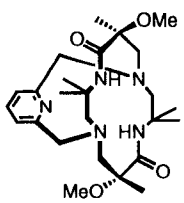

Pyridine-Capped Dioxocyclam (3a). Purification by flash chromatography on silica gel (95:5 CH_2Cl_2/MeOH) afforded white solid in 69% yield.

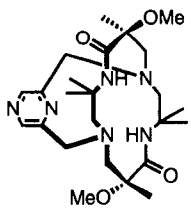

Pyrazine-Capped Dioxocyclam (3b). Purification by flash chromatography on silica gel (1.5:1 Hexanes/THF) afforded white solid in 40% yield.

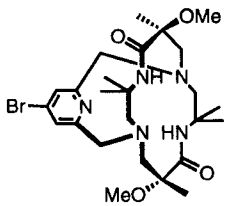

4-Bromopyridine-Capped Dioxocyclam (3d). Purification by flash chromatography on silica gel (97:3 $CHCl_3$/MeOH) afforded a white solid in 75% yield.

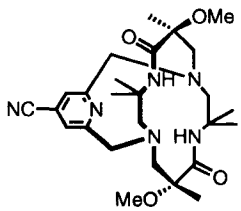

4-Cyanopyridine-Capped Dioxocyclam (3f). Purification by flash chromatography on silica gel (97:3 CH_2Cl_2/MeOH) afforded a white solid in 64% yield.

Preparation of Cobalt(III) (Ring-Opened 2a) Acetate Complex (43).

Method A: 5,12 dioxocyclam **1**, (40 mg, 0.1 mmol) $Co(CH_3CO_2)_2{\cdot}4H_2O$ (213 mg, 0.855 mmol), and iPr$_2$NEt (0.15 mL, 0.86 mmol) were combined in a screw-cap pressure tube. The mixture was suspended in MeOH (4 mL) then degassed with argon for 20 minutes. The reaction vessel was sealed tightly and microwaved an average 15 times for periods of two minutes at a power level of 20%. The tube was allowed to cool to room temperature between microwave sets. The solution was initially clear pink in color. After each microwave cycle the solution became deep purple. The resulting purple solution was passed through a Celite pad and concentrated under vacuum. Purification by flash chromatography on silica gel (10% EtOH/CH_2Cl_2) gave a purple solid **43** in 31% yield.

Method B: 5,12 dioxocyclam **1**, (60 mg 0.16 mmol) $Co(CH_3CO_2)_2 \cdot 4H_2O$ (320 mg, 1.2 mmol), and iPr$_2$NEt (0.220 mL, 1.26 mmol) were combined in a screw-cap pressure tube. The mixture was suspended in MeOH (6 mL) then degassed with argon for 20 minutes. The reaction vessel was sealed tightly and was heated to reflux under argon for 5 days. The resulting purple solution was passed through a Celite pad and concentrated under vacuum. Purification by flash chromatography on silica gel (10% EtOH/CH_2Cl_2) afforded a purple solid **43** in 44% yield.

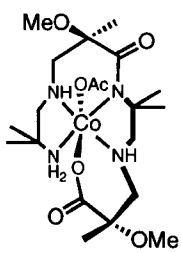

Cobalt(III) (Ring-Opened 2a) Acetate Complex (43). X-ray quality crystals were obtained by recrystallization from CH_2Cl_2 and hexanes; mp 185-187 °C; ^{1}H NMR ($CDCl_3$, 300 MHz) δ 7.75 (s, 1H), 6.63-6.57 (m, 1H), 6.09 (d, J=10.6, 1H), 5.57 (d, J=10.2, 1H), 3.41 (d, J=6.2, 1H), 3.37 (s,1H), 3.35 (s, 3H), 3.31 (s, 3H), 3.24-3.10 (m, 2H), 2.85 (dd, J=5.1, 12.4, 1H), 2.63-2.51 (m, 4H), 1.76 (s, 3H), 1.71 (s, 3H), 1.49 (s, 3H), 1.46 (s, 3H), 1.36 (s, 3H), 1.33 (s, 3H), 1.29 (s, 3H); ^{13}C NMR ($CDCl_3$, 100 MHz) δ 184.0, 172.7, 171.7, 79.4, 78.3, 67.1, 64.1, 64.1, 58.8, 57.8, 54.6, 52.3, 51.4, 29.4, 28.7, 27.9, 26.9, 24.8, 21.4, 20.6; FT-IR (film) 1639, 1567 cm^{-1}; UV-vis (MeOH) $\lambda_{max}(\varepsilon)$ 561 (110); HRMS (FAB$^+$, m/z) calcd for $C_{20}H_{40}CoN_4O_7$ (M+H$^+$) 507.2229, found 507.2237.

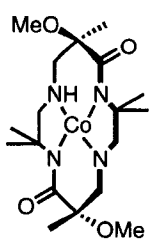

Preparation of Cobalt(III) (3-3H) Complex (44). Dioxocyclam **1** (100 mg, 0.228 mmol), $Co(acac)_3$ (100 mg, 0.280 mmol) were combined in a 50 mL round bottom flask fitted with a reflux condenser. The mixture was suspended in EtOH (10 mL). The reaction was heated at reflux under

nitrogen for 2 days. The resulting green solution was passed through a Celite pad and concentrated under vacuum. Purification by flash chromatography on silica gel (5% MeOH/$CHCl_3$) afforded 20 mg of a pink solid **44**: yield 20%; ^1H NMR (CD_3OD, 400 MHz) δ 5.43 (t, 1H), 5.10 (t, 1H), 3.60 (d, *J*=4.7 Hz, 1H), 3.23 (s, 3H), 3.19 (d, *J*=11.9 Hz, 1H), 2.88 (m, 5H), 2.58 (m, 2H), 2.42 (dd, *J*=4.3, 11.5 Hz, 1H), 1.54 (s, 6H), 1.53 (s, 3H), 1.37 (s, 3H), 1.30 (s, 3H), 1.25 (s, 3H); ^{13}C NMR (CD_3OD, 100 MHz) δ177.1, 175.1, 80.0, 79.7, 70.1, 67.0, 63.4, 63.2, 63.0, 59.8, 52.0, 51.6, 27.3, 26.5, 24.7, 23.5, 20.3, 20.0; FT-IR (film) 1550, 1445 cm^{-1}; UV-vis (MeOH) $\lambda_{max}(\varepsilon)$ 538(176); LRMS (ES^-, *m/z*) calcd for $C_{18}H_{32}CoN_4O_4$ ($M-H^+$) 427.41, found 427.17.

General Procedure for the Preparation of Cobalt(III) Complexes. The capped dioxocyclam **3** (0.287 mmol), $Co(CH_3CO_2)_2{\cdot}4H_20$ (35 mg, 1.436 mmol), and iPr$_2$NEt (0.25 mL, 1.436 mmol) were combined in a screw cap pressure tube. The mixture was suspended in MeOH (2 mL) then degassed with argon for 20 minutes. During this time the cobalt acetate completely dissolved resulting in a clear pink solution. The reaction vessel was sealed tightly and microwaved an average of 60 times for periods of two minutes at a power level of 20%, or until no starting material was present by TLC. The tube was allowed to cool to room temperature between each microwave set. After several microwave sets a blue precipitate began to form. Once the precipitate had formed the precipitate was suspended in solution prior to each microwave set by shaking the tube to prevent bumping and/or explosions of the reaction mixture. The solution was initially clear and pink in color. After each microwave cycle the solution became deep purple and would fade back to pink as the

solution cooled. The resulting pink solution was passed through a Celite pad to remove precipitate and concentrated in vacuo.

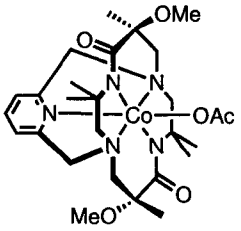

Pyridine-Capped Cobalt(III) (2g-2h) Acetate Complex (5a). Purification by flash chromatography on silica gel (10% MeOH/CH_2Cl_2) afforded a pink solid. X-ray quality crystals were obtained by recrystallization from hot THF and CH_2Cl_2: yield 78%; mp 207 °C dec; ^{1}H NMR ($CDCl_3$, 300 MHz) δ 7.73 (t, 1H), 7.04 (dd, *J*=6.7, 13.6 Hz, 2H), 5.32 (d, *J*=17.9 Hz, 1H), 4.83 (d, *J*=2.1 Hz, 2H), 4.78 (d, *J*=18.0 Hz, 1H), 4.59 (d, *J*=12.9 Hz, 1H), 4.39 (d, *J*=13.1 Hz, 1H), 3.91 (dd, *J*=13.6, 26.0 Hz, 2H), 3.44 (s, 1H), 3.38 (s, 3H), 2.89 (s, 3H), 2.68 (dd, *J*=12.8, 19.6 Hz, 2H), 2.52 (d, *J*=12.1 Hz, 1H), 1.96 (s, 3H), 1.65 (s, 3H), 1.58 (s, 3H), 1.56 (s, 3H), 1.55 (s, 3H), 1.39 (s, 3H), 1.32 (s, 3H); ^{13}C NMR ($CDCl_3$, 75 MHz) δ 178.5, 173.8, 173.0, 164.3, 160.6, 139.0, 117.7, 117.4, 81.0, 79.8, 79.1, 78.7, 69.6, 68.3, 68.2, 67.7, 63.7, 62.7, 52.5, 50.8, 31.2, 29.5, 28.7, 28.6, 28.2, 26.9, 22.2; FT-IR (film) 1613, 1564 cm^{-1}; UV-vis (MeOH) $\lambda_{max}(\varepsilon)$ 526 (156); LRMS (ES$^-$, *m/z*) calcd for $C_{27}H_{41}CoN_5O_6$ (M-H$^+$) 590.25, found 590.20.

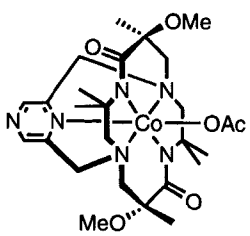

Pyrazine-Capped Cobalt(III) (2b-2h) Acetate Complex (5b). Purification by flash chromatography on silica gel (10% MeOH/CH_2Cl_2) afforded a pink solid. X-ray quality crystals were obtained by recrystallization from hot THF and CH_2Cl_2: yield 54%; mp 155-160 °C dec; ^{1}H NMR ($CDCl_3$, 300 MHz) δ 8.35 (s, 1H), 8.33 (s, 1H), 5.20 (d, *J*=17.6 Hz, 1H), 4.86 (m, 1H), 4.62 (d, *J*=12.8 Hz, 2H), 4.38 (d, *J*=13.2 Hz,

1H), 3.81-3.75 (m, 4H), 3.38 (s, 3H), 2.85 (d, *J*=13.5 Hz, 1H), 2.78 (s, 3H), 2.68 (d, *J*=12.8 Hz, 1H), 2.52 (d, *J*=12.1 Hz, 1H), 1.98 (s, 3H), 1.74 (s, 3H), 1.56 (s, 3H), 1.54 (s, 3H), 1.43 (s, 3H), 1.41 (s, 3H), 1.37 (s, 3H); ^{13}C NMR ($CDCl_3$, 75 MHz) δ 178.7, 174.2, 172.5, 143.5, 138.8, 138.1, 81.4, 79.5, 78.8, 78.1, 68.7, 68.3, 67.7, 66.5, 64.0, 63.0, 52.7, 50.6, 32.2, 30.1, 29.6, 29.0, 28.8, 28.1, 26.8, 21.7; FT-IR (film) 1616, 1559 cm^{-1}; UV-vis (CH_2Cl_2) $\lambda_{max}(\varepsilon)$ 530 (160); LRMS (ES^-, *m/z*) calcd for $C_{26}H_{40}CoN_6O_6$ ($M-H^+$) 591.23, found 591.20.

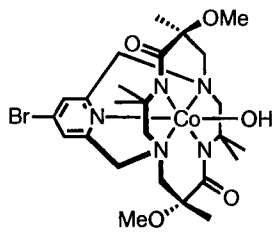

4-Bromopyridine-Capped Cobalt(III) (2b-2h) Hydroxy Complex (5d″). Purification by flash chromatography on silica gel (10% $MeOH/CH_2Cl_2$) and a second and third column by flash chromatography on alumina neutral (2% $MeOH/CH_2Cl_2$) to yield a brown solid: yield 20%; mp 105-110 °C; ^{1}H NMR ($CDCl_3$, 300 MHz) δ 7.28 (s, 1H), 6.32 (d, *J*=18.7 Hz, 1H), 5.15 (d, *J*=19.4 Hz, 1H), 4.75 (d, *J*=19.4 Hz, 1H), 4.17-4.11 (m, 4H), 4.02 (d, *J*=12.1 Hz, 1H), 3.42 (s, 3H), 3.38 (s, 1H), 2.99 (d, *J*=13.5 Hz, 1H), 2.83 (d, *J*=13.2 Hz, 1H), 2.68 (d, *J*=12.1 Hz, 1H), 2.58 (d, *J*=12.1 Hz, 1H), 1.69 (s, 3H), 1.63 (s, 3H), 1.62 (s, 3H), 1.51 (s, 3H), 1.46 (s, 3H), 1.44 (s, 3H); ^{13}C NMR ($CDCl_3$, 75 MHz) δ 174.1, 172.7, 164.1, 161.3, 136.7, 122.2, 121.9, 81.3, 80.8, 79.9, 78.8, 77.6, 67.8, 67.4, 67.3, 67.1, 63.8, 63.1, 52.9, 51.7, 31.2, 29.3, 28.7, 28.2, 23.6; FT-IR (film) 1597, 1560 cm^{-1}; UV-vis (CH_2Cl_2) $\lambda_{max}(\varepsilon)$ 556 (160) ; LRMS (ES^-, *m/z*) calcd for $C_{25}H_{38}CoBrN_5O_5$ ($M-H^+$) 626.14 found 626.13.

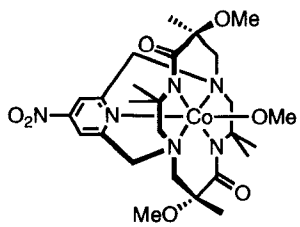

Cobalt(III) Methoxy Complex (5e′). Purification by flash chromatography on silica gel (10% MeOH/CH_2Cl_2) afforded a pink solid: yield 10%; ^{1}H NMR ($CDCl_3$, 400 MHz) δ 6.65 (d, *J*=10.0 Hz, 1H), 5.11 (d, *J*=17.7 Hz, 1H), 4.63-4.54 (m, 3H), 4.26 (d, *J*=13.6 Hz, 1H), 3.91 (s, 3H), 3.68 (dd, *J*=12.8, 35.7 Hz, 2H), 3.45 (d, *J*=20.4 Hz, 1H), 3.42 (s, 3H), 3.28 (s, 1H), 2.93 (s, 3H), 2.76 (d, *J*=13.6 Hz, 1H), 2.56 (dd, *J*=13.2, 29.0 Hz, 2H), 2.38 (d, *J*=12.6 Hz, 1H), 1.58 (s, 3H), 1.50 (s, 3H), 1.49 (s, 3H), 1.48 (s, 3H), 1.37 (s, 3H), 1.29 (s, 3H); ^{13}C NMR ($CDCl_3$, 100 MHz) δ 173.4, 172.8, 168.8, 163.2, 159.6, 104.6, 104.0, 81.1, 80.0, 79.3, 78.6, 71.0, 70.3, 68.1, 67.9, 64.2, 63.4, 56.6, 52.5, 51.0, 30.9, 29.4, 28.1, 28.0, 27.8, 22.3; FT-IR (film) 1570, 1379, 1323 cm^{-1}; LRMS (ES$^-$, *m/z*) calcd for $C_{26}H_{41}CoN_6O_7$ ($M-H^+$) 607.24, found 607.07.

Procedure for the Acetate/Cyanide Ligand Exchange of Cobalt Complexes (5a, 5b, 5d″). The cobalt acetate complex (0.217 mmol) was dissolved in abs. MeOH (2 mL) giving a dark pink solution. NaCN (10.6 mg, 0.217 mmol) was added to the stirring solution. The mixture was stirred at room temperature for 48 h over which time the solution changed from dark pink to orange. The solvent was removed under an air stream in the hood. The orange solid was brought up in CH_2Cl_2 and the remaining white solid was removed by filtration and the solvent was removed in vacuo.

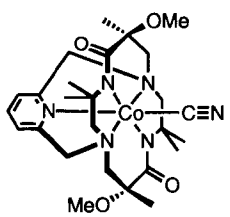

Cobalt Cyanide Complex (6a). Purification by flash chromatography on silica gel (10% MeOH/CH_2Cl_2) to yield an orange solid. X-ray quality crystals were obtained from a mixture of CH_2Cl_2 and Et_2O; mp 226 °C dec.; ^{1}H NMR ($CDCl_3$, 400 MHz) δ 7.87 (t, 1H), 7.25 (d,

J=7.7 Hz, 1H), 5.90 (d, J=18.4 Hz, 1H), 4.96 (d, J=19.0 Hz, 1H), 4.66 (d, J=18.9 Hz, 1H), 4.43 (d, J=18.3 Hz, 1H), 3.97 (d, J=13.2 Hz, 1H), 3.80-3.65 (m, 3H), 3.48 (s, 3H), 3.47 (s, 1H), 3.20 (s, 3H), 3.06 (d, J=13.6 Hz, 1H), 2.88 (d, J=13.0 Hz, 1H), 2.67 (d, J=12.2 Hz, 1H), 2.55 (d, J=12.4 Hz, 1H), 1.70 (s, 3H), 1.66 (s, 3H), 1.50 (s, 3H), 1.46 (s, 3H), 1.44 (s, 6H); ^{13}C NMR ($CDCl_3$, 100 MHz) δ 173.0, 172.5, 162.2, 159.3, 139.5, 129.6, 118.9, 118.5, 82.5, 81.8, 79.7, 78.4, 69.5, 69.2, 68.6, 67.8, 63.6, 62.7, 52.7, 51.4, 50.9, 30.2, 28.8, 28.7, 27.7, 27.2, 22.9; FT-IR (film) 2123, 1566 cm^{-1}; UV-vis (MeOH) $\lambda_{max}(\varepsilon)$ 463 (313); LRMS (ES$^-$, *m/z*) calcd for $C_{26}H_{39}CoN_6O_4$ (M-H$^+$) 557.24, found 557.18.

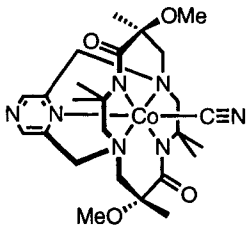

Cobalt Cyanide Complex (6b). Purification by flash chromatography on silica gel (10% MeOH/CH_2Cl_2) to yield an orange solid: yield 93%; X-ray quality crystals were obtained from a mixture of acetone and THF; mp <260 °C dec; ^{1}H NMR ($CDCl_3$, 300 MHz) δ 8.62 (s, 1 H), 8.60 (s, 1 H), 5.77 (d, J=18.3 Hz, 1 H), 4.98 (d, J=19.4 Hz, 1H), 4.77 (d, J=19.4 Hz, 1H), 4.60 (d, J=18.3 Hz, 1H), 3.89 (d, J=13.2, 1H), 3.77 (d, J=12.5, 1H), 3.68-3.58 (m, 4H), 3.41 (s, 3H), 3.07 (s, 3H), 3.03 (d, J=13.9 Hz, 1H), 2.88 (d, J=13.18 Hz, 1H), 2.72 (d, J=12.27 Hz, 1H), 2.58 (d, J=12.27 Hz, 1H), 1.71 (s, 3H), 1.68 (s, 3H), 1.52 (s, 3H), 1.49 (s, 3H), 1.43 (s, 3H), 1.39 (s, 3H); ^{13}C NMR ($CDCl_3$, 75 MHz) δ 172.9, 172.5, 157.3, 154.4, 140.3, 139.8, 127.9 82.5, 81.4, 79.9, 78.3, 69.7, 69.1, 67.4, 66.4, 64.0, 63.1, 52.7, 51.4, 29.9, 29.7, 29.3, 27.7, 27.4, 22.4; FT-IR (film) 2128, 1558 cm^{-1}; UV-vis (CH_2Cl_2) $\lambda_{max}(\varepsilon)$ 454 (475); LRMS (ES$^+$, *m/z*) calcd for $C_{25}H_{39}CoN_7O_4$ (M+H$^+$) 560.55, found 560.13.

Cobalt Cyanide Complex (6d'). Purification by flash chromatography on silica gel (10% $MeOH/CH_2Cl_2$) to yield an orange solid: yield 53%; mp <260 °C dec; ^1H NMR ($CDCl_3$, 300 MHz) δ 6.72 (s, 1H), 6.71 (s, 1H), 5.89 (d, *J*=18.3 Hz, 1H), 4.87 (d, *J*=18.7 Hz, 1H), 4.58 (d, *J*=19.0 Hz, 1H), 4.28 (d, *J*=18.3 Hz, 1H), 3.96 (d, *J*=13.1 Hz, 1H), 3.91 (s, 3H) 3.78-3.62 (m, 4H), 3.47 (s, 3H), 3.27 (s, 3H), 3.04 (d, *J*=13.9 Hz, 1H), 2.86 (d, *J*=13.2 Hz, 1H), 2.64 (d, *J*=12.45 Hz, 1H), 2.53 (d, *J*=12.45 Hz, 1H), 1.69 (s, 3H), 1.64 (s, 3H), 1.52 (s, 3H), 1.48 (s, 3H), 1.44 (s, 6H); ^{13}C NMR ($CDCl_3$, 75 MHz) δ 173.3, 172.4, 168.8, 163.0, 160.3, 105.5, 104.9, 82.6, 82.0, 79.6, 78.5, 69.3, 69.2, 68.5, 67.8, 63.4, 62.7, 56.7, 52.7, 51.6, 30.5, 28.7, 28.5, 27.7, 27.2, 23.2; FT-IR (film) 2123, 1560 cm^{-1}; UV-vis (MeOH) $\lambda_{max}(\varepsilon)$ 462 (317); LRMS (ES^+, *m/z*) calcd for $C_{27}H_{42}CoN_6O_5$ ($M+H^+$) 589.25, found 589.13.

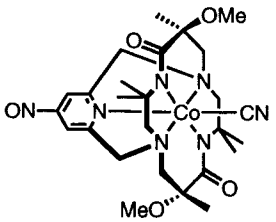

Cobalt Cyanide Complex (6e). Purification by flash chromatography on silica gel (10% $MeOH/CH_2Cl_2$) to yield an orange solid: yield 6%; ^1H NMR ($CDCl_3$, 400 MHz) δ 6.77 (d, *J*=23.6 Hz, 2H), 5.88 (d, *J*=18.2 Hz, 1H), 4.91 (d, *J*=18.5 Hz, 1H), 4.60 (d, *J*=19.0 Hz, 1H), 4.31 (d, *J*=18.3 Hz, 1H), 4.19 (s, 1H), 3.95 (s, 1H), 3.92 (s, 3H), 3.77-3.63 (m, 4H), 3.46 (s, 2H), 3.35 (s, 2H), 3.25 (s, 3H), 3.05 (d, *J*=13.6 Hz, 1H), 2.89 (d, *J*=13.4 Hz, 1H), 2.67 (d, *J*=12.3 Hz, 1H), 2.55 (d, *J*=12.4 Hz, 1H), 1.69 (s, 3H), 1.64 (s, 3H), 1.53 (s, 3H), 1.48 (s, 3H), 1.44 (s, 3H), 1.24 (s, 3H); ^{13}C NMR ($CDCl_3$, 100 MHz) δ 173.2, 172.3, 168.7, 162.9, 160.2, 130.2, 105.4, 104.9, 82.5, 81.8, 79.5, 78.5, 69.4, 69.1, 68.4, 67.7, 63.4, 62.7, 56.7, 53.6, 52.7, 51.5, 50.3, 30.3, 29.9, 28.6, 28.4, 27.6,

27.1, 23.1; FT-IR (film) 2125, 1560, 1448, 1360 cm^{-1}; LRMS (ES^-, *m/z*) calcd for $C_{26}H_{38}CoN_7O_5$ (M-H^+) 586.22, found 587.30.

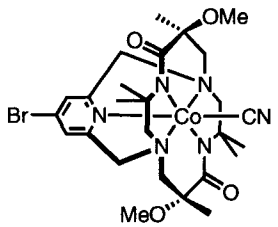

Procedure for the Ligand Exchange of Cobalt Complex (6d). Complex **5d″** (14 mg, 0.02 mmol) was dissolved in acetonitrile (3 mL) giving a dark pink solution. KCN (4.0 mg, 0.06 mmol) and 18-crown-6 (2 mg, 0.0075 mmol) were added to the stirring solution. The mixture was stirred at reflux for 7 h over which time the solution changed from dark pink to orange. The solvent was removed by air stream in the hood. The orange solid was brought up in CH_2Cl_2 and the resulting white solid was filtered off through Celite. Solvent removed in vacuo. Purification by flash chromatography on silica gel (10% MeOH/CH_2Cl_2) afforded an orange solid in 86% yield.

Cobalt Cyanide Complex (6d). Mp <260 °C dec; ^1H NMR ($CDCl_3$, 300 MHz) δ 7.44 (s, 1H), 7.42 (s, 1H), 5.86 (d, *J*=18.3 Hz, 1H), 4.92 (d, *J*=19.4 Hz, 1H), 4.66 (d, *J*=19.4 Hz, 1 H), 4.42 (d, *J*=18.3 Hz, 1 H), 3.94 (d, *J*=13.2 Hz 1 H), 3.94 (d, *J*=12.4 Hz 1H) 3.71-3.70 (m, 4H), 3.45 (s, 3H), 3.22 (s, 3H), 3.03 (d, *J*=13.5 Hz, 1H), 2.87 (d, *J*=13.2 Hz, 1H), 2.68 (d, *J*=12.45 Hz, 1H), 2.55 (d, *J*=12.45 Hz, 1H), 1.71 (s, 3H), 1.68 (s, 3H), 1.50 (s, 3H), 1.49 (s, 3H), 1.43 (s, 3H); ^{13}C NMR ($CDCl_3$, 75 MHz) δ 173.1, 172.6, 163.1, 160.2, 136.7, 122.4, 122.1, 82.5, 81.7, 79.7, 78.3, 77.5, 69.7, 69.2, 68.4, 67.5, 63.6, 62.8, 52.7, 51.6, 30.2, 29.2, 29.1, 27.6, 27.3, 22.9; FT-IR (film) 2124, 1567 cm^{-1}; UV-vis (MeOH) $\lambda_{max}(\varepsilon)$ 462 (238); LRMS (ES^+, *m/z*) calcd for $C_{26}H_{38}CoBrN_6O_4$ (M+H^+) 637.15, found 637.07.

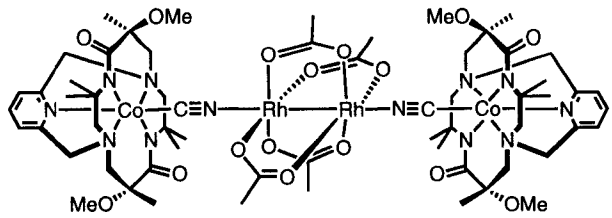

Synthesis of Rhodium Acetate Bridged Cobalt Cyanide Pyridine Complex (7). A solution of cobalt complex **6a** (32.8 mg, 0.059 mmol) and rhodium(II)acetate (13 mg, 0.029 mmol) in 6 mL abs. MeOH was stirred at reflux for 3 hours. The color of the solution turned from orange to a greenish brown. The solution was filtered through a cotton plug. Evaporation of the solvent gave a brown solid. Recrystallization by vapor diffusion of MeOH and Et_2O gave red plate crystals: yield 95%; ^{1}H NMR ($CDCl_3$, 400 MHz) δ 7.89 (t, 1H), 7.26 (d, *J*=7.9 Hz, 2H), 5.89 (d, *J*=18.1 Hz, 1H), 5.02 (d, *J*=18.8 Hz, 1H), 4.72 (d, *J*=18.7 Hz, 1H), 4.54 (d, *J*=18.1 Hz, 1H), 3.48 (s, 3H), 3.20 (s, 3H), 3.12 (d, *J*=14.7 Hz, 1H), 2.88 (d, *J*=13.4 Hz, 1H), 2.65 (dd, *J*=11.4, 23.5 Hz, 2H), 1.83 (s, 12H), 1.70 (s, 6H), 1.53 (s, 3H), 1.51 (s, 3H), 1.50 (s, 3H), 1.48 (s, 3H); ^{13}C NMR ($CDCl_3$, 100 MHz) δ 191.1, 173.1, 172.8, 162.4, 159.5, 139.4, 118.8, 118.3, 82.4, 81.9, 79.8, 78.5, 77.4, 69.1, 68.2, 63.8, 63.0, 53.0, 51.4, 30.6, 29.2, 28.8, 27.8, 27.0, 23.7, 22.8; FT-IR (film) 2228, 2200, 2142, 1595, 1566 cm^{-1}; UV-vis (MeOH) $\lambda_{max}(\varepsilon)$ 455 (744), 574 (246); LRMS (FAB$^+$, *m/z*) calcd for $C_{60}H_{90}Co_2N_{12}O_{16}Rh_2$ (M+H$^+$) 1559.34, found 1559.40.

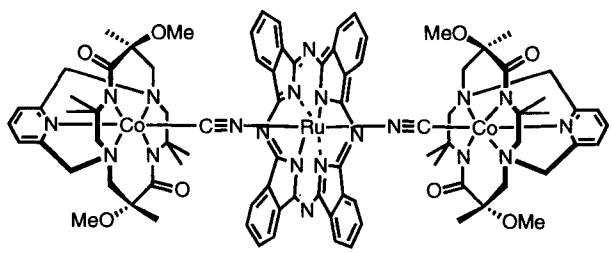

Synthesis of Ruthenium(II) Phthalocyanine Bridged Cobalt Cyanide Pyridine Complex (8). A solution of bis(benzonitrile)-phthalocyaninate ruthenium(II)[28] (10 mg, 0.012 mmol) and 18 mg (0.032 mmol) of cobalt

cyanide complex **6a** in 5 mL dry CH_2Cl_2 was heated at 65 °C under nitrogen for 24 hours. Evaporation of solvent gave a blue product. Purification by flash chromatography on silica gel (10% MeOH/$CHCl_3$) afforded a blue solid. X-ray quality crystals were obtained by recrystallization via vapor diffusion of MeOH and Et_2O giving blue crystals: yield 71%, mp <260 °C dec; ^{1}H NMR ($CDCl_3$, 400 MHz) δ 8.94 (s, 8H), 7.70 (s, 8H), 7.38 (t, *J*=7.8 Hz, 2H), 6.68 (d, *J*=7.8 Hz 2H), 6.67 (d, *J*=7.8 Hz, 2H), 5.23 (d, *J*=19.2 Hz, 2H), 3.98 (d, *J*=20.2 Hz, 2H), 3.89 (d, *J*=19.2 Hz, 2H), 3.64 (m, 8H), 3.45 (d, *J*=12.4 Hz, 2H), 2.77 (s, 6H), 1.73 (s, 6H), 1.65 (d, *J*=14.8 Hz, 2H), 1.58 (d, *J*=12.6 Hz, 2H), 1.47 (d, *J*=14.8 Hz, 2H), 1.38 (d, *J*=12.6 Hz, 2H), 0.81 (s, 6H), 0.77(s, 6H), 0.73 (s, 6H), 0.61 (s, 6H), -0.03 (s, 6H), -0.19 (s, 6H); ^{13}C NMR ($CDCl_3$, 100 MHz) δ 171.5, 171.1, 161.3, 158.2, 140.2, 139.3, 130.0, 127.3, 121.4, 118.7, 118.2, 117.9, 81.2, 79.5, 78.3, 76.5, 70.5, 66.9, 66.8, 66.2, 61.5, 60.8, 50.8, 50.6, 29.6, 29.1, 28.3, 26.0, 25.0, 21.7 ; FT-IR (film) 2920, 2125, 1562 cm^{-1}; UV-vis (CH_2Cl_2) $\lambda_{max}(\varepsilon)$ 320 (42201), 412 (2500), 571 (sh), 628 (26871); LRMS (FAB^+, *m/z*) calcd for $C_{84}H_{94}Co_2RuN_{20}O_8$ ($M+H^+$) 1730.5, found 1730.7.

References

1 Curtis, N. F. *Coord. Chem. Rev.* **1968**, *3*, 3.
2 Kimura, E. *J. Coord. Chem.* **1986**, *15*, 1.
3 Kimura, E. *Tetrahedron* **1992**, *48*, 6175.
4 Busch, D. H.; Alcock, N. W. *Chem. Rev.* **1994**, *94*, 585.
5 Betshaart, C.; Hegedus, L. S. *J. Am. Chem. Soc.* **1991**, *113*, 5884.
6 Hegedus, L. S.; Moser, W. H. *J. Org. Chem.* **1994**, *55*, 7779.
7 Dumas, S.; Lastra, E.; Hegedus, L. S. *J. Am. Chem. Soc.* **1995**, *117*, 3368.
8 Hsiao, Y.; Hegedus, L. S. *J. Org. Chem.* **1997**, *62*, 3586.
9 Motekaitis, R. J.; Sun, Y.; Martell, A. E.; Welch, M. J. *Can. J. Chem.* **1999**, *77*, 614.
10 (a) Machida, R.; Kimura, E.; Kodama, M. *Inorg. Chem.* **1983**, *22*, 2055. (b) Hu, C. H.; Chin, R. M.; Nguyen, T. D.; Nguyen, K. T.; Wagenknecht, P. S. *Inorg. Chem.* **2003**, *42, 7602.*
11 Goeta, A. E.; Howard, J. A. K.; Maffeo, D.; Puschmann, H.; Williams, J. A. G.; Yufit, D. S. *J. Chem. Soc., Dalton Trans.* **2000**, 1873.
12 (a) Denat, F.; Lacour, S.; Brandes, S.; Guilard, R. *Tetrahedron Lett.* **1997**, *38*, 4417. (b) Brandes, S.; Lacour, S.; Denat, F.; Pullumbi, P.; Guilard, R. *J. Chem. Soc., Perkin Trans. 1* **1998**, 639. (c) Brandes, S.; Denat, F.; Lacour, S.; Rabiet, F.; Pullumbi, P.; Guilard, R. *Eur. J. Org. Chem.* **1998**, 2349. (d) Denat, F.; Brandes, S.; Guilard, R. *Synlett* **2000**, 561. (e) Fremond, L.; Espinosa, E.; Meyer, M.; Denat, F.; Guilard, R.; Huch, V.; Veith, M. *New J. Chem.* **2000**, *24*, 959.
13 (a) Lackkar, M.; Guilard, R.; Atmani, A.; De Cran, A.; Fischer, J.; Weiss, R. *Inorg. Chem.* **1998**, *37*, 1575. (b) Brandes, S.; Denat, F.; Lacour, S.; Rabiet, F.; Pullumbi, P.; Guilard, R. *Eur. J. Org. Chem.* **1998**, 2349. (c) Denat, F.; Brandes, S.; Guilard, R. *Synlett* **2000**, 561.
14 Meyer, M.; Fremond, L.; Espinosa, E.; Guilard, R.; Ou, Z.; Kadish, K. M. *Inorg. Chem.* **2004**, *43*, 5572.
15 (a) De Clercq, E.; Yamamoto, N.; Pauwels, R.; Baba, M.; Schols, D.; Nakashima, H.; Balzarini, J.; Debyser, Z.; Murrer, B. A.; Schwarts, D.; Thorton, D.; Bridger, G.; Fricker, S.; Hensen, G.; Abrams, M.; Picker, D. *Proc. Natl. Acad. Sci. USA* **1992**, *89*, 5286. (b) Inouye, Y.; Kanamori, T.; Yoshida, T.; Bu, X.; Shionoya, M.; Koike, T.; Kimura, E. *Biol. Pharm. Bull.* **1994**, *17*, 243.
16 Wynn, T.; Hegedus, L. S. *J. Am. Chem. Soc.* **2000**, *122*, 5034.
17 Hegedus, L. S.; Sundermann, M. J.; Dorhout, P. K. *Inorg. Chem.* **2003**, *42*, 4346.
18 (a) Lehn, J. *Angew. Chem. Int. Ed.* **1988**, *27*, 89. (b) Ringsdorf, H.; Schlarb, B.; Venzmer, J. *Angew. Chem. Int. Ed.* **1990**, *29*, 1304. (c) Balzani, V. *Tetrahedron* **1992**, *48*, 10443.
19 Sauvage, J. P.; Colling, J. P.; Chambron, J. C.; Guillerez, S.; Coudret, C. *Chem. Rev.* **1994**, *94*, 993. (b) Walielewski, M. R. *Chem. Rev.* **1992**, *92*, 435.
20 Astruc, D. *Acc. Chem. Res.* **1997**, *30*, 383.
21 Barigelletti, F.; Flamigni, L. *Chem. Soc. Rev.* **2000**, 1.
22 (a) Baranoff, E.; Collin, J. P.; Flamingni, L.; Sauvage, J. P. *Chem. Soc. Rev.* **2004**, *33*, 147. (b) Yu, L.; Muthkumaran, K.; Sazanerrich, I. V.; Kirmaier, C.; Hindin, E.; Diers, J. R.; Boyle, P. D.; Bocian, D. F.; Holten, D.; Lindsey, J. E.

Inorg. Chem. **2003**, *42*, 629.
23 Ziessel, R.; Hissler, M.; El-ghayoury, a.; Harriman, A. *Coord. Chem. Rev.* **1998**, *178-180*, 1251.
24 Carcel, C. M.; Laha, J. K.; Loewe, R. S.; Thamyongkit, P.; Schweikert, K. H.; Misra, V.; Bocian, D. F.; Lindsey, J. S. *J. Org. Chem.* **2004**, *69*, 1435.
25 (a) Shen, X.; Moriuchi, T.; Hirao, T. *Tetrahedron Lett.* **2003**, *44*, 7711. (b) Nishihara, H. *Bull. Chem. Soc. Jpn.* **2004**, *77*, 407.
26 (a) Launay, J. P. *Chem. Soc. Rev.* **2001**, *30*, 386. (b) Patoux, C.; Launay, J. P.; Beley, M.; Chodorowski-Kimmes, S.; Collin, J. P.; James, S.; Sauvage, J. P. *J. Am. Chem. Soc.* **1998**, *120*, 3717.
27 *Crystal Engineering*; Seddon, K. R.; Zaworotko, M. J., Eds. Kluwer Academic Publishers: Dordrecht, The Netherlands, **1999**.
28 (a) Robson, R. *J. Chem. Soc., Dalton Trans.* **2000**, 3735. (b) Liang, K.; Zheng, H.; Song, Y.; Lappert, M. F.; Li, Y.; Xin, X.; Huang, Z.; Chen, J.; Lu, S. *Angew. Chem. Int. Ed.* **2004**, *43*, 5776.
29 (a) Journaux, Y.; Sletten, J.; Kahn, O. *Inorg. Chem.* **1986**, *25*, 439. (b) Adachi, K.; Sugiyama, Y.; Kumagai, H.; Inoue, K.; Kitagawa, S.; Kawata, S. *Polyhedron* **2001**, *20*, 1411. (c) Weickowska, A.; Bilewicz, R.; Domagala, S.; Wozniak, K.; Korybut-Daszkiewicz, B.; Tomkiewicz, A.; Mrozinski, J. *Inorg. Chem.* **2003**, *42*, 5513.
30 Rosokha, S. V.; Lampeka, Y. D.; Maloshtan, I. M. *J. Chem. Soc., Dalton Trans.* **1993**, 631.
31 Ishida, T.; Kawakami, T.; Mitsubori, S.; Nogami, T.; Yamaguchi, K.; Iwamura, H. *J. Chem. Soc., Dalton Trans.* **2002**, 3177.
32 Ruminski, R. R.; Petersen, J. D. *Inorg. Chem.* **1982**, *21*, 3706.
33 Kaim, W.; Klein, A.; Glockle, M. *Acc. Chem. Res.* **2000**, *33*, 755.
34 (a) Ward, M. D. *Chem. Soc. Rev.* **1995**, *64*, 135. (b) Astruc, D. *Acc. Chem. Res.* **1997**, *30*, 383. (c) McCleverty, J. A.; Ward, M. D. *Acc. Chem. Res.* **1998**, *31*, 842.
35 Lambert, C.; Noll, G. *J. Am. Chem. Soc.* **1999**, *121*, 8434.
36 Ito, T.; Hamaguchi, T.; Nagino, H.; Yamaguchi, T.; Kido, H.; Zavarine, I. S.; Richmond, T.; Washington, H.; Kubiak, C. P. *J. Am. Chem. Soc.* **1999**, *121*, 4625.
37 (a) Creutz, C.; Taube, H. *J. Am. Chem. Soc.* **1969**, *91*, 3988. (b) Creutz, C.; Taube, H. *J. Am. Chem. Soc.* **1973**, *95*, 1086. (c) Lau, V. C.; Berben, L. A.; Long, J. R. *J. Am. Chem. Soc.* **2002**, *124*, 9042.
38 (a) Launay, J. P. *Chem. Soc. Rev.* **2001**, *30*, 386. (b) Kuhn, F. E.; Zuo, J. L.; Fabrizi de Biani, F.; Santos, A. M.; Zhang, Y.; Zhao, J.; Sandulache, A.; Herdtweck, E. *New. J. Chem.* **2004**, *28*, 43. (c) Benniston, A. C.; Mitchell, S.; Rostron, S. A.; Yang, S. *Tetrahedron Lett.* **2004**, *45*, 7883.
39 Contakes, S. M.; Klausmeyer, K. K.; Rauchfuss, T. B. *Inorg. Chem.* **2000**, *39*, 2069.
40 Vahrenkamp, H.; Geiss, A.; Richardson, G. N. *J. Chem. Soc., Dalton Trans.* **1997**, 3643.
41 (a) Albores, P.; Slep, L. D.; Weyhermuller, T.; Baraldo, L. M. *Inorg. Chem.*

2004, *43*, 6762. (b) Flay, M.; Vahrenkamp, H. *Eur. J. Inorg. Chem.* **2003**, 1719.
42 (a) Sheng, T.; Varhenkamp, H. *Eur. J. Inorg. Chem.* **2004**, 1198. (b) Geiss, A.; Vahrenkamp, H. *Inorg. Chem.* **2000**, *39*, 4029. (c) Geiss, A.; Kolm, M. J.; Janiak, C.; Vahrenkamp, H. *Inorg. Chem.* **2000**, *39*, 4037. (d) Geiss, A.; Vahrenkamp, H. *Eur. J. Inorg. Chem.* **1999**, 1793. (e) Cordiner, R. L.; Corcoran, D.; Yufit, D. S.; Goeta, A. E.; Howard, J. A. K.; Low, P. J. *J. Chem. Soc., Dalton Trans.* **2003**, 3541. (f) Bernhardt, P. V.; Bozoglian, F.; Macpherson, B. P.; Martinez, M. *J. Chem. Soc., Dalton Trans.* **2004**, 2582. (g) Sheng, T.; Appelt, R.; Comte, V.; Vahrenkamp, H. *Eur. J. Inorg. Chem.* **2003**, 3731.
43 (a) Collman, J. P.; McDevitt, J. T.; Leidner, C. R.; Yee, G. T.; Torrance, J. B.; Little, W. A. *J. Am. Chem. Soc.* **1987**, *109*, 4606. (b) Ma, B.; Gao, S.; Yi, T.; Xu, G. *Polyhedron* **2001**, *20*, 1255.
44 Sheng, T.; Appelt, R.; Comte, V.; Vahrenkamp, H. *Eur. J. Inorg. Chem.* **2003**, 3731.
45 (a) Gonzalez-Cabello, A.; Vazquez, P.; Torres, T.; Guldi, D. M. *J. Org. Chem.* **2003**, *68*, 8635. (b) de la Torre, G.; Vazquez, P.; Agullo-Lopez; Torres, T. *Chem. Rev.* **2004**, *104*, 3723.
46 Bu, X. H.; An, D. L.; Cao, X. C.; Zhang, R. H.; Clifford, T.; Kimura, E. *J. Chem. Soc., Dalton Trans.* **1998**, 2247
47 Slocik, J. M.; Ward, M. S.; Shepherd, R. E. *Inorg. Chim. Acta.* **2001**, *317*, 290.
48 *The Chemistry of Macrocyclic Ligand Complexes*; Lindoy, L. F. Cambridge University Press: New York, New York. **1989**.
49 Ochiai, E. *J. Org. Chem.* **1953**, *18*, 534.
50 Craig, J. C.; Purushothaman, K. K. *J. Org. Chem.* **1970**, *35*, 1721.
51 (a) Diwu, Z.; Beachdel, C.; Klaubert, D. H. *Tetrahedron Lett.* **1998**, *39*, 4987. (b) Hirao, T.; Masunaga, T.; Ohshiro, Y.; Agawa, T. *J. Org. Chem.* **1981**, *46*, 3745. (c) Hirao, T.; Masunaga, T.; Hayashi, K.; Ohshiro, Y. *Nippon Kagaku Kaishi* **1987**, 1277. (d) Hirao, T.; Kohno, S.; Ohshiro, Y.; Agawa, T. *Bull. Chem. Soc. Jpn.* **1983**, *56*, 1881.
52 Liu, P.; Chem, Y.; Deng, J.; Tu, Y. *Synthesis* **2001**, 2078.
53 (a) Malinowski, M.; Kaczmarek, L. *Journal f. Prakt. Chemie.* **1988**, *330*, 154. (b) Kaczmarek, L.; Balicki, R.; Malinowski, M. *Journal f. Prakt. Chemie.* **1990**, *332*, 423.
54 Kelly, T. A.; McNiel, D. W. *Tetrahedron Lett.* **1994**, *35*, 9003.
55 Tahri, A.; Cielen, E.; Van Aken, K. J.; Hoornaert, G. J.; De Schryver, F. C.; Boens, N. *J. Chem. Soc., Perkin Trans. 2* **1999**, *8*, 1739.
56 Mager, H. I. X.; Berends, W. *Rec. Trav. Chim.* **1958**, *77*, 827.
57 (a) Hull, J. W. Jr.; Wang, C. *Heterocycles* **2004**, *63*, 411. (b) Takeuchi, R.; Suzuki, K.; Sato, N. *J. Mol. Cat.* **1991**, *66*, 277.
58 (a) Zeynizadeh, B. *Bull. Chem. Soc. Jpn.* **2003**, *76*, 317. (b) Gensler, W. J.; Johnson, F.; Sloan, D. B. *J. Am. Chem. Soc.* **1960**, *82*, 6074.
59 Achmatowicz, M.; Hegedus, L. S.; David, S. *J. Org. Chem.* **2003**, *68*, 7661.
60 Hayes, B. *Aldrichimica Acta* **2004**, *37*, 66.
61 Gowenlock, B. G.; Cameron, M.; Boyd, A. S. F. *J. Chem. Res. Synth.* **1995**, 358.
62 Marty, M.; Clyde-Watson, Z.; Twyman, L. J.; Nakash, M.; Sanders, J. K. M.

Chem. Comm. **1998**, 2265.
63 (a) Yam, V. W. W.; Lau, V. C. Y.; Cheung, K. K. *Organometallics* **1995**, *14*, 2749. (b) Xu, G. L.; Jablonski, C. G.; Ren, T. *J. Organometallic Chem.* **2003**, *683*, 388.
64 Yam, V. W. W.; Lau, V. C. Y.; Cheung, K. K. *Organometallics* **1996**, *15*, 1740.
65 Handa, M.; Yoshioka, D.; Mikuriya, M.; Hiromitsu, I.; Kasuga, K. *Mol. Cryst. Liq. Cryst.* **2002**, *376*, 257.
66 (a) Stephenson, T. A.; Wilkinson, G. *J. Inorg. Nucl. Chem.* **1966**, *28*, 2285. (b) Cooke, M. W.; Murphy, C. A.; Cameron, T. S.; Beck, E. J.; Vamvounis, G.; Aquino, M. A. S. *Polyhedron* **2002**, *21*, 1235.
67 Alessio, E.; Mestroni, G.; Nardin, G.; Attia, W. M.; Calligaris, M.; Sava, G.; Zorzet, S. *Inorg. Chem.* **1988**, *27*, 4099.
68 Reiff, A. L.; Garcia-Frutos, E. M.; Gil, J. M.; Anderson, O. P.; Hegedus, L. S. **2005**, submitted.
69 Balzani, V. *Tetrahedron* **1992**, *48*, 10443.
70 Berber, G.; Cammidge, A. N.; Chambrier, I.; Cook, M. J.; Hough P. W. *Tetrahedron Lett.* **2003**, *44*, 5527.
71 (a) Bossard, G. E.; Abrams, M. J.; Darkes, M. C.; Vollano, J. F.; Brooks, R. C. *Inorg. Chem.* **1995**, *34*, 1524. (b) Weber, A.; Ertel, T. S.; Reinohl, U.; Feth, M.; Bertagnolli, H.; Leuze, M.; Hanak, M. *Eur. J. Inorg. Chem.* **2001**, 679.
72 (a) Wagner, F.; Barefield, K. *Inorg. Chem.* **1976**, *15*, 408. (b) Kang, S.; Kim, M.; Whang, D.; Kim, K. *Inorg. Chim. Acta.* **1998**, *279*, 238.

CHAPTER TWO

SYNTHESIS OF COPPER (II) AND COBALT(III) COMPLEXES OF 4-SUBSTITUTED-PYRIDINE-CAPPED BIS-DIOXOCYCLAMS

Introduction

I. Bis-Dioxocyclams

Bis-cyclams are formed by the covalent connection of two mono-cyclams. They are of interest because when two complexed metals are held in close proximity the properties of the two metal centers can change. The methods for synthesis of bis-cyclams are extensions of cyclam synthesis. One of the simplest methods for the linking of two cyclams together is through the ring nitrogens (Scheme 1).[1] However, selective protection of the amines is required for this approach and tosylation of the monocyclam occurred in very low yields (24%). After linking the cyclams with $(COClCH_2)_2$, *p*- or *m*-dibromoxylene, the tosyl protecting groups were removed. The linear linkers were not extended beyond four carbon atoms as seen in Scheme 1.

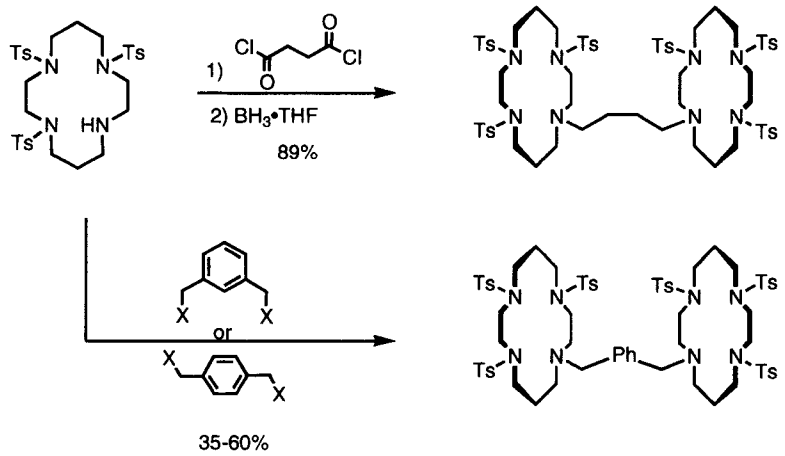

Scheme 1. Bis-cyclam synthesis via nitrogen linking.

Treatment of the detosylated bis-cyclams with nickel(II) and copper(II) perchlorates afforded dimetallic complexes for all three of the bis-cyclams. However, no yields were reported (Scheme 2).

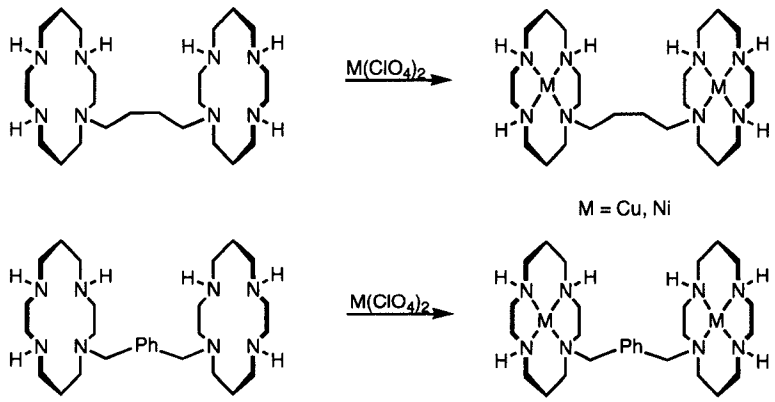

Scheme 2. Copper(II) and nickel(II) bis-cyclam complexes.

As demonstrated in chapter one, bis-dioxocyclams can also be formed by linking the ring nitrogens, resulting in the two rings having a face-to-face orientation (Scheme 3).[2,3] A stepwise synthesis was required to affect the macrocyclization, since capping resulted if one of the amine nitrogens was not protected. No metal complexes have been reported for this bis-dioxocyclam.

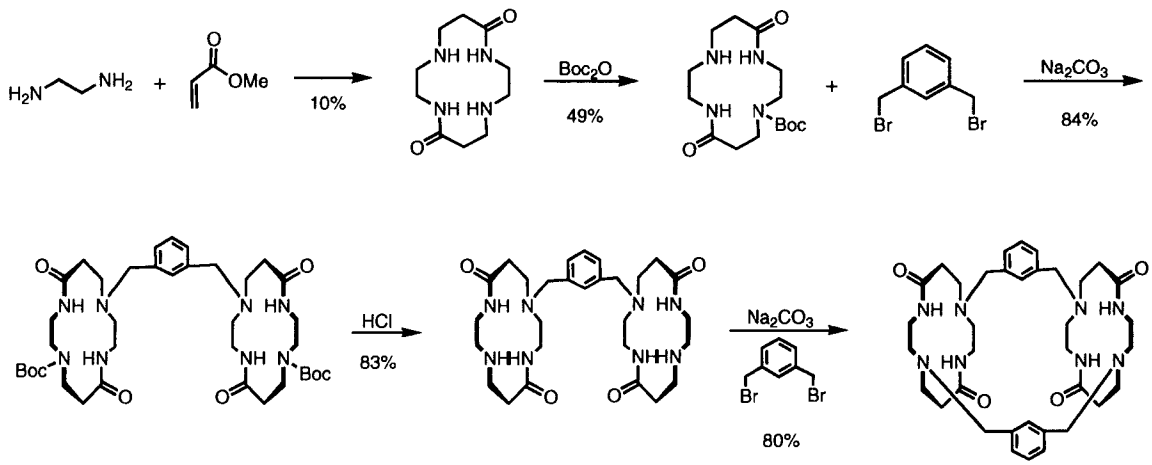

Scheme 3. Bis-dioxocyclam synthesis via nitrogen linking.

Linking of the two cyclams through the carbon backbone of the cyclam has also been developed. This is advantageous because metal complexes of N-substituted cyclams are generally less stable than cyclams with only secondary amines. Fabbrizzi developed and studied the metal complexes of carbon linked bis-cyclams and bis-dioxocyclams using an extension of Tabushi's dioxocyclam synthesis (Scheme 4).[4] The corresponding copper(II) complex was obtained by treatment of the bis-dioxocyclam with copper(II) perchlorate.

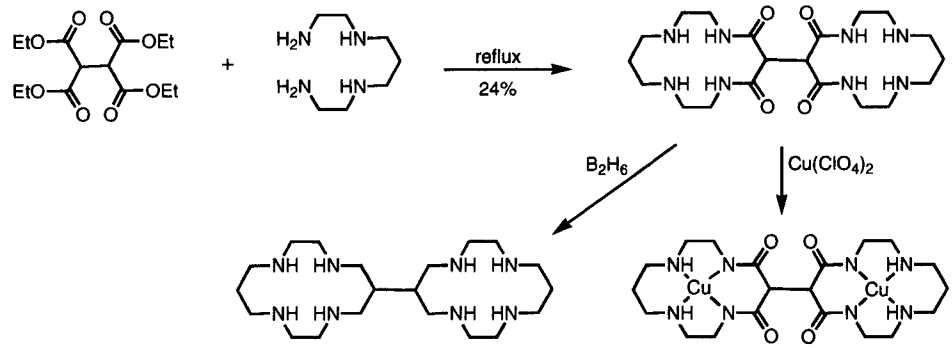

Scheme 4. Bis-dioxocyclam via carbon linking.

The synthesis of bis-dioxocylams in a controlled manner is not trivial. Unfortunately, their construction typically employs the use of protecting groups to selectively link two mono-cyclams (Scheme 1) or low yielding condensation reactions (Scheme 4).

Highly functionalized carbon bridged bis-dioxocyclams have been synthesized in the Hegedus laboratories in good yields without the use of protecting groups or condensation reactions. These bis-dioxocyclams are generated in a face-to-face manner and the carbon bridge length can easily be varied (n = 0, 1, 2, 8). Similar to mono-dioxocyclams, acid-catalyzed opening of the bis-azapenam forms a seven-membered imine, which undergoes dimerization to form an imine bis-dioxocyclam (Scheme 5).[5]

Reduction of the imine affords bis-dioxocyclam **1** (n = 0, 1, 2, 8) in a mixture of *meso* and *d,l* diastereomers, which differ by the absolute configuration at the apical etherates. The complexity inherent to the dimerization process for bis-azapenams warrants further discussion.

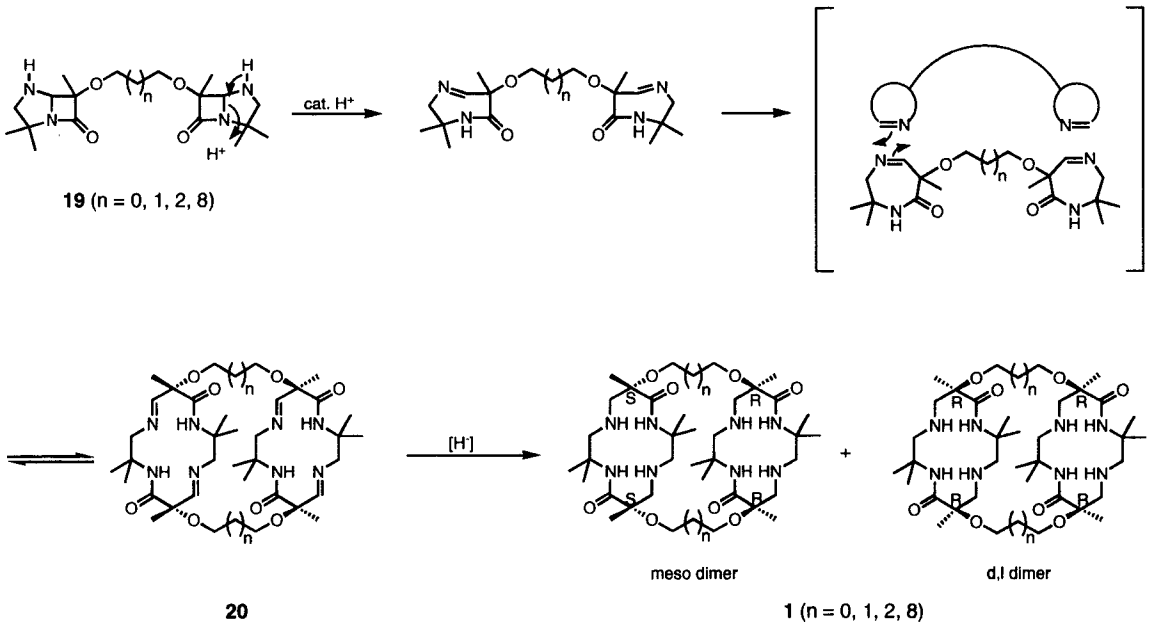

Scheme 5. Hegedus' synthesis of *meso* and *d,l* bis-dioxocyclams.

As demonstrated in chapter 1, the dimerization of racemic mono-azapenams result in a 1:1 mixture of the C_2 (R,R;S,S) and C_i (R,S) mono-cyclam. With bis-azapenams, the situation is stereochemically much more complex. Dimerization of the racemic mixture of diastereomers (*d,l-d,l*; *meso-meso*; *meso-d,l*) could lead to seven possible hetero- or homo-isomeric bis-dioxocyclams (Figure 1).

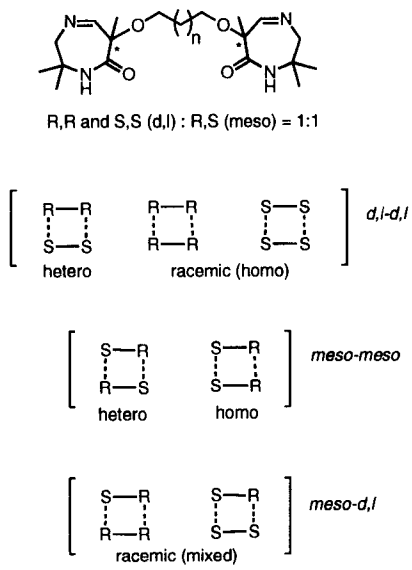

Figure 1. Isomer possibilities.

Fortunately, the diastereomers of bisazapenam **19** (n = 1) were separable so that dimerization could be studied with either the *meso* or *d,l* isomer. Dimerization of the *meso* bis-azapenam **19** (n = 1) afforded the *meso* homo dimer **1** only, not a mixture of homo and hetero dimers as confirmed by X-ray crystallography. The stepwise and reversible dimerization process effects the selectivity for centers of like configuration to combine, favoring the formation of homo bis-dioxocyclams over hetero bis-dioxocyclams. Scheme 6 shows the stepwise cyclization of both homo and heterodimerization of *d,l* **19** (n = 1). If dimerization occurs between imines of like configuration (homo), the resulting compound has the remaining two imines ideally located for a second cyclization, to form the homo dimer. In contrast, dimerization between imines of opposite configuration (hetero), results in a compound having the remaining two imines on opposite faces, making heterodimerization more difficult. Since cyclam formation is reversible, it can equilibrate to the homo dimer precursor or it can oligomerize. It has been observed that bis-dioxocyclam formation is very sensitive to

reaction conditions. High concentrations of bis-azapenam, additional camphorsulfonic acid, prolonged reaction times, and high temperatures decreased the yield of bis-dioxocyclam and resulted in an increase of oligomeric byproducts. Leaving the imine bis-dioxocyclams standing in solution allowed slow formation of insoluble oligomeric byproducts and loss of bis-dioxocyclam. Additionally, the necessity for separation of *meso* and *d,l* bis-azapenams before conversion to bis-dioxocyclams was verified for compound **19** (n = 2) for which the bis-azapenams could not be separated. Treatment of the mixture to acid-catalyzed dimerization conditions resulted in an inseparable mixture of *meso* and *d,l* bis-dioxocyclams.

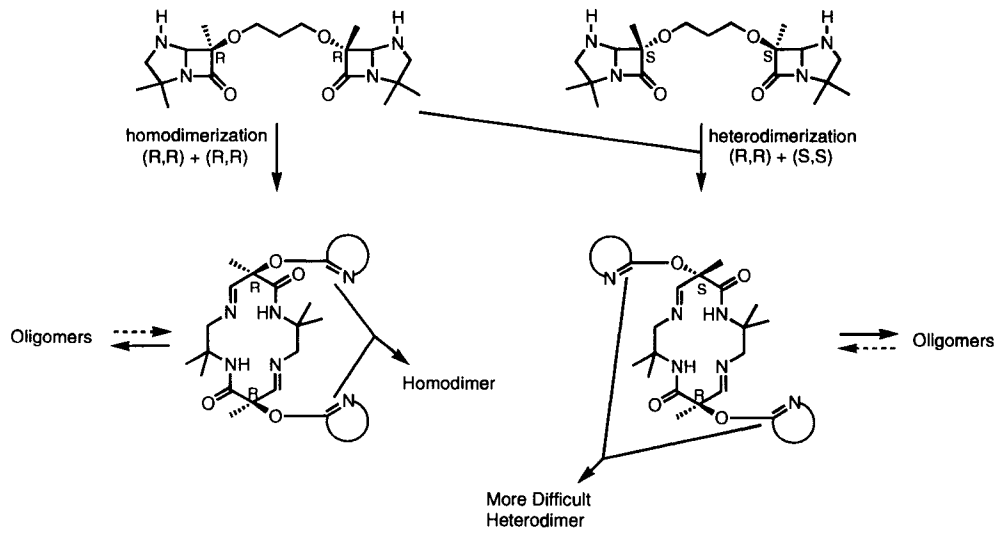

Scheme 6. Homodimerization vs Heterodimerization.

The formation of oligomeric byproducts were minimized by monitoring reaction conditions during dimerization and by reducing the imine bis-dioxocyclam **20** immediately upon its isolation. Separation of the *meso* and *d,l* bis-azapenams prior to dimerization provided simplified conditions that afforded the homo dimer preferentially.

The *meso* and *d,l* bis-dioxocyclams **1** were obtained from azapenams **19** in ≈50% yield, depending on bridge length.[5]

X-ray crystal structures were previously obtained of both *meso* and *d,l* bis-dioxocyclams **1** (n = 1).[5] For the *meso* ligand, the two centers of coordination are ≈6.3 Å apart and the planes of the two rings are virtually parallel and eclipsed. The structure of the *d,l* ligand is quite different from the *meso*. Its two centers of coordination are much farther apart at 7.448 Å and the two rings are at an angle of ≈75 °, similar to an open book, and gauche.

Both nickel(II)[5] and copper(II)[6] complexes of the 1,3-propanediol-linked bis-dioxocyclams have been synthesized. Treatment of **1** (n = 1) with one equivalent of nickel(II) bromide afforded a mono-nickel *d,l* complex (Scheme 7).[5] X-ray crystallography of this complex showed, upon mono-complexation, the two rings move closer together to 6.758 Å from 7.448 Å in the free ligand. The two rings also align, becoming almost parallel while the torsion angle closes slightly from 75 °.

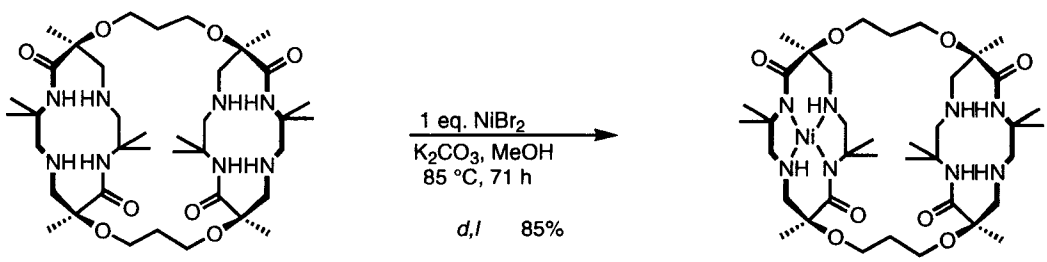

Scheme 7. Mono nickel complex of *d,l* bis-dioxocyclam.

Treatment of *meso* and *d,l* **1** (n = 1) with excess nickel(II) bromide or copper(II) tetrafluoroborate afforded complexed bis-dioxocyclams (Scheme 8). The structure of the metal complexes of the two *meso* and *d,l* diastereomers again change substantially from uncomplexed and mono-complexed structures. The *meso* complex has the two planar

metal dioxocyclam rings strictly face-to-face and eclipsed while the *d,l* rings are at an angle of ≈70 ° and gauche. In both of these metal complexes the metal ions are now separated by a distance of ≈7.5 Å.

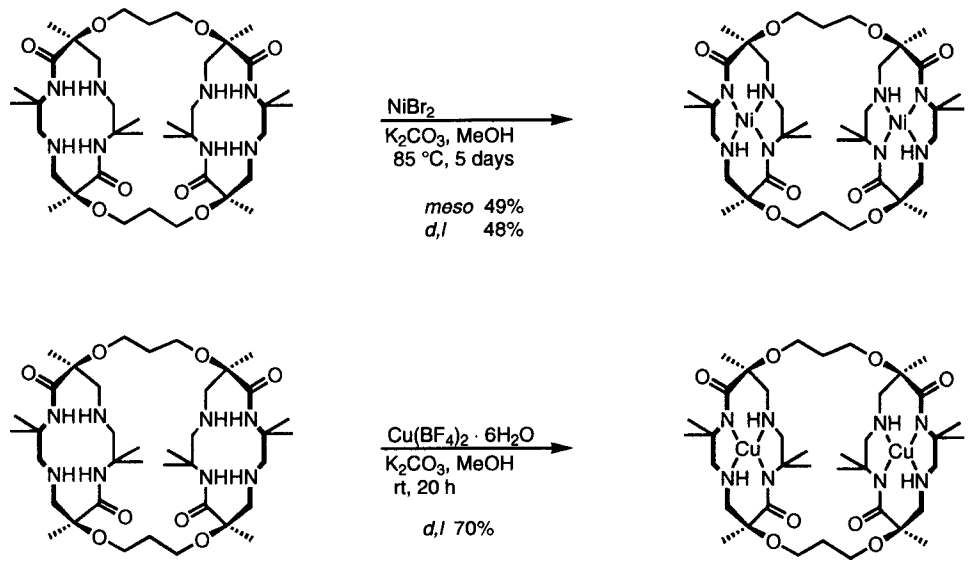

Scheme 8. Nickel and copper coordination of bis-dioxocyclams.

Pyridine-capped bis-dioxocyclams have been synthesized. Treatment of *meso* bis-dioxocyclam **1** (n = 1) with bis-(bromomethyl)pyridine and Na_2CO_3 gave pyridine-capped bis-dioxocyclam **3a** in 58% yield, while identical reaction conditions with the *d,l* bis-dioxocyclam **1** (n = 1) gave **3b** in 24% yield (Scheme 9).[7] Capping occurs from the face opposite the bridge, since the bridge face is very sterically hindered. This process is believed to proceed in a stepwise manner since formation of the mono-capped bis-dioxocyclam is observed by TLC prior to formation of bis-capped **3a/b**. Capping reactions with 4-substituted pyridine or pyrazine capping reagents and complexation of metals to capped bis-dioxocyclams have not yet been examined.

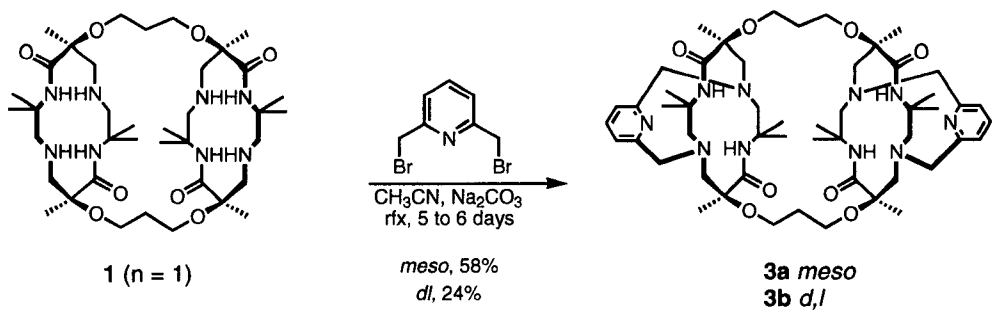

Scheme 9. Pyridine-capped bis-dioxocyclam.

Highly functionalized polyether-linked bis-dioxocyclams have also been synthesized in the Hegedus laboratories. *O*-acylation of the tetramethylammonium carbene complex **9** followed by acyl group replacement with tri- (n = 1) and tetra(ethylene glycol) (n = 2) to give the corresponding bis-carbene complexes **10** in good yield (Scheme 10).[8] The polyether-linked bis-azapenams were synthesized by photolysis in the presence of Cbz protected imidazoline. Hydrogenolysis of the Cbz group followed by acid-catalyzed dimerization and imine reduction afforded dioxocyclams **12** and **13**. Surprisingly, instead of obtaining a mixture of *meso* and *d,l* bis-dioxocyclams similar to the ether-linked dioxocyclams (above), a mixture of polyether-linked bis-dioxocyclam **13** and "basket" homo monocyclam **12** from the (R,R)/(S,S) bis-azapenam cyclizing on itself were obtained. This result also demonstrates the preference for centers of like configuration to undergo dimerization. The (R,R)/(S,S) pair brings two centers of like configuration together to give the "basket" homo monocyclam while the only way the (R,S) bis-azapenam could bring centers of like configuration together was through formation of the bis-dioxocyclam.

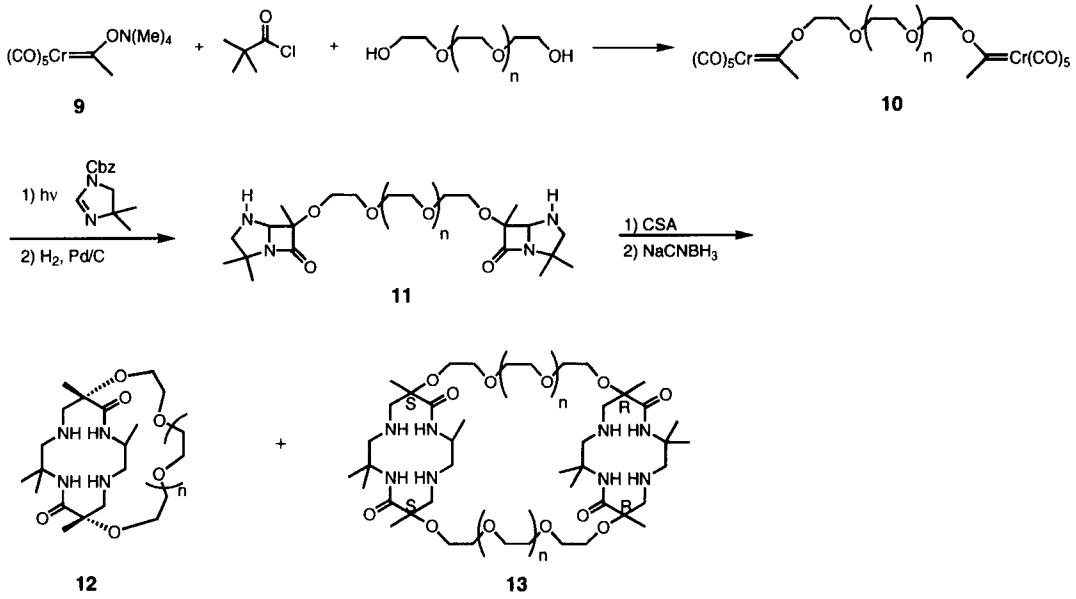

Scheme 10. Synthesis of polyether linked "basket" and bis-dioxocyclams.

Treatment of the "basket" monocyclams with nickel(II) bromide·3DMF or nickel(II) tetrafluoroborate in THF produced neutral nickel(II) monocyclam complex **14** (Scheme 11).[8] Likewise, the polyether-linked bis-dioxocyclams formed bis-nickel complex **15** when treated with nickel(II) tetrafluoroborate (Scheme 11). The structure of the bis-metal complexes of **15** are askew from a strictly face-to-face orientation at an angle of 27.3 °. Additionally, the two rings are not aligned parallel, rather they are rotated almost 90 ° with respect to one another, with the amide nitrogens of one ring aligning with the amines of the other. The metal-metal distance is also much longer compared to the ether-linked bis-dioxocyclam at 9.466 Å.

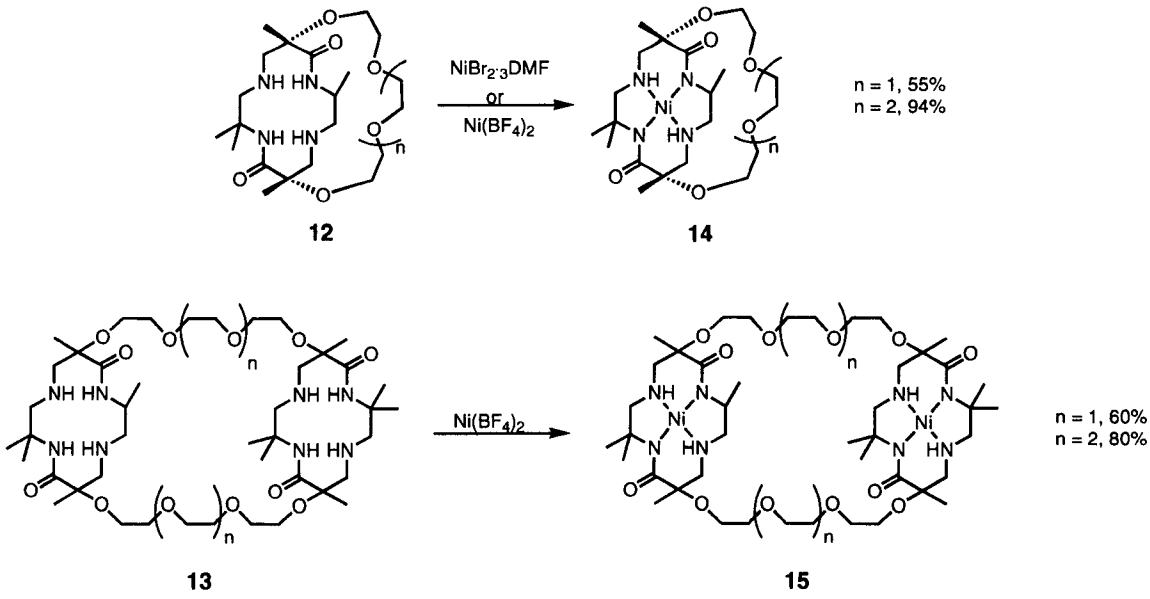

Scheme 11. Nickel complexes of "basket" and polyether-linked bis-dioxocyclams.

Capping of these polyether-linked bis-dioxocyclams was also investigated. Treatment of bis-dioxocyclam **13** (n = 2) with bis-(bromomethyl)pyridine and Na_2CO_3 afforded a bis-capped dioxocyclam (Scheme 12).[8] Surprisingly, the polyether-linked bis-dioxocyclams did not cap away from the bridging atoms but rather inside the cavity of the bis-dioxocyclam as was confirmed by X-ray crystallography (Figure 2).

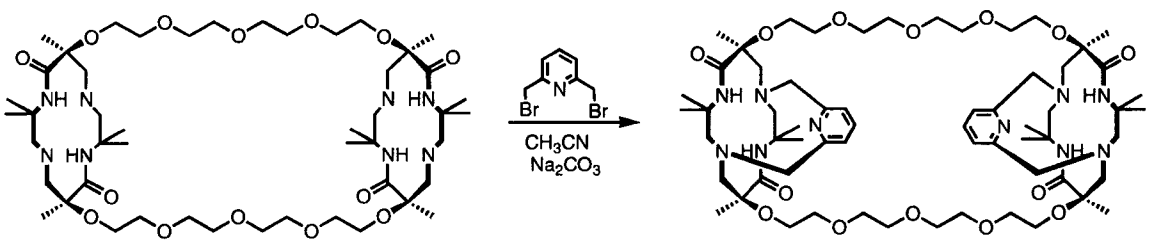

Scheme 12. Bis-capped polyether-linked bis-dioxocyclams.

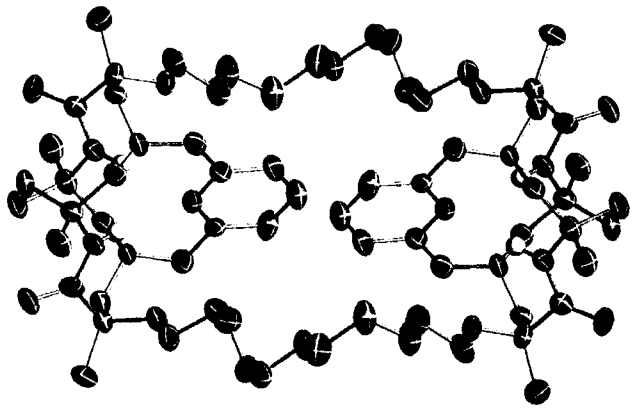

Figure 2. ORTEP of bis-capped polyether-linked bis-dioxocyclam.

The coordination of metals to bis-dioxocyclams and capped bis-dioxocyclams is relatively undeveloped, with nickel and copper the only examples in the literature.[4,5] Most importantly, their application to the synthesis of polymetallic complexes has yet to be examined. Metal complexes of bis-dioxocyclams would provide a polymetallic system that is covalently connected. Furthermore, capped bis-dioxocyclams with coordination sites at the 4-position of the capping reagent would allow coordination to additional metal complexes for the construction of coordination oligomers.

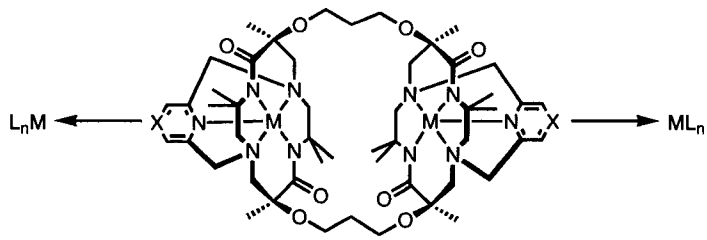

Figure 3. Polymetallic complexes of bis-dioxocyclams.

Additionally, the face-to-face ether-linked bis-dioxocyclams **1** synthesized in the Hegedus laboratories have a cavity between two coordinated metal centers, the dimensions of which can be controlled by choice of diastereomer and length of bridging alkyl groups. Control over the dimension of the cavity allows metal coordinated bis-

dioxocyclams to be "tuned" for the encapsulation of small bridging molecules such as pyrazine. These elaborations of bis-dioxocyclams will result in the synthesis of a new class of coordination complexes for use as building blocks in the synthesis of coordination polymers.

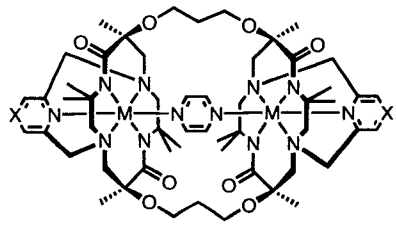

Figure 4. Encapsulation of small molecules.

Rationale

I. Bis-Dioxocyclam Incorporation into Polymetallic Complexes.

As presented in chapter 1, polymetallic complexes connected by π-conjugated bridging ligands often exhibit metal-metal interaction.[9] The challenges in synthesizing these complexes lie in controlling their construction, and in predicting their physical properties from structural features.[10,11]

Currently, research is focused on the synthesis of novel capped bis-dioxocyclams and their metal derivatives for use as building blocks for the synthesis of polymetallic complexes. To prepare bis-dioxocyclams for use in polymetallic complexes, four items must be addressed (Figure 5). 1) Incorporation of electron-donating and electron-withdrawing capping substituents to influence metal-metal interaction. 2) Introduction of redox active metals into the bis-dioxocyclam core. 3) Examination of bridging ligands that can coordinate to both of the metals within the bis-dioxocyclam. 4) Coordination of metal complexes such as bridging metals to the 4-position of the capping reagent.

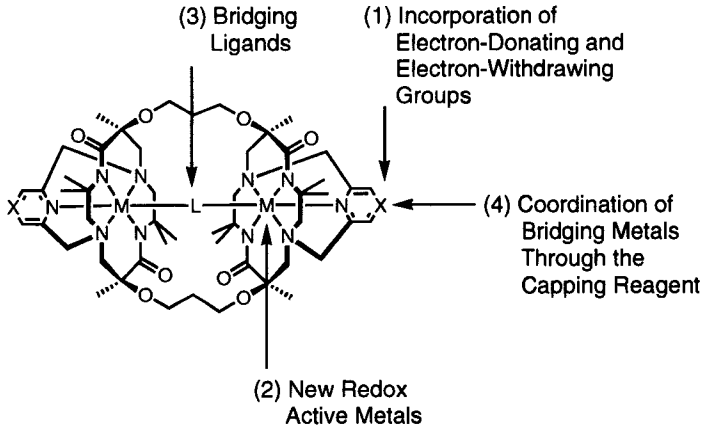

Figure 5. Bis-dioxocyclam modifications.

A. Ligand Manipulation

Similar to mono-dioxocyclams, synthetic approaches to a variety of 4-substituted capped dioxocyclams were investigated (Figure 6). Previous capping studies of bis-dioxocyclams have shown that capping is a stepwise process, probably due to conformational changes after one of the rings has been capped. A stepwise process could be advantageous for capping the bis-dioxocyclam with two different capping reagents (Figure 6).

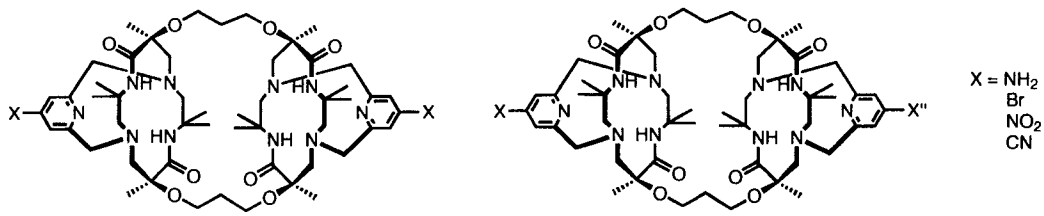

Figure 6. Incorporation of electron donating and withdrawing substituents.

B. Metal Coordination

Capped bis-dioxocyclams have two pentacoordinate sites for metal coordination. To synthesize the polymetallic complexes pictured in Figure 3 and Figure 4, metals capable of octahedral coordination were desired. Since metal coordination of capped bis-

dioxocyclams has never been investigated, studies began with copper and cobalt since methodology has been developed for their coordination to capped and uncapped mono-dioxocyclams. Ruthenium and iron coordination studies followed.

C. Incorporation of Bridging Ligands

Bis-dioxocyclams differ from mono-dioxocyclams in that they have a coordination cavity in-between the two rings. X-ray crystal analysis of nickel complexes of **1** (n=1) showed that the metal ions are separated by ≈7.5 Å (Figure 7). This distance is ideal for the encapsulation of small bridging molecules such as pyrazine. Pyrazine easily bridges distances between 6.8-7.8 Å[12], making pyrazine of interest for its coordination.

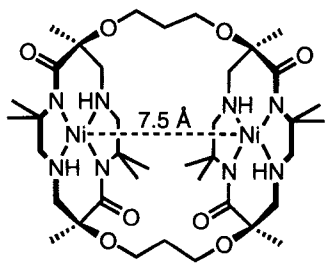

Figure 7. Distance between the metal faces for **1** (n = 1).

D. Incorporation of Bridging Metals

For capped bis-dioxocyclams, coordination can only occur through the 4-position of the capping reagent (Figure 8). Their coordination with rhodium acetates or ruthenium phthalocyanines could afford polymetallic complexes containing bridging metals. Alternatively, metal complexes of uncapped bis-dioxocyclams could lead to coordination through bridging ligands to provide polymetallic complexes (Figure 8).

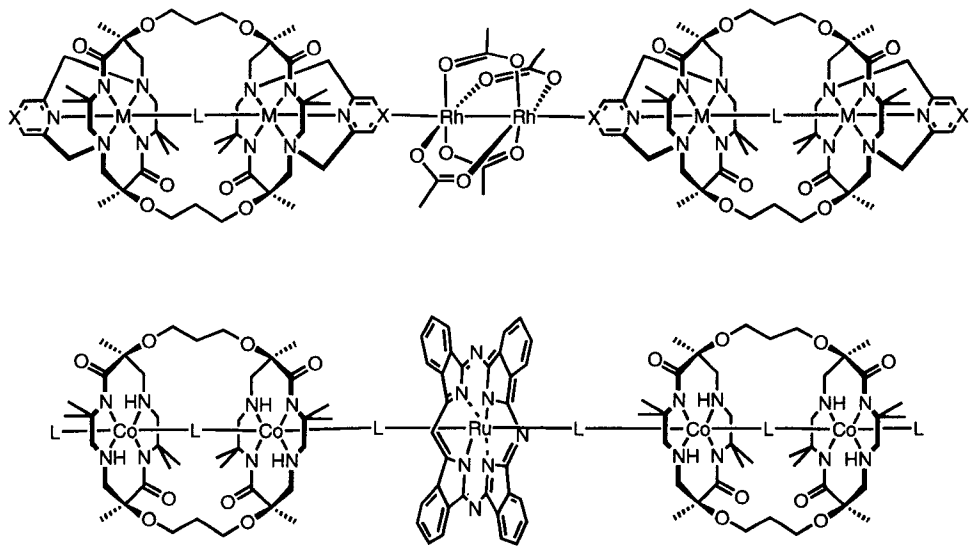

Figure 8. Metal bridging agents for polymetallic complexes.

Results and Discussion

Meso bis-dioxocyclam **1a** was synthesized following methodology previously established in the Hegedus group. The bis-carbene complex **16** was synthesized in a straightforward manner by *O*-acylation of tetramethylammonium carbene complex **9** followed by treatment with 1,3-propane diol. Photolysis of bis-chromium carbene complex **16** in the presence of benyloxycarbonyl (Cbz)-protected imidazoline **17** gave a protected bis-azapenam **18** in 59% yield as a 1:1 mixture of racemic diastereomers at the two alkoxy-methyl centers. Fortunately, the *d,l* diastereomer could be isolated by recrystallization while the *meso* remained in the mother liquor. The two diastereomers could be carried on separately. The N-protecting group was removed with Pd/C hydrogenation giving bis-azapenam **19a** or **19b**. Treatment with CSA opened the bis-azapenam to seven-membered cyclic imine, which underwent dimerization giving either **20a** or **20b**. Reduction of imine **20a** or **20b** with sodium cyanoborohydride in the

presence of benzoic acid gave *meso* bis-dioxocyclam **1a** or *d,l* bis-dioxocyclam **1b** respectively and in good yields (Scheme 13).[5]

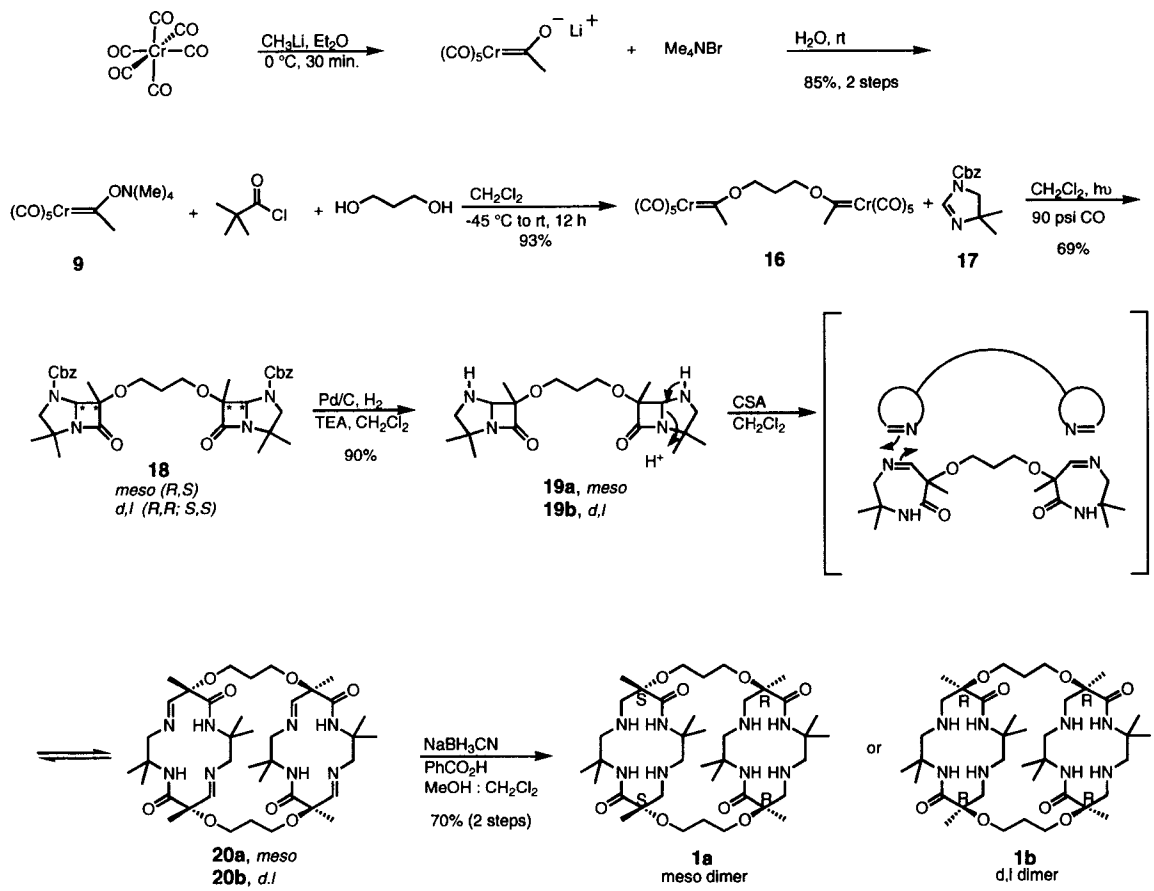

Scheme 13. *Meso* and *d,l* bis-dioxocyclam syntheses.

I. Capping Reagents

The same set of capping reagents used for the capping of mono dioxocyclams in chapter 1 were examined for capping the bis-dioxocyclams. The series included 2,6-bis(tosylmethyl)pyridine **2a**, 2,6-bis(bromomethyl)pyrazine **2b**, 4-amino-2,6-bis(bromomethyl)pyridine **2c**, 4-bromo-2,6-bis(tosylmethyl)pyridine **2d**, 4-nitro-2,6-bis(bromomethyl)pyridine **2e**, and 4-cyano-2,6-bis(bromomethyl)pyridine **2f** (Figure 9).

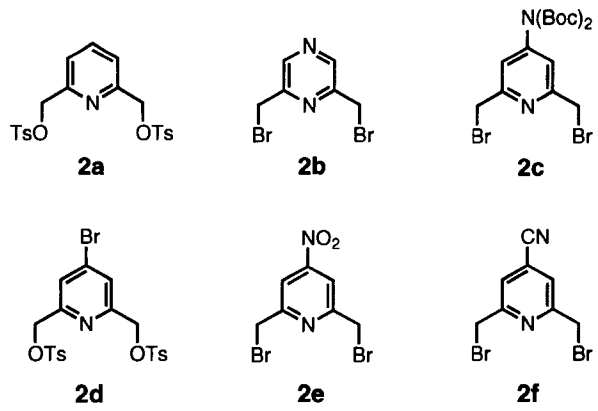

Figure 9. Capping reagents.

II. Bis-Dioxocyclam Capping Conditions

The first capping reagent examined was 4-nitro-2,6-bis(bromomethyl)pyridine **2e** (Table 1). Capping reactions were executed according to methodology previously developed in the Hegedus laboratories. Unfortunately, no capped bis-dioxocyclam was obtained with those conditions. A variety of capping conditions were examined, all of which resulted in recovery of starting material albeit in low yields (Table 1). The capping reactions were very complex showing the presence of multiple products by TLC. Expected products include starting material, mono-capped, bis-capped, and dioxocyclam oligomers resulting from the capping reagent reacting to two different bis-dioxocyclams. Chromatographic separation of the reaction mixtures never resulted in obtaining pure mono- or bis-capped dioxocyclam. Instead, ^{1}H NMR spectra of the separated aliquots resembled that of crude complex mixtures.

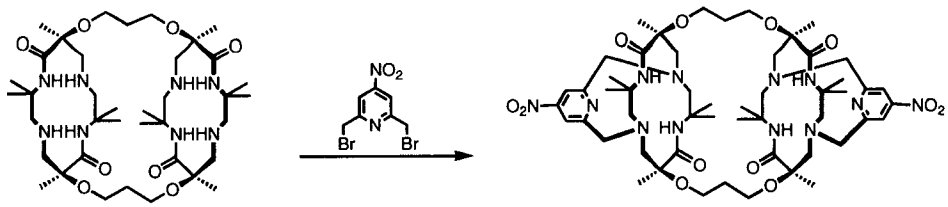

	Base	Solvent	Reaction Conditions	Product
1	Na_2CO_3	CH_3CN	70 °C, 4 days	starting material
			90 °C, 3 days	starting material
			80 °C, 5 days	starting material
			110 °C, 56 h	starting material
			105 °C, 3 days	starting material
2	$(i\text{-}Pr)_2NEt$	CH_3CN	70 °C, 4 days	starting material
		THF	rfx., $(Bu)_4NI$	starting material
		THF	sonication	starting material
		DMF	rfx. 3 days	decomposition

Table 1. Bis(bromomethyl)4-nitro pyridine capping reactions.

The problems with the 4-nitropyridine capping reagent were reminiscent to those encountered during microwave capping of the mono-dioxocyclam with 4-nitro-2,6-bis(bromomethyl)pyridine. Previously described capping conditions using heat for 3-4 days led to good yields of the 4-nitro-capped dioxocyclam **22** (Scheme 14). However, capping reactions carried out under microwave radiation afforded only a 6% yield of capped dioxocyclam. Perhaps the extended reactions times required for capping the bis-dioxocyclam resulted in decomposition, similar to the harsh conditions of microwave capping. To test this, mono-dioxocyclam **21** was treated with 4-nitropyridine capping reagent **2e** and heat for 7 days, conditions similar to that for bis-dioxocyclams (Scheme 14). The reaction was monitored by TLC, which showed the formation of capped dioxocyclam during the first few days. However, after day five, the capped dioxocyclam began to disappear. After a total of seven days, no capped dioxocyclam could be detected by TLC or isolated after purification. For reasons unknown to the investigators,

the 4-nitropyridine-capped dioxocyclam seemed to be unstable to the reaction conditions. If the mono-capped or bis-capped bis-dioxocyclam is also unstable, bis-capped material may be impossible to obtain with the 4-nitro capping reagent under these conditions.

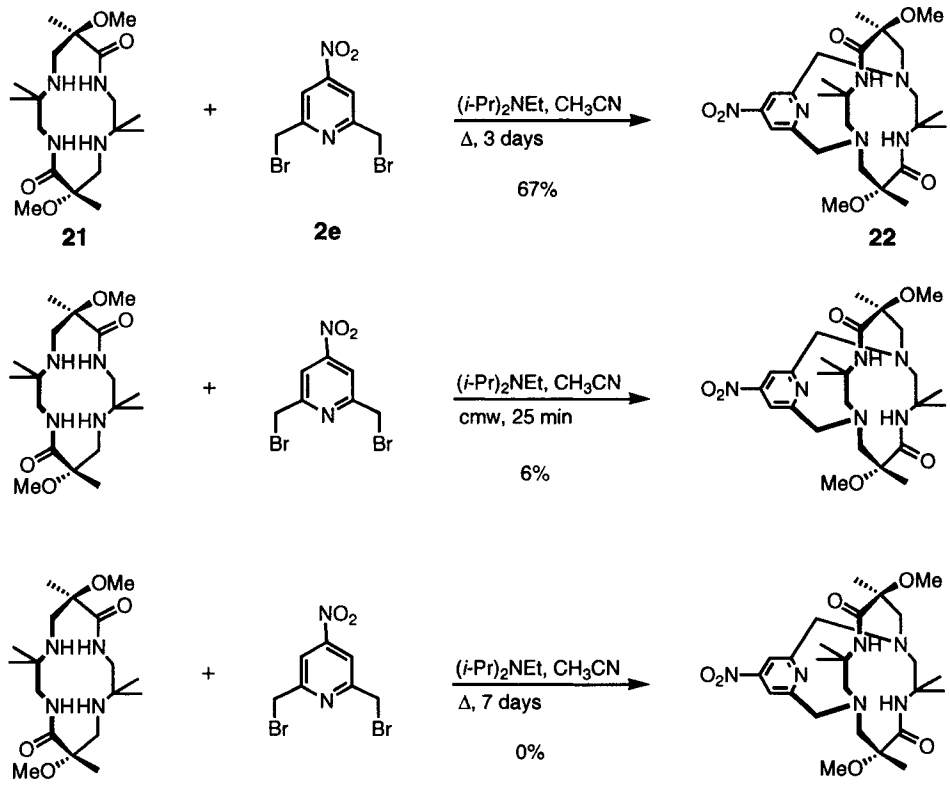

Scheme 14. The effect of capping conditions on the formation of **22**.

Fortunately, there were other capping reagents to examine. Capping studies continued with the 4-amino capping reagent **2c**. Treatment of *meso* bis-dioxocyclam with base in acetonitrile unfortunately did not result in mono- or bis-capped dioxocyclam (Table 2).

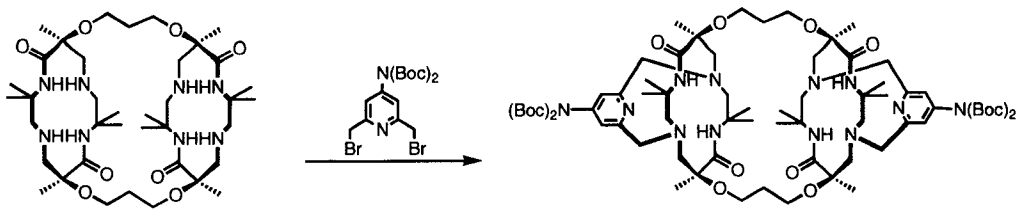

	Base	Solvent	Reaction Conditions	Product
1	Na_2CO_3	CH_3CN	70 °C, 4 days	starting material
2	Na_2CO_3	CH_3CN	65 °C, 8 days	starting material
3	$(i\text{-}Pr)_2NEt$	CH_3CN	65 °C, 6 days	starting material

Table 2. 4-amino capping reactions.

Capping of the bis-dioxocyclam proved to be more difficult than anticipated. To determine why the bis-capping reactions were not working, *meso* and *d,l* pyridine-capped bis-dioxocyclams were prepared according to literature procedure. As expected, both *meso* **3a** and *d,l* bis-pyridine-capped bis-dioxocyclams **3b** were obtained in good yields (Table 3, entry 1). With this inspiring result, capping with bis-(bromomethyl)pyrazine ensued. Treatment of *meso* and *d,l* bis-dioxocyclams with bis-(bromomethyl)pyrazine and sodium carbonate in CH_3CN afforded bis-capped dioxocyclams **4a** and **4b** albeit in modest yields (Table 3, entry 2). The instability of the capping reagent and the long reaction time (6-12 days) were responsible for the low yields of the reaction. It is important to note that the pyrazine capping reagent **2b** was added portion-wise throughout the reaction. Small amounts of the mono-capped dioxocyclam were isolated after purification. Surprisingly, only 2-5% of starting material was recovered from the reaction, a clear indication that the bis-dioxocyclam was decomposing or falling victim to oligomerization. **4a** and **4b** were characterized by mass spectrometry with a parent ion at

977.1 m/z. Single crystals of the mono-pyrazine-capped *d,l* bis-dioxocyclam **4b'** were obtained and examined by X-ray diffraction (Figure 10). Figure 10 shows the pyrazine-capped ring on the left and the uncapped ring to the right.

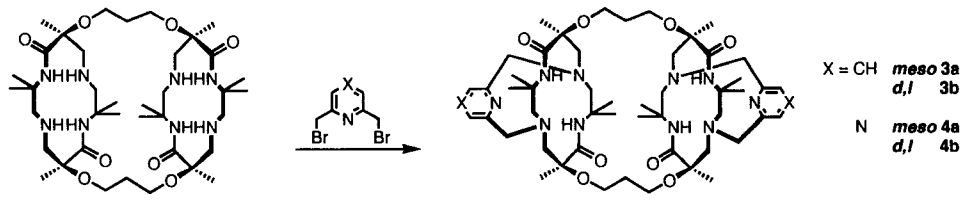

	Cap	*m/d,l*	Base	Solvent	Reaction Conditions	Yield
1	X = CH	*meso*	Na_2CO_3	CH_3CN	70 °C, 7 days	bis-capped 62%
		d,l	Na_2CO_3	CH_3CN	70 °C, 4 days	bis-capped 42%
2	X = N	*meso*	Na_2CO_3	CH_3CN	75 °C, 12 days	bis-capped 15% mono-capped 4% starting material 5%
		d,l	Na_2CO_3	CH_3CN	75 °C, 6 days	bis-capped 16% mono-capped 14% starting material 2%

Table 3. Pyridine and pyrazine capping reactions.

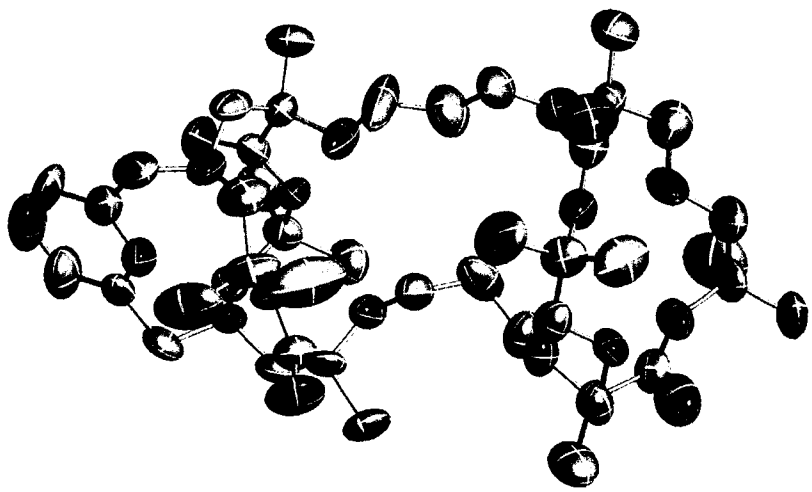

Figure 10. ORTEP drawing of mono-pyrazine-capped *d,l* bis-dioxocyclam **4b'**.

Capping the bis-dioxocyclam with reagents besides pyridine proved to be more difficult than expected. X-ray structure analysis of the mono-capped dioxocyclam **4b′** provided some insight into the capping reactions. When compared to the uncapped bis-cyclam **1b**, the conformation of the uncapped ring of the mono-capped cyclam **4b′** changed quite a bit, reminiscent of the mono-nickel bis-dioxocyclam complex. First, the distance between the two amine and amide nitrogens across the face of the ring changed. Dioxocyclam **1b** has the amine nitrogens at 3.865 and 3.804 Å separation across the ring face while the amide nitrogens are 4.125 and 4.111 Å separation (Figure 12). After one capping reagent is attached, the second uncapped ring flattens with the amine nitrogens for **4b′** being 4.081 Å apart, similar to the amide nitrogens that are separated by 4.061 Å. Additionally, the lone pairs (l.p.) of the amine nitrogens in the uncapped ring **4b′** now seem to be pointing in toward the middle of the ring and could be involved in hydrogen bonding with the amide hydrogens (Figure 11).[13] The two dioxocyclam rings also move away from each other after mono-capping. Remember, the two faces of the *d,l* dioxocyclam resemble an open book. For **1b**, the nitrogens making up the spine of the book are 5.888 and 5.997 Å apart while the external nitrogens are 9.037 and 9.059 Å apart (Figure 12).[14] For **4b′**, the nitrogens making up the spine of the book are now 7.306 and 7.978 Å apart with the external at 8.289 and 9.505 Å. This is a significant difference in the relative arrangement of the two macrocyclic rings. These structural factors could have a drastic effect on capping of the second ring making long reaction times necessary. Decomposition or instability of the intermediates and starting materials due to long reaction times could have a detrimental effect on obtaining bis-capped bis-dioxocyclams.

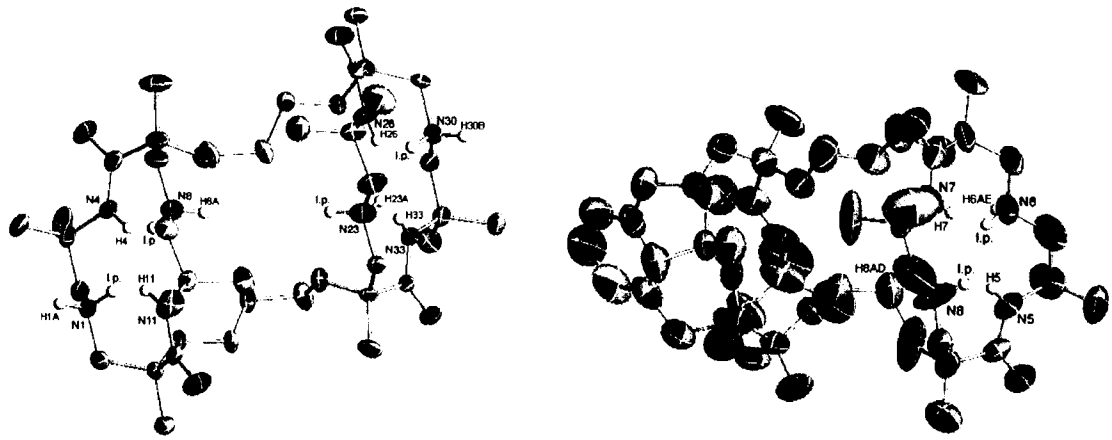

Figure 11. ORTEP diagrams of **1** (left) and **4b′** (right) bis-dioxocyclams

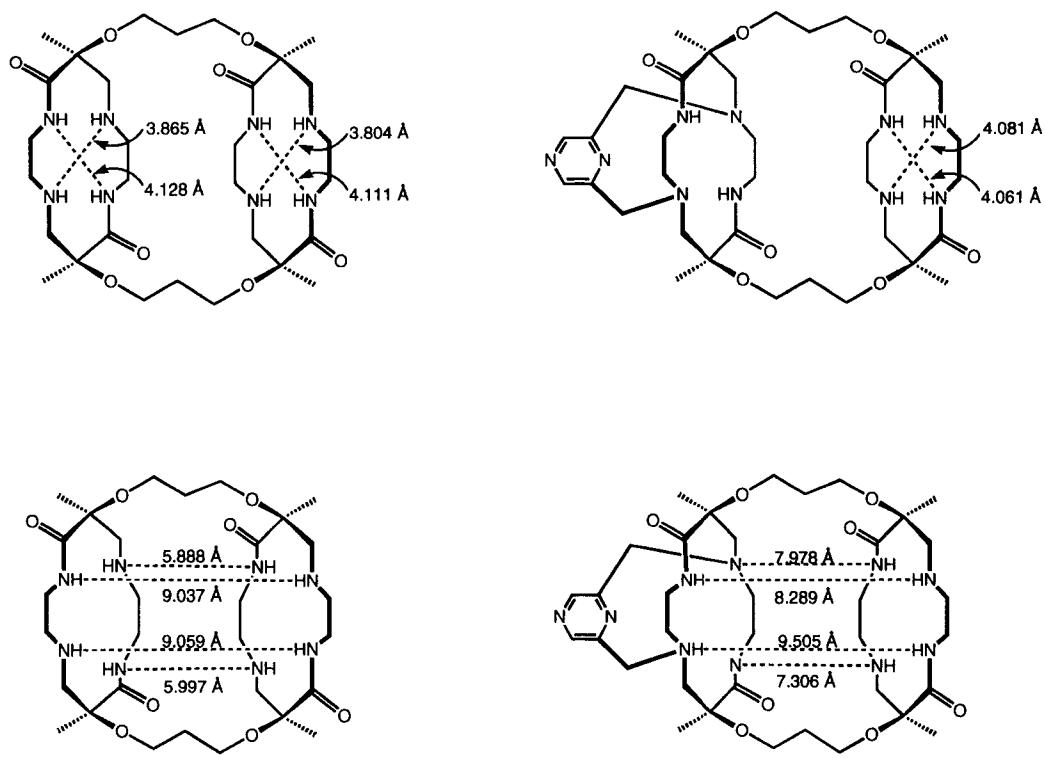

Figure 12. Nitrogen distance comparisons for **1** (left) and **4b′** (right) bis-dioxocyclams.

Microwave capping conditions were examined since the long reaction times seem to be problematic. Treatment of *meso* bis-dioxocyclam **1a** with the pyridine capping reagent **2a** and $(i\text{-Pr})_2$NEt in acetonitrile under microwave radiation for periods of 2 minutes at a power level of 2 did not result in capped bis-dioxocyclam. Radiation for

nearly 3 hours resulted in no reaction with recovery of bis-dioxocyclam. This result was very surprising since the mono-dioxocyclams cap in the microwave within a matter of minutes. Since capping conditions could not be improved with microwave radiation, pyridine- and pyrazine-capped bis-dioxocyclams obtained by heating were carried on for metal coordination studies.

III. Metal Coordination

A. Copper Coordination

Treatment of **4b** with copper(II) tetrafluoroborate with K_2CO_3 afforded the bis-copper complex **5** in excellent yields (Scheme 15). An IR carbonyl stretch was observed at1572 cm^{-1}, demonstrating that the amide nitrogens were coordinated. Mass spectrometry of **5** confirmed a parent ion at 1101 m/z (calc. 1100). The difference in mass may be a result of one of the amide nitrogens being protonated. The isotopic distribution however, did not exactly match that which is expected for **5**. Six isotope peaks were observed (expected) but not with the correct distribution. Similar peculiarities were observed in a related complex which was also coordinated to copper(II).[15] Further study is needed to determine the exact nature **5** and to determine the exact coordination motif of the complex.

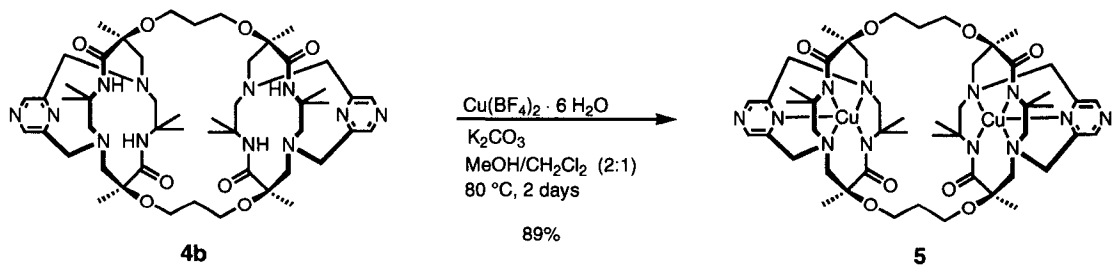

4b **5**

Scheme 15. Copper coordination with pyrazine-capped bis-dioxocyclam.

Coordination of an additional ligand between the two copper centers was examined. Treatment of **5** with pyrazine in CH_2Cl_2 unfortunately resulted in no further coordination (Scheme 16), again demonstrating the need for metals that coordinate in an octahedral environment.

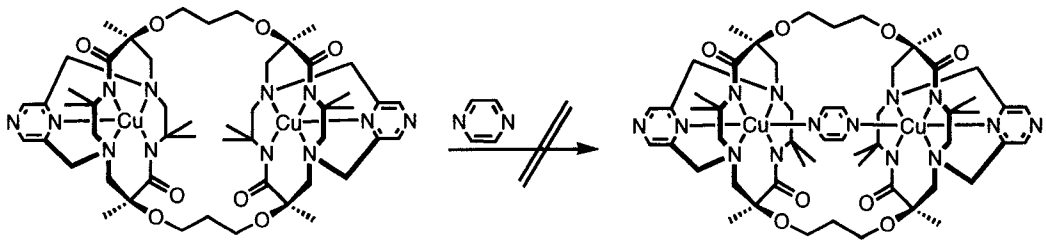

5

Scheme 16. Pyrazine-copper coordination.

B. Cobalt Coordination

Cobalt coordination of uncapped bis-dioxocyclams were examined first because of ease of introduction. Treatment of *d,l* bis-dioxocyclam **1b** with cobalt(II) acetate in MeOH afforded the mono-ring opened bis-dioxocyclam **6**, similar to the observed mono-dioxocyclam system. Infrared spectroscopy showed several carbonyl stretches at 1773 cm^{-1}, 1709 cm^{-1}, 1670 cm^{-1}, and 1572 cm^{-1}. These absorptions corresponded to the four different carbonyls present in the ring opened bis-dioxocyclam.

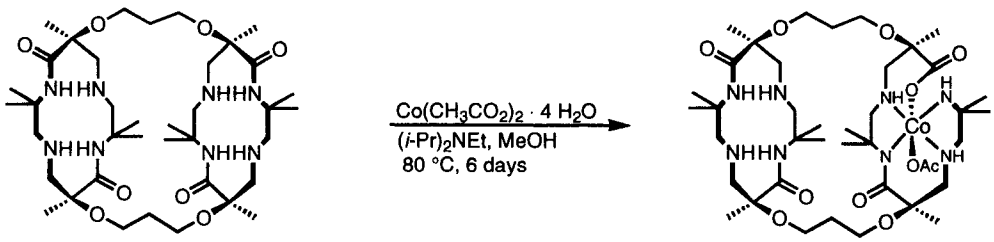

1b **6**

Scheme 17. Cobalt coordination resulting in a ring opened bis-dioxocyclam.

The coordination of mono-dioxocyclam with Co(III) acetylacetonate proved to be successful without hydrolysis of the amide bond. These reaction conditions were then applied to the bis-dioxocyclam system. Reaction of *meso* bis-dioxocyclam with Co(II) and Co(III) acetylacetonate has been inconclusive. Examination of the crude mixture by infrared spectroscopy showed carbonyl stretches at 1666 cm^{-1} corresponding to uncoordinated amide nitrogens, and 1580 cm^{-1} corresponding to metal-coordinated amide nitrogens. Mass spectroscopy of the crude mixture also identified the formation of **7** having a parent peak at 926.4 m/z. However, purification of the crude material on did not result in isolation of coordinated product. Instead, starting material was recovered.

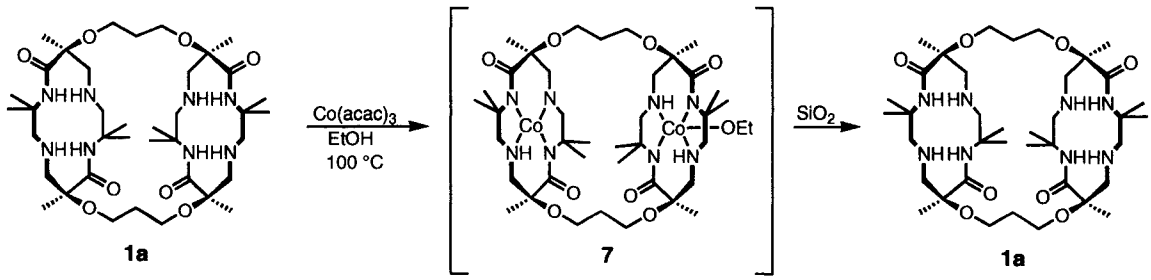

Scheme 18. Uncapped bis-dioxocyclam cobalt coordination.

Cobalt coordination of capped bis-dioxocyclams was also examined. Bis-pyridine-capped bis-dioxocyclam **1b** was treated with cobalt(II) acetate and $(i\text{-Pr})_2NEt$ in MeOH under microwave radiation for increments of 2 minutes at a power level of 2 for a total of 1 hour and 40 minutes (Scheme 19). Surprisingly, instead of bis-coordinated product, only mono-cobalt complex **8** was obtained in very low yields. Infrared spectroscopy confirmed this structure with a carbonyl stretches at 1659 cm^{-1}, 1617 cm^{-1}, and 1572 cm^{-1}.

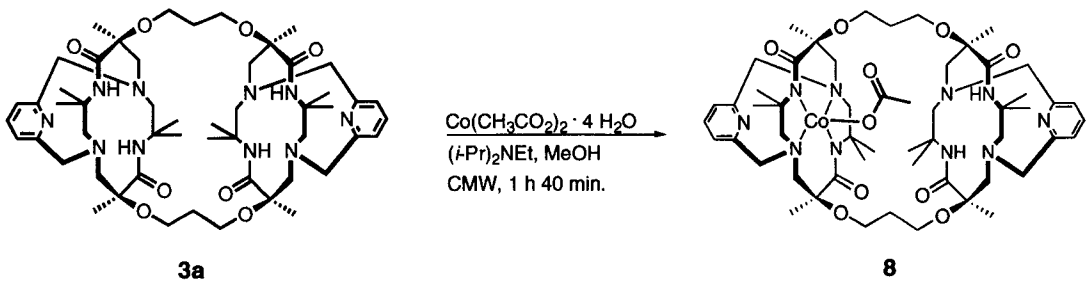

3a 8

Scheme 19. Bis-pyridine-capped bis-dioxocyclam cobalt(II) coordination.

Future Work

There is much work to be done on the bis-dioxocyclam project. For the uncapped bis-dioxocyclams, coordination of cobalt acetylacetonate to uncapped bis-dioxocyclams may require additional time, or the use of base. This methodology may prove useful for the coordination of ruthenium and iron. For the bis-capped bis-dioxocyclams, longer reaction times for the microwave assisted coordination of cobalt(II) acetate with pyridine- and pyrazine-capped bis-dioxocyclams should be examined. It may be possible that acetate ligand attached to cobalt could sterically hinder coordination of a second cobalt atom. Copper complexes of pyridine- and pyrazine-capped **3a,b** and **4a,b** could be examined for magnetic based metal-metal interactions. Additionally, the copper complexes of pyrazine capped **4a,b** would allow for coordination to other metal complexes through the 4-position of the capping reagent. Once synthesized, these novel compounds could be tested for metal-metal communication.

Conclusions

The difficulty of capping bis-dioxocyclams was completely underestimated. Fortunately, even with the difficulties experienced with capping, both pyridine- and pyrazine-capped *meso* and *d,l* bis-dioxocyclams were obtained. The synthesis of copper coordinated bis-capped bis-dioxocyclams was demonstrated with the synthesis of **5**.

Experimental Section

General Procedures. Acetonitrile was distilled over calcium hydride. Methanol was distilled over calcium hydride and dried over molecular sieves. NMR spectra were recorded on a Varian JS-300. Infrared spectra were recorded on a Nicolet Magna-IR 760 spectrometer. UV-vis spectra were recorded on an Agilent G 1103 spectrometer. Electrochemical measurements were conducted with an EG and G, Princeton Applied Research, model 75 universal programmer, model 179 digital coulometer, and model 173 potentiostat/galvanostat. The complex was dissolved in a 0.1 M solution of tetrabutylammonium hexafluorophosphate in acetonitrile or CH_2Cl_2. The working electrode was either a glassy carbon or platinum. The counter electrode was a platinum wire. The reference electrode was a silver wire. Potentials were calculated versus SCE. Cyclic voltammograms were obtained at a scan rate of 100 mV/s. Data were plotted with the *x*-axis equal to 100 mV/cm. Microwave reactions were performed in a GE countertop microwave oven, model number JES1339WC, which had a capacity of 1.3 cubic feet (1.21 L) and a watt output of 1,100W. X-ray crystallographic studies were performed on a Bruker SMART CCD diffractometer, and the intensity of the data set was integrated using Bruker SAINT software. The structures were solved using Bruker SHELXTL V6.1 software. Compounds **2a-2g** and **2i-2k** were synthesized by published procedures.

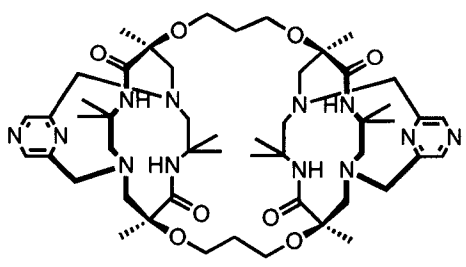

Bis-pyrazine-capped *meso* bis-dioxocyclam (4a). *Meso* bis-dioxocyclam **1a** (65.1 mg, 0.0847 mmol), bis-(bromomethyl)pyrazine **2b** (49.5 mg, 0.1862 mmol), Na_2CO_3 (89.7 mg, 0.847 mmol) and 4 mL

CH_3CN were combined in a pressure tube, oven dried under argon, and heated to 80 °C for 12 days. The solution was cooled to room temperature and filter over Celite. The solvent was removed in vacuo. Purification by flash chromatography on silica gel (7% MeOH:CH2Cl2) afforded **4a** as a white solid in 15% yield. ^{1}H NMR ($CDCl_3$, 300 MHz) δ 8.14 (s, 4H), 7.57 (s, 4H), 3.82 (d, *J*=4.0 Hz, 4H), 3.60 (m, 8H), 3.50 (s, 2H), 3.44 (m, 4H), 3.14 (d, *J*=15.3 Hz, 4H), 2.84 (dd, J=15.0, 13.1 Hz, 8H), 2.67 (d, *J*=13.1 Hz, 4H), 1.33 (s, 12H), 1.28 (s, 12H), 1.22 (s, 12H). FT-IR (film) 1658 cm^{-1}; LRMS (FAB^+, *m/z*) calcd for $C_{50}H_{80}N_{12}O_8$ ($M+H^+$) 977.62, found 977.1.

Preparation of mono- and bis-pyrazine-capped *d,l* bis-dioxocyclams. *d,l* Bis-dioxocyclam **1b** (147.0 mg, 0.191 mmol), bis-(bromomethyl)pyrazine **2b** (111.8 mg, 0.4205 mmol), Na_2CO_3 (202.6 mg, 1.911 mmol) and 8 mL CH_3CN were combined in a pressure tube, oven dried under argon, and heated to 80 °C for 6 days. The solution was cooled to room temperature and filter over Celite. The solvent was removed in vacuo. Purification by flash chromatography on silica gel (7% MeOH:CH_2Cl_2) afforded **4b** as a white solid in 16% yield and **4b′** as a white solid in 14% yield.

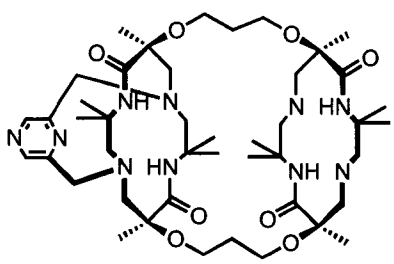

Monopyrazine-capped *d,l* bis-dioxocyclam (4b′). ^{1}H NMR ($CDCl_3$, 300 MHz) δ 8.79 (s, 2H), 8.13 (s, 1H) 7.721 (s, 1H), 3.89 (s, 2H), 3.49 (m, 7H), 3.26 (s, 1H), 3.19 (d, *J*=15.3 Hz, 2H), 2.86 (d, *J*=15.0 Hz, 3H), 2.75 (d, *J*=7.8 Hz, 6H), 2.63 (d, *J*=17.5 Hz, 6H), 1.41 (s, 6H), 1.35 (s, 6H), 1.28 (s, 6H), 1.25 (s, 6H), 1.24 (s, 6H), 1.19 (s, 6H).

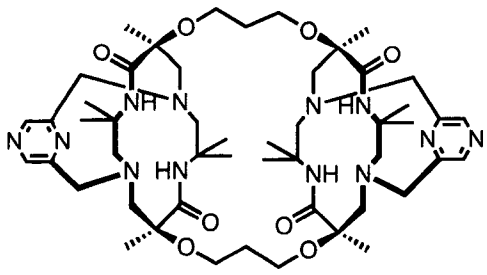

Bis-pyrazine-capped d.l bis-dioxocyclam (4b). ^{1}H NMR ($CDCl_3$, 300 MHz) δ 8.14 (s, 3H), 7.57 (s, 3H), 3.84 (s, 5H), 3.56 (m, 12 H), 3.18 (d, *J*=15.0 Hz, 4H), 2.77 (m, 14H), 1.32 (s, 12H), 1.27 (s, 12H), 1.22 (s, 12H); ^{13}C NMR ($CDCl_3$, 100 MHz) δ 172.3, 154.6, 140.3, 84.2, 67.8, 65.4, 63.4, 60.6, 54.2, 41.2, 29.0, 25.3, 21.5; FT-IR (film) 1659 cm^{-1}; LRMS (FAB$^+$, *m/z*) calcd for $C_{50}H_{80}N_{12}O_8$ (M+H$^+$) 977.62, found 977.1.

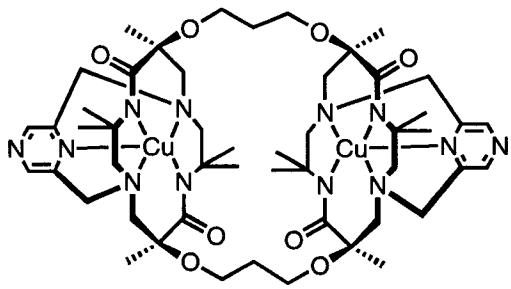

Bis-pyrazine-capped *d,l* bis-dioxocyclam copper(II) complex (5). The bis-pyrazine-capped bis-dioxocyclam **4b** (22.2 mg, 0.0227 mmol), copper(II) tetrafluoroborate·6H_2O (107.7 mg, 0.4543 mmol), and K_2CO_3 (31.9 mg, 0.2272 mmol) were combined in a screw cap pressure tube along with 1 mL CH_2Cl_2 and 2.6 mL MeOH. The solution was stirred at 80 °C. Over the course of two days, the solution turned from a pale yellow/blue color to dark green. The solution was then filtered over Celite and solvent was removed in vacuo. The crude was brought up in a 1:1 mixture of MeOH:CH_2Cl_2 and washed with distilled water. The organic layer was isolated and the aqueous layer was washed 3×10 mL CH_2Cl_2. The solvent was removed in vacuo providing 22.1 mg or **5** as a pale green solid in 89% yield. Single crystal X-ray quality crystals were not obtained under a variety of conditions. FT-IR (film) 1572 cm^{-1}; LRMS (FAB$^+$, *m/z*) calcd for $C_{50}H_{76}Cu_2N_{12}O_8$ (M+H$^+$) 1099.45, found 1100.0.

References

1 (a) Ciampolini, M.; Fabbrizzi, L.; Perottti, A.; Seghi, B.; Zanobini, F. *Inorg. Chem.* **1987**, *26*, 3527. (b) Schneider, R.; Reisen, A.; Kaden, T. A. *Helv. Chim. Acta* **1986**, *69*, 53. (c) Weighardt, K.; Tolksdorf, J.; Hermann, W. *Inorg. Chem.* **1985**, *24*, 1230. (d) Garcia-Espana, E.; Micheloni, M.; Paoletti, P.; Bianchi, A. *Gazz. Chim. Ital.* **1985**, 115. (e) Ciampolini, M.; Micheloni, M.; Nardi, N.; Vizza, F.; Buttafava, A.; Fabbrizzi, L.; Perotti, A. *J. Chem. Soc., Chem. Comm.* **1984**, 998.

2 Brandes, S.; Denat, F.; Lacour, S.; Rabiet, F.; Barbette, F.; Pullumbi, P.; Guilard, R. *Eur. J. Org. Chem.* **1998**, 2349.

3 Tomalia, D. A.; Wilson, L. R. U. S. Patent 4,517,122, **1986**.

4 (a) Fabbrizzi, L.; Forlini, L.; Perotti, A.; Seghi, B. *Inorg. Chem.* **1984**, *23*, 807. (b) Buttafava, A.; Fabbrizzi, L.; Perotti, A.; Poggo, A.; Seghi, B. *Inorg. Chem.* **1984**, *23*, 3917. (c) Fabbrizzi, L.; Montagna, L.; Poggo, A.; Kaden, T. A.; Siegfried, L. C. *Inorg. Chem.* **1988**, *27*, 1986.

5 Dumas, S.; Lastra, E.; Hegedus, L. S. *J. Am. Chem. Soc.* **1995**, *117*, 3368.

6 Wynn, T. *Ph.D. Dissertation, Colorado State University* **2000**.

7 Wynn, T.; Hegedus, L. S. *J. Am. Chem. Soc.* **2000**, *122*, 5034

8 Puntener, K.; Hellman, M. D.; Kuester, E.; Hegedus, L. S. *J. Org. Chem.* **2000**, *65*, 8301.

9 (a) Ito, T.; Hamaguchi, T.; Nagino, H.; Yamaguchi, T.; Kido, H.; Zavarine, I. S.; Richmond, T.; Washington, H.; Kubiak, C. P. *J. Am. Chem. Soc.* **1999**, *121*, 4625. (b) Creutz, C.; Taube, H. *J. Am. Chem. Soc.* **1969**, *91*, 3988. (b) Creutz, C.; Taube, H. *J. Am. Chem. Soc.* **1973**, *95*, 1086. (c) Launay, J. P. *Chem. Soc. Rev.* **2001**, *30*, 386. (d) Kuhn, F. E.; Zuo, J. L.; Fabrizi de Biani, F.; Santos, A. M.; Zhang, Y.; Zhao, J.; Sandulache, A.; Herdtweck, E. *New. J. Chem.* **2004**, *28*, 43. (e) Benniston, A. C.; Mitchell, S.; Rostron, S. A.; Yang, S. *Tetrahedron Lett.* **2004**, *45*, 7883. (f) Contakes, S. M.; Klausmeyer, K. K.; Rauchfuss, T. B. *Inorg. Chem.* **2000**, *39*, 2069. (g) Vahrenkamp, H.; Geiss, A.; Richardson, G. N. *J. Chem. Soc., Dalton Trans.* **1997**, 3643.

10 *Crystal Engineering*; Seddon, K. R.; Zaworotko, M. J., Eds. Kluwer Academic Publishers: Dordrecht, The Netherlands, 1999.

11 (a) Robson, R. *J. Chem. Soc., Dalton Trans.* **2000**, 3735. (b) Liang, K.; Zheng, H.; Song, Y.; Lappert, M. F.; Li, Y.; Xin, X.; Huang, Z.; Chen, J.; Lu, S. *Angew. Chem. Int. Ed.* **2004**, *43*, 5776.

12 (a) Collman, J. P.; McDevitt, J. T.; Leidner, C. R.; Yee, G. T.; Torrance, J. B.; Little, W. A. *J. Am. Chem. Soc.* **1987**, *109*, 4606. (b) Ma, B.; Gao, S.; Yi, T.; Xu, G. *Polyhedron*, **2001**, *20*, 1255.

13 The lone pairs of the nitrogen atoms are labeled l.p. on the ORTEP diagram. The hydrogen atoms are labeled Hx, with x being a number that relates the hydrogen to its corresponding nitrogen atom (i.e. N7-H7).

14 The gem dimethyl groups of the bis-dioxocyclam were omitted for clarity.

15 Bolig, A. *Ph.D. Dissertation, Colorado State University* **2005**.

CHAPTER THREE

X-RAY CRYSTAL STRUCTURES

The X-ray crystal structures discussed in chapters 1 and 2 and all other single crystals from the Hegedus labs for the period of three years were solved by the author with the assistance of Susie Miller. Crystallography training from Susie Miller included the mounting of single crystals on the diffractometer, collection of data, integration of data, and solving the data to obtain the crystal structure. Additionally, many structures were prepared for publication, which involved the checking of CIF files followed by further changing of the crystal data or explanations to account for alerts found during CIF checking. Much time was spent in understanding the intricate details required to solve the large-molecule structures of dioxocyclams.

Obtaining good data for X-ray crystal structures for the compounds discussed in Chapters 1 and 2 was not a facile process. As discussed in chapter 1, the crystals of the dioxocyclam complexes were often poor, suffering from powdering and low reflection. Once a suitable data set was obtained, much time was spent trying to optimize that data due to poor data to parameter ratios. Disordered solvent molecules and poor data to parameter ratios contributed to the high R values observed for almost all data sets. Optimizing the data often took several days or weeks so that R values suitable for publication could be obtained.

X-ray crystal structures were fundamental to understanding how the dioxocyclam complex was affected by the different capping reagents and their coordination to rhodium and ruthenium complexes. Solving the X-ray crystal structures was extremely challenging but also equally enjoyable.

I. Chapter 1 X-Ray Crystal Structures

A. lsh129m, 43

Table 1. Crystal data and structure refinement for lsh129m, **43**.

Identification code	lsh129m	
Empirical formula	C_{20} H_{39} Co N_4 O_7	
Formula weight	506.48	
Temperature	173(2) K	
Wavelength	0.71073 Å	
Crystal system	Monoclinic	
Space group	P2(1)/n	
Unit cell dimensions	a = 10.130(2) Å	α= 90°.
	b = 22.392(5) Å	β= 93.177(3)°.
	c = 10.637(2) Å	γ= 90°.
Volume	2409.0(8) $Å^3$	
Z	4	
Density (calculated)	1.396 Mg/m^3	
Absorption coefficient	0.759 mm^{-1}	
F(000)	1080	
Crystal size	0.50 x 0.50 x 0.20 mm^3	
Theta range for data collection	1.82 to 28.43°.	
Index ranges	-13<=h<=13, -30<=k<=29, -13<=l<=13	
Reflections collected	22051	
Independent reflections	5911 [R(int) = 0.0639]	
Completeness to theta = 28.43°	97.4 %	
Absorption correction	Semi-empirical from equivalents	
Max. and min. transmission	0.8630 and 0.7028	
Refinement method	Full-matrix least-squares on F^2	
Data / restraints / parameters	5911 / 0 / 299	
Goodness-of-fit on F^2	1.166	
Final R indices [I>2sigma(I)]	R1 = 0.0510, wR2 = 0.1188	
R indices (all data)	R1 = 0.0574, wR2 = 0.1229	
Extinction coefficient	0.041(2)	
Largest diff. peak and hole	1.712 and -0.831 e.$Å^{-3}$	

Table 2. Atomic coordinates (x 10^4) and equivalent isotropic displacement parameters ($Å^2$x 10^3) for lsh129m. U(eq) is defined as one third of the trace of the orthogonalized U^{ij} tensor.

	x	y	z	U(eq)
Co(1)	1757(1)	8929(1)	2541(1)	17(1)
O(1)	4174(2)	7815(1)	550(1)	31(1)
O(2)	2620(1)	8948(1)	-730(1)	23(1)
O(3)	-1623(1)	8758(1)	346(1)	35(1)
O(5)	401(1)	8824(1)	1235(1)	20(1)
O(6)	3260(1)	9085(1)	3721(1)	23(1)
O(7)	-1628(1)	8955(1)	3319(1)	27(1)
O(8)	2201(2)	9172(1)	5522(1)	38(1)
N(1)	2807(2)	8275(1)	1919(2)	20(1)
N(2)	2437(1)	9533(1)	1429(1)	18(1)
N(3)	812(1)	9608(1)	3284(1)	20(1)
N(4)	962(2)	8337(1)	3623(2)	21(1)
C(1)	3566(2)	8264(1)	925(2)	21(1)
C(2)	3732(2)	8852(1)	153(2)	20(1)
C(3)	2176(2)	8437(1)	-1439(2)	33(1)
C(4)	5007(2)	8825(1)	-561(2)	26(1)
C(5)	3765(2)	9416(1)	966(2)	20(1)
C(6)	2349(2)	10133(1)	2023(2)	21(1)
C(7)	1012(2)	10192(1)	2622(2)	21(1)
C(8)	-125(2)	10277(1)	1633(2)	26(1)
C(9)	1060(2)	10712(1)	3561(2)	31(1)
C(15)	1985(2)	7861(1)	3850(2)	25(1)
C(16)	2698(2)	7704(1)	2643(2)	24(1)
C(17)	1955(2)	7228(1)	1820(2)	38(1)
C(18)	4052(2)	7449(1)	3117(2)	39(1)
C(19)	-844(2)	8692(1)	1264(2)	21(1)
C(20)	3224(2)	9145(1)	4926(2)	27(1)
C(21)	-1366(2)	8450(1)	2519(2)	23(1)
C(22)	-2753(2)	9319(1)	2929(2)	39(1)
C(23)	-2606(2)	8065(1)	2261(2)	33(1)
C(24)	-342(2)	8059(1)	3234(2)	29(1)

C(25)	4564(2)	9174(1)	5636(2)	45(1)

Table 3. Bond lengths [Å] and angles [°] for lsh129m.

Co(1)-O(5)	1.9137(13)	N(2)-C(6)	1.489(2)
Co(1)-N(1)	1.9465(15)	N(3)-C(7)	1.506(2)
Co(1)-N(2)	1.9487(15)	N(4)-C(15)	1.496(2)
Co(1)-O(6)	1.9497(14)	N(4)-C(24)	1.497(2)
Co(1)-N(4)	1.9576(15)	C(1)-C(2)	1.565(3)
Co(1)-N(3)	1.9851(15)	C(2)-C(5)	1.531(3)
O(1)-C(1)	1.256(2)	C(2)-C(4)	1.535(3)
O(2)-C(3)	1.429(2)	C(6)-C(7)	1.534(3)
O(2)-C(2)	1.442(2)	C(7)-C(8)	1.527(3)
O(3)-C(19)	1.229(2)	C(7)-C(9)	1.533(3)
O(5)-C(19)	1.297(2)	C(15)-C(16)	1.547(3)
O(6)-C(20)	1.292(2)	C(16)-C(18)	1.545(3)
O(7)-C(22)	1.442(3)	C(16)-C(17)	1.548(3)
O(7)-C(21)	1.449(2)	C(19)-C(21)	1.560(3)
O(8)-C(20)	1.246(2)	C(20)-C(25)	1.517(3)
N(1)-C(1)	1.342(2)	C(21)-C(24)	1.527(3)
N(1)-C(16)	1.500(2)	C(21)-C(23)	1.535(3)
N(2)-C(5)	1.481(2)		

O(5)-Co(1)-N(1)	92.57(6)	C(3)-O(2)-C(2)	115.86(14)
O(5)-Co(1)-N(2)	84.70(6)	C(19)-O(5)-Co(1)	132.10(12)
N(1)-Co(1)-N(2)	95.64(7)	C(20)-O(6)-Co(1)	126.45(12)
O(5)-Co(1)-O(6)	173.09(5)	C(22)-O(7)-C(21)	116.05(16)
N(1)-Co(1)-O(6)	86.11(6)	C(1)-N(1)-C(16)	116.84(15)
N(2)-Co(1)-O(6)	88.68(6)	C(1)-N(1)-Co(1)	128.97(13)
O(5)-Co(1)-N(4)	92.40(6)	C(16)-N(1)-Co(1)	114.16(12)
N(1)-Co(1)-N(4)	86.61(7)	C(5)-N(2)-C(6)	112.18(13)
N(2)-Co(1)-N(4)	176.40(6)	C(5)-N(2)-Co(1)	115.85(11)
O(6)-Co(1)-N(4)	94.29(6)	C(6)-N(2)-Co(1)	109.71(11)
O(5)-Co(1)-N(3)	92.29(6)	C(7)-N(3)-Co(1)	113.53(11)
N(1)-Co(1)-N(3)	175.12(6)	C(15)-N(4)-C(24)	109.98(15)
N(2)-Co(1)-N(3)	84.49(6)	C(15)-N(4)-Co(1)	105.85(11)
O(6)-Co(1)-N(3)	89.03(6)	C(24)-N(4)-Co(1)	120.26(12)
N(4)-Co(1)-N(3)	93.51(7)	O(1)-C(1)-N(1)	125.23(17)

O(1)-C(1)-C(2)	115.97(16)
N(1)-C(1)-C(2)	118.80(15)
O(2)-C(2)-C(5)	103.69(14)
O(2)-C(2)-C(4)	109.39(15)
C(5)-C(2)-C(4)	108.65(15)
O(2)-C(2)-C(1)	111.34(15)
C(5)-C(2)-C(1)	113.37(15)
C(4)-C(2)-C(1)	110.16(15)
N(2)-C(5)-C(2)	110.04(14)
N(2)-C(6)-C(7)	109.22(14)
N(3)-C(7)-C(8)	108.30(15)
N(3)-C(7)-C(9)	110.79(15)
C(8)-C(7)-C(9)	110.52(16)
N(3)-C(7)-C(6)	105.29(14)
C(8)-C(7)-C(6)	111.97(15)
C(9)-C(7)-C(6)	109.84(15)
N(4)-C(15)-C(16)	112.27(15)
N(1)-C(16)-C(18)	113.13(16)
N(1)-C(16)-C(15)	106.47(15)
C(18)-C(16)-C(15)	105.10(17)
N(1)-C(16)-C(17)	110.10(17)
C(18)-C(16)-C(17)	109.00(18)
C(15)-C(16)-C(17)	112.99(16)
O(3)-C(19)-O(5)	122.42(17)
O(3)-C(19)-C(21)	119.14(16)
O(5)-C(19)-C(21)	118.43(16)
O(8)-C(20)-O(6)	125.40(18)
O(8)-C(20)-C(25)	119.44(19)
O(6)-C(20)-C(25)	115.16(18)
O(7)-C(21)-C(24)	107.17(16)
O(7)-C(21)-C(23)	111.60(16)
C(24)-C(21)-C(23)	107.14(16)
O(7)-C(21)-C(19)	108.25(14)
C(24)-C(21)-C(19)	111.84(15)
C(23)-C(21)-C(19)	110.82(16)
N(4)-C(24)-C(21)	117.72(16)

Table 4. Anisotropic displacement parameters ($Å^2 x\ 10^3$) for lsh129m. The anisotropic displacement factor exponent takes the form: $-2\pi^2[\ h^2\ a^{*2}U^{11} + ... + 2\ h\ k\ a^*\ b^*\ U^{12}\ ]$

	U^{11}	U^{22}	U^{33}	U^{23}	U^{13}	U^{12}
Co(1)	15(1)	19(1)	16(1)	2(1)	2(1)	1(1)
O(1)	36(1)	26(1)	33(1)	-1(1)	10(1)	9(1)
O(2)	24(1)	24(1)	22(1)	-3(1)	-3(1)	3(1)
O(3)	23(1)	56(1)	25(1)	8(1)	-2(1)	-8(1)
O(5)	18(1)	24(1)	19(1)	3(1)	2(1)	-3(1)
O(6)	21(1)	29(1)	20(1)	1(1)	0(1)	2(1)
O(7)	20(1)	37(1)	24(1)	-1(1)	3(1)	2(1)
O(8)	32(1)	60(1)	21(1)	2(1)	3(1)	3(1)
N(1)	21(1)	20(1)	21(1)	2(1)	2(1)	1(1)
N(2)	16(1)	20(1)	18(1)	0(1)	3(1)	0(1)
N(3)	18(1)	23(1)	18(1)	1(1)	3(1)	1(1)
N(4)	21(1)	24(1)	20(1)	6(1)	4(1)	1(1)
C(1)	20(1)	22(1)	22(1)	-1(1)	2(1)	2(1)
C(2)	18(1)	24(1)	20(1)	0(1)	3(1)	2(1)
C(3)	36(1)	28(1)	34(1)	-7(1)	-9(1)	2(1)
C(4)	21(1)	32(1)	27(1)	1(1)	9(1)	4(1)
C(5)	15(1)	23(1)	22(1)	-1(1)	5(1)	-3(1)
C(6)	21(1)	19(1)	24(1)	-1(1)	5(1)	-1(1)
C(7)	22(1)	20(1)	21(1)	0(1)	5(1)	1(1)
C(8)	25(1)	26(1)	27(1)	6(1)	3(1)	4(1)
C(9)	35(1)	26(1)	31(1)	-6(1)	9(1)	1(1)
C(15)	22(1)	26(1)	26(1)	9(1)	1(1)	3(1)
C(16)	23(1)	20(1)	29(1)	7(1)	5(1)	3(1)
C(17)	44(1)	26(1)	45(1)	-4(1)	16(1)	-9(1)
C(18)	31(1)	41(1)	45(1)	20(1)	8(1)	13(1)
C(19)	20(1)	21(1)	21(1)	1(1)	2(1)	-1(1)
C(20)	26(1)	30(1)	23(1)	3(1)	-3(1)	2(1)
C(21)	18(1)	28(1)	24(1)	5(1)	4(1)	-1(1)
C(22)	26(1)	48(1)	43(1)	-2(1)	5(1)	11(1)
C(23)	23(1)	37(1)	38(1)	10(1)	1(1)	-9(1)
C(24)	21(1)	31(1)	35(1)	14(1)	3(1)	-4(1)

C(25)	31(1)	72(2)	30(1)	-3(1)	-8(1)	1(1)

Table 5. Hydrogen coordinates (x 10^4) and isotropic displacement parameters ($Å^2$x 10^3) for lsh129m.

	x	y	z	U(eq)
H(2)	1858	9541	719	21
H(3A)	-78	9523	3259	23
H(3B)	1098	9647	4116	23
H(4)	858	8522	4394	26
H(3C)	2926	8254	-1836	50
H(3D)	1509	8560	-2090	50
H(3E)	1787	8147	-876	50
H(4B)	5006	8461	-1074	40
H(4C)	5773	8821	43	40
H(4D)	5055	9175	-1109	40
H(5A)	4411	9364	1691	24
H(5B)	4048	9761	464	24
H(6A)	2436	10448	1380	26
H(6B)	3076	10183	2676	26
H(8A)	-193	9924	1088	39
H(8B)	44	10631	1123	39
H(8C)	-953	10330	2053	39
H(9A)	196	10754	3924	46
H(9B)	1278	11082	3126	46
H(9C)	1736	10632	4235	46
H(15A)	1557	7497	4165	29
H(15B)	2646	7998	4507	29
H(17A)	1150	7404	1422	57
H(17B)	1717	6890	2349	57
H(17C)	2526	7087	1168	57
H(18A)	4513	7291	2402	58
H(18B)	3920	7128	3722	58
H(18C)	4584	7767	3526	58
H(22A)	-2717	9415	2033	59
H(22B)	-2737	9688	3423	59

H(22C)	-3569	9099	3067	59
H(23A)	-2954	7942	3062	49
H(23B)	-2378	7711	1778	49
H(23C)	-3279	8298	1778	49
H(24A)	-742	7910	4003	34
H(24B)	-170	7708	2704	34
H(25A)	4495	9413	6401	67
H(25B)	5207	9358	5100	67
H(25C)	4856	8769	5865	67

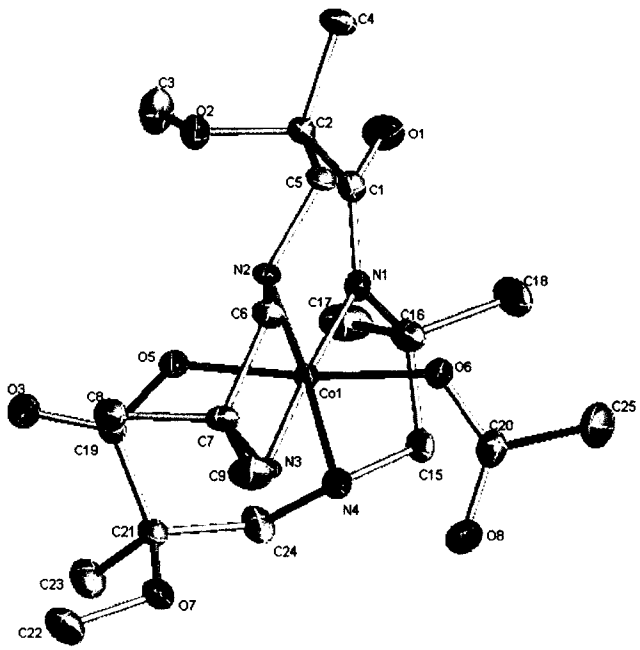

B. lsh132rm, 5a

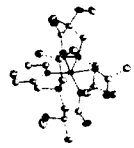

Table 1. Crystal data and structure refinement for lsh132rm, **5a**.

Identification code	lsh132rm	
Empirical formula	$C_{31}\ H_{50}\ Co\ N_5\ O_7$	
Formula weight	663.69	
Temperature	173(2) K	
Wavelength	0.71073 Å	
Crystal system	Monoclinic	
Space group	Cc	
Unit cell dimensions	a = 10.5774(16) Å	α= 90°.
	b = 20.901(3) Å	β= 104.217(3)°.
	c = 14.663(2) Å	γ= 90°.
Volume	3142.2(8) $Å^3$	
Z	4	
Density (calculated)	1.403 Mg/m^3	
Absorption coefficient	0.601 mm^{-1}	
F(000)	1416	
Crystal size	0.40 x 0.30 x 0.20 mm^3	
Theta range for data collection	1.95 to 28.32°.	
Index ranges	-13<=h<=14, -27<=k<=27, -19<=l<=19	
Reflections collected	14404	
Independent reflections	7178 [R(int) = 0.0386]	
Completeness to theta = 28.32°	98.2 %	
Absorption correction	Semi-empirical from equivalents	
Max. and min. transmission	0.8892 and 0.7950	
Refinement method	Full-matrix least-squares on F^2	
Data / restraints / parameters	7178 / 2 / 407	
Goodness-of-fit on F^2	1.065	
Final R indices [I>2sigma(I)]	R1 = 0.0463, wR2 = 0.1086	
R indices (all data)	R1 = 0.0526, wR2 = 0.1113	
Absolute structure parameter	0.022(12)	
Extinction coefficient	0.0029(5)	
Largest diff. peak and hole	0.765 and -0.511 $e.Å^{-3}$	

Table 2. Atomic coordinates (x 10^4) and equivalent isotropic displacement parameters ($Å^2$x 10^3) for lsh132rm. U(eq) is defined as one third of the trace of the orthogonalized U^{ij} tensor.

	x	y	z	U(eq)
Co(1)	3278(1)	3458(1)	170(1)	19(1)
O(1)	2446(2)	3769(1)	3072(2)	36(1)
O(2)	2610(3)	4835(1)	2059(2)	38(1)
O(3)	5148(2)	3517(1)	-1643(2)	31(1)
O(4)	3879(3)	2119(1)	-1779(2)	35(1)
O(5)	1501(2)	3172(1)	29(2)	26(1)
O(6)	451(3)	2995(1)	-1485(2)	42(1)
N(1)	2742(3)	4207(1)	804(2)	23(1)
N(2)	3111(2)	4061(1)	-888(2)	23(1)
N(3)	3646(2)	2695(1)	-501(2)	23(1)
N(4)	3806(2)	2905(1)	1294(2)	22(1)
N(5)	5023(2)	3715(1)	491(2)	22(1)
C(1)	3280(3)	3764(2)	2433(2)	26(1)
C(2)	4604(4)	3930(2)	3065(3)	39(1)
C(3)	1083(4)	3806(2)	2672(3)	44(1)
C(4)	2855(3)	4316(2)	1706(2)	27(1)
C(5)	2032(3)	4712(1)	143(2)	28(1)
C(6)	603(4)	4760(2)	213(3)	39(1)
C(7)	2663(4)	5385(2)	334(3)	39(1)
C(8)	1963(3)	4468(1)	-862(2)	28(1)
C(9)	2879(3)	3763(2)	-1837(2)	26(1)
C(10)	3853(3)	3250(2)	-1950(2)	26(1)
C(11)	3565(4)	3097(2)	-3000(2)	33(1)
C(12)	6203(4)	3088(2)	-1560(3)	45(1)
C(13)	3766(3)	2636(2)	-1380(2)	25(1)
C(14)	3677(3)	2077(1)	31(2)	27(1)
C(15)	4994(4)	1732(2)	158(3)	40(1)
C(16)	2593(4)	1610(2)	-455(3)	39(1)
C(17)	3374(3)	2251(1)	969(2)	27(1)
C(18)	3136(3)	3084(1)	2043(2)	25(1)
C(19)	5268(3)	2906(2)	1660(2)	25(1)

C(20)	5874(3)	3416(1)	1197(2)	26(1)
C(21)	7174(3)	3591(2)	1439(2)	30(1)
C(22)	7581(3)	4068(2)	930(3)	37(1)
C(23)	6692(3)	4376(2)	202(2)	31(1)
C(24)	5400(3)	4185(1)	-2(2)	26(1)
C(25)	4310(3)	4483(1)	-718(2)	27(1)
C(26)	553(3)	2962(2)	-630(2)	30(1)
C(27)	-518(3)	2656(2)	-251(3)	41(1)
C(28)	6524(5)	5806(2)	1420(4)	59(1)
C(29)	6425(9)	5314(2)	2260(6)	119(4)
C(30)	7685(8)	5165(3)	2932(3)	85(2)
C(31)	8666(10)	5527(3)	2377(6)	139(4)
O(7)	7968(5)	5646(2)	1441(3)	87(1)

Table 3. Bond lengths [Å] and angles [°] for lsh132rm.

Co(1)-N(5)	1.868(3)	N(5)-C(20)	1.347(4)
Co(1)-O(5)	1.935(2)	C(1)-C(2)	1.518(5)
Co(1)-N(3)	1.963(2)	C(1)-C(18)	1.526(4)
Co(1)-N(2)	1.973(3)	C(1)-C(4)	1.560(4)
Co(1)-N(1)	1.973(2)	C(5)-C(8)	1.543(5)
Co(1)-N(4)	1.978(2)	C(5)-C(6)	1.544(5)
O(1)-C(3)	1.419(5)	C(5)-C(7)	1.554(5)
O(1)-C(1)	1.436(4)	C(9)-C(10)	1.523(4)
O(2)-C(4)	1.257(4)	C(10)-C(11)	1.529(4)
O(3)-C(12)	1.414(4)	C(10)-C(13)	1.547(4)
O(3)-C(10)	1.445(4)	C(14)-C(17)	1.531(4)
O(4)-C(13)	1.248(4)	C(14)-C(15)	1.539(5)
O(5)-C(26)	1.287(4)	C(14)-C(16)	1.540(5)
O(6)-C(26)	1.233(4)	C(19)-C(20)	1.492(4)
N(1)-C(4)	1.317(4)	C(20)-C(21)	1.383(5)
N(1)-C(5)	1.503(4)	C(21)-C(22)	1.376(5)
N(2)-C(9)	1.489(4)	C(22)-C(23)	1.394(5)
N(2)-C(8)	1.490(4)	C(23)-C(24)	1.385(5)
N(2)-C(25)	1.514(4)	C(24)-C(25)	1.492(4)
N(3)-C(13)	1.331(4)	C(26)-C(27)	1.521(5)
N(3)-C(14)	1.506(4)	C(28)-O(7)	1.557(6)
N(4)-C(17)	1.482(4)	C(28)-C(29)	1.628(7)
N(4)-C(18)	1.494(4)	C(29)-C(30)	1.482(11)
N(4)-C(19)	1.507(4)	C(30)-C(31)	1.652(13)
N(5)-C(24)	1.338(4)	C(31)-O(7)	1.412(8)
N(5)-Co(1)-O(5)	171.81(10)	N(3)-Co(1)-N(1)	174.92(11)
N(5)-Co(1)-N(3)	93.10(11)	N(2)-Co(1)-N(1)	83.28(10)
O(5)-Co(1)-N(3)	90.09(10)	N(5)-Co(1)-N(4)	84.19(11)
N(5)-Co(1)-N(2)	84.65(11)	O(5)-Co(1)-N(4)	88.66(10)
O(5)-Co(1)-N(2)	102.49(10)	N(3)-Co(1)-N(4)	83.82(10)
N(3)-Co(1)-N(2)	96.63(10)	N(2)-Co(1)-N(4)	168.84(11)
N(5)-Co(1)-N(1)	91.95(11)	N(1)-Co(1)-N(4)	97.25(10)
O(5)-Co(1)-N(1)	84.98(10)	C(3)-O(1)-C(1)	117.1(3)

C(12)-O(3)-C(10)	116.7(3)	C(8)-C(5)-C(7)	112.9(3)
C(26)-O(5)-Co(1)	138.1(2)	C(6)-C(5)-C(7)	108.2(3)
C(4)-N(1)-C(5)	115.8(3)	N(2)-C(8)-C(5)	111.4(3)
C(4)-N(1)-Co(1)	130.0(2)	N(2)-C(9)-C(10)	115.8(2)
C(5)-N(1)-Co(1)	114.11(19)	O(3)-C(10)-C(9)	108.0(2)
C(9)-N(2)-C(8)	108.4(2)	O(3)-C(10)-C(11)	109.5(3)
C(9)-N(2)-C(25)	109.7(2)	C(9)-C(10)-C(11)	106.5(3)
C(8)-N(2)-C(25)	108.6(2)	O(3)-C(10)-C(13)	109.3(2)
C(9)-N(2)-Co(1)	115.44(19)	C(9)-C(10)-C(13)	113.2(3)
C(8)-N(2)-Co(1)	105.11(18)	C(11)-C(10)-C(13)	110.3(3)
C(25)-N(2)-Co(1)	109.44(18)	O(4)-C(13)-N(3)	125.3(3)
C(13)-N(3)-C(14)	115.2(2)	O(4)-C(13)-C(10)	116.1(3)
C(13)-N(3)-Co(1)	129.7(2)	N(3)-C(13)-C(10)	118.5(3)
C(14)-N(3)-Co(1)	114.83(18)	N(3)-C(14)-C(17)	106.1(2)
C(17)-N(4)-C(18)	107.6(2)	N(3)-C(14)-C(15)	111.6(3)
C(17)-N(4)-C(19)	108.9(2)	C(17)-C(14)-C(15)	112.7(3)
C(18)-N(4)-C(19)	111.7(2)	N(3)-C(14)-C(16)	112.7(3)
C(17)-N(4)-Co(1)	105.63(17)	C(17)-C(14)-C(16)	105.7(3)
C(18)-N(4)-Co(1)	112.25(18)	C(15)-C(14)-C(16)	107.9(3)
C(19)-N(4)-Co(1)	110.56(18)	N(4)-C(17)-C(14)	113.1(2)
C(24)-N(5)-C(20)	121.6(3)	N(4)-C(18)-C(1)	119.1(2)
C(24)-N(5)-Co(1)	118.8(2)	C(20)-C(19)-N(4)	110.9(2)
C(20)-N(5)-Co(1)	119.5(2)	N(5)-C(20)-C(21)	120.7(3)
O(1)-C(1)-C(2)	102.9(3)	N(5)-C(20)-C(19)	113.7(3)
O(1)-C(1)-C(18)	103.3(2)	C(21)-C(20)-C(19)	125.7(3)
C(2)-C(1)-C(18)	115.7(3)	C(22)-C(21)-C(20)	118.4(3)
O(1)-C(1)-C(4)	108.7(3)	C(21)-C(22)-C(23)	120.5(3)
C(2)-C(1)-C(4)	108.4(3)	C(24)-C(23)-C(22)	118.5(3)
C(18)-C(1)-C(4)	116.6(2)	N(5)-C(24)-C(23)	120.3(3)
O(2)-C(4)-N(1)	125.8(3)	N(5)-C(24)-C(25)	113.9(3)
O(2)-C(4)-C(1)	114.2(3)	C(23)-C(24)-C(25)	125.7(3)
N(1)-C(4)-C(1)	119.9(3)	C(24)-C(25)-N(2)	110.1(2)
N(1)-C(5)-C(8)	106.5(2)	O(6)-C(26)-O(5)	127.0(3)
N(1)-C(5)-C(6)	110.2(3)	O(6)-C(26)-C(27)	120.6(3)
C(8)-C(5)-C(6)	105.6(3)	O(5)-C(26)-C(27)	112.5(3)
N(1)-C(5)-C(7)	113.2(3)	O(7)-C(28)-C(29)	95.4(5)

C(30)-C(29)-C(28)	114.9(6)
C(29)-C(30)-C(31)	98.5(4)
O(7)-C(31)-C(30)	108.5(6)
C(31)-O(7)-C(28)	109.5(6)

Table 4. Anisotropic displacement parameters ($Å^2 x\ 10^3$) for lsh132rm. The anisotropic displacement factor exponent takes the form: $-2\pi^2[\ h^2\ a^{*2}U^{11} + ... + 2\ h\ k\ a^*\ b^*\ U^{12}\ ]$

	U^{11}	U^{22}	U^{33}	U^{23}	U^{13}	U^{12}
Co(1)	20(1)	19(1)	18(1)	1(1)	5(1)	1(1)
O(1)	44(1)	43(1)	25(1)	0(1)	16(1)	4(1)
O(2)	58(2)	27(1)	34(1)	-6(1)	21(1)	3(1)
O(3)	26(1)	33(1)	36(1)	-3(1)	10(1)	-1(1)
O(4)	48(2)	29(1)	29(1)	-8(1)	10(1)	7(1)
O(5)	23(1)	30(1)	27(1)	-4(1)	7(1)	-3(1)
O(6)	44(2)	53(2)	27(1)	-3(1)	5(1)	-11(1)
N(1)	29(1)	22(1)	22(1)	-2(1)	10(1)	1(1)
N(2)	24(1)	24(1)	22(1)	1(1)	6(1)	4(1)
N(3)	26(1)	21(1)	23(1)	2(1)	6(1)	2(1)
N(4)	26(1)	21(1)	20(1)	2(1)	6(1)	-1(1)
N(5)	25(1)	22(1)	19(1)	-1(1)	7(1)	-1(1)
C(1)	32(2)	29(2)	19(1)	1(1)	10(1)	0(1)
C(2)	41(2)	36(2)	36(2)	-10(1)	2(2)	1(2)
C(3)	41(2)	44(2)	55(2)	-3(2)	27(2)	-4(2)
C(4)	29(2)	27(2)	28(2)	-3(1)	11(1)	0(1)
C(5)	34(2)	23(1)	29(2)	3(1)	13(1)	5(1)
C(6)	36(2)	42(2)	41(2)	5(2)	12(2)	14(2)
C(7)	56(2)	25(2)	40(2)	-2(1)	18(2)	3(2)
C(8)	32(2)	26(1)	29(2)	5(1)	11(1)	9(1)
C(9)	30(2)	30(2)	19(1)	4(1)	5(1)	6(1)
C(10)	24(2)	30(2)	23(1)	-2(1)	7(1)	-1(1)
C(11)	46(2)	34(2)	22(2)	2(1)	13(1)	-2(1)
C(12)	28(2)	46(2)	64(3)	1(2)	13(2)	4(2)
C(13)	23(2)	28(2)	25(2)	0(1)	5(1)	4(1)
C(14)	35(2)	21(1)	24(2)	-1(1)	6(1)	0(1)
C(15)	53(2)	37(2)	31(2)	6(1)	9(2)	20(2)
C(16)	56(2)	29(2)	35(2)	-9(1)	15(2)	-15(2)
C(17)	34(2)	21(1)	25(2)	2(1)	8(1)	-3(1)
C(18)	29(2)	25(1)	21(1)	3(1)	6(1)	-1(1)
C(19)	22(2)	28(1)	25(2)	3(1)	5(1)	3(1)

C(20)	26(2)	27(2)	24(1)	-2(1)	6(1)	2(1)
C(21)	24(2)	37(2)	31(2)	-3(1)	6(1)	-1(1)
C(22)	27(2)	44(2)	41(2)	-5(2)	8(1)	-7(1)
C(23)	34(2)	30(2)	32(2)	-2(1)	12(1)	-10(1)
C(24)	31(2)	27(2)	25(2)	-2(1)	14(1)	0(1)
C(25)	31(2)	27(1)	25(1)	5(1)	11(1)	2(1)
C(26)	25(2)	33(2)	29(2)	-2(1)	5(1)	5(1)
C(27)	27(2)	60(2)	37(2)	-7(2)	6(2)	-7(2)
C(28)	88(3)	41(2)	74(3)	-25(2)	66(3)	-34(2)
C(29)	230(10)	41(3)	144(7)	-10(3)	159(8)	-11(4)
C(30)	151(6)	64(3)	29(2)	-5(2)	2(3)	21(4)
C(31)	175(9)	73(4)	112(6)	-17(4)	-73(6)	20(5)
O(7)	102(3)	77(3)	84(3)	2(2)	28(3)	-13(2)

Table 5. Hydrogen coordinates (x 10^4) and isotropic displacement parameters ($Å^2$x 10^3) for lsh132rm.

	x	y	z	U(eq)
H(2A)	4554	4345	3365	59
H(2B)	5250	3953	2687	59
H(2C)	4864	3600	3549	59
H(3A)	663	4027	3109	66
H(3B)	724	3373	2554	66
H(3C)	920	4043	2078	66
H(6A)	184	4340	89	59
H(6B)	134	5070	-250	59
H(6C)	582	4902	847	59
H(7A)	2291	5611	793	59
H(7B)	2489	5630	-254	59
H(7C)	3607	5340	585	59
H(8A)	1153	4217	-1090	34
H(8B)	1931	4838	-1288	34
H(9A)	2885	4105	-2302	31
H(9B)	1997	3571	-1992	31
H(11A)	3806	3464	-3338	49
H(11B)	2633	3007	-3238	49
H(11C)	4072	2722	-3097	49
H(12A)	6259	2811	-1012	68
H(12B)	7016	3330	-1482	68
H(12C)	6064	2824	-2129	68
H(15A)	5036	1527	-436	60
H(15B)	5081	1405	649	60
H(15C)	5705	2042	341	60
H(16A)	1753	1832	-604	59
H(16B)	2559	1250	-34	59
H(16C)	2779	1449	-1037	59
H(17A)	2422	2217	902	32
H(17B)	3808	1939	1453	32

H(18A)	3448	2788	2579	30
H(18B)	2193	3000	1794	30
H(19A)	5495	2977	2349	30
H(19B)	5620	2484	1539	30
H(21)	7772	3387	1945	37
H(22)	8474	4188	1075	45
H(23)	6967	4710	-145	38
H(25A)	4576	4543	-1315	32
H(25B)	4106	4909	-495	32
H(27A)	-1210	2498	-777	62
H(27B)	-880	2974	106	62
H(27C)	-155	2298	162	62
H(28A)	5916	5696	812	71
H(28B)	6403	6258	1583	71
H(29A)	5828	5499	2615	143
H(29B)	6032	4909	1974	143
H(30A)	7850	4699	2992	102
H(30B)	7742	5352	3561	102
H(31A)	8980	5936	2695	167
H(31B)	9432	5254	2383	167

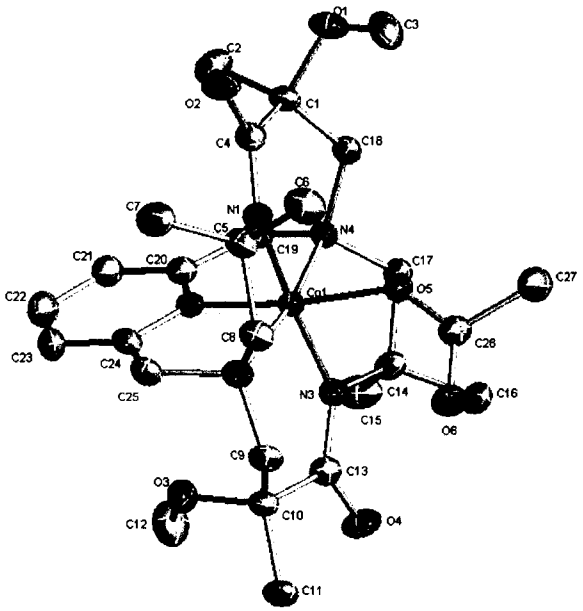

C. lsh133m, 5b

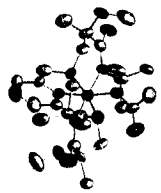

Table 1. Crystal data and structure refinement for lsh133m, **5b**.

Identification code	lsh133m	
Empirical formula	$C_{30}\ H_{49}\ Co\ N_6\ O_7$	
Formula weight	664.68	
Temperature	298(2) K	
Wavelength	0.71073 Å	
Crystal system	Monoclinic	
Space group	Cc	
Unit cell dimensions	a = 10.6644(19) Å	α= 90°.
	b = 21.732(4) Å	β= 102.815(5)°.
	c = 14.189(3) Å	γ = 90°.
Volume	3206.5(11) $Å^3$	
Z	4	
Density (calculated)	1.360 Mg/m^3	
Absorption coefficient	0.590 mm^{-1}	
F(000)	1384	
Crystal size	0.28 x 0.25 x 0.18 mm^3	
Theta range for data collection	2.17 to 25.04°.	
Index ranges	-12<=h<=12, -25<=k<=25, -16<=l<=16	
Reflections collected	11992	
Independent reflections	5592 [R(int) = 0.0937]	
Completeness to theta = 25.04°	99.8 %	
Absorption correction	Semi-empirical from equivalents	
Max. and min. transmission	0.9013 and 0.8523	
Refinement method	Full-matrix least-squares on F^2	
Data / restraints / parameters	5592 / 11 / 397	
Goodness-of-fit on F^2	0.951	
Final R indices [I>2sigma(I)]	R1 = 0.0672, wR2 = 0.1069	
R indices (all data)	R1 = 0.1655, wR2 = 0.1323	
Absolute structure parameter	0.00(2)	
Largest diff. peak and hole	0.352 and -0.220 e.$Å^{-3}$	

Table 2. Atomic coordinates (x 10^4) and equivalent isotropic displacement parameters ($Å^2$x 10^3) for lsh133m. U(eq) is defined as one third of the trace of the orthogonalized U^{ij} tensor.

	x	y	z	U(eq)
Co(1)	2088(1)	6522(1)	7986(1)	44(1)
N(1)	1611(6)	5791(3)	8662(4)	46(2)
N(2)	1970(6)	5946(3)	6902(5)	45(2)
N(3)	2393(6)	7262(3)	7289(5)	44(2)
N(4)	2590(6)	7059(3)	9136(4)	39(2)
N(5)	3806(6)	6309(3)	8274(4)	38(2)
N(6)	6396(7)	6027(4)	8632(6)	71(2)
O(1)	1237(6)	6197(3)	10981(4)	71(2)
O(2)	1537(5)	5188(2)	9967(4)	66(2)
O(3)	3872(5)	6523(2)	6030(4)	63(1)
O(4)	2547(6)	7835(3)	5969(4)	73(2)
O(5)	321(5)	6769(3)	7867(4)	53(1)
O(6)	-692(6)	6953(3)	6334(5)	90(2)
C(1)	2101(8)	6222(4)	10323(6)	51(2)
C(2)	3376(8)	6079(4)	10994(6)	70(3)
C(3)	-101(10)	6159(5)	10559(8)	100(4)
C(4)	1739(7)	5682(4)	9602(6)	49(2)
C(5)	960(8)	5288(4)	7998(6)	62(2)
C(6)	-440(8)	5216(4)	8108(6)	83(3)
C(7)	1639(10)	4643(3)	8210(6)	94(3)
C(8)	879(8)	5529(3)	6962(5)	55(2)
C(9)	1703(8)	6236(4)	5919(5)	53(2)
C(10)	2580(8)	6763(4)	5769(6)	49(2)
C(11)	2229(8)	6889(4)	4700(5)	63(2)
C(12)	4881(9)	6935(4)	6021(8)	101(3)
C(13)	2477(7)	7341(4)	6370(6)	46(2)
C(14)	2406(8)	7855(3)	7828(6)	49(2)
C(15)	3691(9)	8201(4)	7928(6)	80(3)
C(16)	1338(8)	8292(3)	7379(5)	71(3)
C(17)	2141(7)	7678(3)	8803(5)	47(2)
C(18)	1954(8)	6877(4)	9912(5)	53(2)

C(19)	4035(8)	7067(3)	9510(5)	54(2)
C(20)	4642(8)	6602(4)	8988(5)	44(2)
C(21)	5928(8)	6453(4)	9148(6)	56(2)
C(22)	5560(9)	5751(4)	7951(7)	66(3)
C(23)	4253(8)	5875(4)	7759(5)	48(2)
C(24)	3193(8)	5584(3)	7033(6)	57(2)
C(25)	-621(9)	6954(4)	7201(7)	62(3)
C(26)	-1724(8)	7188(4)	7593(7)	88(3)
O(7)	7220(20)	5239(13)	5440(20)	363(13)
C(27)	6200(30)	4948(9)	5863(12)	205(13)
C(28)	5203(15)	5189(8)	5038(15)	138(6)
C(29)	5660(20)	5610(8)	4466(13)	165(6)
C(30)	7100(40)	5649(10)	4760(30)	290(20)

Table 3. Bond lengths [Å] and angles [°] for lsh133m.

Co(1)-N(5)	1.845(6)	O(4)-C(13)	1.224(8)
Co(1)-O(5)	1.930(6)	O(5)-C(25)	1.282(9)
Co(1)-N(3)	1.951(6)	O(6)-C(25)	1.215(9)
Co(1)-N(2)	1.965(6)	C(1)-C(2)	1.509(10)
Co(1)-N(1)	1.980(7)	C(1)-C(18)	1.534(11)
Co(1)-N(4)	1.981(6)	C(1)-C(4)	1.549(11)
N(1)-C(4)	1.331(9)	C(5)-C(6)	1.544(10)
N(1)-C(5)	1.509(9)	C(5)-C(8)	1.545(10)
N(2)-C(8)	1.492(9)	C(5)-C(7)	1.577(10)
N(2)-C(24)	1.500(9)	C(9)-C(10)	1.522(10)
N(2)-C(9)	1.500(9)	C(10)-C(11)	1.504(10)
N(3)-C(13)	1.339(9)	C(10)-C(13)	1.535(11)
N(3)-C(14)	1.498(9)	C(14)-C(16)	1.511(10)
N(4)-C(18)	1.470(9)	C(14)-C(17)	1.521(10)
N(4)-C(17)	1.471(8)	C(14)-C(15)	1.541(11)
N(4)-C(19)	1.515(9)	C(19)-C(20)	1.483(10)
N(5)-C(23)	1.344(9)	C(20)-C(21)	1.378(10)
N(5)-C(20)	1.352(9)	C(22)-C(23)	1.385(10)
N(6)-C(22)	1.307(10)	C(23)-C(24)	1.491(10)
N(6)-C(21)	1.343(10)	C(25)-C(26)	1.497(11)
O(1)-C(3)	1.422(10)	O(7)-C(30)	1.29(3)
O(1)-C(1)	1.452(9)	O(7)-C(27)	1.50(3)
O(2)-C(4)	1.232(9)	C(27)-C(28)	1.49(2)
O(3)-C(12)	1.403(9)	C(28)-C(29)	1.38(2)
O(3)-C(10)	1.443(9)	C(29)-C(30)	1.50(3)
N(5)-Co(1)-O(5)	172.3(3)	N(3)-Co(1)-N(1)	174.8(3)
N(5)-Co(1)-N(3)	92.9(2)	N(2)-Co(1)-N(1)	83.6(3)
O(5)-Co(1)-N(3)	89.8(2)	N(5)-Co(1)-N(4)	83.8(3)
N(5)-Co(1)-N(2)	84.4(3)	O(5)-Co(1)-N(4)	89.3(2)
O(5)-Co(1)-N(2)	102.5(2)	N(3)-Co(1)-N(4)	83.6(3)
N(3)-Co(1)-N(2)	96.7(3)	N(2)-Co(1)-N(4)	168.2(3)
N(5)-Co(1)-N(1)	92.3(3)	N(1)-Co(1)-N(4)	97.2(2)
O(5)-Co(1)-N(1)	85.1(2)	C(4)-N(1)-C(5)	115.3(7)

C(4)-N(1)-Co(1)	130.4(6)	N(1)-C(5)-C(7)	113.4(7)
C(5)-N(1)-Co(1)	114.2(5)	C(6)-C(5)-C(7)	107.7(7)
C(8)-N(2)-C(24)	110.0(6)	C(8)-C(5)-C(7)	114.2(7)
C(8)-N(2)-C(9)	108.6(6)	N(2)-C(8)-C(5)	112.3(6)
C(24)-N(2)-C(9)	108.4(5)	N(2)-C(9)-C(10)	116.8(6)
C(8)-N(2)-Co(1)	105.0(4)	O(3)-C(10)-C(11)	109.5(6)
C(24)-N(2)-Co(1)	109.6(5)	O(3)-C(10)-C(9)	105.8(6)
C(9)-N(2)-Co(1)	115.2(5)	C(11)-C(10)-C(9)	104.7(7)
C(13)-N(3)-C(14)	113.0(7)	O(3)-C(10)-C(13)	109.6(6)
C(13)-N(3)-Co(1)	130.9(6)	C(11)-C(10)-C(13)	112.3(7)
C(14)-N(3)-Co(1)	115.7(5)	C(9)-C(10)-C(13)	114.6(7)
C(18)-N(4)-C(17)	108.4(6)	O(4)-C(13)-N(3)	126.1(8)
C(18)-N(4)-C(19)	110.1(5)	O(4)-C(13)-C(10)	116.1(7)
C(17)-N(4)-C(19)	109.6(5)	N(3)-C(13)-C(10)	117.6(8)
C(18)-N(4)-Co(1)	111.9(4)	N(3)-C(14)-C(16)	113.9(7)
C(17)-N(4)-Co(1)	105.4(4)	N(3)-C(14)-C(17)	105.4(6)
C(19)-N(4)-Co(1)	111.3(4)	C(16)-C(14)-C(17)	105.5(6)
C(23)-N(5)-C(20)	118.9(7)	N(3)-C(14)-C(15)	112.0(6)
C(23)-N(5)-Co(1)	120.7(5)	C(16)-C(14)-C(15)	107.7(6)
C(20)-N(5)-Co(1)	120.3(6)	C(17)-C(14)-C(15)	112.4(7)
C(22)-N(6)-C(21)	116.4(8)	N(4)-C(17)-C(14)	114.2(6)
C(3)-O(1)-C(1)	116.9(6)	N(4)-C(18)-C(1)	120.6(6)
C(12)-O(3)-C(10)	117.2(6)	C(20)-C(19)-N(4)	109.9(6)
C(25)-O(5)-Co(1)	137.9(6)	N(5)-C(20)-C(21)	118.7(7)
O(1)-C(1)-C(2)	101.4(6)	N(5)-C(20)-C(19)	114.0(7)
O(1)-C(1)-C(18)	104.6(6)	C(21)-C(20)-C(19)	127.3(8)
C(2)-C(1)-C(18)	115.6(7)	N(6)-C(21)-C(20)	123.3(8)
O(1)-C(1)-C(4)	107.2(7)	N(6)-C(22)-C(23)	123.2(8)
C(2)-C(1)-C(4)	108.6(7)	N(5)-C(23)-C(22)	119.5(7)
C(18)-C(1)-C(4)	117.6(7)	N(5)-C(23)-C(24)	111.5(7)
O(2)-C(4)-N(1)	126.1(8)	C(22)-C(23)-C(24)	128.9(8)
O(2)-C(4)-C(1)	115.1(7)	C(23)-C(24)-N(2)	111.6(6)
N(1)-C(4)-C(1)	118.8(8)	O(6)-C(25)-O(5)	127.5(9)
N(1)-C(5)-C(6)	109.3(7)	O(6)-C(25)-C(26)	119.9(8)
N(1)-C(5)-C(8)	105.7(6)	O(5)-C(25)-C(26)	112.6(8)
C(6)-C(5)-C(8)	106.2(7)	C(30)-O(7)-C(27)	129(2)

C(28)-C(27)-O(7)	89.6(14)
C(29)-C(28)-C(27)	114.3(15)
C(28)-C(29)-C(30)	110.2(17)
O(7)-C(30)-C(29)	96(2)

Table 4. Anisotropic displacement parameters ($Å^2 x\ 10^3$) for lsh133m. The anisotropic displacement factor exponent takes the form: $-2\pi^2[\ h^2\ a^{*2}U^{11} + ... + 2\ h\ k\ a^*\ b^*\ U^{12}\ ]$

	U^{11}	U^{22}	U^{33}	U^{23}	U^{13}	U^{12}
Co(1)	51(1)	44(1)	36(1)	0(1)	9(1)	-3(1)
N(1)	52(5)	51(5)	35(5)	-8(4)	13(4)	-7(4)
N(2)	50(5)	45(4)	40(4)	1(3)	11(3)	-1(4)
N(3)	46(4)	41(4)	47(5)	2(4)	11(3)	-4(3)
N(4)	41(5)	38(4)	37(4)	2(3)	6(3)	-4(3)
N(5)	41(4)	42(4)	31(4)	1(3)	5(3)	0(4)
N(6)	62(6)	72(6)	77(6)	-11(5)	11(5)	4(4)
O(1)	85(5)	84(5)	54(4)	-1(3)	37(4)	-15(4)
O(2)	107(5)	42(4)	55(4)	15(3)	31(3)	-11(3)
O(3)	47(4)	69(4)	77(4)	4(3)	23(3)	-11(4)
O(4)	120(5)	50(4)	46(4)	7(3)	16(3)	-14(4)
O(5)	51(4)	62(4)	44(4)	6(3)	9(3)	-1(3)
O(6)	95(5)	121(6)	51(4)	4(4)	11(4)	20(4)
C(1)	68(7)	46(6)	38(5)	-2(4)	13(5)	2(5)
C(2)	84(7)	62(6)	56(6)	3(4)	-1(5)	5(5)
C(3)	100(9)	90(8)	131(10)	16(7)	71(8)	7(7)
C(4)	47(6)	57(7)	46(6)	5(5)	15(4)	3(5)
C(5)	79(7)	68(7)	42(5)	0(5)	19(5)	-16(5)
C(6)	74(7)	121(9)	55(6)	5(5)	16(5)	-50(6)
C(7)	173(11)	46(6)	66(7)	-10(5)	34(6)	-21(6)
C(8)	72(6)	48(5)	48(5)	-9(4)	18(4)	-8(5)
C(9)	69(6)	50(5)	33(5)	-10(4)	-2(4)	7(5)
C(10)	41(6)	53(6)	53(6)	16(5)	10(4)	-17(5)
C(11)	80(7)	75(6)	35(5)	-1(4)	16(4)	-7(5)
C(12)	77(8)	91(8)	147(10)	18(7)	53(7)	-9(7)
C(13)	50(6)	38(6)	52(6)	5(5)	14(5)	-1(4)
C(14)	70(7)	37(5)	39(5)	4(4)	14(4)	3(5)
C(15)	102(8)	75(7)	62(6)	1(5)	15(5)	-31(6)
C(16)	108(8)	49(6)	54(5)	0(4)	17(5)	2(5)
C(17)	63(6)	37(5)	43(5)	4(4)	15(4)	3(4)
C(18)	56(6)	61(7)	41(5)	-18(5)	11(4)	0(5)

C(19)	80(7)	38(5)	49(5)	-7(4)	22(5)	4(5)
C(20)	40(6)	54(6)	34(5)	5(4)	-2(4)	-9(5)
C(21)	45(6)	62(6)	57(5)	2(5)	3(4)	-10(5)
C(22)	51(7)	77(7)	79(7)	-11(6)	33(6)	16(6)
C(23)	66(7)	43(5)	37(5)	-2(4)	14(5)	-9(5)
C(24)	87(7)	49(6)	40(5)	-8(5)	22(5)	12(5)
C(25)	62(7)	77(7)	43(6)	12(5)	4(5)	-6(6)
C(26)	53(7)	117(8)	94(8)	8(6)	15(6)	24(6)
O(7)	210(20)	400(30)	420(30)	-80(30)	-58(19)	90(20)
C(27)	380(30)	197(17)	54(8)	-48(10)	86(15)	-190(20)
C(28)	153(14)	154(14)	147(14)	-44(11)	120(13)	-45(11)
C(29)	208(19)	135(15)	152(14)	-18(12)	41(14)	17(14)
C(30)	310(40)	130(16)	500(50)	160(20)	240(40)	38(19)

Table 5. Hydrogen coordinates (x 10^4) and isotropic displacement parameters ($Å^2$x 10^3) for lsh133m.

	x	y	z	U(eq)
H(2A)	3623	6415	11435	105
H(2B)	4018	6020	10623	105
H(2C)	3298	5711	11351	105
H(3A)	-574	6143	11060	150
H(3B)	-270	5794	10170	150
H(3C)	-361	6514	10161	150
H(6B)	-877	5604	7983	124
H(6C)	-442	5086	8754	124
H(6D)	-873	4915	7656	124
H(7A)	2517	4675	8154	141
H(7B)	1199	4346	7753	141
H(7C)	1614	4513	8853	141
H(8A)	879	5182	6531	66
H(8B)	75	5749	6745	66
H(9A)	826	6387	5777	63
H(9B)	1755	5918	5450	63
H(11A)	2734	7226	4552	94
H(11B)	1333	6992	4511	94
H(11C)	2396	6529	4355	94
H(12A)	5688	6723	6211	151
H(12B)	4850	7265	6464	151
H(12C)	4797	7098	5381	151
H(15A)	4389	7933	8210	120
H(15B)	3697	8555	8334	120
H(15C)	3786	8331	7301	120
H(16A)	525	8087	7302	106
H(16B)	1457	8423	6758	106
H(16C)	1355	8644	7790	106
H(17A)	2554	7976	9281	57
H(17B)	1222	7702	8762	57

H(18A)	1041	6952	9680	63
H(18B)	2250	7157	10448	63
H(19A)	4368	7472	9415	65
H(19B)	4243	6977	10197	65
H(21A)	6501	6658	9637	67
H(22A)	5856	5457	7576	79
H(24A)	3047	5170	7242	69
H(24B)	3445	5554	6418	69
H(26A)	-2408	7315	7068	132
H(26B)	-1444	7533	8011	132
H(26C)	-2025	6867	7952	132

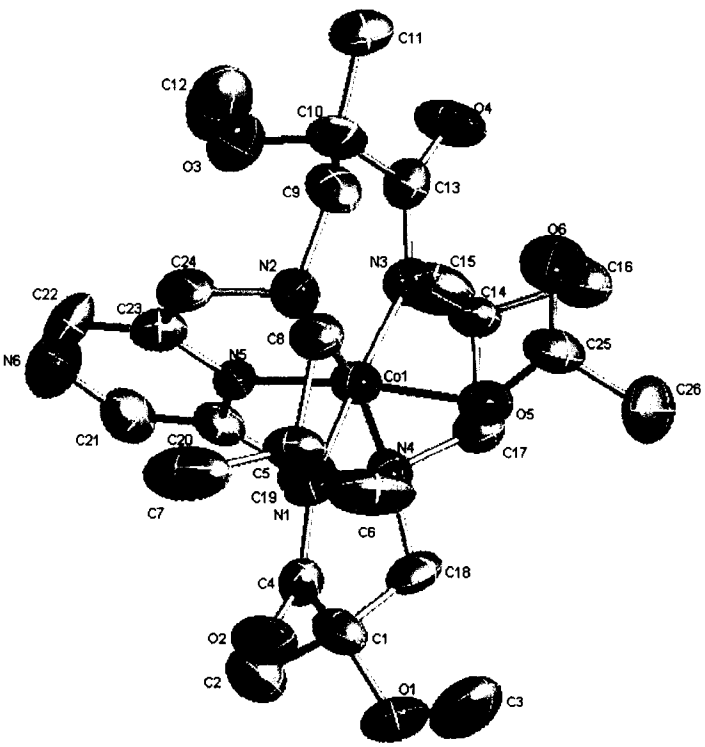

D. lsh149m, 6a

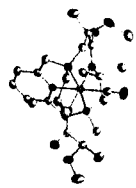

Table 1. Crystal data and structure refinement for lsh149m, **6a**.

Identification code	lsh149m	
Empirical formula	$C_{59}\ H_{106}\ Co_2\ N_{12}\ O_{15}$	
Formula weight	1341.41	
Temperature	173(2) K	
Wavelength	0.71073 Å	
Crystal system	Orthorhombic	
Space group	Pbca	
Unit cell dimensions	a = 14.7441(13) Å	α= 90°.
	b = 13.4537(12) Å	β= 90°.
	c = 32.905(3) Å	γ = 90°.
Volume	6527.1(10) $Å^3$	
Z	4	
Density (calculated)	1.353 Mg/m^3	
Absorption coefficient	0.581 mm^{-1}	
F(000)	2824	
Crystal size	0.40 x 0.40 x 0.04 mm^3	
Theta range for data collection	1.24 to 26.37°.	
Index ranges	-18<=h<=18, -16<=k<=16, -40<=l<=41	
Reflections collected	52023	
Independent reflections	6675 [R(int) = 0.1177]	
Completeness to theta = 26.37°	100.0 %	
Absorption correction	Semi-empirical from equivalents	
Max. and min. transmission	0.9771 and 0.8009	
Refinement method	Full-matrix least-squares on F^2	
Data / restraints / parameters	6675 / 5 / 417	
Goodness-of-fit on F^2	1.042	
Final R indices [I>2sigma(I)]	R1 = 0.0588, wR2 = 0.1287	
R indices (all data)	R1 = 0.0997, wR2 = 0.1492	
Extinction coefficient	0.0024(2)	
Largest diff. peak and hole	1.139 and -0.442 $e.Å^{-3}$	

Table 2. Atomic coordinates (x 10^4) and equivalent isotropic displacement parameters ($Å^2$x 10^3) for lsh149m. U(eq) is defined as one third of the trace of the orthogonalized U^{ij} tensor.

	x	y	z	U(eq)
Co(1)	9481(1)	497(1)	3837(1)	22(1)
O(1)	11631(2)	-1378(2)	3281(1)	42(1)
O(2)	9835(2)	-2185(2)	3228(1)	34(1)
O(3)	7592(2)	2011(2)	4667(1)	37(1)
O(4)	8745(2)	3243(2)	4297(1)	36(1)
N(1)	9564(2)	-910(2)	3674(1)	24(1)
N(2)	8521(2)	98(2)	4219(1)	23(1)
N(3)	9406(2)	1896(2)	3997(1)	25(1)
N(4)	10243(2)	936(2)	3382(1)	27(1)
N(5)	8511(2)	685(2)	3470(1)	24(1)
N(6)	11033(2)	276(3)	4439(1)	43(1)
C(1)	10834(3)	-811(3)	3170(1)	32(1)
C(2)	10814(3)	-972(3)	2710(1)	45(1)
C(3)	11761(3)	-1615(4)	3703(1)	51(1)
C(4)	10004(2)	-1328(3)	3366(1)	28(1)
C(5)	8904(2)	-1566(3)	3898(1)	25(1)
C(6)	8078(2)	-1834(3)	3637(1)	30(1)
C(7)	9348(3)	-2527(3)	4054(1)	33(1)
C(8)	8664(3)	-989(3)	4282(1)	28(1)
C(9)	8614(3)	585(3)	4627(1)	27(1)
C(10)	8529(3)	1711(3)	4642(1)	29(1)
C(11)	9084(3)	2048(3)	5011(1)	44(1)
C(12)	7151(3)	1888(4)	5048(1)	56(1)
C(13)	8897(3)	2325(3)	4281(1)	27(1)
C(14)	9952(3)	2573(3)	3732(1)	29(1)
C(15)	10541(3)	3298(3)	3985(1)	41(1)
C(16)	9362(3)	3185(3)	3440(1)	35(1)
C(17)	10638(3)	1904(3)	3519(1)	30(1)
C(18)	11030(2)	261(3)	3298(1)	31(1)
C(19)	9685(3)	1072(3)	3000(1)	32(1)
C(20)	8699(3)	946(3)	3085(1)	27(1)

C(21)	8002(3)	1080(3)	2808(1)	33(1)
C(22)	7121(3)	927(3)	2938(1)	33(1)
C(23)	6940(3)	657(3)	3334(1)	30(1)
C(24)	7659(2)	550(3)	3600(1)	25(1)
C(25)	7593(2)	311(3)	4043(1)	28(1)
C(26)	10444(3)	340(3)	4211(1)	29(1)
O(5)	548(3)	6050(3)	2978(1)	85(1)
C(27)	1074(5)	5679(5)	3277(2)	94(2)
O(6A)	8180(30)	4300(30)	5740(11)	318(18)
C(28A)	8262(10)	4231(11)	5693(5)	61(3)
O(6B)	7603(6)	3744(7)	5814(3)	79(2)
C(28B)	8003(18)	4289(19)	5392(9)	170(9)
O(7)	3692(9)	337(8)	5145(3)	128(5)
C(29)	4644(12)	-28(17)	5090(10)	158(15)
O(8)	8973(2)	7638(3)	2473(1)	59(1)
C(30)	8255(3)	8325(4)	2455(2)	63(2)

Table 3. Bond lengths [Å] and angles [°] for lsh149m.

Co(1)-N(5)	1.888(3)	C(1)-C(18)	1.531(5)
Co(1)-C(26)	1.892(4)	C(1)-C(4)	1.548(5)
Co(1)-N(3)	1.958(3)	C(5)-C(8)	1.525(5)
Co(1)-N(4)	1.963(3)	C(5)-C(6)	1.533(5)
Co(1)-N(2)	1.967(3)	C(5)-C(7)	1.537(5)
Co(1)-N(1)	1.971(3)	C(9)-C(10)	1.521(5)
O(1)-C(3)	1.437(5)	C(10)-C(11)	1.534(5)
O(1)-C(1)	1.448(5)	C(10)-C(13)	1.545(5)
O(2)-C(4)	1.264(4)	C(14)-C(17)	1.525(5)
O(3)-C(12)	1.420(5)	C(14)-C(16)	1.536(5)
O(3)-C(10)	1.441(5)	C(14)-C(15)	1.549(5)
O(4)-C(13)	1.257(4)	C(19)-C(20)	1.490(5)
N(1)-C(4)	1.328(5)	C(20)-C(21)	1.384(5)
N(1)-C(5)	1.507(4)	C(21)-C(22)	1.382(6)
N(2)-C(8)	1.492(4)	C(22)-C(23)	1.379(5)
N(2)-C(9)	1.501(4)	C(23)-C(24)	1.383(5)
N(2)-C(25)	1.513(4)	C(24)-C(25)	1.495(5)
N(3)-C(13)	1.329(5)	O(5)-C(27)	1.349(7)
N(3)-C(14)	1.495(5)	O(6A)-O(6B)	1.15(4)
N(4)-C(17)	1.497(5)	O(6A)-C(28B)	1.17(4)
N(4)-C(18)	1.499(5)	C(28A)-C(28B)	1.06(3)
N(4)-C(19)	1.513(5)	C(28A)-O(6B)	1.239(17)
N(5)-C(24)	1.340(4)	O(6B)-C(28B)	1.68(3)
N(5)-C(20)	1.343(5)	O(7)-C(29)	1.50(2)
N(6)-C(26)	1.150(5)	C(29)-C(29)#1	1.21(6)
C(1)-C(2)	1.528(6)	O(8)-C(30)	1.408(5)
N(5)-Co(1)-C(26)	178.51(15)	C(26)-Co(1)-N(2)	95.41(13)
N(5)-Co(1)-N(3)	90.09(12)	N(3)-Co(1)-N(2)	92.86(12)
C(26)-Co(1)-N(3)	88.47(14)	N(4)-Co(1)-N(2)	168.85(12)
N(5)-Co(1)-N(4)	84.56(13)	N(5)-Co(1)-N(1)	90.09(12)
C(26)-Co(1)-N(4)	95.73(14)	C(26)-Co(1)-N(1)	91.35(14)
N(3)-Co(1)-N(4)	87.05(13)	N(3)-Co(1)-N(1)	179.61(14)
N(5)-Co(1)-N(2)	84.29(12)	N(4)-Co(1)-N(1)	92.62(12)

N(2)-Co(1)-N(1)	87.50(12)	N(1)-C(5)-C(7)	112.4(3)
C(3)-O(1)-C(1)	118.0(3)	C(8)-C(5)-C(7)	104.5(3)
C(12)-O(3)-C(10)	117.3(3)	C(6)-C(5)-C(7)	109.1(3)
C(4)-N(1)-C(5)	116.2(3)	N(2)-C(8)-C(5)	114.5(3)
C(4)-N(1)-Co(1)	130.2(3)	N(2)-C(9)-C(10)	117.2(3)
C(5)-N(1)-Co(1)	112.9(2)	O(3)-C(10)-C(9)	111.1(3)
C(8)-N(2)-C(9)	106.8(3)	O(3)-C(10)-C(11)	112.5(3)
C(8)-N(2)-C(25)	111.5(3)	C(9)-C(10)-C(11)	106.0(3)
C(9)-N(2)-C(25)	110.0(3)	O(3)-C(10)-C(13)	103.4(3)
C(8)-N(2)-Co(1)	104.8(2)	C(9)-C(10)-C(13)	118.6(3)
C(9)-N(2)-Co(1)	112.7(2)	C(11)-C(10)-C(13)	105.4(3)
C(25)-N(2)-Co(1)	110.8(2)	O(4)-C(13)-N(3)	123.9(3)
C(13)-N(3)-C(14)	116.6(3)	O(4)-C(13)-C(10)	115.4(3)
C(13)-N(3)-Co(1)	129.7(2)	N(3)-C(13)-C(10)	120.4(3)
C(14)-N(3)-Co(1)	113.5(2)	N(3)-C(14)-C(17)	105.4(3)
C(17)-N(4)-C(18)	106.3(3)	N(3)-C(14)-C(16)	112.8(3)
C(17)-N(4)-C(19)	110.9(3)	C(17)-C(14)-C(16)	113.8(3)
C(18)-N(4)-C(19)	110.0(3)	N(3)-C(14)-C(15)	111.8(3)
C(17)-N(4)-Co(1)	104.8(2)	C(17)-C(14)-C(15)	104.3(3)
C(18)-N(4)-Co(1)	113.7(2)	C(16)-C(14)-C(15)	108.5(3)
C(19)-N(4)-Co(1)	111.0(2)	N(4)-C(17)-C(14)	113.2(3)
C(24)-N(5)-C(20)	122.0(3)	N(4)-C(18)-C(1)	118.3(3)
C(24)-N(5)-Co(1)	119.2(2)	C(20)-C(19)-N(4)	111.2(3)
C(20)-N(5)-Co(1)	118.8(2)	N(5)-C(20)-C(21)	120.1(3)
O(1)-C(1)-C(2)	101.0(3)	N(5)-C(20)-C(19)	114.0(3)
O(1)-C(1)-C(18)	105.8(3)	C(21)-C(20)-C(19)	125.9(3)
C(2)-C(1)-C(18)	114.2(3)	C(22)-C(21)-C(20)	118.4(4)
O(1)-C(1)-C(4)	107.4(3)	C(23)-C(22)-C(21)	120.8(4)
C(2)-C(1)-C(4)	109.5(3)	C(22)-C(23)-C(24)	118.5(4)
C(18)-C(1)-C(4)	117.2(3)	N(5)-C(24)-C(23)	120.2(3)
O(2)-C(4)-N(1)	124.3(3)	N(5)-C(24)-C(25)	113.7(3)
O(2)-C(4)-C(1)	114.6(3)	C(23)-C(24)-C(25)	126.1(3)
N(1)-C(4)-C(1)	120.9(3)	C(24)-C(25)-N(2)	110.8(3)
N(1)-C(5)-C(8)	105.0(3)	N(6)-C(26)-Co(1)	178.0(4)
N(1)-C(5)-C(6)	112.1(3)	O(6B)-O(6A)-C(28B)	92(3)
C(8)-C(5)-C(6)	113.6(3)	C(28B)-C(28A)-O(6B)	93.3(17)

O(6A)-O(6B)-C(28A)	10(2)
O(6A)-O(6B)-C(28B)	44(2)
C(28A)-O(6B)-C(28B)	39.3(10)
C(28A)-C(28B)-O(6A)	10(2)
C(28A)-C(28B)-O(6B)	47.4(13)
O(6A)-C(28B)-O(6B)	43(2)
C(29)#1-C(29)-O(7)	149(4)

Symmetry transformations used to generate equivalent atoms: #1 -x+1,-y,-z+1

Table 4. Anisotropic displacement parameters ($Å^2 x\ 10^3$) for lsh149m. The anisotropic displacement factor exponent takes the form: $-2\pi^2[\ h^2\ a^{*2}U^{11} + ... + 2\ h\ k\ a^*\ b^*\ U^{12}\ ]$

	U^{11}	U^{22}	U^{33}	U^{23}	U^{13}	U^{12}
Co(1)	21(1)	22(1)	23(1)	2(1)	-1(1)	-2(1)
O(1)	29(2)	45(2)	51(2)	3(2)	9(1)	12(1)
O(2)	35(2)	29(2)	37(2)	-6(1)	2(1)	3(1)
O(3)	40(2)	38(2)	34(2)	-1(1)	11(1)	6(1)
O(4)	46(2)	22(2)	39(2)	0(1)	2(1)	0(1)
N(1)	23(2)	22(2)	26(2)	4(1)	-1(1)	-1(1)
N(2)	23(2)	22(2)	24(2)	1(1)	-2(1)	-1(1)
N(3)	27(2)	23(2)	25(2)	3(1)	-2(1)	-4(1)
N(4)	26(2)	29(2)	27(2)	5(1)	2(1)	0(1)
N(5)	25(2)	22(2)	24(2)	-4(1)	-1(1)	0(1)
N(6)	33(2)	57(3)	39(2)	10(2)	-10(2)	-3(2)
C(1)	28(2)	31(2)	38(2)	2(2)	4(2)	6(2)
C(2)	53(3)	45(3)	36(2)	-2(2)	16(2)	3(2)
C(3)	37(3)	56(3)	59(3)	11(2)	-5(2)	12(2)
C(4)	27(2)	28(2)	28(2)	4(2)	-2(2)	4(2)
C(5)	25(2)	19(2)	32(2)	2(2)	2(2)	-2(2)
C(6)	25(2)	27(2)	39(2)	-2(2)	-2(2)	-1(2)
C(7)	35(2)	25(2)	37(2)	1(2)	1(2)	0(2)
C(8)	29(2)	24(2)	31(2)	4(2)	3(2)	-3(2)
C(9)	33(2)	27(2)	21(2)	0(2)	0(2)	-2(2)
C(10)	34(2)	28(2)	26(2)	-1(2)	-1(2)	0(2)
C(11)	64(3)	37(2)	31(2)	-6(2)	-6(2)	-5(2)
C(12)	59(3)	62(3)	46(3)	-1(2)	24(2)	3(3)
C(13)	32(2)	25(2)	25(2)	0(2)	-6(2)	-3(2)
C(14)	34(2)	22(2)	32(2)	6(2)	-1(2)	-6(2)
C(15)	38(2)	33(2)	53(3)	2(2)	-7(2)	-10(2)
C(16)	39(2)	29(2)	36(2)	9(2)	1(2)	0(2)
C(17)	27(2)	30(2)	33(2)	7(2)	1(2)	-6(2)
C(18)	23(2)	35(2)	36(2)	4(2)	8(2)	1(2)
C(19)	31(2)	43(2)	23(2)	6(2)	1(2)	2(2)
C(20)	33(2)	22(2)	27(2)	-1(2)	-2(2)	1(2)

C(21)	43(2)	30(2)	27(2)	0(2)	-7(2)	4(2)
C(22)	33(2)	30(2)	35(2)	-4(2)	-14(2)	5(2)
C(23)	26(2)	25(2)	40(2)	-6(2)	-7(2)	2(2)
C(24)	25(2)	18(2)	31(2)	-4(2)	-3(2)	0(2)
C(25)	22(2)	30(2)	32(2)	-3(2)	3(2)	2(2)
C(26)	29(2)	28(2)	29(2)	5(2)	2(2)	-3(2)
O(5)	125(4)	68(3)	61(2)	-17(2)	-1(2)	43(3)
C(27)	137(6)	64(4)	80(5)	2(3)	13(4)	48(4)
O(7)	159(10)	98(8)	128(8)	-71(7)	76(8)	-86(7)
C(29)	140(20)	74(9)	260(30)	-38(15)	-150(30)	6(18)
O(8)	60(2)	64(2)	54(2)	-7(2)	-2(2)	3(2)
C(30)	54(3)	61(3)	75(4)	11(3)	-5(3)	27(3)

Table 5. Hydrogen coordinates (x 10^4) and isotropic displacement parameters ($Å^2$x 10^3) for lsh149m.

	x	y	z	U(eq)
H(2A)	11275	-553	2581	67
H(2B)	10213	-795	2605	67
H(2C)	10940	-1672	2650	67
H(3A)	11797	-1000	3861	76
H(3B)	12326	-1991	3735	76
H(3C)	11250	-2016	3799	76
H(6A)	7835	-1231	3510	45
H(6B)	7611	-2137	3809	45
H(6C)	8260	-2306	3425	45
H(7A)	9451	-2980	3825	49
H(7B)	8946	-2845	4253	49
H(7C)	9928	-2368	4183	49
H(8A)	8104	-1276	4400	33
H(8B)	9156	-1081	4483	33
H(9A)	9213	402	4740	32
H(9B)	8147	300	4809	32
H(11A)	8981	2758	5059	66
H(11B)	9730	1932	4959	66
H(11C)	8895	1669	5251	66
H(12A)	7266	1217	5151	83
H(12B)	6497	1985	5013	83
H(12C)	7386	2378	5241	83
H(15A)	10835	2933	4207	62
H(15B)	10157	3823	4098	62
H(15C)	11006	3595	3810	62
H(16A)	9747	3482	3230	52
H(16B)	9052	3712	3591	52
H(16C)	8912	2750	3312	52
H(17A)	10885	2260	3280	36
H(17B)	11148	1769	3707	36

H(18A)	11409	238	3547	37
H(18B)	11401	572	3082	37
H(19A)	9794	1745	2888	39
H(19B)	9877	580	2794	39
H(21)	8127	1271	2536	40
H(22)	6635	1010	2751	39
H(23)	6334	547	3422	36
H(25A)	7197	-276	4081	34
H(25B)	7316	878	4189	34
H(5)	403	6638	3034	127
H(27A)	1581	6133	3328	141
H(27B)	1311	5029	3195	141
H(27C)	714	5606	3525	141
H(8C)	9230	7680	2700	89
H(30A)	7906	8297	2708	95
H(30B)	7858	8160	2226	95
H(30C)	8499	8996	2418	95

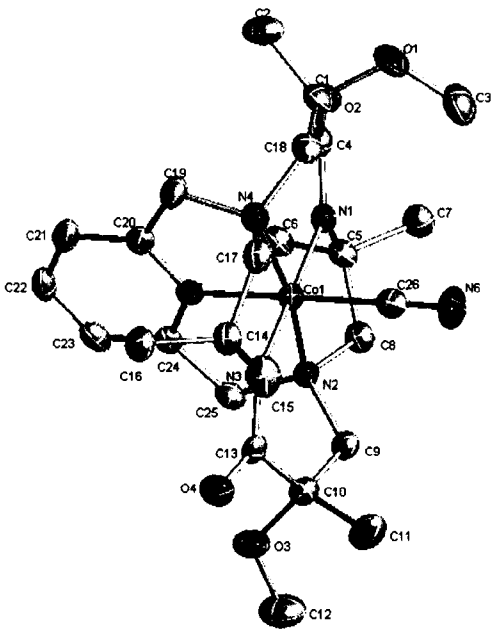

E. lsh154m, 6b

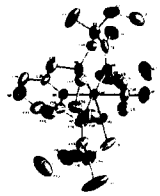

Table 7. Crystal data and structure refinement for lsh154m, **6b**.

Identification code	lsh154m	
Empirical formula	$C_{25}\ H_{40}\ Co\ N_7\ O_5$	
Formula weight	577.56	
Temperature	173(2) K	
Wavelength	0.71073 Å	
Crystal system	Monoclinic	
Space group	P2(1)/c	
Unit cell dimensions	a = 16.167(4) Å	α= 90°.
	b = 11.435(3) Å	β= 102.626(5)°.
	c = 15.670(4) Å	γ = 90°.
Volume	2826.9(12) $Å^3$	
Z	4	
Density (calculated)	1.352 Mg/m^3	
Absorption coefficient	0.654 mm^{-1}	
F(000)	1216	
Crystal size	0.25 x 0.20 x 0.10 mm^3	
Theta range for data collection	1.29 to 22.22°.	
Index ranges	-17<=h<=17, -12<=k<=12, -16<=l<=16	
Reflections collected	15951	
Independent reflections	3567 [R(int) = 0.0990]	
Completeness to theta = 22.22°	99.9 %	
Absorption correction	Semi-empirical from equivalents	
Max. and min. transmission	0.9375 and 0.8536	
Refinement method	Full-matrix least-squares on F^2	
Data / restraints / parameters	3567 / 0 / 353	
Goodness-of-fit on F^2	1.038	
Final R indices [I>2sigma(I)]	R1 = 0.0659, wR2 = 0.1562	
R indices (all data)	R1 = 0.1235, wR2 = 0.1997	
Extinction coefficient	0.0019(5)	
Largest diff. peak and hole	0.907 and -0.490 $e.Å^{-3}$	

Table 2. Atomic coordinates (x 10^4) and equivalent isotropic displacement parameters ($Å^2$x 10^3) for lsh154m. U(eq) is defined as one third of the trace of the orthogonalized U^{ij} tensor.

	x	y	z	U(eq)
Co(1)	7510(1)	9152(1)	2771(1)	32(1)
O(1)	10095(4)	7966(5)	4362(5)	68(2)
O(2)	9471(4)	6746(5)	2848(4)	61(2)
O(3)	5655(4)	10264(6)	999(4)	75(2)
O(4)	5548(4)	11542(5)	2697(4)	67(2)
N(1)	8225(4)	7768(5)	2723(4)	39(2)
N(2)	6652(4)	8301(5)	1921(4)	38(2)
N(3)	6779(4)	10482(5)	2902(4)	36(2)
N(4)	8441(4)	10152(5)	3401(4)	35(2)
N(5)	7794(4)	9785(5)	1773(4)	35(2)
N(6)	8236(5)	10610(8)	292(5)	76(3)
N(7)	7039(5)	8020(7)	4345(5)	73(2)
C(1)	9590(5)	8543(7)	3592(6)	53(2)
C(2)	10260(7)	8983(9)	3133(9)	107(5)
C(3)	9647(6)	7152(9)	4804(6)	73(3)
C(4)	9054(6)	7624(7)	3006(5)	46(2)
C(5)	7762(6)	6747(7)	2261(6)	63(3)
C(6)	8055(7)	6468(9)	1406(7)	94(4)
C(7)	7900(8)	5656(8)	2844(8)	114(5)
C(8)	6815(6)	7042(6)	2128(6)	57(2)
C(9)	5748(5)	8578(8)	1967(6)	62(3)
C(10)	5442(6)	9827(8)	1811(8)	71(3)
C(11)	4506(6)	9962(11)	1712(11)	146(7)
C(12)	5534(9)	11520(10)	789(8)	123(5)
C(13)	5953(5)	10695(8)	2542(5)	46(2)
C(14)	7194(5)	11387(7)	3547(6)	49(2)
C(15)	7243(6)	12565(7)	3098(7)	82(3)
C(16)	6731(6)	11582(9)	4299(6)	75(3)
C(17)	8047(5)	10898(7)	3985(5)	45(2)
C(18)	9118(5)	9479(6)	3986(5)	44(2)
C(19)	8799(5)	10913(7)	2771(5)	50(2)

C(20)	8417(5)	10560(7)	1848(5)	43(2)
C(21)	8644(6)	10963(9)	1091(6)	67(3)
C(22)	7608(6)	9841(10)	247(6)	70(3)
C(23)	7387(5)	9407(7)	976(5)	42(2)
C(24)	6725(5)	8520(7)	1000(5)	46(2)
C(25)	7221(5)	8477(7)	3760(6)	45(2)
O(5A)	4704(11)	3790(20)	-259(13)	158(10)
O(5B)	5255(16)	4556(19)	670(20)	188(12)

Table 3. Bond lengths [Å] and angles [°] for lsh154m.

Co(1)-N(5)	1.869(6)	N(5)-C(20)	1.328(9)
Co(1)-C(25)	1.879(8)	N(5)-C(23)	1.351(9)
Co(1)-N(2)	1.959(6)	N(6)-C(22)	1.333(12)
Co(1)-N(3)	1.964(6)	N(6)-C(21)	1.344(12)
Co(1)-N(1)	1.971(6)	N(7)-C(25)	1.147(10)
Co(1)-N(4)	1.975(6)	C(1)-C(2)	1.513(12)
O(1)-C(3)	1.446(11)	C(1)-C(18)	1.522(11)
O(1)-C(1)	1.458(11)	C(1)-C(4)	1.533(12)
O(2)-C(4)	1.263(9)	C(5)-C(7)	1.533(13)
O(3)-C(10)	1.475(12)	C(5)-C(8)	1.537(13)
O(3)-C(12)	1.477(12)	C(5)-C(6)	1.549(13)
O(4)-C(13)	1.222(9)	C(9)-C(10)	1.514(13)
N(1)-C(4)	1.326(10)	C(10)-C(11)	1.496(13)
N(1)-C(5)	1.487(10)	C(10)-C(13)	1.601(13)
N(2)-C(8)	1.486(9)	C(14)-C(17)	1.506(11)
N(2)-C(24)	1.494(10)	C(14)-C(15)	1.531(12)
N(2)-C(9)	1.512(10)	C(14)-C(16)	1.545(12)
N(3)-C(13)	1.354(10)	C(19)-C(20)	1.498(11)
N(3)-C(14)	1.499(9)	C(20)-C(21)	1.394(11)
N(4)-C(18)	1.480(9)	C(22)-C(23)	1.363(11)
N(4)-C(17)	1.493(9)	C(23)-C(24)	1.481(11)
N(4)-C(19)	1.522(9)	O(5A)-O(5B)	1.76(3)

N(5)-Co(1)-C(25)	178.5(3)	C(25)-Co(1)-N(4)	97.2(3)
N(5)-Co(1)-N(2)	83.7(3)	N(2)-Co(1)-N(4)	167.6(2)
C(25)-Co(1)-N(2)	95.2(3)	N(3)-Co(1)-N(4)	84.8(2)
N(5)-Co(1)-N(3)	92.9(3)	N(1)-Co(1)-N(4)	95.4(2)
C(25)-Co(1)-N(3)	88.2(3)	C(3)-O(1)-C(1)	116.0(6)
N(2)-Co(1)-N(3)	95.9(2)	C(10)-O(3)-C(12)	118.5(8)
N(5)-Co(1)-N(1)	91.5(2)	C(4)-N(1)-C(5)	115.4(7)
C(25)-Co(1)-N(1)	87.4(3)	C(4)-N(1)-Co(1)	130.2(5)
N(2)-Co(1)-N(1)	84.8(3)	C(5)-N(1)-Co(1)	114.3(5)
N(3)-Co(1)-N(1)	175.6(3)	C(8)-N(2)-C(24)	109.0(6)
N(5)-Co(1)-N(4)	83.9(3)	C(8)-N(2)-C(9)	108.7(6)

C(24)-N(2)-C(9)	107.0(6)	C(11)-C(10)-C(9)	113.6(9)
C(8)-N(2)-Co(1)	105.5(5)	O(3)-C(10)-C(13)	103.1(7)
C(24)-N(2)-Co(1)	112.3(4)	C(11)-C(10)-C(13)	111.2(8)
C(9)-N(2)-Co(1)	114.3(5)	C(9)-C(10)-C(13)	111.8(8)
C(13)-N(3)-C(14)	114.4(6)	O(4)-C(13)-N(3)	125.5(7)
C(13)-N(3)-Co(1)	131.1(5)	O(4)-C(13)-C(10)	114.8(7)
C(14)-N(3)-Co(1)	114.4(5)	N(3)-C(13)-C(10)	119.6(7)
C(18)-N(4)-C(17)	105.9(6)	N(3)-C(14)-C(17)	106.4(6)
C(18)-N(4)-C(19)	111.4(6)	N(3)-C(14)-C(15)	111.0(7)
C(17)-N(4)-C(19)	110.2(6)	C(17)-C(14)-C(15)	113.7(7)
C(18)-N(4)-Co(1)	112.9(4)	N(3)-C(14)-C(16)	113.2(7)
C(17)-N(4)-Co(1)	104.9(4)	C(17)-C(14)-C(16)	104.7(7)
C(19)-N(4)-Co(1)	111.3(4)	C(15)-C(14)-C(16)	107.8(8)
C(20)-N(5)-C(23)	120.2(7)	N(4)-C(17)-C(14)	113.8(6)
C(20)-N(5)-Co(1)	120.3(5)	N(4)-C(18)-C(1)	118.8(7)
C(23)-N(5)-Co(1)	119.4(5)	C(20)-C(19)-N(4)	109.7(6)
C(22)-N(6)-C(21)	117.4(8)	N(5)-C(20)-C(21)	118.7(8)
O(1)-C(1)-C(2)	102.3(8)	N(5)-C(20)-C(19)	114.2(7)
O(1)-C(1)-C(18)	102.8(7)	C(21)-C(20)-C(19)	127.1(7)
C(2)-C(1)-C(18)	115.7(7)	N(6)-C(21)-C(20)	121.8(8)
O(1)-C(1)-C(4)	109.1(6)	N(6)-C(22)-C(23)	122.1(9)
C(2)-C(1)-C(4)	108.3(8)	N(5)-C(23)-C(22)	119.7(8)
C(18)-C(1)-C(4)	117.2(7)	N(5)-C(23)-C(24)	113.8(7)
O(2)-C(4)-N(1)	125.2(8)	C(22)-C(23)-C(24)	126.5(8)
O(2)-C(4)-C(1)	114.0(8)	C(23)-C(24)-N(2)	110.5(6)
N(1)-C(4)-C(1)	120.8(7)	N(7)-C(25)-Co(1)	177.1(8)
N(1)-C(5)-C(7)	110.9(7)		
N(1)-C(5)-C(8)	105.9(7)		
C(7)-C(5)-C(8)	105.7(9)		
N(1)-C(5)-C(6)	111.5(8)		
C(7)-C(5)-C(6)	108.4(9)		
C(8)-C(5)-C(6)	114.3(8)		
N(2)-C(8)-C(5)	111.5(7)		
N(2)-C(9)-C(10)	118.3(7)		
O(3)-C(10)-C(11)	107.2(11)		
O(3)-C(10)-C(9)	109.3(7)		

Table 4. Anisotropic displacement parameters ($Å^2 x\ 10^3$) for lsh154m. The anisotropic displacement factor exponent takes the form: $-2\pi^2[\ h^2\ a^{*2}U^{11} + ... + 2\ h\ k\ a^*\ b^*\ U^{12}\ ]$

	U^{11}	U^{22}	U^{33}	U^{23}	U^{13}	U^{12}
Co(1)	39(1)	23(1)	38(1)	-6(1)	15(1)	-8(1)
O(1)	38(3)	55(4)	106(6)	-13(4)	5(4)	3(3)
O(2)	67(4)	46(4)	71(4)	1(3)	18(3)	20(3)
O(3)	90(5)	64(4)	62(4)	1(4)	-1(4)	14(4)
O(4)	55(4)	49(4)	91(5)	-20(4)	2(3)	15(3)
N(1)	47(4)	24(3)	50(4)	-6(3)	18(3)	-7(3)
N(2)	36(4)	30(4)	50(4)	-11(3)	18(3)	-5(3)
N(3)	39(4)	27(3)	41(4)	-12(3)	10(3)	-3(3)
N(4)	43(4)	28(3)	34(4)	2(3)	9(3)	-2(3)
N(5)	33(4)	34(4)	40(4)	0(3)	13(3)	-2(3)
N(6)	61(5)	120(7)	48(5)	18(5)	13(4)	-27(5)
N(7)	78(6)	79(6)	65(6)	19(5)	25(5)	-16(5)
C(1)	52(6)	32(5)	80(7)	3(5)	28(5)	0(4)
C(2)	92(8)	55(7)	204(14)	-11(8)	100(9)	-19(6)
C(3)	76(7)	72(7)	69(7)	16(6)	15(6)	28(6)
C(4)	63(6)	30(5)	50(5)	15(4)	26(5)	11(5)
C(5)	90(8)	30(5)	60(6)	-5(4)	1(6)	7(5)
C(6)	92(8)	96(8)	83(8)	-40(7)	-3(6)	62(7)
C(7)	124(10)	43(6)	146(12)	23(7)	-32(9)	-30(7)
C(8)	75(7)	26(5)	67(6)	-15(4)	9(5)	-13(4)
C(9)	38(5)	72(6)	80(7)	-34(5)	26(5)	-23(5)
C(10)	56(6)	53(6)	121(9)	-9(6)	55(6)	19(5)
C(11)	47(7)	106(10)	290(20)	-103(12)	59(9)	-24(7)
C(12)	170(14)	70(8)	104(10)	10(7)	-23(9)	12(9)
C(13)	35(5)	55(6)	52(5)	-16(5)	16(4)	-6(4)
C(14)	50(5)	38(5)	53(6)	-18(4)	-3(4)	1(4)
C(15)	74(7)	32(5)	120(9)	0(6)	-26(6)	-5(5)
C(16)	67(7)	85(7)	69(7)	-41(6)	7(5)	19(6)
C(17)	53(5)	38(5)	42(5)	-19(4)	8(4)	-2(4)
C(18)	38(5)	37(5)	54(5)	-5(4)	7(4)	-2(4)
C(19)	55(5)	35(5)	64(6)	-4(4)	20(5)	-19(4)

C(20)	38(5)	43(5)	53(6)	3(4)	18(4)	-13(4)
C(21)	59(6)	79(7)	68(7)	13(6)	26(6)	-25(5)
C(22)	47(6)	119(9)	44(6)	1(6)	9(5)	-7(6)
C(23)	35(5)	58(6)	35(5)	-3(4)	15(4)	5(4)
C(24)	29(4)	52(5)	53(6)	-9(4)	2(4)	-1(4)
C(25)	57(6)	37(5)	49(5)	2(4)	27(5)	-12(4)
O(5A)	95(13)	280(30)	123(16)	89(18)	77(12)	80(16)
O(5B)	160(20)	113(17)	320(40)	-50(20)	120(20)	6(15)

Table 5. Hydrogen coordinates (x 10^4) and isotropic displacement parameters ($Å^2$x 10^3) for lsh154m.

	x	y	z	U(eq)
H(2A)	10603	9561	3490	160
H(2B)	9992	9325	2582	160
H(2C)	10612	8343	3035	160
H(3A)	10034	6823	5298	109
H(3B)	9409	6538	4408	109
H(3C)	9201	7554	4998	109
H(6A)	7974	7144	1033	141
H(6B)	7728	5828	1111	141
H(6C)	8644	6259	1543	141
H(7A)	7721	5814	3378	171
H(7B)	8490	5452	2975	171
H(7C)	7574	5019	2543	171
H(8A)	6495	6571	1654	69
H(8B)	6622	6850	2655	69
H(9A)	5673	8347	2541	74
H(9B)	5377	8087	1544	74
H(11A)	4216	9433	1271	218
H(11B)	4344	10751	1544	218
H(11C)	4356	9788	2258	218
H(12A)	5698	11679	248	184
H(12B)	5876	11975	1248	184
H(12C)	4948	11721	733	184
H(15A)	7526	12466	2624	124
H(15B)	7554	13111	3513	124
H(15C)	6681	12857	2875	124
H(16A)	6689	10853	4590	112
H(16B)	6173	11882	4066	112
H(16C)	7043	12132	4709	112
H(17A)	8426	11542	4198	54
H(17B)	7983	10439	4487	54

H(18A)	8868	9106	4426	52
H(18B)	9534	10034	4289	52
H(19A)	8673	11728	2857	60
H(19B)	9410	10824	2885	60
H(21A)	9090	11490	1141	80
H(22A)	7311	9592	-300	84
H(24A)	6867	7797	743	55
H(24B)	6185	8793	659	55

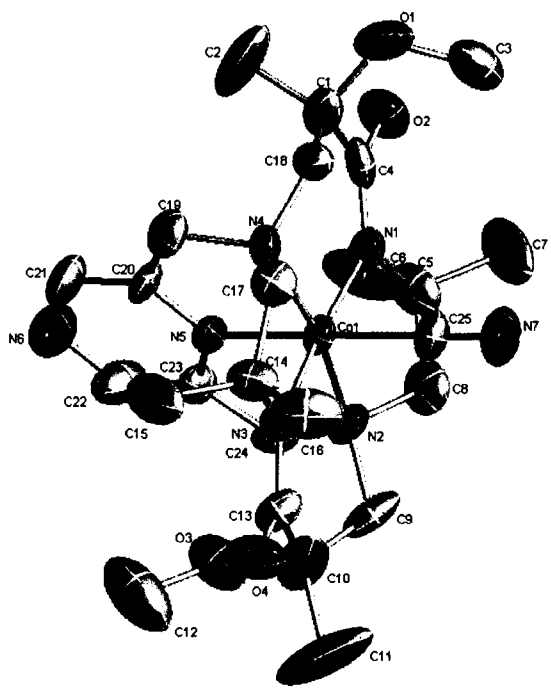

F. lsh144m, 7

Table 1. Crystal data and structure refinement for lsh144m, 7.

Identification code	lsh144m	
Empirical formula	$C_{62}\ H_{98}\ Co_2\ N_{12}\ O_{22}\ Rh_2$	
Formula weight	1687.19	
Temperature	169(2) K	
Wavelength	0.71073 Å	
Crystal system	Trigonal	
Space group	R-3	
Unit cell dimensions	a = 39.468(10) Å	α= 90°.
	b = 39.468(10) Å	β= 90°.
	c = 14.566(4) Å	γ= 120°.
Volume	19650(9) $Å^3$	
Z	9	
Density (calculated)	1.277 Mg/m^3	
Absorption coefficient	0.812 mm^{-1}	
F(000)	7794	
Crystal size	0.40 x 0.30 x 0.15 mm^3	
Theta range for data collection	1.52 to 23.29°.	
Index ranges	-43<=h<=43, -43<=k<=43, -16<=l<=16	
Reflections collected	42637	
Independent reflections	6307 [R(int) = 0.1265]	
Completeness to theta = 23.29°	100.0 %	
Absorption correction	Semi-empirical from equivalents	
Max. and min. transmission	0.8880 and 0.7372	
Refinement method	Full-matrix least-squares on F^2	
Data / restraints / parameters	6307 / 0 / 471	
Goodness-of-fit on F^2	1.082	
Final R indices [I>2sigma(I)]	R1 = 0.0741, wR2 = 0.1961	
R indices (all data)	R1 = 0.1288, wR2 = 0.2248	
Extinction coefficient	0.00012(3)	
Largest diff. peak and hole	0.901 and -0.485 $e.Å^{-3}$	

Table 2. Atomic coordinates (x 10^4) and equivalent isotropic displacement parameters ($Å^2$x 10^3) for lsh144m. U(eq) is defined as one third of the trace of the orthogonalized U^{ij} tensor.

	x	y	z	U(eq)
Rh(1)	1652(1)	3095(1)	7806(1)	55(1)
Co(1)	2015(1)	2257(1)	5840(1)	39(1)
O(1)	2154(3)	1662(3)	8194(8)	125(4)
O(2)	1438(2)	1254(2)	7399(6)	85(2)
O(3)	1916(2)	3045(2)	3771(5)	83(2)
O(4)	2686(2)	3199(2)	4115(5)	66(2)
O(5)	1650(3)	2779(3)	8891(6)	113(3)
O(6)	2245(2)	3378(3)	7816(6)	104(3)
O(7)	1658(3)	3436(3)	6786(5)	93(3)
O(8)	1062(2)	2830(3)	7876(5)	91(3)
N(1)	1643(3)	1770(2)	6460(6)	63(2)
N(2)	1666(2)	2071(2)	4775(5)	58(2)
N(3)	2388(3)	2761(2)	5254(6)	61(2)
N(4)	2410(2)	2394(2)	6804(5)	51(2)
N(5)	2269(2)	2013(2)	5261(5)	43(2)
N(6)	1653(2)	2667(2)	6847(5)	56(2)
C(1)	1953(3)	1870(3)	7934(9)	78(3)
C(2)	1698(5)	1866(4)	8722(9)	133(6)
C(3)	2342(6)	1752(7)	9126(14)	214(12)
C(4)	1656(3)	1617(3)	7188(9)	74(3)
C(5)	1271(3)	1515(3)	5861(7)	66(3)
C(6)	1265(4)	1148(4)	5452(8)	94(4)
C(7)	894(3)	1375(4)	6396(9)	91(4)
C(8)	1271(3)	1792(3)	5170(7)	61(3)
C(9)	1638(3)	2397(3)	4312(7)	61(3)
C(10)	2012(3)	2732(3)	3904(7)	64(3)
C(11)	2103(4)	2657(4)	2944(8)	111(5)
C(12)	1952(4)	3282(4)	4591(11)	101(4)
C(13)	2403(4)	2910(3)	4476(8)	67(3)
C(14)	2773(3)	3005(3)	5810(6)	54(2)
C(15)	2877(3)	3419(3)	5949(7)	70(3)

C(16)	3109(3)	2974(3)	5412(7)	69(3)
C(17)	2658(3)	2829(3)	6775(6)	49(2)
C(18)	2243(3)	2297(3)	7727(6)	62(3)
C(19)	2646(3)	2185(3)	6632(8)	71(3)
C(20)	2575(3)	2029(3)	5674(7)	52(3)
C(21)	2785(3)	1886(3)	5210(9)	73(3)
C(22)	2672(3)	1734(3)	4362(8)	62(3)
C(23)	2350(3)	1710(3)	3971(7)	61(3)
C(24)	2139(3)	1855(3)	4435(6)	49(2)
C(25)	1796(3)	1863(4)	4093(7)	73(3)
C(26)	1776(2)	2506(3)	6443(6)	43(2)
C(27)	1659(6)	3747(5)	6976(10)	123(6)
C(28)	1620(9)	3968(6)	6160(11)	245(15)
C(29)	913(3)	2982(5)	8379(10)	117(6)
C(30)	459(4)	2782(6)	8324(14)	199(12)
O(9)	335(11)	1799(9)	8100(20)	404(19)
C(35)	707(10)	1913(11)	8610(20)	241(14)
O(10)	926(12)	881(7)	8959(17)	270(20)
O(11)	871(11)	1025(11)	2994(16)	230(17)
O(12)	973(5)	1661(8)	2679(18)	372(17)

Table 3. Bond lengths [Å] and angles [°] for lsh144m.

Rh(1)-O(7)	1.998(9)	N(4)-C(18)	1.462(12)
Rh(1)-O(5)	2.009(9)	N(4)-C(17)	1.492(11)
Rh(1)-O(8)	2.021(7)	N(4)-C(19)	1.541(12)
Rh(1)-O(6)	2.028(7)	N(5)-C(20)	1.324(11)
Rh(1)-N(6)	2.192(8)	N(5)-C(24)	1.335(11)
Rh(1)-Rh(1)#1	2.3879(15)	N(6)-C(26)	1.140(10)
Co(1)-C(26)	1.887(9)	C(1)-C(18)	1.519(14)
Co(1)-N(5)	1.896(7)	C(1)-C(2)	1.522(18)
Co(1)-N(2)	1.958(8)	C(1)-C(4)	1.544(17)
Co(1)-N(1)	1.960(8)	C(5)-C(8)	1.486(15)
Co(1)-N(4)	1.962(7)	C(5)-C(7)	1.520(15)
Co(1)-N(3)	1.980(8)	C(5)-C(6)	1.556(14)
O(1)-C(1)	1.448(14)	C(9)-C(10)	1.527(14)
O(1)-C(3)	1.50(2)	C(10)-C(11)	1.508(14)
O(2)-C(4)	1.287(12)	C(10)-C(13)	1.576(15)
O(3)-C(10)	1.475(13)	C(14)-C(15)	1.487(13)
O(3)-C(12)	1.481(15)	C(14)-C(16)	1.508(13)
O(4)-C(13)	1.246(12)	C(14)-C(17)	1.532(13)
O(5)-C(27)#1	1.272(15)	C(19)-C(20)	1.494(14)
O(6)-C(29)#1	1.257(15)	C(20)-C(21)	1.388(13)
O(7)-C(27)	1.258(15)	C(21)-C(22)	1.349(15)
O(8)-C(29)	1.264(14)	C(22)-C(23)	1.353(14)
N(1)-C(4)	1.234(13)	C(23)-C(24)	1.395(13)
N(1)-C(5)	1.567(13)	C(24)-C(25)	1.457(13)
N(2)-C(8)	1.502(12)	C(27)-O(5)#1	1.272(15)
N(2)-C(9)	1.505(12)	C(27)-C(28)	1.527(19)
N(2)-C(25)	1.532(12)	C(29)-O(6)#1	1.257(15)
N(3)-C(13)	1.265(13)	C(29)-C(30)	1.558(17)
N(3)-C(14)	1.558(12)	O(9)-C(35)	1.50(3)
O(7)-Rh(1)-O(5)	176.2(3)	O(5)-Rh(1)-O(6)	89.0(4)
O(7)-Rh(1)-O(8)	90.6(4)	O(8)-Rh(1)-O(6)	176.2(3)
O(5)-Rh(1)-O(8)	89.6(4)	O(7)-Rh(1)-N(6)	92.3(3)
O(7)-Rh(1)-O(6)	90.6(4)	O(5)-Rh(1)-N(6)	91.5(3)

O(8)-Rh(1)-N(6)	94.5(3)	C(25)-N(2)-Co(1)	110.6(6)
O(6)-Rh(1)-N(6)	89.0(3)	C(13)-N(3)-C(14)	111.9(9)
O(7)-Rh(1)-Rh(1)#1	88.1(2)	C(13)-N(3)-Co(1)	133.8(9)
O(5)-Rh(1)-Rh(1)#1	88.1(2)	C(14)-N(3)-Co(1)	113.7(6)
O(8)-Rh(1)-Rh(1)#1	88.1(2)	C(18)-N(4)-C(17)	106.2(7)
O(6)-Rh(1)-Rh(1)#1	88.4(2)	C(18)-N(4)-C(19)	108.7(8)
N(6)-Rh(1)-Rh(1)#1	177.4(2)	C(17)-N(4)-C(19)	112.8(7)
C(26)-Co(1)-N(5)	178.2(3)	C(18)-N(4)-Co(1)	113.2(6)
C(26)-Co(1)-N(2)	97.0(3)	C(17)-N(4)-Co(1)	105.8(5)
N(5)-Co(1)-N(2)	84.8(3)	C(19)-N(4)-Co(1)	110.1(6)
C(26)-Co(1)-N(1)	88.3(4)	C(20)-N(5)-C(24)	124.0(8)
N(5)-Co(1)-N(1)	92.0(3)	C(20)-N(5)-Co(1)	118.4(6)
N(2)-Co(1)-N(1)	87.5(4)	C(24)-N(5)-Co(1)	117.6(6)
C(26)-Co(1)-N(4)	93.4(3)	C(26)-N(6)-Rh(1)	157.6(7)
N(5)-Co(1)-N(4)	84.9(3)	O(1)-C(1)-C(18)	111.0(9)
N(2)-Co(1)-N(4)	169.7(3)	O(1)-C(1)-C(2)	110.0(12)
N(1)-Co(1)-N(4)	92.5(4)	C(18)-C(1)-C(2)	106.9(11)
C(26)-Co(1)-N(3)	89.5(3)	O(1)-C(1)-C(4)	105.7(10)
N(5)-Co(1)-N(3)	90.1(3)	C(18)-C(1)-C(4)	119.0(10)
N(2)-Co(1)-N(3)	93.7(4)	C(2)-C(1)-C(4)	103.9(10)
N(1)-Co(1)-N(3)	177.6(3)	N(1)-C(4)-O(2)	125.5(12)
N(4)-Co(1)-N(3)	86.7(3)	N(1)-C(4)-C(1)	119.5(11)
C(1)-O(1)-C(3)	116.7(14)	O(2)-C(4)-C(1)	115.0(11)
C(10)-O(3)-C(12)	116.1(8)	C(8)-C(5)-C(7)	104.7(9)
C(27)#1-O(5)-Rh(1)	118.3(9)	C(8)-C(5)-C(6)	114.9(9)
C(29)#1-O(6)-Rh(1)	117.7(7)	C(7)-C(5)-C(6)	107.6(10)
C(27)-O(7)-Rh(1)	119.2(8)	C(8)-C(5)-N(1)	104.5(8)
C(29)-O(8)-Rh(1)	118.2(7)	C(7)-C(5)-N(1)	112.4(9)
C(4)-N(1)-C(5)	114.8(9)	C(6)-C(5)-N(1)	112.5(9)
C(4)-N(1)-Co(1)	133.0(9)	C(5)-C(8)-N(2)	114.6(8)
C(5)-N(1)-Co(1)	112.0(7)	N(2)-C(9)-C(10)	117.5(8)
C(8)-N(2)-C(9)	107.7(8)	O(3)-C(10)-C(11)	103.1(10)
C(8)-N(2)-C(25)	111.1(8)	O(3)-C(10)-C(9)	103.5(8)
C(9)-N(2)-C(25)	110.8(8)	C(11)-C(10)-C(9)	114.4(9)
C(8)-N(2)-Co(1)	104.5(6)	O(3)-C(10)-C(13)	107.6(8)
C(9)-N(2)-Co(1)	112.0(6)	C(11)-C(10)-C(13)	107.6(9)

C(9)-C(10)-C(13)	119.2(9)
O(4)-C(13)-N(3)	128.1(12)
O(4)-C(13)-C(10)	114.5(10)
N(3)-C(13)-C(10)	117.3(11)
C(15)-C(14)-C(16)	111.8(9)
C(15)-C(14)-C(17)	103.3(8)
C(16)-C(14)-C(17)	112.9(8)
C(15)-C(14)-N(3)	113.5(8)
C(16)-C(14)-N(3)	112.0(8)
C(17)-C(14)-N(3)	102.7(7)
N(4)-C(17)-C(14)	115.0(7)
N(4)-C(18)-C(1)	117.8(9)
C(20)-C(19)-N(4)	109.5(8)
N(5)-C(20)-C(21)	118.5(10)
N(5)-C(20)-C(19)	114.9(8)
C(21)-C(20)-C(19)	126.6(10)
C(22)-C(21)-C(20)	119.6(10)
C(21)-C(22)-C(23)	120.5(9)
C(22)-C(23)-C(24)	119.9(10)
N(5)-C(24)-C(23)	117.5(9)
N(5)-C(24)-C(25)	116.1(8)
C(23)-C(24)-C(25)	126.4(9)
C(24)-C(25)-N(2)	110.8(8)
N(6)-C(26)-Co(1)	175.3(8)
O(7)-C(27)-O(5)#1	126.1(13)
O(7)-C(27)-C(28)	115.8(13)
O(5)#1-C(27)-C(28)	118.1(14)
O(6)#1-C(29)-O(8)	127.7(10)
O(6)#1-C(29)-C(30)	117.3(12)
O(8)-C(29)-C(30)	114.8(12)

Symmetry transformations used to generate equivalent atoms: #1 -x+1/3,-y+2/3,-z+5/3

Table 4. Anisotropic displacement parameters ($Å^2 x\ 10^3$) for lsh144m. The anisotropic displacement factor exponent takes the form: $-2\pi^2[\ h^2\ a^{*2}U^{11} + ... + 2\ h\ k\ a^*\ b^*\ U^{12}\ ]$

	U^{11}	U^{22}	U^{33}	U^{23}	U^{13}	U^{12}
Rh(1)	49(1)	78(1)	51(1)	-31(1)	-14(1)	42(1)
Co(1)	37(1)	41(1)	40(1)	-3(1)	3(1)	22(1)
O(1)	103(7)	89(7)	154(9)	43(6)	-37(7)	26(6)
O(2)	82(6)	62(5)	96(6)	21(4)	9(5)	25(4)
O(3)	93(6)	87(6)	82(6)	8(5)	-8(5)	56(5)
O(4)	51(4)	61(5)	75(5)	30(4)	17(4)	19(4)
O(5)	194(10)	104(7)	76(6)	-42(5)	-26(6)	100(7)
O(6)	53(5)	157(8)	110(7)	-97(7)	-30(4)	59(5)
O(7)	140(8)	96(6)	59(5)	-26(5)	-8(5)	70(6)
O(8)	47(4)	126(7)	93(6)	-70(5)	-16(4)	37(5)
N(1)	76(6)	47(5)	62(6)	8(4)	22(5)	28(5)
N(2)	56(5)	73(6)	50(5)	-22(4)	-3(4)	35(5)
N(3)	89(7)	66(6)	51(5)	10(4)	17(5)	55(5)
N(4)	43(4)	52(5)	62(5)	-8(4)	-12(4)	28(4)
N(5)	45(5)	33(4)	50(5)	2(4)	10(4)	20(4)
N(6)	53(5)	74(6)	54(5)	-24(4)	-7(4)	42(5)
C(1)	65(8)	68(8)	90(9)	6(7)	-13(7)	26(7)
C(2)	129(13)	114(12)	79(10)	5(9)	18(10)	4(10)
C(3)	162(19)	260(30)	180(20)	93(19)	-51(16)	76(19)
C(4)	76(8)	62(8)	90(9)	19(7)	28(7)	37(7)
C(5)	51(7)	72(7)	67(7)	-17(6)	-2(5)	25(6)
C(6)	146(12)	86(9)	80(9)	-8(7)	-5(8)	80(9)
C(7)	76(9)	93(9)	88(9)	7(7)	-7(7)	30(7)
C(8)	59(7)	61(7)	63(7)	-17(5)	-11(5)	30(6)
C(9)	67(7)	80(8)	44(6)	-9(5)	-12(5)	43(6)
C(10)	56(7)	73(7)	64(7)	-9(6)	-5(5)	33(6)
C(11)	91(10)	128(12)	73(9)	-32(8)	15(7)	24(9)
C(12)	85(9)	96(10)	142(13)	-7(9)	-4(9)	60(9)
C(13)	87(9)	75(8)	64(7)	0(6)	12(6)	58(7)
C(14)	49(6)	57(6)	54(6)	-4(5)	-9(5)	25(5)
C(15)	70(7)	61(7)	64(7)	-1(6)	0(6)	21(6)

C(16)	39(6)	97(9)	71(7)	21(6)	13(5)	33(6)
C(17)	45(6)	50(6)	50(6)	-8(5)	-1(4)	22(5)
C(18)	64(7)	73(7)	42(6)	4(5)	-6(5)	28(6)
C(19)	67(7)	76(8)	79(8)	-19(6)	-20(6)	43(6)
C(20)	46(6)	46(6)	76(7)	-7(5)	-5(5)	32(5)
C(21)	62(7)	69(7)	105(10)	-19(7)	0(7)	45(6)
C(22)	69(7)	53(6)	80(8)	3(6)	26(6)	42(6)
C(23)	83(8)	60(7)	46(6)	-6(5)	11(6)	39(6)
C(24)	53(6)	44(6)	50(6)	-3(5)	12(5)	25(5)
C(25)	79(8)	95(9)	60(7)	-32(6)	-15(6)	56(7)
C(26)	37(5)	54(6)	34(5)	-8(4)	-4(4)	21(5)
C(27)	220(20)	110(12)	71(10)	-18(9)	-28(10)	105(13)
C(28)	560(50)	180(20)	84(12)	-17(13)	-50(20)	250(30)
C(29)	43(7)	186(16)	119(12)	-84(12)	-23(7)	54(9)
C(30)	51(9)	270(20)	220(20)	-165(19)	-18(11)	44(12)
O(9)	450(50)	350(40)	330(40)	50(30)	-70(30)	150(30)
C(35)	270(40)	350(40)	170(30)	-40(30)	-20(20)	210(40)
O(10)	470(60)	92(17)	114(19)	21(15)	70(30)	40(30)
O(11)	400(50)	370(50)	95(18)	50(20)	20(20)	320(40)
O(12)	162(15)	510(40)	500(40)	-330(30)	-190(20)	220(20)

Table 5. Hydrogen coordinates (x 10^4) and isotropic displacement parameters ($Å^2$x 10^3) for lsh144m.

	x	y	z	U(eq)
H(2A)	1479	1599	8807	199
H(2B)	1598	2042	8581	199
H(2C)	1854	1953	9287	199
H(3A)	2461	2032	9250	321
H(3B)	2545	1678	9142	321
H(3C)	2144	1603	9593	321
H(6A)	1035	1006	5057	142
H(6B)	1254	976	5953	142
H(6C)	1503	1230	5091	142
H(7A)	882	1601	6632	137
H(7B)	886	1211	6910	137
H(7C)	670	1222	5991	137
H(8A)	1164	1946	5460	73
H(8B)	1093	1640	4662	73
H(9A)	1535	2509	4765	73
H(9B)	1442	2281	3813	73
H(11A)	1868	2560	2561	167
H(11B)	2187	2462	2963	167
H(11C)	2313	2901	2683	167
H(12A)	1789	3110	5086	152
H(12B)	1867	3470	4438	152
H(12C)	2226	3424	4791	152
H(15A)	2642	3429	6121	105
H(15B)	2984	3566	5378	105
H(15C)	3072	3536	6438	105
H(16A)	3193	3120	4834	104
H(16B)	3026	2699	5297	104
H(16C)	3328	3084	5847	104
H(17A)	2900	2907	7130	59
H(17B)	2516	2944	7085	59

H(18A)	2112	2450	7847	75
H(18B)	2462	2387	8169	75
H(19A)	2928	2371	6723	85
H(19B)	2564	1967	7074	85
H(21)	3008	1896	5488	88
H(22)	2818	1642	4038	74
H(23)	2267	1596	3381	74
H(25A)	1580	1592	3995	87
H(25B)	1859	2001	3496	87
H(28A)	1359	3941	6165	367
H(28B)	1656	3860	5588	367
H(28C)	1819	4246	6205	367
H(30A)	384	2848	7739	298
H(30B)	363	2873	8832	298
H(30C)	344	2497	8366	298

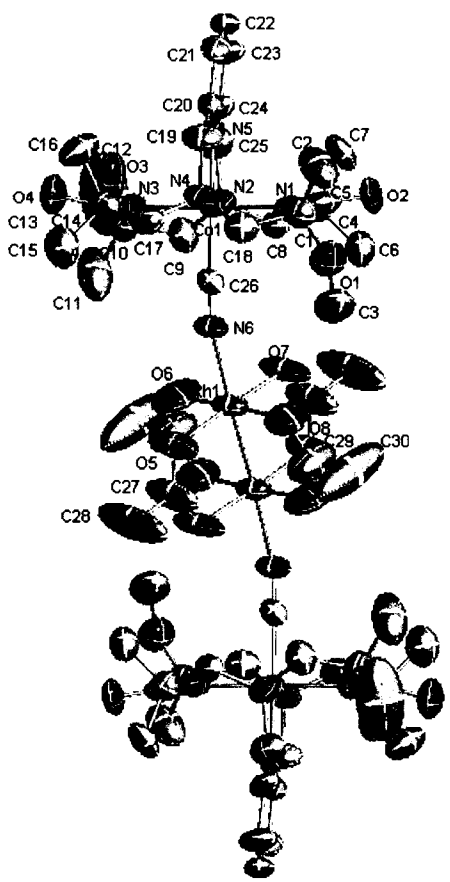

G. lsh146m, 8

Table 1. Crystal data and structure refinement for lsh146m, **8**.

Identification code	lsh146m	
Empirical formula	$C_{88}\ H_{110}\ Co_2\ N_{20}\ O_{12}\ Ru$	
Formula weight	1858.88	
Temperature	173(2) K	
Wavelength	0.71073 Å	
Crystal system	Monoclinic	
Space group	P2(1)/n	
Unit cell dimensions	a = 12.0984(12) Å	α= 90°.
	b = 11.8549(12) Å	β= 99.127(2)°.
	c = 29.740(3) Å	γ = 90°.
Volume	4211.5(7) $Å^3$	
Z	2	
Density (calculated)	1.460 Mg/m^3	
Absorption coefficient	0.642 mm^{-1}	
F(000)	1928	
Crystal size	0.40 x 0.34 x 0.18 mm^3	
Theta range for data collection	1.39 to 25.03°.	
Index ranges	-14<=h<=14, -14<=k<=14, -35<=l<=35	
Reflections collected	30862	
Independent reflections	7443 [R(int) = 0.0802]	
Completeness to theta = 25.03°	100.0 %	
Absorption correction	Semi-empirical from equivalents	
Max. and min. transmission	0.8932 and 0.7833	
Refinement method	Full-matrix least-squares on F^2	
Data / restraints / parameters	7443 / 0 / 567	
Goodness-of-fit on F^2	1.130	
Final R indices [I>2sigma(I)]	R1 = 0.0812, wR2 = 0.1847	
R indices (all data)	R1 = 0.1184, wR2 = 0.2036	
Extinction coefficient	0.0045(4)	
Largest diff. peak and hole	1.248 and -0.595 e.$Å^{-3}$	

Table 2. Atomic coordinates (x 10^4) and equivalent isotropic displacement parameters ($Å^2$x 10^3) for lsh146m. U(eq) is defined as one third of the trace of the orthogonalized U^{ij} tensor.

	x	y	z	U(eq)
Ru(1)	10000	0	0	30(1)
Co(1)	10266(1)	1272(1)	1647(1)	37(1)
O(1)	11410(6)	4682(5)	1664(2)	73(2)
O(2)	13172(5)	3198(5)	1732(2)	59(2)
O(3)	8822(6)	-2246(6)	1717(2)	80(2)
O(4)	7346(6)	-482(6)	1758(3)	78(2)
N(1)	11786(7)	1906(7)	1649(2)	63(2)
N(2)	11047(6)	-35(6)	1949(2)	52(2)
N(3)	8786(6)	643(7)	1620(2)	62(2)
N(4)	9513(6)	2704(6)	1468(2)	57(2)
N(5)	10285(6)	1787(6)	2251(2)	47(2)
N(6)	10104(4)	447(5)	660(2)	29(1)
N(7)	11472(5)	-770(5)	167(2)	36(1)
N(8)	10826(5)	-2655(5)	319(2)	36(1)
N(9)	9214(5)	-1439(5)	97(2)	31(1)
N(10)	7293(5)	-824(5)	-113(2)	35(1)
C(1)	11336(9)	3720(8)	1344(3)	65(3)
C(2)	11899(9)	4052(9)	936(3)	78(3)
C(3)	11002(12)	5775(9)	1463(4)	103(4)
C(4)	12221(10)	2849(9)	1613(3)	69(3)
C(5)	12765(8)	983(7)	1797(3)	57(2)
C(6)	13536(9)	883(9)	1427(4)	81(3)
C(7)	13496(9)	1207(10)	2251(4)	86(3)
C(8)	12129(7)	-116(8)	1777(3)	61(2)
C(9)	10438(8)	-1098(7)	1831(3)	65(3)
C(10)	9224(9)	-1200(8)	1918(4)	73(3)
C(11)	9087(9)	-1419(9)	2421(3)	78(3)
C(12)	8500(11)	-2168(12)	1245(4)	101(4)
C(13)	8368(10)	-248(9)	1754(3)	72(3)
C(14)	7792(8)	1494(8)	1413(3)	61(2)
C(15)	7116(9)	1920(9)	1763(4)	80(3)

C(16)	6977(10)	999(9)	1010(4)	89(4)
C(17)	8430(8)	2428(8)	1200(3)	58(2)
C(18)	10155(9)	3371(7)	1162(3)	60(3)
C(19)	9376(10)	3407(9)	1883(3)	81(3)
C(20)	9787(9)	2785(8)	2313(3)	62(3)
C(21)	9751(12)	3176(10)	2747(3)	96(4)
C(22)	10231(14)	2545(10)	3112(4)	116(6)
C(23)	10714(12)	1545(11)	3041(3)	99(4)
C(24)	10750(9)	1162(8)	2596(3)	62(3)
C(25)	11252(9)	102(9)	2465(3)	68(3)
C(26)	10203(5)	754(6)	1041(2)	32(2)
C(27)	14579(7)	-2927(7)	713(3)	48(2)
C(28)	13415(6)	-3032(7)	603(2)	42(2)
C(29)	12812(6)	-2081(6)	433(2)	35(2)
C(30)	11627(6)	-1871(6)	301(2)	34(2)
C(31)	9733(6)	-2443(6)	219(2)	33(2)
C(32)	8874(6)	-3319(6)	226(2)	36(2)
C(33)	8930(7)	-4460(6)	305(2)	41(2)
C(34)	7935(7)	-5043(7)	275(3)	50(2)
C(35)	6900(7)	-4520(7)	169(3)	45(2)
C(36)	6843(6)	-3359(6)	83(2)	40(2)
C(37)	7832(6)	-2771(6)	112(2)	35(2)
C(38)	8084(6)	-1592(6)	27(2)	31(2)
C(39)	7513(6)	252(6)	-203(2)	32(2)
C(40)	6645(6)	1075(6)	-374(2)	38(2)
C(41)	5489(6)	968(7)	-480(3)	45(2)
C(42)	4896(6)	1913(7)	-656(3)	47(2)
O(5)	4889(6)	4214(7)	1410(3)	86(2)
C(45)	4984(9)	3815(10)	979(4)	83(3)
O(6)	7105(12)	5088(16)	1691(6)	230(8)
C(46)	7680(30)	5639(19)	2098(10)	310(20)

Table 3. Bond lengths [Å] and angles [°] for lsh146m.

Ru(1)-N(7)#1	1.992(6)	N(8)-C(30)	1.350(9)
Ru(1)-N(7)	1.992(6)	N(9)-C(38)	1.362(8)
Ru(1)-N(9)#1	1.996(6)	N(9)-C(31)	1.367(9)
Ru(1)-N(9)	1.996(6)	N(10)-C(38)	1.338(9)
Ru(1)-N(6)#1	2.018(5)	N(10)-C(39)	1.338(9)
Ru(1)-N(6)	2.018(5)	C(1)-C(18)	1.503(13)
Co(1)-N(5)	1.892(6)	C(1)-C(2)	1.535(14)
Co(1)-C(26)	1.895(7)	C(1)-C(4)	1.606(14)
Co(1)-N(3)	1.930(7)	C(5)-C(8)	1.510(12)
Co(1)-N(2)	1.958(7)	C(5)-C(7)	1.518(12)
Co(1)-N(4)	1.960(7)	C(5)-C(6)	1.556(14)
Co(1)-N(1)	1.985(8)	C(9)-C(10)	1.535(14)
O(1)-C(1)	1.478(10)	C(10)-C(11)	1.552(14)
O(1)-C(3)	1.478(12)	C(10)-C(13)	1.557(14)
O(2)-C(4)	1.221(11)	C(14)-C(15)	1.510(13)
O(3)-C(12)	1.400(12)	C(14)-C(16)	1.542(13)
O(3)-C(10)	1.427(11)	C(14)-C(17)	1.543(13)
O(4)-C(13)	1.268(12)	C(19)-C(20)	1.492(13)
N(1)-C(4)	1.248(12)	C(20)-C(21)	1.378(11)
N(1)-C(5)	1.621(12)	C(21)-C(22)	1.369(17)
N(2)-C(9)	1.474(11)	C(22)-C(23)	1.353(17)
N(2)-C(8)	1.483(11)	C(23)-C(24)	1.408(13)
N(2)-C(25)	1.524(10)	C(24)-C(25)	1.474(14)
N(3)-C(13)	1.263(12)	C(27)-C(42)#1	1.382(11)
N(3)-C(14)	1.615(12)	C(27)-C(28)	1.400(11)
N(4)-C(17)	1.459(11)	C(28)-C(29)	1.394(10)
N(4)-C(18)	1.509(11)	C(29)-C(40)#1	1.385(10)
N(4)-C(19)	1.520(10)	C(29)-C(30)	1.447(10)
N(5)-C(24)	1.317(10)	C(31)-C(32)	1.472(10)
N(5)-C(20)	1.354(11)	C(32)-C(33)	1.373(10)
N(6)-C(26)	1.177(8)	C(32)-C(37)	1.411(10)
N(7)-C(39)#1	1.362(9)	C(33)-C(34)	1.379(11)
N(7)-C(30)	1.370(9)	C(34)-C(35)	1.388(11)
N(8)-C(31)	1.333(9)	C(35)-C(36)	1.399(11)

C(36)-C(37)	1.375(10)	C(40)-C(41)	1.391(10)
C(37)-C(38)	1.461(10)	C(41)-C(42)	1.388(11)
C(39)-N(7)#1	1.362(9)	C(42)-C(27)#1	1.382(11)
C(39)-C(40)	1.464(9)	O(5)-C(45)	1.390(12)
C(40)-C(29)#1	1.385(10)	O(6)-C(46)	1.45(3)

N(7)#1-Ru(1)-N(7)	180.0(5)	C(1)-O(1)-C(3)	115.7(7)
N(7)#1-Ru(1)-N(9)#1	90.0(2)	C(12)-O(3)-C(10)	112.6(9)
N(7)-Ru(1)-N(9)#1	90.0(2)	C(4)-N(1)-C(5)	109.1(9)
N(7)#1-Ru(1)-N(9)	90.0(2)	C(4)-N(1)-Co(1)	137.9(8)
N(7)-Ru(1)-N(9)	90.0(2)	C(5)-N(1)-Co(1)	112.5(5)
N(9)#1-Ru(1)-N(9)	180.0(4)	C(9)-N(2)-C(8)	107.3(7)
N(7)#1-Ru(1)-N(6)#1	87.9(2)	C(9)-N(2)-C(25)	109.0(7)
N(7)-Ru(1)-N(6)#1	92.1(2)	C(8)-N(2)-C(25)	110.1(7)
N(9)#1-Ru(1)-N(6)#1	92.4(2)	C(9)-N(2)-Co(1)	112.4(5)
N(9)-Ru(1)-N(6)#1	87.6(2)	C(8)-N(2)-Co(1)	106.3(5)
N(7)#1-Ru(1)-N(6)	92.1(2)	C(25)-N(2)-Co(1)	111.5(6)
N(7)-Ru(1)-N(6)	87.9(2)	C(13)-N(3)-C(14)	109.3(8)
N(9)#1-Ru(1)-N(6)	87.6(2)	C(13)-N(3)-Co(1)	136.5(8)
N(9)-Ru(1)-N(6)	92.4(2)	C(14)-N(3)-Co(1)	113.9(6)
N(6)#1-Ru(1)-N(6)	180.00(8)	C(17)-N(4)-C(18)	107.0(6)
N(5)-Co(1)-C(26)	178.4(3)	C(17)-N(4)-C(19)	111.2(8)
N(5)-Co(1)-N(3)	92.1(3)	C(18)-N(4)-C(19)	109.6(7)
C(26)-Co(1)-N(3)	86.4(3)	C(17)-N(4)-Co(1)	107.0(5)
N(5)-Co(1)-N(2)	83.6(3)	C(18)-N(4)-Co(1)	110.9(5)
C(26)-Co(1)-N(2)	97.1(3)	C(19)-N(4)-Co(1)	111.0(5)
N(3)-Co(1)-N(2)	95.2(3)	C(24)-N(5)-C(20)	122.0(7)
N(5)-Co(1)-N(4)	85.1(3)	C(24)-N(5)-Co(1)	119.8(6)
C(26)-Co(1)-N(4)	94.3(3)	C(20)-N(5)-Co(1)	118.2(5)
N(3)-Co(1)-N(4)	86.3(4)	C(26)-N(6)-Ru(1)	176.4(5)
N(2)-Co(1)-N(4)	168.6(3)	C(39)#1-N(7)-C(30)	109.1(6)
N(5)-Co(1)-N(1)	90.2(3)	C(39)#1-N(7)-Ru(1)	124.9(5)
C(26)-Co(1)-N(1)	91.3(3)	C(30)-N(7)-Ru(1)	125.8(5)
N(3)-Co(1)-N(1)	177.7(3)	C(31)-N(8)-C(30)	123.6(6)
N(2)-Co(1)-N(1)	85.4(3)	C(38)-N(9)-C(31)	109.4(6)
N(4)-Co(1)-N(1)	93.6(3)	C(38)-N(9)-Ru(1)	125.6(5)

C(31)-N(9)-Ru(1)	124.9(5)	C(20)-C(19)-N(4)	111.2(8)
C(38)-N(10)-C(39)	123.7(6)	N(5)-C(20)-C(21)	120.2(9)
O(1)-C(1)-C(18)	113.7(8)	N(5)-C(20)-C(19)	114.2(7)
O(1)-C(1)-C(2)	108.7(8)	C(21)-C(20)-C(19)	125.5(10)
C(18)-C(1)-C(2)	107.5(7)	C(22)-C(21)-C(20)	119.1(11)
O(1)-C(1)-C(4)	102.0(6)	C(23)-C(22)-C(21)	119.7(10)
C(18)-C(1)-C(4)	121.5(9)	C(22)-C(23)-C(24)	120.4(10)
C(2)-C(1)-C(4)	102.4(8)	N(5)-C(24)-C(23)	118.6(10)
O(2)-C(4)-N(1)	132.0(11)	N(5)-C(24)-C(25)	114.7(7)
O(2)-C(4)-C(1)	116.7(9)	C(23)-C(24)-C(25)	126.7(9)
N(1)-C(4)-C(1)	111.2(10)	C(24)-C(25)-N(2)	110.4(7)
C(8)-C(5)-C(7)	114.0(8)	N(6)-C(26)-Co(1)	176.4(6)
C(8)-C(5)-C(6)	105.4(8)	C(42)#1-C(27)-C(28)	120.9(7)
C(7)-C(5)-C(6)	108.3(8)	C(29)-C(28)-C(27)	117.5(7)
C(8)-C(5)-N(1)	103.0(7)	C(40)#1-C(29)-C(28)	120.7(7)
C(7)-C(5)-N(1)	114.9(8)	C(40)#1-C(29)-C(30)	106.7(6)
C(6)-C(5)-N(1)	110.8(7)	C(28)-C(29)-C(30)	132.6(7)
N(2)-C(8)-C(5)	113.8(8)	N(8)-C(30)-N(7)	127.0(6)
N(2)-C(9)-C(10)	118.9(8)	N(8)-C(30)-C(29)	123.9(6)
O(3)-C(10)-C(9)	105.7(8)	N(7)-C(30)-C(29)	109.0(6)
O(3)-C(10)-C(11)	100.1(8)	N(8)-C(31)-N(9)	128.4(6)
C(9)-C(10)-C(11)	115.2(8)	N(8)-C(31)-C(32)	122.8(6)
O(3)-C(10)-C(13)	109.5(8)	N(9)-C(31)-C(32)	108.8(6)
C(9)-C(10)-C(13)	119.8(9)	C(33)-C(32)-C(37)	120.8(7)
C(11)-C(10)-C(13)	104.7(9)	C(33)-C(32)-C(31)	133.0(7)
N(3)-C(13)-O(4)	128.8(11)	C(37)-C(32)-C(31)	106.1(6)
N(3)-C(13)-C(10)	115.1(10)	C(32)-C(33)-C(34)	117.7(8)
O(4)-C(13)-C(10)	116.0(9)	C(33)-C(34)-C(35)	122.5(8)
C(15)-C(14)-C(16)	108.3(9)	C(34)-C(35)-C(36)	119.8(7)
C(15)-C(14)-C(17)	113.8(8)	C(37)-C(36)-C(35)	118.0(7)
C(16)-C(14)-C(17)	104.7(7)	C(36)-C(37)-C(32)	121.1(7)
C(15)-C(14)-N(3)	113.5(7)	C(36)-C(37)-C(38)	132.6(7)
C(16)-C(14)-N(3)	113.8(8)	C(32)-C(37)-C(38)	106.2(6)
C(17)-C(14)-N(3)	102.4(7)	N(10)-C(38)-N(9)	127.4(6)
N(4)-C(17)-C(14)	113.6(7)	N(10)-C(38)-C(37)	123.1(6)
C(1)-C(18)-N(4)	118.5(7)	N(9)-C(38)-C(37)	109.5(6)

N(10)-C(39)-N(7)#1	128.2(6)
N(10)-C(39)-C(40)	123.4(6)
N(7)#1-C(39)-C(40)	108.3(6)
C(29)#1-C(40)-C(41)	122.0(7)
C(29)#1-C(40)-C(39)	106.8(6)
C(41)-C(40)-C(39)	131.1(7)
C(42)-C(41)-C(40)	116.9(8)
C(27)#1-C(42)-C(41)	

Symmetry transformations used to generate equivalent atoms: #1 -x+2,-y,-z

Table 4. Anisotropic displacement parameters ($Å^2 x\ 10^3$) for lsh146m. The anisotropic displacement factor exponent takes the form: $-2\pi^2[\ h^2\ a^{*2}U^{11} + ... + 2\ h\ k\ a^*\ b^*\ U^{12}\ ]$

	U^{11}	U^{22}	U^{33}	U^{23}	U^{13}	U^{12}
Ru(1)	35(1)	31(1)	25(1)	-3(1)	6(1)	2(1)
Co(1)	47(1)	41(1)	23(1)	-1(1)	5(1)	0(1)
O(1)	104(5)	46(4)	65(4)	-19(3)	-1(4)	-3(4)
O(2)	48(4)	75(4)	48(3)	-13(3)	-10(3)	-17(3)
O(3)	88(5)	74(5)	76(5)	-7(4)	6(4)	-5(4)
O(4)	56(4)	80(5)	106(6)	23(4)	38(4)	-5(4)
N(1)	99(6)	57(5)	36(4)	-11(3)	18(4)	-31(5)
N(2)	59(4)	54(4)	38(3)	3(3)	-4(3)	-6(4)
N(3)	60(5)	89(6)	38(4)	-2(4)	14(3)	-20(4)
N(4)	78(5)	54(5)	34(4)	-10(3)	-2(3)	18(4)
N(5)	61(4)	50(4)	27(3)	0(3)	4(3)	-12(4)
N(6)	31(3)	27(3)	30(3)	0(2)	6(2)	0(2)
N(7)	40(4)	40(4)	28(3)	-3(3)	8(3)	-3(3)
N(8)	40(4)	33(3)	33(3)	-2(3)	2(3)	3(3)
N(9)	35(3)	36(3)	22(3)	-1(2)	3(2)	3(3)
N(10)	37(3)	33(3)	35(3)	0(3)	8(3)	-2(3)
C(1)	86(7)	65(6)	38(5)	-18(4)	-11(5)	19(5)
C(2)	106(9)	81(7)	43(5)	3(5)	-5(5)	16(6)
C(3)	145(12)	47(6)	105(9)	-9(6)	-10(8)	21(7)
C(4)	93(8)	78(7)	37(5)	-15(5)	16(5)	-16(6)
C(5)	63(6)	43(5)	60(5)	15(4)	-8(5)	7(4)
C(6)	69(7)	57(6)	112(9)	5(6)	0(6)	0(5)
C(7)	78(7)	89(8)	79(7)	20(6)	-22(6)	-13(6)
C(8)	54(5)	59(6)	65(6)	8(5)	-7(4)	16(5)
C(9)	80(7)	44(5)	59(6)	0(4)	-23(5)	-4(5)
C(10)	65(6)	40(5)	102(8)	-14(5)	-22(6)	0(5)
C(11)	84(8)	77(7)	75(7)	16(6)	16(6)	-4(6)
C(12)	118(10)	124(11)	64(7)	-1(7)	18(7)	-9(9)
C(13)	90(8)	71(7)	57(6)	-10(5)	19(6)	-12(6)
C(14)	78(7)	51(5)	50(5)	2(4)	1(5)	16(5)
C(15)	87(8)	76(7)	77(7)	2(6)	17(6)	28(6)

C(16)	117(10)	67(7)	74(7)	29(6)	-11(7)	-20(7)
C(17)	76(6)	50(5)	46(5)	2(4)	1(4)	19(5)
C(18)	110(8)	35(5)	34(4)	-1(4)	4(5)	10(5)
C(19)	119(9)	76(7)	48(5)	-24(5)	13(6)	27(7)
C(20)	93(7)	56(6)	40(5)	-12(4)	22(5)	-10(5)
C(21)	180(13)	75(8)	39(5)	-19(5)	38(7)	-18(8)
C(22)	247(18)	54(7)	57(7)	-15(6)	58(9)	-42(9)
C(23)	182(13)	85(9)	25(5)	9(5)	5(6)	-40(9)
C(24)	92(7)	61(6)	29(4)	8(4)	-3(4)	-19(5)
C(25)	86(7)	73(7)	37(5)	15(5)	-14(4)	-15(6)
C(26)	28(4)	29(4)	38(4)	-1(3)	5(3)	-3(3)
C(27)	43(5)	48(5)	50(5)	2(4)	0(4)	16(4)
C(28)	48(5)	41(4)	37(4)	1(3)	5(3)	7(4)
C(29)	33(4)	41(4)	30(4)	-4(3)	2(3)	4(3)
C(30)	40(4)	33(4)	29(4)	-3(3)	4(3)	2(3)
C(31)	45(4)	35(4)	21(3)	-3(3)	11(3)	3(3)
C(32)	48(4)	31(4)	29(4)	-3(3)	5(3)	0(3)
C(33)	42(4)	38(4)	40(4)	1(3)	2(3)	0(4)
C(34)	62(5)	38(4)	50(5)	4(4)	7(4)	-9(4)
C(35)	49(5)	38(4)	51(5)	3(4)	15(4)	-13(4)
C(36)	38(4)	42(4)	40(4)	-3(3)	7(3)	-3(3)
C(37)	43(4)	36(4)	26(3)	-3(3)	9(3)	-1(3)
C(38)	33(4)	32(4)	28(3)	-2(3)	5(3)	0(3)
C(39)	35(4)	29(4)	32(4)	-1(3)	2(3)	5(3)
C(40)	29(4)	46(5)	36(4)	3(3)	0(3)	7(3)
C(41)	41(5)	51(5)	45(4)	-1(4)	9(4)	10(4)
C(42)	26(4)	64(6)	49(5)	-5(4)	-1(3)	8(4)
O(5)	81(5)	99(6)	77(5)	-8(4)	5(4)	-30(5)
C(45)	82(8)	84(8)	84(8)	21(6)	12(6)	18(6)
O(6)	160(13)	270(20)	266(19)	42(16)	43(12)	87(13)
C(46)	520(50)	170(20)	320(30)	-200(20)	310(30)	-220(30)

Table 5. Hydrogen coordinates (x 10^4) and isotropic displacement parameters ($Å^2$x 10^3) for lsh146m.

	x	y	z	U(eq)
H(2A)	11426	4596	746	118
H(2B)	12001	3378	756	118
H(2C)	12630	4393	1045	118
H(3A)	11457	6001	1233	154
H(3B)	11061	6349	1702	154
H(3C)	10218	5699	1319	154
H(6A)	14043	240	1497	122
H(6B)	13975	1576	1422	122
H(6C)	13076	769	1128	122
H(7A)	13033	1494	2468	128
H(7B)	14068	1768	2211	128
H(7C)	13860	505	2369	128
H(8A)	11985	-381	1457	73
H(8B)	12602	-688	1958	73
H(9A)	10874	-1712	2002	78
H(9B)	10440	-1241	1504	78
H(11A)	8343	-1735	2431	117
H(11B)	9170	-707	2590	117
H(11C)	9661	-1953	2558	117
H(12A)	7753	-1828	1178	152
H(12B)	8482	-2924	1111	152
H(12C)	9038	-1698	1116	152
H(15A)	6550	2455	1620	119
H(15B)	7614	2298	2010	119
H(15C)	6745	1283	1888	119
H(16A)	6534	396	1120	134
H(16B)	7403	692	784	134
H(16C)	6475	1595	870	134
H(17A)	8546	2183	892	70
H(17B)	7962	3117	1163	70

H(18A)	10174	2920	883	72
H(18B)	9722	4063	1068	72
H(19A)	9800	4120	1878	97
H(19B)	8576	3599	1872	97
H(21)	9398	3874	2792	115
H(22)	10225	2809	3413	139
H(23)	11030	1097	3294	119
H(25A)	10920	-544	2607	81
H(25B)	12067	108	2578	81
H(27)	15014	-3561	829	58
H(28)	13050	-3726	642	50
H(34)	9629	-4835	378	49
H(35)	7958	-5832	330	60
H(36)	6232	-4949	154	54
H(37)	6142	-2988	8	48
H(43)	5121	278	-435	54
H(44)	4106	1863	-740	57
H(5)	4265	4025	1476	129
H(45A)	5590	4216	864	125
H(45B)	4279	3941	773	125
H(45C)	5151	3005	995	125

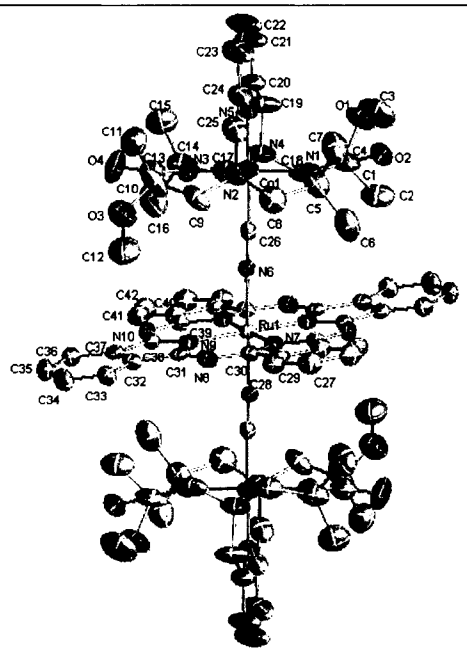

II. Chapter 2 X-Ray Crystal Structures

A. lsh124rt, 4b′

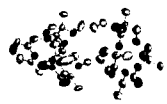

Table 1. Crystal data and structure refinement for lsh124rt, **4b′**.

Identification code	lsh124m	
Empirical formula	C88 H152 N20 O16	
Formula weight	1746.30	
Temperature	298(2) K	
Wavelength	0.71073 Å	
Crystal system	Monoclinic	
Space group	P2(1)/n	
Unit cell dimensions	a = 19.840(6) Å	α= 90°.
	b = 13.990(4) Å	β= 103.411(6)°.
	c = 36.256(11) Å	γ= 90°.
Volume	9788(5) $Å^3$	
Z	4	
Density (calculated)	1.185 Mg/m^3	
Absorption coefficient	0.083 mm^{-1}	
F(000)	3792	
Crystal size	0.30 x 0.20 x 0.08 mm^3	
Theta range for data collection	3.08 to 17.28°.	
Index ranges	-16<=h<=16, -11<=k<=11, -30<=l<=30	
Reflections collected	29675	
Independent reflections	5934 [R(int) = 0.0870]	
Completeness to theta = 17.28°	99.1 %	
Absorption correction	SABADS	
Refinement method	Full-matrix least-squares on F^2	
Data / restraints / parameters	5934 / 0 / 1117	
Goodness-of-fit on F^2	1.186	
Final R indices [I>2sigma(I)]	R1 = 0.0879, wR2 = 0.1731	
R indices (all data)	R1 = 0.1178, wR2 = 0.1872	
Largest diff. peak and hole	0.378 and -0.177 $e.Å^{-3}$	

Room temperature data with 2 molecules in the asymmetric unit. High mosaic quality.

Table 2. Atomic coordinates (x 10^4) and equivalent isotropic displacement parameters ($Å^2$x 10^3) for lsh124rt. U(eq) is defined as one third of the trace of the orthogonalized U^{ij} tensor.

	x	y	z	U(eq)
N(1)	4982(5)	9337(6)	1228(3)	66(2)
N(2)	4077(5)	10855(7)	831(2)	75(2)
N(3)	4114(4)	10795(6)	1892(3)	60(2)
N(4)	5597(4)	10647(6)	1920(2)	53(2)
N(5)	3399(6)	4766(5)	2236(2)	73(3)
N(6)	2142(4)	5564(7)	1873(3)	83(3)
N(7)	2636(6)	5672(6)	1155(2)	72(3)
N(8)	3833(4)	4509(5)	1548(3)	67(2)
N(9)	5582(9)	13438(9)	1240(5)	117(4)
N(10)	5322(7)	11500(6)	1197(4)	72(3)
N(1A)	7973(4)	1865(5)	813(3)	61(2)
N(2A)	8565(6)	1646(8)	154(2)	79(3)
N(3A)	9896(4)	2686(6)	995(4)	84(3)
N(4A)	9364(5)	1175(7)	1404(2)	68(2)
N(5A)	7629(4)	7062(7)	1683(3)	68(2)
N(6A)	7783(6)	7690(6)	995(3)	126(4)
N(7A)	6724(6)	6452(7)	543(3)	100(3)
N(8A)	6544(5)	5880(7)	1243(4)	121(4)
N(9A)	9911(8)	-1123(10)	558(7)	163(6)
N(10A)	9033(5)	278(7)	706(5)	80(3)
O(1)	5837(4)	8223(6)	1325(2)	105(3)
O(2)	4020(3)	12190(6)	1567(2)	80(2)
O(3)	4831(4)	8796(4)	1954(2)	66(2)
O(4)	4360(3)	6053(6)	2015(2)	70(2)
O(5)	4269(4)	4689(5)	2759(3)	105(3)
O(6)	1658(4)	5689(6)	674(3)	124(3)
O(7)	1892(4)	7182(7)	1430(2)	85(2)
O(8)	3252(3)	9910(6)	1354(2)	87(2)
O(1A)	7305(5)	1361(6)	1196(2)	121(3)
O(2A)	10234(4)	1721(7)	572(3)	121(3)
O(3A)	8655(3)	3019(6)	1404(2)	63(2)

O(4A)	7574(4)	4920(5)	1717(2)	129(3)
O(5A)	7941(4)	6730(5)	2308(2)	96(3)
O(6A)	6578(4)	6652(5)	-81(2)	101(3)
O(7A)	8161(5)	6698(8)	455(2)	104(3)
O(8A)	9047(4)	3591(6)	490(2)	85(2)
C(1)	5518(6)	8819(8)	1881(3)	63(3)
C(2)	5921(5)	7942(7)	2073(3)	98(4)
C(3)	5467(6)	8782(9)	1450(4)	67(3)
C(4)	4784(7)	9304(9)	817(4)	89(4)
C(5)	5387(7)	9637(10)	648(3)	137(5)
C(6)	4580(7)	8256(9)	694(3)	164(6)
C(7)	4111(6)	9886(10)	689(3)	96(4)
C(8)	3402(6)	11137(7)	894(3)	80(3)
C(9)	3279(6)	10908(8)	1287(4)	67(3)
C(10)	2611(5)	11424(7)	1318(3)	104(4)
C(11)	3856(5)	11353(9)	1594(4)	58(3)
C(12)	4609(6)	11083(7)	2248(3)	61(3)
C(13)	4614(5)	10288(7)	2538(3)	84(3)
C(14)	4358(5)	12003(7)	2408(3)	88(3)
C(15)	5332(5)	11278(7)	2172(3)	62(3)
C(16)	5857(4)	9726(8)	2077(3)	66(3)
C(17)	4368(6)	8067(8)	1768(3)	83(3)
C(18)	3977(5)	7620(9)	2039(4)	99(4)
C(19)	4333(6)	6813(9)	2274(3)	90(3)
C(20)	4558(5)	5132(8)	2174(3)	56(3)
C(21)	5302(5)	5123(8)	2407(3)	107(4)
C(22)	4039(8)	4851(7)	2415(4)	67(3)
C(23)	2802(7)	4583(9)	2403(4)	80(3)
C(24)	2771(6)	5345(10)	2710(3)	142(5)
C(25)	2845(5)	3610(8)	2580(4)	128(5)
C(26)	2180(7)	4704(9)	2092(4)	110(4)
C(27)	1502(6)	5693(8)	1593(4)	104(4)
C(28)	1534(7)	6334(9)	1256(4)	81(4)
C(29)	793(6)	6577(8)	1046(3)	116(4)
C(30)	1955(9)	5881(8)	1001(4)	80(4)
C(31)	3094(7)	5185(8)	951(3)	74(3)

C(32)	3165(6)	5788(8)	610(3)	115(4)
C(33)	2808(6)	4189(7)	838(3)	110(4)
C(34)	3806(6)	5136(7)	1223(3)	75(3)
C(35)	4501(5)	4519(6)	1823(3)	63(3)
C(36)	1956(5)	7916(9)	1168(3)	91(4)
C(37)	2455(6)	8634(10)	1350(3)	108(4)
C(38)	2676(7)	9384(10)	1145(4)	137(5)
C(39)	4420(7)	11591(10)	654(3)	98(4)
C(40)	4970(7)	12114(14)	940(4)	80(3)
C(41)	5105(8)	13072(13)	957(5)	100(4)
C(42)	5920(7)	12832(15)	1495(4)	101(4)
C(43)	5791(7)	11872(11)	1474(5)	65(3)
C(44)	6133(5)	11141(8)	1769(3)	67(3)
C(1A)	8343(6)	2170(9)	1498(3)	62(3)
C(2A)	7968(5)	2321(7)	1818(3)	95(4)
C(3A)	7841(6)	1734(8)	1159(4)	70(3)
C(4A)	7506(6)	1644(7)	450(4)	65(3)
C(5A)	7305(5)	583(7)	418(3)	98(4)
C(6A)	6840(5)	2249(7)	404(3)	101(4)
C(7A)	7860(7)	1966(7)	134(3)	84(3)
C(8A)	9009(6)	2327(9)	21(3)	89(3)
C(9A)	9452(7)	2972(9)	310(4)	74(3)
C(10A)	9970(6)	3536(8)	142(3)	127(5)
C(11A)	9891(6)	2391(11)	643(5)	86(4)
C(12A)	10343(7)	2377(12)	1361(4)	105(4)
C(13A)	10295(6)	3206(10)	1670(4)	149(5)
C(14A)	11073(6)	2430(10)	1353(4)	158(6)
C(15A)	10100(7)	1484(9)	1484(3)	116(4)
C(16A)	8954(7)	1507(8)	1663(3)	91(4)
C(17A)	8212(5)	3770(8)	1234(3)	72(3)
C(18A)	8477(5)	4708(8)	1419(3)	92(3)
C(19A)	8301(6)	4864(7)	1791(3)	89(3)
C(20A)	7210(6)	5572(8)	1899(3)	69(3)
C(21A)	7124(5)	5164(7)	2267(3)	101(4)
C(22A)	7636(5)	6531(9)	1987(4)	62(3)
C(23A)	8022(6)	7967(9)	1678(3)	76(3)

C(24A)	8793(6)	7738(7)	1798(3)	108(4)
C(25A)	7817(7)	8710(8)	1928(3)	134(5)
C(26A)	7813(7)	8317(9)	1274(4)	126(5)
C(27A)	7675(6)	8093(7)	620(4)	112(4)
C(28A)	7613(9)	7368(9)	311(4)	93(4)
C(29A)	7703(7)	7834(7)	-58(3)	132(5)
C(30A)	6930(8)	6790(9)	248(4)	85(4)
C(31A)	6143(7)	5847(9)	553(4)	76(3)
C(32A)	6243(6)	4898(8)	394(4)	152(6)
C(33A)	5472(7)	6264(11)	342(4)	169(6)
C(34A)	6093(7)	5735(10)	953(5)	157(7)
C(35A)	6509(5)	5694(6)	1617(4)	71(3)
C(36A)	8271(7)	5998(11)	235(4)	131(5)
C(37A)	8759(7)	5236(10)	444(3)	112(4)
C(38A)	8683(7)	4327(11)	265(3)	117(4)
C(39A)	8630(6)	662(10)	26(3)	94(4)
C(40A)	9076(7)	91(10)	357(6)	85(4)
C(41A)	9503(11)	-626(14)	276(5)	131(5)
C(42A)	9867(8)	-890(12)	903(6)	137(6)
C(43A)	9445(8)	-190(11)	992(5)	90(5)
C(44A)	9337(6)	154(10)	1362(4)	96(4)

Table 3. Bond lengths [Å] and angles [°] for lsh124rt.

N(1)-C(3)	1.348(11)	N(5A)-C(22A)	1.326(11)
N(1)-C(4)	1.451(11)	N(5A)-C(23A)	1.490(11)
N(2)-C(7)	1.457(11)	N(6A)-C(26A)	1.331(12)
N(2)-C(39)	1.464(12)	N(6A)-C(27A)	1.441(11)
N(2)-C(8)	1.464(11)	N(7A)-C(30A)	1.319(13)
N(3)-C(11)	1.334(11)	N(7A)-C(31A)	1.437(12)
N(3)-C(12)	1.485(11)	N(8A)-C(34A)	1.228(12)
N(4)-C(16)	1.453(10)	N(8A)-C(35A)	1.400(11)
N(4)-C(15)	1.453(10)	N(9A)-C(42A)	1.315(16)
N(4)-C(44)	1.475(10)	N(9A)-C(41A)	1.342(16)
N(5)-C(22)	1.291(11)	N(10A)-C(40A)	1.314(13)
N(5)-C(23)	1.471(11)	N(10A)-C(43A)	1.333(12)
N(6)-C(26)	1.435(11)	O(1)-C(3)	1.231(11)
N(6)-C(27)	1.442(11)	O(2)-C(11)	1.225(10)
N(7)-C(30)	1.369(13)	O(3)-C(17)	1.433(10)
N(7)-C(31)	1.466(11)	O(3)-C(1)	1.447(10)
N(8)-C(34)	1.460(10)	O(4)-C(20)	1.429(9)
N(8)-C(35)	1.461(10)	O(4)-C(19)	1.430(11)
N(9)-C(42)	1.317(14)	O(5)-C(22)	1.247(10)
N(9)-C(41)	1.327(14)	O(6)-C(30)	1.225(12)
N(10)-C(43)	1.307(12)	O(7)-C(36)	1.425(11)
N(10)-C(40)	1.339(13)	O(7)-C(28)	1.450(11)
N(1A)-C(3A)	1.352(11)	O(8)-C(9)	1.420(10)
N(1A)-C(4A)	1.456(11)	O(8)-C(38)	1.421(12)
N(2A)-C(8A)	1.454(12)	O(1A)-C(3A)	1.220(10)
N(2A)-C(7A)	1.453(11)	O(2A)-C(11A)	1.220(13)
N(2A)-C(39A)	1.468(11)	O(3A)-C(17A)	1.416(9)
N(3A)-C(11A)	1.338(13)	O(3A)-C(1A)	1.417(10)
N(3A)-C(12A)	1.479(13)	O(4A)-C(19A)	1.407(10)
N(4A)-C(44A)	1.436(12)	O(4A)-C(20A)	1.418(10)
N(4A)-C(16A)	1.454(11)	O(5A)-C(22A)	1.214(11)
N(4A)-C(15A)	1.486(12)	O(6A)-C(30A)	1.248(11)
		O(7A)-C(36A)	1.314(12)
		O(7A)-C(28A)	1.440(13)
		O(8A)-C(38A)	1.405(12)

O(8A)-C(9A)	1.436(11)	C(1A)-C(3A)	1.520(14)
C(1)-C(16)	1.532(12)	C(1A)-C(2A)	1.530(11)
C(1)-C(2)	1.539(11)	C(1A)-C(16A)	1.535(12)
C(1)-C(3)	1.543(13)	C(4A)-C(5A)	1.534(11)
C(4)-C(5)	1.537(14)	C(4A)-C(7A)	1.543(12)
C(4)-C(7)	1.540(13)	C(4A)-C(6A)	1.546(11)
C(4)-C(6)	1.559(14)	C(8A)-C(9A)	1.501(13)
C(8)-C(9)	1.534(12)	C(9A)-C(10A)	1.528(12)
C(9)-C(11)	1.532(13)	C(9A)-C(11A)	1.548(15)
C(9)-C(10)	1.535(11)	C(12A)-C(15A)	1.446(14)
C(12)-C(13)	1.530(11)	C(12A)-C(14A)	1.457(13)
C(12)-C(14)	1.541(11)	C(12A)-C(13A)	1.630(16)
C(12)-C(15)	1.546(11)	C(17A)-C(18A)	1.512(12)
C(17)-C(18)	1.522(13)	C(18A)-C(19A)	1.489(12)
C(18)-C(19)	1.490(13)	C(20A)-C(21A)	1.499(11)
C(20)-C(35)	1.517(11)	C(20A)-C(35A)	1.531(12)
C(20)-C(21)	1.522(11)	C(20A)-C(22A)	1.580(13)
C(20)-C(22)	1.546(13)	C(23A)-C(25A)	1.497(13)
C(23)-C(26)	1.475(13)	C(23A)-C(26A)	1.508(13)
C(23)-C(25)	1.499(13)	C(23A)-C(24A)	1.525(12)
C(23)-C(24)	1.555(13)	C(27A)-C(28A)	1.496(13)
C(27)-C(28)	1.529(13)	C(28A)-C(29A)	1.534(13)
C(28)-C(30)	1.520(15)	C(28A)-C(30A)	1.548(15)
C(28)-C(29)	1.529(12)	C(31A)-C(32A)	1.479(13)
C(31)-C(34)	1.525(12)	C(31A)-C(34A)	1.487(15)
C(31)-C(33)	1.524(12)	C(31A)-C(33A)	1.491(13)
C(31)-C(32)	1.532(12)	C(36A)-C(37A)	1.519(14)
C(36)-C(37)	1.456(12)	C(37A)-C(38A)	1.420(13)
C(37)-C(38)	1.412(13)	C(39A)-C(40A)	1.536(14)
C(39)-C(40)	1.508(14)	C(40A)-C(41A)	1.388(17)
C(40)-C(41)	1.365(15)	C(42A)-C(43A)	1.374(17)
C(42)-C(43)	1.367(14)	C(43A)-C(44A)	1.489(15)
C(43)-C(44)	1.520(12)		

C(3)-N(1)-C(4)	125.7(9)	C(7)-N(2)-C(8)	115.2(9)
C(7)-N(2)-C(39)	115.7(10)	C(39)-N(2)-C(8)	114.5(9)

C(11)-N(3)-C(12)	126.6(8)	C(16)-C(1)-C(3)	114.6(9)
C(16)-N(4)-C(15)	116.0(8)	C(2)-C(1)-C(3)	109.6(9)
C(16)-N(4)-C(44)	110.0(8)	O(1)-C(3)-N(1)	123.2(10)
C(15)-N(4)-C(44)	110.2(7)	O(1)-C(3)-C(1)	119.5(12)
C(22)-N(5)-C(23)	127.0(9)	N(1)-C(3)-C(1)	117.2(11)
C(26)-N(6)-C(27)	114.8(9)	N(1)-C(4)-C(5)	110.4(9)
C(30)-N(7)-C(31)	124.1(9)	N(1)-C(4)-C(7)	107.6(10)
C(34)-N(8)-C(35)	113.7(8)	C(5)-C(4)-C(7)	114.9(10)
C(42)-N(9)-C(41)	116.7(14)	N(1)-C(4)-C(6)	108.3(10)
C(43)-N(10)-C(40)	116.3(11)	C(5)-C(4)-C(6)	110.2(11)
C(3A)-N(1A)-C(4A)	126.2(9)	C(7)-C(4)-C(6)	105.2(10)
C(8A)-N(2A)-C(7A)	115.5(9)	N(2)-C(7)-C(4)	119.6(9)
C(8A)-N(2A)-C(39A)	113.9(10)	N(2)-C(8)-C(9)	115.8(8)
C(7A)-N(2A)-C(39A)	115.3(9)	O(8)-C(9)-C(11)	109.0(9)
C(11A)-N(3A)-C(12A)	129.4(11)	O(8)-C(9)-C(8)	112.6(9)
C(44A)-N(4A)-C(16A)	111.8(10)	C(11)-C(9)-C(8)	109.8(9)
C(44A)-N(4A)-C(15A)	108.7(9)	O(8)-C(9)-C(10)	112.5(9)
C(16A)-N(4A)-C(15A)	116.8(10)	C(11)-C(9)-C(10)	105.5(9)
C(22A)-N(5A)-C(23A)	125.6(9)	C(8)-C(9)-C(10)	107.1(9)
C(26A)-N(6A)-C(27A)	115.4(9)	O(2)-C(11)-N(3)	124.5(10)
C(30A)-N(7A)-C(31A)	129.2(11)	O(2)-C(11)-C(9)	119.7(12)
C(34A)-N(8A)-C(35A)	127.4(10)	N(3)-C(11)-C(9)	115.6(10)
C(42A)-N(9A)-C(41A)	115.8(15)	N(3)-C(12)-C(13)	107.3(8)
C(40A)-N(10A)-C(43A)	119.2(12)	N(3)-C(12)-C(14)	110.3(8)
C(17)-O(3)-C(1)	117.3(8)	C(13)-C(12)-C(14)	107.3(8)
C(20)-O(4)-C(19)	116.9(8)	N(3)-C(12)-C(15)	110.3(8)
C(36)-O(7)-C(28)	114.1(8)	C(13)-C(12)-C(15)	113.2(8)
C(9)-O(8)-C(38)	118.4(8)	C(14)-C(12)-C(15)	108.3(8)
C(17A)-O(3A)-C(1A)	117.6(7)	N(4)-C(15)-C(12)	119.4(8)
C(19A)-O(4A)-C(20A)	123.7(8)	N(4)-C(16)-C(1)	118.3(7)
C(36A)-O(7A)-C(28A)	118.9(10)	O(3)-C(17)-C(18)	110.8(9)
C(38A)-O(8A)-C(9A)	116.4(8)	C(19)-C(18)-C(17)	115.9(9)
O(3)-C(1)-C(16)	105.4(8)	O(4)-C(19)-C(18)	105.8(9)
O(3)-C(1)-C(2)	108.2(8)	O(4)-C(20)-C(35)	102.1(8)
C(16)-C(1)-C(2)	109.0(9)	O(4)-C(20)-C(21)	111.9(8)
O(3)-C(1)-C(3)	109.8(8)	C(35)-C(20)-C(21)	109.6(9)

O(4)-C(20)-C(22)	107.5(8)	N(10)-C(40)-C(39)	110.2(15)
C(35)-C(20)-C(22)	113.6(8)	C(41)-C(40)-C(39)	127.6(18)
C(21)-C(20)-C(22)	111.8(10)	N(9)-C(41)-C(40)	120.7(13)
O(5)-C(22)-N(5)	125.1(11)	N(9)-C(42)-C(43)	122.4(14)
O(5)-C(22)-C(20)	118.4(12)	N(10)-C(43)-C(42)	121.6(12)
N(5)-C(22)-C(20)	116.5(10)	N(10)-C(43)-C(44)	113.2(14)
N(5)-C(23)-C(26)	106.1(10)	C(42)-C(43)-C(44)	125.0(18)
N(5)-C(23)-C(25)	111.3(9)	N(4)-C(44)-C(43)	109.6(8)
C(26)-C(23)-C(25)	112.6(11)	O(3A)-C(1A)-C(3A)	112.4(9)
N(5)-C(23)-C(24)	110.2(9)	O(3A)-C(1A)-C(2A)	112.7(9)
C(26)-C(23)-C(24)	107.6(10)	C(3A)-C(1A)-C(2A)	109.1(10)
C(25)-C(23)-C(24)	108.9(10)	O(3A)-C(1A)-C(16A)	104.4(9)
N(6)-C(26)-C(23)	116.5(10)	C(3A)-C(1A)-C(16A)	112.5(9)
N(6)-C(27)-C(28)	116.2(9)	C(2A)-C(1A)-C(16A)	105.5(9)
O(7)-C(28)-C(30)	108.9(10)	O(1A)-C(3A)-N(1A)	121.5(12)
O(7)-C(28)-C(29)	110.6(10)	O(1A)-C(3A)-C(1A)	120.3(13)
C(30)-C(28)-C(29)	113.0(12)	N(1A)-C(3A)-C(1A)	117.8(11)
O(7)-C(28)-C(27)	103.8(10)	N(1A)-C(4A)-C(5A)	111.9(8)
C(30)-C(28)-C(27)	111.9(10)	N(1A)-C(4A)-C(7A)	107.8(9)
C(29)-C(28)-C(27)	108.2(11)	C(5A)-C(4A)-C(7A)	112.4(9)
O(6)-C(30)-N(7)	123.8(12)	N(1A)-C(4A)-C(6A)	109.2(8)
O(6)-C(30)-C(28)	118.2(14)	C(5A)-C(4A)-C(6A)	108.7(8)
N(7)-C(30)-C(28)	117.9(12)	C(7A)-C(4A)-C(6A)	106.7(9)
N(7)-C(31)-C(34)	106.5(9)	N(2A)-C(7A)-C(4A)	118.0(8)
N(7)-C(31)-C(33)	109.0(9)	N(2A)-C(8A)-C(9A)	117.7(9)
C(34)-C(31)-C(33)	111.3(9)	O(8A)-C(9A)-C(8A)	112.3(9)
N(7)-C(31)-C(32)	109.6(9)	O(8A)-C(9A)-C(10A)	111.6(9)
C(34)-C(31)-C(32)	107.6(10)	C(8A)-C(9A)-C(10A)	111.9(11)
C(33)-C(31)-C(32)	112.7(9)	O(8A)-C(9A)-C(11A)	103.5(10)
N(8)-C(34)-C(31)	113.8(9)	C(8A)-C(9A)-C(11A)	111.1(10)
N(8)-C(35)-C(20)	117.2(8)	C(10A)-C(9A)-C(11A)	105.9(10)
O(7)-C(36)-C(37)	110.6(10)	O(2A)-C(11A)-N(3A)	123.8(13)
C(38)-C(37)-C(36)	122.4(11)	O(2A)-C(11A)-C(9A)	118.6(14)
C(37)-C(38)-O(8)	114.5(10)	N(3A)-C(11A)-C(9A)	117.5(13)
N(2)-C(39)-C(40)	112.1(10)	C(15A)-C(12A)-C(14A)	117.1(12)
N(10)-C(40)-C(41)	122.2(13)	C(15A)-C(12A)-N(3A)	110.9(11)

C(14A)-C(12A)-N(3A)	111.1(10)
C(15A)-C(12A)-C(13A)	108.9(11)
C(14A)-C(12A)-C(13A)	101.2(12)
N(3A)-C(12A)-C(13A)	106.8(11)
C(12A)-C(15A)-N(4A)	125.0(9)
N(4A)-C(16A)-C(1A)	116.8(8)
O(3A)-C(17A)-C(18A)	109.5(8)
C(19A)-C(18A)-C(17A)	113.5(9)
O(4A)-C(19A)-C(18A)	106.2(9)
O(4A)-C(20A)-C(21A)	110.3(10)
O(4A)-C(20A)-C(35A)	104.0(8)
C(21A)-C(20A)-C(35A)	111.3(9)
O(4A)-C(20A)-C(22A)	109.6(8)
C(21A)-C(20A)-C(22A)	108.0(10)
C(35A)-C(20A)-C(22A)	113.6(9)
O(5A)-C(22A)-N(5A)	125.2(10)
O(5A)-C(22A)-C(20A)	120.9(12)
N(5A)-C(22A)-C(20A)	113.9(11)
N(5A)-C(23A)-C(25A)	111.4(9)
N(5A)-C(23A)-C(26A)	105.2(9)
C(25A)-C(23A)-C(26A)	108.1(11)
N(5A)-C(23A)-C(24A)	108.1(9)
C(25A)-C(23A)-C(24A)	111.6(10)
C(26A)-C(23A)-C(24A)	112.2(10)
N(6A)-C(26A)-C(23A)	118.5(11)
N(6A)-C(27A)-C(28A)	114.2(9)
O(7A)-C(28A)-C(27A)	104.2(11)
O(7A)-C(28A)-C(29A)	111.2(11)
C(27A)-C(28A)-C(29A)	111.0(10)
O(7A)-C(28A)-C(30A)	106.0(9)
C(27A)-C(28A)-C(30A)	112.5(11)
C(29A)-C(28A)-C(30A)	111.6(12)
O(6A)-C(30A)-N(7A)	120.6(14)
O(6A)-C(30A)-C(28A)	119.9(15)
N(7A)-C(30A)-C(28A)	119.5(12)
N(7A)-C(31A)-C(32A)	109.8(10)
N(7A)-C(31A)-C(34A)	108.8(10)
C(32A)-C(31A)-C(34A)	109.3(12)
N(7A)-C(31A)-C(33A)	112.5(11)
C(32A)-C(31A)-C(33A)	109.6(10)
C(34A)-C(31A)-C(33A)	106.8(11)
N(8A)-C(34A)-C(31A)	128.1(12)
N(8A)-C(35A)-C(20A)	115.2(9)
O(7A)-C(36A)-C(37A)	113.3(12)
C(38A)-C(37A)-C(36A)	114.3(11)
O(8A)-C(38A)-C(37A)	113.9(10)
N(2A)-C(39A)-C(40A)	108.5(10)
N(10A)-C(40A)-C(41A)	121.6(13)
N(10A)-C(40A)-C(39A)	119.6(16)
C(41A)-C(40A)-C(39A)	118.7(19)
N(9A)-C(41A)-C(40A)	120.3(15)
N(9A)-C(42A)-C(43A)	125.3(15)
N(10A)-C(43A)-C(42A)	117.6(14)
N(10A)-C(43A)-C(44A)	110.7(16)
C(42A)-C(43A)-C(44A)	131.6(18)
N(4A)-C(44A)-C(43A)	113.9(10)

Table 4. Anisotropic displacement parameters ($Å^2 x\ 10^3$) for lsh124rt. The anisotropic displacement factor exponent takes the form: $-2\pi^2[\ h^2\ a^{*2}U^{11} + ... + 2\ h\ k\ a^*\ b^*\ U^{12}\ ]$

	U^{11}	U^{22}	U^{33}	U^{23}	U^{13}	U^{12}
N(1)	62(6)	58(6)	66(8)	-7(5)	-7(5)	14(5)
N(2)	66(8)	66(8)	80(7)	18(6)	-8(5)	3(6)
N(3)	55(6)	46(6)	77(7)	17(6)	12(6)	6(5)
N(4)	45(6)	40(6)	73(6)	-7(5)	13(5)	8(5)
N(5)	66(7)	100(7)	54(7)	15(5)	14(7)	-11(6)
N(6)	48(6)	117(8)	72(6)	18(6)	-8(6)	-11(5)
N(7)	70(7)	66(6)	74(7)	0(6)	6(7)	-8(5)
N(8)	57(6)	75(6)	70(6)	-2(6)	15(5)	-13(5)
N(9)	147(12)	69(10)	149(13)	5(10)	62(10)	-18(9)
N(10)	66(7)	64(8)	84(8)	11(8)	14(6)	-7(8)
N(1A)	54(6)	56(6)	66(7)	-15(5)	-4(7)	-6(4)
N(2A)	111(9)	62(8)	64(6)	-2(6)	21(6)	-3(7)
N(3A)	56(7)	99(8)	106(9)	45(8)	36(8)	5(5)
N(4A)	57(7)	53(7)	86(7)	20(5)	1(5)	0(5)
N(5A)	76(7)	83(8)	38(7)	-9(6)	-3(5)	-5(6)
N(6A)	268(13)	44(6)	52(8)	-3(7)	10(7)	-70(7)
N(7A)	171(12)	60(7)	52(8)	9(6)	-8(7)	-32(7)
N(8A)	86(8)	229(12)	45(8)	-2(8)	8(6)	-98(7)
N(9A)	221(15)	104(11)	202(18)	15(12)	127(15)	75(10)
N(10A)	88(8)	63(8)	101(9)	-10(9)	45(9)	-2(6)
O(1)	111(6)	95(6)	107(7)	-27(5)	21(5)	47(5)
O(2)	95(6)	39(5)	108(6)	4(5)	24(4)	-4(4)
O(3)	56(5)	51(5)	87(5)	-1(4)	7(4)	0(4)
O(4)	97(5)	50(5)	70(5)	-9(5)	32(4)	-9(4)
O(5)	112(7)	139(7)	64(6)	9(5)	20(5)	-18(5)
O(6)	124(8)	139(8)	90(7)	-26(6)	-15(6)	7(5)
O(7)	91(6)	91(6)	72(5)	-2(6)	19(4)	9(5)
O(8)	81(6)	50(5)	106(6)	12(5)	-25(4)	-20(4)
O(1A)	99(7)	154(8)	118(7)	-22(5)	44(6)	-60(6)
O(2A)	102(7)	113(7)	159(9)	8(6)	52(6)	36(6)
O(3A)	54(5)	61(5)	73(5)	7(4)	12(4)	3(5)

O(4A)	57(6)	110(6)	215(9)	-92(6)	25(6)	0(5)
O(5A)	133(7)	98(6)	46(5)	-11(5)	-2(5)	-26(5)
O(6A)	110(6)	115(7)	66(6)	-6(5)	-6(5)	28(5)
O(7A)	161(8)	65(6)	69(6)	16(5)	-3(5)	4(6)
O(8A)	113(6)	58(5)	79(5)	23(5)	10(5)	32(5)
C(1)	43(8)	63(9)	85(11)	-1(7)	18(7)	21(7)
C(2)	82(8)	71(8)	135(10)	22(7)	15(7)	37(7)
C(3)	68(9)	63(9)	64(11)	-16(8)	3(8)	5(7)
C(4)	96(11)	100(11)	52(10)	-19(7)	-21(8)	44(9)
C(5)	147(12)	186(14)	88(10)	-7(9)	49(10)	73(11)
C(6)	177(14)	110(12)	160(13)	-84(10)	-48(10)	44(10)
C(7)	96(11)	97(11)	76(9)	-5(8)	-15(7)	14(9)
C(8)	51(9)	62(8)	106(11)	9(7)	-25(7)	1(7)
C(9)	59(9)	51(10)	91(10)	18(8)	17(8)	5(7)
C(10)	57(8)	105(9)	145(11)	21(8)	16(7)	23(7)
C(11)	49(8)	36(9)	90(10)	-8(9)	18(8)	-1(8)
C(12)	58(8)	71(9)	57(8)	-7(7)	17(7)	5(6)
C(13)	89(8)	95(8)	68(8)	7(7)	21(6)	-7(6)
C(14)	88(8)	82(8)	105(9)	-41(7)	44(7)	0(7)
C(15)	57(8)	56(7)	76(8)	-7(6)	20(6)	0(6)
C(16)	42(7)	73(9)	76(8)	-9(8)	-1(6)	7(7)
C(17)	64(8)	61(8)	118(10)	8(8)	8(8)	-4(7)
C(18)	76(9)	75(9)	157(12)	-35(9)	50(9)	-6(8)
C(19)	115(10)	63(9)	98(10)	-1(9)	37(8)	0(8)
C(20)	73(9)	36(8)	62(8)	-2(7)	18(8)	-2(6)
C(21)	75(9)	150(11)	82(9)	4(8)	-12(7)	-16(8)
C(22)	92(12)	72(8)	36(9)	0(7)	16(10)	-12(7)
C(23)	76(10)	109(11)	65(9)	21(8)	40(9)	-4(8)
C(24)	151(12)	187(14)	105(10)	-31(11)	64(9)	23(10)
C(25)	103(10)	103(10)	205(14)	74(10)	90(9)	10(8)
C(26)	94(11)	128(12)	114(11)	56(10)	36(10)	-2(9)
C(27)	107(12)	101(10)	100(10)	8(9)	16(10)	-9(8)
C(28)	85(11)	50(9)	89(11)	9(8)	-17(9)	-15(8)
C(29)	69(9)	116(10)	154(11)	14(8)	10(9)	-1(7)
C(30)	108(15)	56(8)	79(12)	-16(8)	31(12)	-5(8)
C(31)	88(10)	85(10)	50(9)	-17(7)	22(9)	13(8)

C(32)	151(11)	148(11)	55(8)	24(8)	41(8)	22(9)
C(33)	137(10)	72(9)	99(9)	-44(7)	-15(7)	-3(8)
C(34)	92(10)	70(8)	67(8)	5(7)	29(8)	5(6)
C(35)	73(9)	41(7)	81(8)	-6(7)	33(7)	-5(6)
C(36)	67(8)	74(9)	121(11)	1(10)	2(7)	-24(7)
C(37)	101(10)	102(11)	118(11)	-8(10)	20(9)	-34(9)
C(38)	134(12)	93(10)	140(12)	60(10)	-57(10)	-56(10)
C(39)	80(9)	116(11)	92(10)	43(10)	6(9)	21(9)
C(40)	74(10)	81(14)	91(12)	21(12)	31(9)	6(11)
C(41)	129(14)	44(12)	133(15)	31(10)	43(11)	7(9)
C(42)	120(12)	60(13)	127(14)	0(11)	38(10)	-19(10)
C(43)	47(9)	52(12)	102(12)	5(10)	34(9)	5(8)
C(44)	40(7)	84(9)	75(8)	-17(7)	6(7)	-13(7)
C(1A)	59(8)	72(9)	55(9)	16(7)	11(8)	1(8)
C(2A)	94(9)	130(10)	77(8)	-10(7)	51(7)	-16(7)
C(3A)	55(10)	76(9)	78(12)	4(8)	16(10)	-5(7)
C(4A)	67(8)	48(8)	74(10)	-7(7)	5(8)	1(7)
C(5A)	90(8)	62(9)	131(10)	-9(7)	6(7)	-9(7)
C(6A)	79(9)	89(8)	124(10)	-2(7)	1(7)	23(7)
C(7A)	97(10)	69(8)	75(9)	13(7)	-1(8)	13(8)
C(8A)	112(10)	80(9)	83(10)	-4(9)	38(9)	13(8)
C(9A)	88(9)	50(8)	84(10)	12(9)	18(9)	11(8)
C(10A)	148(11)	103(10)	152(12)	40(9)	79(10)	-24(9)
C(11A)	62(10)	105(13)	99(13)	18(12)	36(10)	-3(9)
C(12A)	56(10)	131(14)	115(13)	64(11)	-5(9)	3(9)
C(13A)	123(12)	153(14)	148(13)	13(12)	-17(10)	-43(10)
C(14A)	43(10)	215(16)	205(15)	60(12)	6(9)	-4(9)
C(15A)	95(12)	101(11)	125(11)	50(9)	-30(8)	-16(9)
C(16A)	115(10)	102(10)	60(8)	27(7)	26(8)	10(8)
C(17A)	71(8)	63(8)	76(8)	-11(7)	5(6)	7(7)
C(18A)	92(9)	73(9)	105(10)	-12(8)	8(8)	-3(7)
C(19A)	60(10)	84(9)	110(11)	-34(7)	-5(8)	3(6)
C(20A)	76(10)	70(9)	67(9)	-17(7)	31(8)	-1(8)
C(21A)	90(9)	106(9)	89(10)	23(8)	-12(7)	-19(7)
C(22A)	62(8)	74(10)	48(10)	-13(9)	9(7)	0(7)
C(23A)	73(9)	84(10)	64(10)	-1(8)	2(7)	-29(8)

C(24A)	95(11)	105(10)	112(10)	12(7)	-2(8)	-31(8)
C(25A)	202(14)	82(9)	137(11)	-49(9)	81(11)	-28(9)
C(26A)	177(13)	86(10)	89(12)	4(11)	-21(10)	-72(9)
C(27A)	213(14)	45(8)	59(9)	4(9)	-11(8)	-26(8)
C(28A)	151(13)	38(8)	73(11)	0(9)	-4(9)	-11(10)
C(29A)	244(15)	80(9)	57(8)	42(7)	5(9)	-30(9)
C(30A)	142(14)	49(9)	44(11)	-1(9)	-19(11)	29(9)
C(31A)	95(10)	52(9)	61(10)	-20(7)	-20(8)	-2(8)
C(32A)	122(11)	81(10)	267(17)	-89(11)	77(11)	-38(8)
C(33A)	123(12)	240(17)	145(12)	58(12)	37(10)	99(12)
C(34A)	171(15)	189(15)	71(12)	26(10)	-54(12)	-120(11)
C(35A)	64(9)	58(7)	84(10)	-7(6)	0(8)	-11(6)
C(36A)	205(15)	60(10)	114(12)	17(11)	7(11)	31(10)
C(37A)	168(13)	76(10)	82(9)	26(10)	11(8)	15(10)
C(38A)	169(13)	80(11)	91(10)	-5(10)	5(9)	39(10)
C(39A)	112(10)	75(10)	100(11)	-23(9)	32(9)	3(8)
C(40A)	91(10)	46(10)	123(17)	5(10)	36(11)	12(8)
C(41A)	203(16)	83(12)	127(15)	27(11)	81(14)	38(12)
C(42A)	138(12)	84(12)	210(20)	55(12)	78(14)	84(11)
C(43A)	83(10)	63(11)	117(14)	37(12)	6(11)	14(8)
C(44A)	109(10)	89(13)	93(11)	23(9)	28(8)	4(8)

Table 5. Hydrogen coordinates (x 10^4) and isotropic displacement parameters ($Å^2$x 10^3) for lsh124rt.

	x	y	z	U(eq)
H(1A)	4772	9745	1339	79
H(3A)	3979	10209	1876	72
H(5A)	3312	4821	1993	88
H(6A)	2476	5971	1906	99
H(7A)	2806	5837	1387	86
H(8A)	3488	4166	1575	81
H(1AA)	8370	2102	806	74
H(3AA)	9595	3118	1011	101
H(5AA)	7375	6866	1471	82
H(6AA)	7826	7085	1035	151
H(7AA)	6973	6617	761	119
H(8AA)	6925	6124	1212	146
H(2A)	5956	7970	2341	146
H(2B)	6376	7939	2025	146
H(2C)	5680	7369	1972	146
H(5B)	5498	10290	719	205
H(5C)	5255	9588	377	205
H(5D)	5785	9242	743	205
H(6B)	4196	8061	796	245
H(6C)	4967	7842	788	245
H(6D)	4450	8220	422	245
H(7B)	4006	9922	414	115
H(7C)	3741	9522	756	115
H(8B)	3044	10823	705	96
H(8C)	3347	11820	852	96
H(10B)	2518	11297	1561	156
H(10C)	2232	11199	1122	156
H(10D)	2667	12100	1289	156
H(13A)	4152	10192	2571	125
H(13B)	4912	10466	2776	125

H(13C)	4780	9706	2450	125
H(14A)	3910	11894	2458	132
H(14B)	4328	12510	2227	132
H(14C)	4681	12177	2639	132
H(15A)	5326	11920	2070	74
H(15D)	5664	11276	2415	74
H(16A)	5816	9708	2339	79
H(16D)	6347	9698	2082	79
H(17A)	4629	7576	1673	100
H(17B)	4040	8341	1553	100
H(18A)	3885	8116	2208	119
H(18B)	3533	7393	1893	119
H(19A)	4796	6999	2408	108
H(19B)	4075	6619	2459	108
H(21A)	5336	5504	2631	161
H(21B)	5602	5382	2259	161
H(21C)	5438	4478	2478	161
H(24A)	2719	5969	2597	213
H(24B)	3191	5323	2905	213
H(24C)	2383	5214	2819	213
H(25A)	2836	3132	2389	192
H(25B)	2457	3518	2693	192
H(25C)	3267	3556	2771	192
H(26A)	2152	4164	1921	132
H(26B)	1776	4679	2200	132
H(27A)	1162	5959	1718	125
H(27B)	1335	5069	1496	125
H(29A)	802	6977	833	174
H(29B)	564	6908	1215	174
H(29C)	546	5998	960	174
H(32A)	3357	6401	696	173
H(32B)	2717	5874	443	173
H(32C)	3466	5468	477	173
H(33A)	2366	4242	662	164
H(33B)	2754	3850	1060	164
H(33C)	3123	3847	722	164

H(34A)	4140	4913	1085	90
H(34B)	3942	5775	1315	90
H(35A)	4850	4734	1693	75
H(35B)	4615	3867	1904	75
H(36A)	1508	8215	1072	109
H(36B)	2105	7640	955	109
H(37A)	2266	8929	1546	129
H(37B)	2868	8292	1478	129
H(38A)	2292	9821	1060	164
H(38B)	2796	9118	922	164
H(39A)	4077	12047	525	118
H(39B)	4630	11296	466	118
H(41A)	4860	13472	768	120
H(42A)	6258	13066	1697	121
H(44A)	6387	10680	1654	81
H(44B)	6457	11459	1973	81
H(2AA)	8286	2576	2037	142
H(2AB)	7791	1720	1883	142
H(2AC)	7591	2760	1736	142
H(5AB)	7713	201	433	146
H(5AC)	6985	470	179	146
H(5AD)	7092	414	621	146
H(6AB)	6601	2068	595	152
H(6AC)	6545	2140	158	152
H(6AD)	6961	2914	432	152
H(7AB)	7575	1753	-107	101
H(7AC)	7860	2659	129	101
H(8AB)	8718	2726	-170	107
H(8AC)	9313	1970	-103	107
H(10E)	9728	3866	-81	191
H(10F)	10302	3105	78	191
H(10G)	10206	3992	326	191
H(13D)	9829	3242	1702	224
H(13E)	10424	3810	1581	224
H(13F)	10605	3054	1908	224
H(14D)	11172	1962	1179	237

H(14E)	11353	2307	1602	237
H(14F)	11175	3056	1272	237
H(15B)	10264	1471	1758	139
H(15C)	10348	983	1387	139
H(16B)	9262	1839	1871	109
H(16C)	8776	951	1769	109
H(17C)	7746	3653	1265	87
H(17D)	8196	3797	965	87
H(18C)	8977	4728	1454	110
H(18D)	8284	5227	1249	110
H(19C)	8469	4338	1962	106
H(19D)	8508	5452	1907	106
H(21D)	6864	4579	2221	151
H(21E)	6880	5614	2389	151
H(21F)	7571	5037	2429	151
H(24D)	8905	7528	2057	162
H(24E)	9057	8301	1774	162
H(24F)	8904	7241	1639	162
H(25D)	7332	8846	1842	201
H(25E)	8079	9282	1919	201
H(25F)	7909	8476	2184	201
H(26C)	7360	8612	1238	151
H(26D)	8135	8817	1244	151
H(27C)	8059	8516	612	135
H(27D)	7257	8477	572	135
H(29D)	8129	8188	-9	198
H(29E)	7322	8258	-153	198
H(29F)	7715	7347	-243	198
H(32D)	6662	4616	539	227
H(32E)	6274	4969	135	227
H(32F)	5857	4494	404	227
H(33D)	5479	6338	80	253
H(33E)	5406	6877	447	253
H(33F)	5099	5846	363	253
H(34C)	5705	6132	978	189
H(34D)	5946	5080	974	189

H(35C)	6240	5116	1620	85
H(35D)	6262	6214	1704	85
H(36C)	8463	6260	34	158
H(36D)	7831	5702	118	158
H(37C)	9232	5452	470	135
H(37D)	8681	5167	697	135
H(38C)	8195	4163	197	141
H(38D)	8842	4370	32	141
H(39C)	8847	661	-188	113
H(39D)	8176	372	-53	113
H(41B)	9506	-763	25	157
H(42B)	10144	-1226	1103	164
H(44C)	8890	-69	1392	115
H(44D)	9689	-126	1564	115

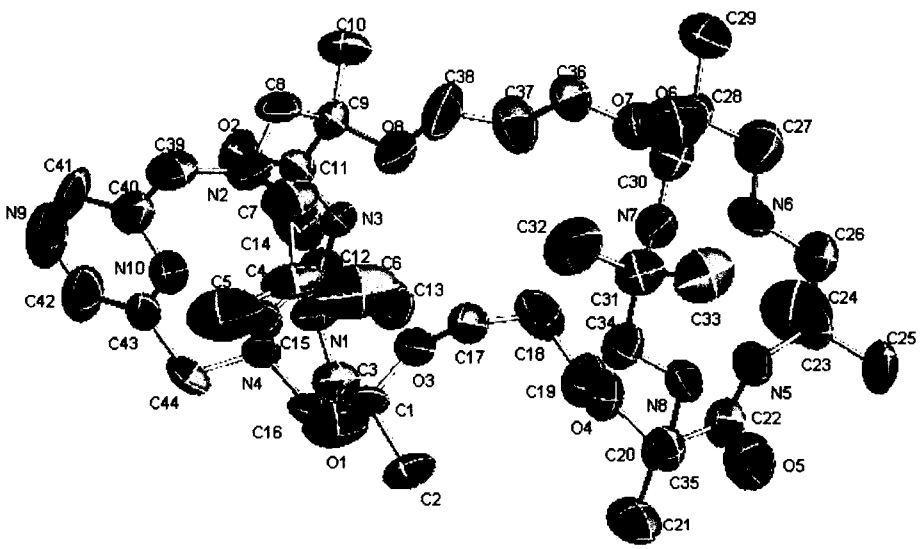

III. Additional X-Ray Crystal Structures

A. lsh107m, Peter Ranslow

Table 1. Crystal data and structure refinement for lsh107m.

Identification code	lsh107m, pbdr – 3466RX	
Empirical formula	$C_{19}\,H_{27}\,N\,O_3\,Si$	
Formula weight	345.51	
Temperature	298(2) K	
Wavelength	0.71073 Å	
Crystal system	Orthorhobmic	
Space group	P(2)1(2)1(2)1	
Unit cell dimensions	a = 8.4892(15) Å	α= 90°.
	b = 15.160(3) Å	β= 90°.
	c = 16.637(3) Å	γ= 90°.
Volume	2141.0(7) $Å^3$	
Z	4	
Density (calculated)	1.072 Mg/m^3	
Absorption coefficient	0.124 mm^{-1}	
F(000)	744	
Crystal size	0.24 x 0.20 x 0.20 mm^3	
Theta range for data collection	3.43 to 23.27°.	
Index ranges	-9<=h<=9, -16<=k<=16, -18<=l<=18	
Reflections collected	13691	
Independent reflections	3080 [R(int) = 0.0793]	
Completeness to theta = 23.27°	99.6 %	
Refinement method	Full-matrix least-squares on F^2	
Data / restraints / parameters	3080 / 0 / 224	
Goodness-of-fit on F^2	0.845	
Final R indices [I>2sigma(I)]	R1 = 0.0466, wR2 = 0.0797	
R indices (all data)	R1 = 0.1394, wR2 = 0.0979	
Absolute structure parameter	0.0(2)	
Extinction coefficient	0.0006(7)	
Largest diff. peak and hole	0.100 and -0.102 e.$Å^{-3}$	

Table 3. Bond lengths [Å] and angles [°] for lsh107m.

Si(1)-C(19)	1.850(4)	C(12)-N(1)-C(5)	124.2(4)
Si(1)-C(20)	1.856(5)	O(1)-C(2)-O(2)	124.8(6)
Si(1)-C(21)	1.856(5)	O(1)-C(2)-N(1)	126.9(6)
Si(1)-C(14)	1.866(4)	O(2)-C(2)-N(1)	108.3(5)
O(1)-C(2)	1.201(5)	O(2)-C(4)-C(5)	107.1(4)
O(2)-C(2)	1.341(6)	N(1)-C(5)-C(6)	113.3(4)
O(2)-C(4)	1.410(5)	N(1)-C(5)-C(4)	99.0(4)
O(3)-C(15)	1.419(4)	C(6)-C(5)-C(4)	113.2(4)
N(1)-C(2)	1.351(6)	C(11)-C(6)-C(7)	119.0(5)
N(1)-C(12)	1.412(5)	C(11)-C(6)-C(5)	118.8(6)
N(1)-C(5)	1.456(5)	C(7)-C(6)-C(5)	122.1(5)
C(4)-C(5)	1.533(5)	C(6)-C(7)-C(8)	121.7(6)
C(5)-C(6)	1.505(5)	C(9)-C(8)-C(7)	114.8(7)
C(6)-C(11)	1.360(6)	C(10)-C(9)-C(8)	130.1(11)
C(6)-C(7)	1.369(6)	C(9)-C(10)-C(11)	112.2(9)
C(7)-C(8)	1.386(6)	C(6)-C(11)-C(10)	122.0(7)
C(8)-C(9)	1.347(8)	C(13)-C(12)-N(1)	123.8(4)
C(9)-C(10)	1.324(11)	C(14)-C(13)-C(12)	178.2(4)
C(10)-C(11)	1.449(9)	C(13)-C(14)-C(15)	120.4(4)
C(12)-C(13)	1.311(5)	C(13)-C(14)-Si(1)	119.0(3)
C(13)-C(14)	1.295(6)	C(15)-C(14)-Si(1)	120.4(3)
C(14)-C(15)	1.512(5)	O(3)-C(15)-C(14)	108.4(4)
C(15)-C(16)	1.528(5)	O(3)-C(15)-C(16)	109.7(4)
C(16)-C(18)	1.524(6)	C(14)-C(15)-C(16)	114.6(4)
C(16)-C(17)	1.534(6)	C(18)-C(16)-C(15)	111.5(4)
C(19)-Si(1)-C(20)	109.5(2)	C(18)-C(16)-C(17)	111.4(4)
C(19)-Si(1)-C(21)	110.7(2)	C(15)-C(16)-C(17)	111.0(4)
C(20)-Si(1)-C(21)	108.7(3)		
C(19)-Si(1)-C(14)	111.8(2)		
C(20)-Si(1)-C(14)	107.4(2)		
C(21)-Si(1)-C(14)	108.7(2)		
C(2)-O(2)-C(4)	111.0(4)		
C(2)-N(1)-C(12)	120.5(5)		
C(2)-N(1)-C(5)	114.1(4)		

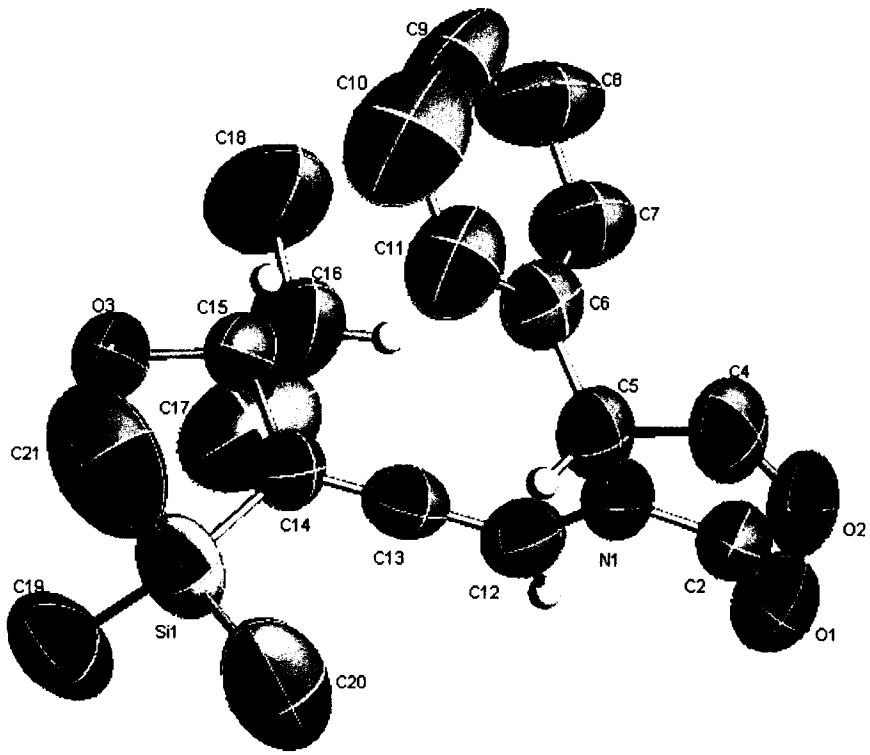

B. lsh125m, Jun Mo Gil

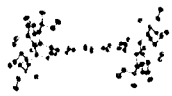

Table 1. Crystal data and structure refinement for lsh125m.

Identification code	lsh125m	
Empirical formula	C50 H80 N12 O8	
Formula weight	977.26	
Temperature	173(2) K	
Wavelength	0.71073 Å	
Crystal system	Monoclinic	
Space group	P2(1)/c	
Unit cell dimensions	a = 9.3537(16) Å	α= 90°.
	b = 18.019(3) Å	β= 97.760(4)°.
	c = 15.890(3) Å	γ = 90°.
Volume	2653.7(8) $Å^3$	
Z	2	
Density (calculated)	1.223 Mg/m^3	
Absorption coefficient	0.084 mm^{-1}	
F(000)	1056	
Crystal size	0.38 x 0.20 x 0.20 mm^3	
Theta range for data collection	3.15 to 23.25°.	
Index ranges	-10<=h<=10, -20<=k<=20, -17<=l<=17	
Reflections collected	17089	
Independent reflections	3812 [R(int) = 0.0864]	
Completeness to theta = 23.25°	99.8 %	
Absorption correction	SADABS	
Max. and min. transmission	0.9833 and 0.9686	
Refinement method	Full-matrix least-squares on F^2	
Data / restraints / parameters	3812 / 0 / 317	
Goodness-of-fit on F^2	1.018	
Final R indices [I>2sigma(I)]	R1 = 0.0676, wR2 = 0.1737	
R indices (all data)	R1 = 0.1053, wR2 = 0.1957	
Extinction coefficient	0.018(3)	
Largest diff. peak and hole	1.261 and -0.211 e.$Å^{-3}$	

Table 3. Bond lengths [Å] and angles [°] for lsh125m.

O(1)-C(3)	1.427(5)	N(6)-C(22)	1.454(5)
O(1)-C(1)	1.428(5)	C(1)-C(18)	1.522(6)
O(2)-C(4)	1.234(5)	C(1)-C(2)	1.529(6)
O(3)-C(12)	1.427(5)	C(1)-C(4)	1.540(6)
O(3)-C(10)	1.440(4)	C(5)-C(6)	1.512(6)
O(4)-C(13)	1.232(4)	C(5)-C(8)	1.534(6)
N(1)-C(4)	1.341(5)	C(5)-C(7)	1.534(6)
N(1)-C(5)	1.470(5)	C(9)-C(10)	1.536(5)
N(2)-C(9)	1.454(5)	C(10)-C(11)	1.514(5)
N(2)-C(25)	1.458(5)	C(10)-C(13)	1.555(5)
N(2)-C(8)	1.471(5)	C(14)-C(16)	1.517(6)
N(3)-C(13)	1.338(5)	C(14)-C(17)	1.529(5)
N(3)-C(14)	1.483(5)	C(14)-C(15)	1.536(5)
N(4)-C(17)	1.454(5)	C(19)-C(20)	1.513(5)
N(4)-C(18)	1.463(5)	C(20)-C(21)	1.392(5)
N(4)-C(19)	1.473(5)	C(21)-C(22)	1.386(5)
N(5)-C(20)	1.329(5)	C(22)-C(23)	1.364(5)
N(5)-C(24)	1.335(5)	C(23)-C(24)	1.386(5)
N(6)-N(6)#1	1.214(7)	C(24)-C(25)	1.503(5)

C(3)-O(1)-C(1)	116.8(3)	C(18)-C(1)-C(2)	107.9(4)
C(12)-O(3)-C(10)	116.3(3)	O(1)-C(1)-C(4)	111.3(3)
C(4)-N(1)-C(5)	126.0(3)	C(18)-C(1)-C(4)	111.5(3)
C(9)-N(2)-C(25)	113.9(3)	C(2)-C(1)-C(4)	109.1(4)
C(9)-N(2)-C(8)	114.5(3)	O(2)-C(4)-N(1)	123.1(4)
C(25)-N(2)-C(8)	110.9(3)	O(2)-C(4)-C(1)	120.1(4)
C(13)-N(3)-C(14)	124.5(3)	N(1)-C(4)-C(1)	116.7(4)
C(17)-N(4)-C(18)	113.8(3)	N(1)-C(5)-C(6)	112.0(3)
C(17)-N(4)-C(19)	114.2(3)	N(1)-C(5)-C(8)	106.4(3)
C(18)-N(4)-C(19)	114.1(3)	C(6)-C(5)-C(8)	113.1(4)
C(20)-N(5)-C(24)	119.2(3)	N(1)-C(5)-C(7)	109.5(4)
N(6)#1-N(6)-C(22)	114.8(4)	C(6)-C(5)-C(7)	109.3(3)
O(1)-C(1)-C(18)	105.8(3)	C(8)-C(5)-C(7)	106.3(3)
O(1)-C(1)-C(2)	111.2(4)	N(2)-C(8)-C(5)	115.9(3)

N(2)-C(9)-C(10)	115.4(3)
O(3)-C(10)-C(11)	110.6(3)
O(3)-C(10)-C(9)	101.4(3)
C(11)-C(10)-C(9)	113.9(3)
O(3)-C(10)-C(13)	107.5(3)
C(11)-C(10)-C(13)	111.8(3)
C(9)-C(10)-C(13)	111.0(3)
O(4)-C(13)-N(3)	122.8(4)
O(4)-C(13)-C(10)	120.1(4)
N(3)-C(13)-C(10)	117.1(3)
N(3)-C(14)-C(16)	112.1(3)
N(3)-C(14)-C(17)	106.3(3)
C(16)-C(14)-C(17)	112.4(3)
N(3)-C(14)-C(15)	109.6(3)
C(16)-C(14)-C(15)	109.2(3)
C(17)-C(14)-C(15)	107.1(3)
N(4)-C(17)-C(14)	116.0(3)
N(4)-C(18)-C(1)	117.1(3)
N(4)-C(19)-C(20)	113.3(3)
N(5)-C(20)-C(21)	122.2(4)
N(5)-C(20)-C(19)	116.2(3)
C(21)-C(20)-C(19)	121.6(4)
C(22)-C(21)-C(20)	117.2(4)
C(23)-C(22)-C(21)	120.8(3)
C(23)-C(22)-N(6)	116.6(3)
C(21)-C(22)-N(6)	122.3(4)
C(22)-C(23)-C(24)	118.0(4)
N(5)-C(24)-C(23)	122.1(4)
N(5)-C(24)-C(25)	116.8(3)
C(23)-C(24)-C(25)	121.2(3)
N(2)-C(25)-C(24)	113.4(3)

Symmetry transformations used to generate equivalent atoms: #1 -x,-y,-z+1

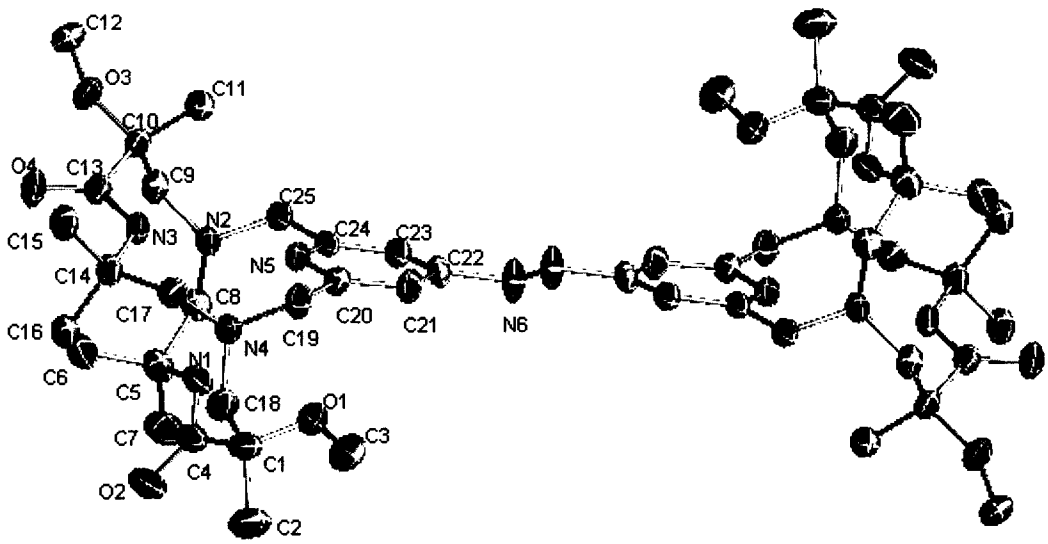

C. lsh135m, Jeff Cross

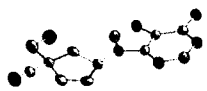

Table 1. Crystal data and structure refinement for lsh135m.

Identification code	lsh135m, JAC-2-291	
Empirical formula	C12 H12 N6 O	
Formula weight	256.28	
Temperature	298(2) K	
Wavelength	0.71073 Å	
Crystal system	Monoclinic	
Space group	P2(1)	
Unit cell dimensions	a = 12.6107(18) Å	α= 90°.
	b = 8.1360(12) Å	β= 105.748(3)°.
	c = 12.7237(19) Å	γ = 90°.
Volume	1256.5(3) $Å^3$	
Z	4	
Density (calculated)	1.355 Mg/m^3	
Absorption coefficient	0.094 mm^{-1}	
F(000)	536	
Crystal size	0.40 x 0.30 x 0.20 mm^3	
Theta range for data collection	1.66 to 20.82°.	
Index ranges	-12<=h<=12, -8<=k<=8, -12<=l<=12	
Reflections collected	6351	
Independent reflections	2623 [R(int) = 0.0156]	
Completeness to theta = 20.82°	100.0 %	
Absorption correction	None	
Refinement method	Full-matrix least-squares on F^2	
Data / restraints / parameters	2623 / 1 / 361	
Goodness-of-fit on F^2	1.044	
Final R indices [I>2sigma(I)]	R1 = 0.0255, wR2 = 0.0665	
R indices (all data)	R1 = 0.0278, wR2 = 0.0680	
Absolute structure parameter	-0.1(14)	
Largest diff. peak and hole	0.089 and -0.118 e.$Å^{-3}$	

Table 3. Bond lengths [Å] and angles [°] for lsh135m.

O(1)-C(7)	1.392(3)	C(1A)-C(5A)	1.493(3)
N(1)-C(6)	1.137(3)	C(1A)-C(7A)	1.524(4)
N(2)-C(8)	1.358(3)	C(1A)-C(2A)	1.548(3)
N(2)-C(10)	1.367(3)	C(2A)-C(3A)	1.535(3)
N(2)-C(3)	1.477(3)	C(3A)-C(4A)	1.488(4)
N(3)-C(8)	1.307(3)	C(4A)-C(5A)	1.312(3)
N(3)-C(9)	1.382(3)	C(9A)-C(10A)	1.376(3)
N(4)-C(11)	1.326(3)	C(9A)-C(12A)	1.394(3)
N(4)-C(10)	1.339(3)		
N(5)-C(11)	1.323(3)	C(8)-N(2)-C(10)	105.44(17)
N(5)-C(12)	1.345(3)	C(8)-N(2)-C(3)	127.5(2)
N(6)-C(12)	1.323(3)	C(10)-N(2)-C(3)	127.04(18)
C(1)-C(6)	1.472(3)	C(8)-N(3)-C(9)	103.5(2)
C(1)-C(5)	1.484(3)	C(11)-N(4)-C(10)	110.6(2)
C(1)-C(7)	1.547(4)	C(11)-N(5)-C(12)	118.7(2)
C(1)-C(2)	1.550(3)	C(6)-C(1)-C(5)	108.63(19)
C(2)-C(3)	1.532(3)	C(6)-C(1)-C(7)	105.2(2)
C(3)-C(4)	1.490(3)	C(5)-C(1)-C(7)	113.4(2)
C(4)-C(5)	1.300(3)	C(6)-C(1)-C(2)	112.1(2)
C(9)-C(10)	1.373(3)	C(5)-C(1)-C(2)	103.56(19)
C(9)-C(12)	1.406(3)	C(7)-C(1)-C(2)	114.0(2)
O(1A)-C(7A)	1.407(3)	C(3)-C(2)-C(1)	106.35(18)
N(1A)-C(6A)	1.139(3)	N(2)-C(3)-C(4)	112.07(19)
N(2A)-C(8A)	1.355(3)	N(2)-C(3)-C(2)	113.11(18)
N(2A)-C(10A)	1.375(3)	C(4)-C(3)-C(2)	103.86(19)
N(2A)-C(3A)	1.465(3)	C(5)-C(4)-C(3)	113.1(2)
N(3A)-C(8A)	1.302(3)	C(4)-C(5)-C(1)	113.2(2)
N(3A)-C(9A)	1.385(3)	N(1)-C(6)-C(1)	176.4(3)
N(4A)-C(11A)	1.330(3)	O(1)-C(7)-C(1)	107.5(2)
N(4A)-C(10A)	1.342(3)	N(3)-C(8)-N(2)	114.3(2)
N(5A)-C(11A)	1.330(3)	C(10)-C(9)-N(3)	110.5(2)
N(5A)-C(12A)	1.347(3)	C(10)-C(9)-C(12)	117.7(2)
N(6A)-C(12A)	1.334(3)	N(3)-C(9)-C(12)	131.7(2)
C(1A)-C(6A)	1.484(3)	N(4)-C(10)-N(2)	127.7(2)

N(4)-C(10)-C(9)	126.1(2)	N(5A)-C(12A)-C(9A)	117.8(2)
N(2)-C(10)-C(9)	106.16(18)		
N(5)-C(11)-N(4)	129.8(2)		
N(6)-C(12)-N(5)	118.0(2)		
N(6)-C(12)-C(9)	125.1(2)		
N(5)-C(12)-C(9)	116.8(2)		
C(8A)-N(2A)-C(10A)	105.16(18)		
C(8A)-N(2A)-C(3A)	127.7(2)		
C(10A)-N(2A)-C(3A)	127.1(2)		
C(8A)-N(3A)-C(9A)	103.6(2)		
C(11A)-N(4A)-C(10A)	110.0(2)		
C(11A)-N(5A)-C(12A)	117.9(2)		
C(6A)-C(1A)-C(5A)	109.34(19)		
C(6A)-C(1A)-C(7A)	105.7(2)		
C(5A)-C(1A)-C(7A)	113.3(2)		
C(6A)-C(1A)-C(2A)	112.14(19)		
C(5A)-C(1A)-C(2A)	102.91(19)		
C(7A)-C(1A)-C(2A)	113.6(2)		
C(3A)-C(2A)-C(1A)	107.15(19)		
N(2A)-C(3A)-C(4A)	112.0(2)		
N(2A)-C(3A)-C(2A)	113.28(19)		
C(4A)-C(3A)-C(2A)	103.7(2)		
C(5A)-C(4A)-C(3A)	112.8(2)		
C(4A)-C(5A)-C(1A)	113.3(2)		
N(1A)-C(6A)-C(1A)	176.5(3)		
O(1A)-C(7A)-C(1A)	107.7(2)		
N(3A)-C(8A)-N(2A)	114.8(2)		
C(10A)-C(9A)-N(3A)	110.3(2)		
C(10A)-C(9A)-C(12A)	117.4(2)		
N(3A)-C(9A)-C(12A)	132.2(2)		
N(4A)-C(10A)-N(2A)	127.3(2)		
N(4A)-C(10A)-C(9A)	126.6(2)		
N(2A)-C(10A)-C(9A)	106.1(2)		
N(4A)-C(11A)-N(5A)	130.1(2)		
N(6A)-C(12A)-N(5A)	117.9(2)		
N(6A)-C(12A)-C(9A)	124.3(2)		

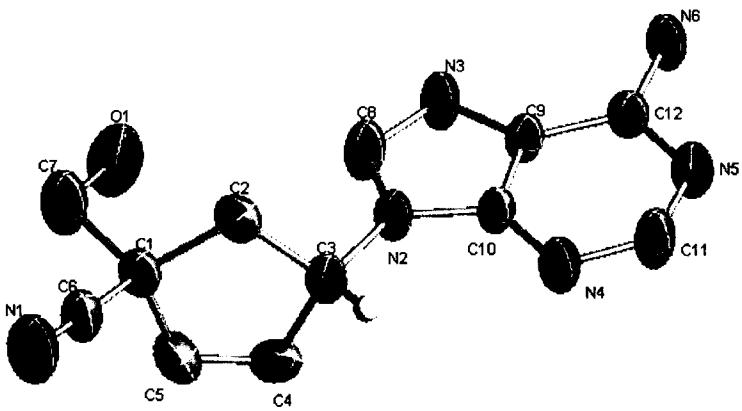

D. lsh136, Jeff Cross

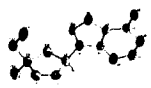

Table 1. Crystal data and structure refinement for lsh136.

Identification code	lsh136	
Empirical formula	C12 H15 N5 O	
Formula weight	245.29	
Temperature	298(2) K	
Wavelength	0.71073 Å	
Crystal system	Orthorhombic	
Space group	P2(1)2(1)2(1)	
Unit cell dimensions	a = 7.0130(14) Å	α= 90°.
	b = 8.3097(17) Å	β= 90°.
	c = 21.272(4) Å	γ= 90°.
Volume	1239.7(4) $Å^3$	
Z	4	
Density (calculated)	1.314 Mg/m^3	
Absorption coefficient	0.090 mm^{-1}	
F(000)	520	
Crystal size	0.40 x 0.30 x 0.28 mm^3	
Theta range for data collection	1.91 to 23.26°.	
Resolution cut off at 0.9 Å in XPREP because the crystal did not scatter beyond that point.		
Index ranges	-7<=h<=7, -9<=k<=9, -23<=l<=23	
Reflections collected	7909	
Independent reflections	1775 [R(int) = 0.0296]	
Completeness to theta = 23.26°	100.0 %	
Absorption correction	SADABS	
Refinement method	Full-matrix least-squares on F^2	
Data / restraints / parameters	1775 / 0 / 171	
Goodness-of-fit on F^2	0.756	
Final R indices [I>2sigma(I)]	R1 = 0.0300, wR2 = 0.0849	
R indices (all data)	R1 = 0.0409, wR2 = 0.0951	
Absolute structure parameter	cannot determine	
Largest diff. peak and hole	0.120 and -0.100 $e.Å^{-3}$	

Table 3. Bond lengths [Å] and angles [°] for lsh136.

N(1)-C(5)	1.366(3)	O(1)-C(12)	1.412(3)
N(1)-C(1)	1.368(3)	C(2)-C(5)	1.387(3)
N(1)-C(6)	1.477(3)	C(2)-C(3)	1.404(3)
N(2)-C(1)	1.311(3)	C(6)-C(7)	1.493(3)
N(2)-C(2)	1.386(3)	C(6)-C(10)	1.542(3)
N(3)-C(3)	1.324(3)	C(7)-C(8)	1.312(3)
N(4)-C(4)	1.332(3)	C(8)-C(9)	1.500(3)
N(4)-C(3)	1.359(3)	C(9)-C(12)	1.523(3)
N(5)-C(4)	1.327(3)	C(9)-C(11)	1.531(3)
N(5)-C(5)	1.345(3)	C(9)-C(10)	1.553(3)
C(5)-N(1)-C(1)	105.83(16)	N(5)-C(5)-C(2)	126.3(2)
C(5)-N(1)-C(6)	126.29(16)	N(1)-C(5)-C(2)	106.10(17)
C(1)-N(1)-C(6)	127.16(18)	N(1)-C(6)-C(7)	111.71(18)
C(1)-N(2)-C(2)	103.93(18)	N(1)-C(6)-C(10)	113.68(18)
C(4)-N(4)-C(3)	118.68(18)	C(7)-C(6)-C(10)	103.88(19)
C(4)-N(5)-C(5)	110.51(19)	C(8)-C(7)-C(6)	112.3(2)
N(2)-C(1)-N(1)	113.89(19)	C(7)-C(8)-C(9)	114.3(2)
N(2)-C(2)-C(5)	110.24(18)	C(8)-C(9)-C(12)	111.36(19)
N(2)-C(2)-C(3)	132.06(19)	C(8)-C(9)-C(11)	111.4(2)
C(5)-C(2)-C(3)	117.62(19)	C(12)-C(9)-C(11)	107.35(19)
N(3)-C(3)-N(4)	117.93(18)	C(8)-C(9)-C(10)	102.22(19)
N(3)-C(3)-C(2)	125.17(19)	C(12)-C(9)-C(10)	112.55(19)
N(4)-C(3)-C(2)	116.87(19)	C(11)-C(9)-C(10)	112.06(19)
N(5)-C(4)-N(4)	129.9(2)	C(6)-C(10)-C(9)	107.37(18)
N(5)-C(5)-N(1)	127.56(19)	O(1)-C(12)-C(9)	109.67(17)

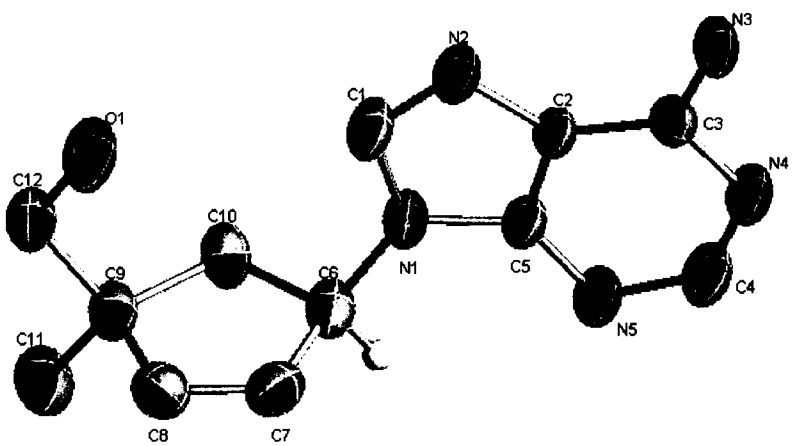

E. lsh138m, Jun Mo Gil

Table 1. Crystal data and structure refinement for lsh138m.

Identification code	lsh138m	
Empirical formula	$C_{52}\ H_{76}\ Co_2\ N_{12}\ O_8$	
Formula weight	1115.11	
Temperature	298(2) K	
Wavelength	0.71073 Å	
Crystal system	Orthorhombic	
Space group	Pbca	
Unit cell dimensions	a = 14.616(3) Å	α= 90°.
	b = 16.517(4) Å	β= 90°.
	c = 26.116(5) Å	γ= 90°.
Volume	6305(2) $Å^3$	
Z	4	
Density (calculated)	1.175 Mg/m^3	
Absorption coefficient	0.581 mm^{-1}	
F(000)	2360	
Crystal size	0.30 x 0.28 x 0.10 mm^3	
Theta range for data collection	1.56 to 20.84°.	
Index ranges	-14<=h<=14, -16<=k<=16, -26<=l<=25	
Reflections collected	29964	

Resolution cut off at 1.0 Å in XPREP because reflection intensities were so low.
Solvent was found in the lattice but due to a possible twin of the crystal the solvent could not be determined with any certainty. The solvents thought to be in the lattice were ethanol and possibly water.

Independent reflections	3305 [R(int) = 0.1256]
Completeness to theta = 20.84°	99.8 %
Absorption correction	SADABS
Refinement method	Full-matrix least-squares on F^2
Data / restraints / parameters	3305 / 0 / 343
Goodness-of-fit on F^2	1.892
Final R indices [I>2sigma(I)]	R1 = 0.1833, wR2 = 0.4677
R indices (all data)	R1 = 0.2330, wR2 = 0.4950
Extinction coefficient	0.0033(15)
Largest diff. peak and hole	2.701 and -0.645 e.$Å^{-3}$

Table 3. Bond lengths [Å] and angles [°] for lsh138m.

Co(1)-N(5)	1.829(13)	C(14)-C(16)	1.47(3)
Co(1)-C(26)	1.91(3)	C(14)-C(17)	1.56(3)
Co(1)-N(4)	1.947(16)	C(14)-C(15)	1.62(3)
Co(1)-N(2)	1.965(14)	C(19)-C(20)	1.45(2)
Co(1)-N(3)	1.971(17)	C(20)-C(21)	1.42(2)
Co(1)-N(1)	1.972(17)	C(21)-C(22)	1.43(2)
N(1)-C(4)	1.26(3)	C(22)-C(23)	1.38(2)
N(1)-C(5)	1.57(3)	C(22)-C(22)#1	1.42(3)
N(2)-C(25)	1.47(2)	C(23)-C(24)	1.41(2)
N(2)-C(9)	1.50(2)	C(24)-C(25)	1.49(2)
N(2)-C(8)	1.50(2)		
N(3)-C(13)	1.23(3)	N(5)-Co(1)-C(26)	178.0(8)
N(3)-C(14)	1.57(3)	N(5)-Co(1)-N(4)	83.9(6)
N(4)-C(17)	1.49(2)	C(26)-Co(1)-N(4)	97.9(8)
N(4)-C(18)	1.50(2)	N(5)-Co(1)-N(2)	83.6(6)
N(4)-C(19)	1.50(2)	C(26)-Co(1)-N(2)	94.6(8)
N(5)-C(20)	1.330(19)	N(4)-Co(1)-N(2)	167.5(6)
N(5)-C(24)	1.366(19)	N(5)-Co(1)-N(3)	90.9(6)
N(6)-C(26)	1.18(2)	C(26)-Co(1)-N(3)	88.3(8)
O(1)-C(3)	1.42(3)	N(4)-Co(1)-N(3)	85.3(7)
O(1)-C(1)	1.50(3)	N(2)-Co(1)-N(3)	94.1(7)
O(2)-C(4)	1.30(3)	N(5)-Co(1)-N(1)	93.6(6)
O(3)-C(10)	1.51(3)	C(26)-Co(1)-N(1)	87.1(8)
O(3)-C(12)	1.52(4)	N(4)-Co(1)-N(1)	96.0(7)
O(4)-C(13)	1.30(3)	N(2)-Co(1)-N(1)	85.7(7)
C(1)-C(18)	1.44(3)	N(3)-Co(1)-N(1)	175.4(6)
C(1)-C(4)	1.50(4)	C(4)-N(1)-C(5)	114(2)
C(1)-C(2)	1.58(3)	C(4)-N(1)-Co(1)	131.6(19)
C(5)-C(6)	1.51(3)	C(5)-N(1)-Co(1)	113.6(14)
C(5)-C(8)	1.52(3)	C(25)-N(2)-C(9)	111.1(14)
C(5)-C(7)	1.63(3)	C(25)-N(2)-C(8)	107.8(15)
C(9)-C(10)	1.48(3)	C(9)-N(2)-C(8)	105.5(13)
C(10)-C(13)	1.54(3)	C(25)-N(2)-Co(1)	112.9(10)
C(10)-C(11)	1.64(3)	C(9)-N(2)-Co(1)	113.0(12)

C(8)-N(2)-Co(1)	106.1(11)	O(3)-C(10)-C(11)	108(2)
C(13)-N(3)-C(14)	112(2)	C(13)-C(10)-C(11)	106(2)
C(13)-N(3)-Co(1)	133.7(19)	N(3)-C(13)-O(4)	124(3)
C(14)-N(3)-Co(1)	114.2(14)	N(3)-C(13)-C(10)	118(2)
C(17)-N(4)-C(18)	107.4(15)	O(4)-C(13)-C(10)	117(2)
C(17)-N(4)-C(19)	107.4(14)	C(16)-C(14)-C(17)	111(2)
C(18)-N(4)-C(19)	110.3(14)	C(16)-C(14)-N(3)	120(2)
C(17)-N(4)-Co(1)	106.9(12)	C(17)-C(14)-N(3)	103.7(18)
C(18)-N(4)-Co(1)	114.3(12)	C(16)-C(14)-C(15)	110(2)
C(19)-N(4)-Co(1)	110.2(11)	C(17)-C(14)-C(15)	102.2(18)
C(20)-N(5)-C(24)	119.4(14)	N(3)-C(14)-C(15)	108(2)
C(20)-N(5)-Co(1)	120.8(11)	N(4)-C(17)-C(14)	112.1(17)
C(24)-N(5)-Co(1)	119.8(11)	C(1)-C(18)-N(4)	116.4(19)
C(3)-O(1)-C(1)	125(3)	C(20)-C(19)-N(4)	111.5(15)
C(10)-O(3)-C(12)	110(3)	N(5)-C(20)-C(21)	122.6(14)
C(18)-C(1)-C(4)	123(2)	N(5)-C(20)-C(19)	112.9(15)
C(18)-C(1)-O(1)	108.0(18)	C(21)-C(20)-C(19)	124.4(16)
C(4)-C(1)-O(1)	105(3)	C(20)-C(21)-C(22)	119.7(16)
C(18)-C(1)-C(2)	112(3)	C(23)-C(22)-C(22)#1	124.7(19)
C(4)-C(1)-C(2)	101(2)	C(23)-C(22)-C(21)	115.1(15)
O(1)-C(1)-C(2)	108(2)	C(22)#1-C(22)-C(21)	120.0(18)
N(1)-C(4)-O(2)	124(3)	C(22)-C(23)-C(24)	123.3(16)
N(1)-C(4)-C(1)	117(2)	N(5)-C(24)-C(23)	119.7(15)
O(2)-C(4)-C(1)	119(2)	N(5)-C(24)-C(25)	113.3(15)
C(6)-C(5)-C(8)	113(2)	C(23)-C(24)-C(25)	126.9(16)
C(6)-C(5)-N(1)	116(2)	N(2)-C(25)-C(24)	109.5(14)
C(8)-C(5)-N(1)	105.2(18)	N(6)-C(26)-Co(1)	179(2)
C(6)-C(5)-C(7)	109(2)		
C(8)-C(5)-C(7)	104.2(19)	Symmetry transformations used to	
N(1)-C(5)-C(7)	109(2)	generate equivalent atoms:	
N(2)-C(8)-C(5)	114.5(15)	#1 -x,-y+1,-z+1	
C(10)-C(9)-N(2)	115.8(16)		
C(9)-C(10)-O(3)	103.7(19)		
C(9)-C(10)-C(13)	120(2)		
O(3)-C(10)-C(13)	108(2)		
C(9)-C(10)-C(11)	111(2)		

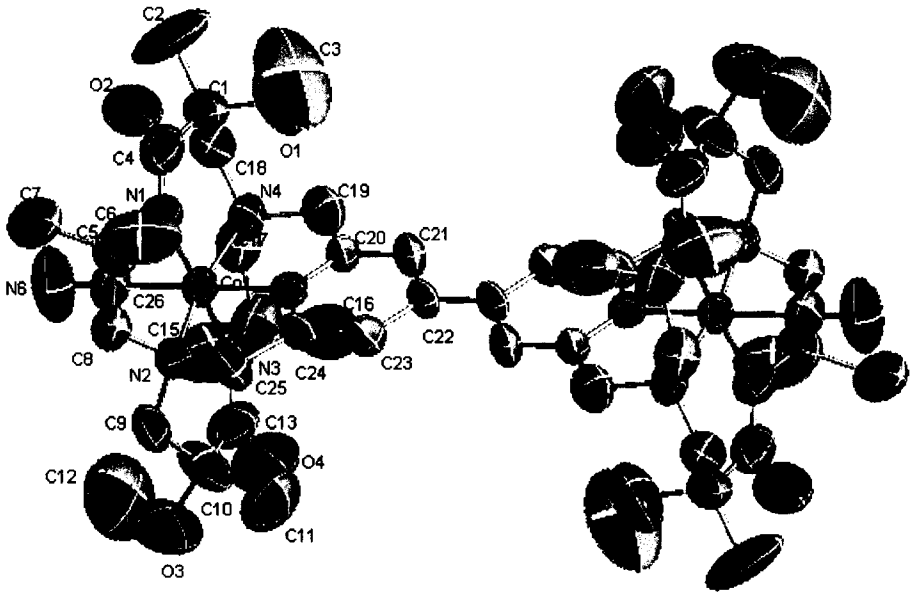

F. lsh151m, Chris Hyland

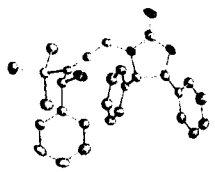

Table 1. Crystal data and structure refinement for lsh151m.

Identification code	lsh151m	
Empirical formula	$C_{29}\ H_{31}\ Cl_2\ N\ O_3\ Si$	
Formula weight	540.54	
Temperature	173(2) K	
Wavelength	0.71073 Å	
Crystal system	Triclinic	
Space group	P-1	
Unit cell dimensions	a = 9.9277(11) Å	α= 79.483(2)°.
	b = 11.5704(12) Å	β= 87.858(2)°.
	c = 13.2704(14) Å	γ= 72.576(2)°.
Volume	1429.7(3) $Å^3$	
Z	2	
Density (calculated)	1.256 Mg/m^3	
Absorption coefficient	0.299 mm^{-1}	
F(000)	568	
Crystal size	0.45 x 0.30 x 0.18 mm^3	
Theta range for data collection	1.88 to 27.88°.	
Index ranges	-13<=h<=13, -15<=k<=15, -17<=l<=17	
Reflections collected	13412	
Independent reflections	6690 [R(int) = 0.0262]	
Completeness to theta = 27.88°	98.2 %	
Absorption correction	Semi-empirical from equivalents	
Max. and min. transmission	0.9482 and 0.8773	
Refinement method	Full-matrix least-squares on F^2	
Data / restraints / parameters	6690 / 0 / 329	
Goodness-of-fit on F^2	1.030	
Final R indices [I>2sigma(I)]	R1 = 0.0499, wR2 = 0.1126	
R indices (all data)	R1 = 0.0778, wR2 = 0.1251	
Largest diff. peak and hole	0.564 and -0.540 $e.Å^{-3}$	

Table 3. Bond lengths [Å] and angles [°] for lsh151m.

Si(1)-C(26)	1.859(2)	C(9)-C(10)	1.514(2)
Si(1)-C(28)	1.861(2)	C(10)-C(15)	1.385(3)
Si(1)-C(27)	1.867(2)	C(10)-C(11)	1.389(3)
Si(1)-C(18)	1.8949(19)	C(11)-C(12)	1.388(3)
O(1)-C(1)	1.211(2)	C(12)-C(13)	1.379(3)
O(2)-C(1)	1.353(3)	C(13)-C(14)	1.380(3)
O(2)-C(2)	1.455(2)	C(14)-C(15)	1.387(3)
O(3)-C(19)	1.426(2)	C(16)-C(17)	1.311(3)
N(1)-C(1)	1.355(2)	C(17)-C(18)	1.305(3)
N(1)-C(16)	1.412(2)	C(18)-C(19)	1.537(3)
N(1)-C(9)	1.455(2)	C(19)-C(20)	1.519(3)
C(2)-C(3)	1.495(3)	C(20)-C(21)	1.388(3)
C(2)-C(9)	1.559(3)	C(20)-C(25)	1.391(3)
C(3)-C(4)	1.389(3)	C(21)-C(22)	1.380(3)
C(3)-C(8)	1.393(3)	C(22)-C(23)	1.384(3)
C(4)-C(5)	1.389(3)	C(23)-C(24)	1.378(4)
C(5)-C(6)	1.373(3)	C(24)-C(25)	1.383(3)
C(6)-C(7)	1.376(3)	Cl(1)-C(29)	1.735(3)
C(7)-C(8)	1.380(3)	Cl(2)-C(29)	1.757(3)
C(26)-Si(1)-C(28)	109.03(11)	O(2)-C(2)-C(9)	103.94(15)
C(26)-Si(1)-C(27)	110.64(11)	C(3)-C(2)-C(9)	117.13(15)
C(28)-Si(1)-C(27)	110.47(11)	C(4)-C(3)-C(8)	119.16(19)
C(26)-Si(1)-C(18)	111.02(9)	C(4)-C(3)-C(2)	122.26(18)
C(28)-Si(1)-C(18)	108.44(9)	C(8)-C(3)-C(2)	118.58(17)
C(27)-Si(1)-C(18)	107.21(10)	C(3)-C(4)-C(5)	119.9(2)
C(1)-O(2)-C(2)	109.08(14)	C(6)-C(5)-C(4)	120.3(2)
C(1)-N(1)-C(16)	122.51(16)	C(5)-C(6)-C(7)	120.0(2)
C(1)-N(1)-C(9)	112.70(16)	C(6)-C(7)-C(8)	120.4(2)
C(16)-N(1)-C(9)	124.58(14)	C(7)-C(8)-C(3)	120.2(2)
O(1)-C(1)-O(2)	122.87(17)	N(1)-C(9)-C(10)	113.41(15)
O(1)-C(1)-N(1)	127.6(2)	N(1)-C(9)-C(2)	99.06(13)
O(2)-C(1)-N(1)	109.54(16)	C(10)-C(9)-C(2)	115.44(15)
O(2)-C(2)-C(3)	110.61(15)	C(15)-C(10)-C(11)	118.83(17)

C(15)-C(10)-C(9)	121.61(16)	O(3)-C(19)-C(20)	107.46(15)
C(11)-C(10)-C(9)	119.51(16)	O(3)-C(19)-C(18)	113.04(15)
C(12)-C(11)-C(10)	120.36(18)	C(20)-C(19)-C(18)	110.24(15)
C(13)-C(12)-C(11)	120.38(19)	C(21)-C(20)-C(25)	118.69(18)
C(12)-C(13)-C(14)	119.55(19)	C(21)-C(20)-C(19)	119.78(17)
C(13)-C(14)-C(15)	120.20(19)	C(25)-C(20)-C(19)	121.51(18)
C(10)-C(15)-C(14)	120.62(18)	C(22)-C(21)-C(20)	120.92(19)
C(17)-C(16)-N(1)	123.84(17)	C(21)-C(22)-C(23)	119.9(2)
C(18)-C(17)-C(16)	176.8(2)	C(24)-C(23)-C(22)	119.8(2)
C(17)-C(18)-C(19)	119.78(17)	C(23)-C(24)-C(25)	120.3(2)
C(17)-C(18)-Si(1)	119.25(14)	C(24)-C(25)-C(20)	120.4(2)
C(19)-C(18)-Si(1)	120.93(13)	Cl(1)-C(29)-Cl(2)	111.89(14)

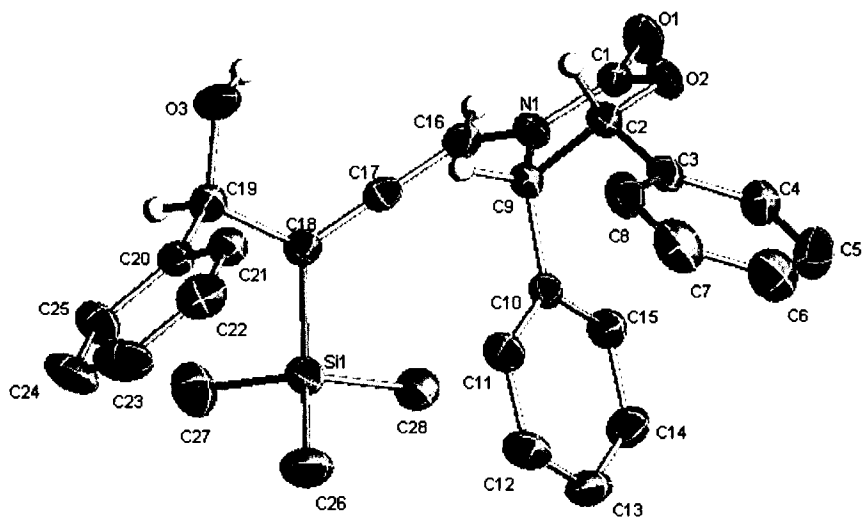

G. lsh152m, Chris Hyland

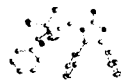

Table 1. Crystal data and structure refinement for lsh152m.

Identification code	lsh152m	
Empirical formula	C_{28} H_{29} N O_3 Si	
Formula weight	455.61	
Temperature	173(2) K	
Wavelength	0.71073 Å	
Crystal system	Orthorhombic	
Space group	Fdd2	
Unit cell dimensions	a = 29.217(3) Å	α= 90°.
	b = 54.471(5) Å	β= 90°.
	c = 6.1768(6) Å	γ = 90°.
Volume	9830.2(16) $Å^3$	
Z	16	
Density (calculated)	1.231 Mg/m^3	
Absorption coefficient	0.125 mm^{-1}	
F(000)	3872	
Crystal size	0.30 x 0.14 x 0.14 mm^3	
Theta range for data collection	1.58 to 25.02°.	
Index ranges	-34<=h<=34, -64<=k<=64, -7<=l<=7	
Reflections collected	18295	
Independent reflections	4344 [R(int) = 0.1015]	
Completeness to theta = 25.02°	100.0 %	
Absorption correction	Semi-empirical from equivalents	
Max. and min. transmission	0.9827 and 0.9635	
Refinement method	Full-matrix least-squares on F^2	
Data / restraints / parameters	4344 / 1 / 303	
Goodness-of-fit on F^2	0.999	
Final R indices [I>2sigma(I)]	R1 = 0.0489, wR2 = 0.0850	
R indices (all data)	R1 = 0.0815, wR2 = 0.0946	
Absolute structure parameter	0.08(15)	
Extinction coefficient	0.00234(10)	
Largest diff. peak and hole	0.199 and -0.201 e.$Å^{-3}$	

Table 3. Bond lengths [Å] and angles [°] for lsh152m.

Si(1)-C(28)	1.851(3)	C(7)-C(8)	1.383(4)
Si(1)-C(26)	1.854(4)	C(9)-C(10)	1.514(4)
Si(1)-C(27)	1.857(3)	C(10)-C(11)	1.378(4)
Si(1)-C(18)	1.888(3)	C(10)-C(15)	1.389(4)
O(1)-C(1)	1.216(3)	C(11)-C(12)	1.395(4)
O(2)-C(1)	1.349(3)	C(12)-C(13)	1.374(5)
O(2)-C(2)	1.453(3)	C(13)-C(14)	1.381(4)
O(3)-C(19)	1.428(3)	C(14)-C(15)	1.381(4)
N(1)-C(1)	1.352(3)	C(16)-C(17)	1.308(4)
N(1)-C(16)	1.409(3)	C(17)-C(18)	1.311(4)
N(1)-C(9)	1.465(3)	C(18)-C(19)	1.534(4)
C(2)-C(3)	1.496(4)	C(19)-C(20)	1.519(4)
C(2)-C(9)	1.570(4)	C(20)-C(21)	1.384(4)
C(3)-C(4)	1.374(4)	C(20)-C(25)	1.387(4)
C(3)-C(8)	1.390(4)	C(21)-C(22)	1.383(4)
C(4)-C(5)	1.380(4)	C(22)-C(23)	1.377(4)
C(5)-C(6)	1.377(5)	C(23)-C(24)	1.374(5)
C(6)-C(7)	1.382(5)	C(24)-C(25)	1.380(4)

C(28)-Si(1)-C(26)	109.76(19)	C(3)-C(2)-C(9)	117.1(2)
C(28)-Si(1)-C(27)	110.60(16)	C(4)-C(3)-C(8)	117.8(3)
C(26)-Si(1)-C(27)	110.7(2)	C(4)-C(3)-C(2)	122.8(3)
C(28)-Si(1)-C(18)	107.32(14)	C(8)-C(3)-C(2)	119.4(3)
C(26)-Si(1)-C(18)	110.17(16)	C(3)-C(4)-C(5)	121.6(3)
C(27)-Si(1)-C(18)	108.23(15)	C(6)-C(5)-C(4)	120.2(3)
C(1)-O(2)-C(2)	110.6(2)	C(5)-C(6)-C(7)	119.3(3)
C(1)-N(1)-C(16)	120.3(2)	C(6)-C(7)-C(8)	119.9(3)
C(1)-N(1)-C(9)	112.8(2)	C(7)-C(8)-C(3)	121.2(3)
C(16)-N(1)-C(9)	122.5(2)	N(1)-C(9)-C(10)	113.8(2)
O(1)-C(1)-O(2)	122.5(2)	N(1)-C(9)-C(2)	100.6(2)
O(1)-C(1)-N(1)	127.1(3)	C(10)-C(9)-C(2)	116.4(2)
O(2)-C(1)-N(1)	110.4(3)	C(11)-C(10)-C(15)	118.6(3)
O(2)-C(2)-C(3)	109.3(2)	C(11)-C(10)-C(9)	119.2(3)
O(2)-C(2)-C(9)	105.0(2)	C(15)-C(10)-C(9)	122.2(3)

C(10)-C(11)-C(12)	120.5(3)
C(13)-C(12)-C(11)	120.1(3)
C(12)-C(13)-C(14)	119.8(3)
C(13)-C(14)-C(15)	119.8(3)
C(14)-C(15)-C(10)	121.1(3)
C(17)-C(16)-N(1)	125.4(3)
C(16)-C(17)-C(18)	172.0(3)
C(17)-C(18)-C(19)	119.1(2)
C(17)-C(18)-Si(1)	117.1(2)
C(19)-C(18)-Si(1)	123.39(19)
O(3)-C(19)-C(20)	110.5(2)
O(3)-C(19)-C(18)	112.4(2)
C(20)-C(19)-C(18)	113.7(2)
C(21)-C(20)-C(25)	118.3(3)
C(21)-C(20)-C(19)	121.0(3)
C(25)-C(20)-C(19)	120.7(3)
C(22)-C(21)-C(20)	120.4(3)
C(23)-C(22)-C(21)	120.6(3)
C(24)-C(23)-C(22)	119.5(3)
C(23)-C(24)-C(25)	120.0(3)
C(24)-C(25)-C(20)	121.2(3)

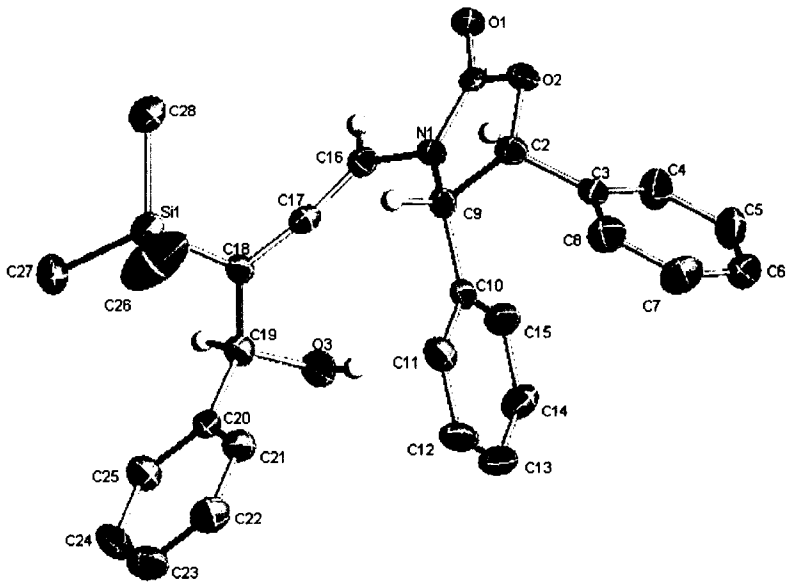

H. lsh156, Cristobal de los Rios Salgado

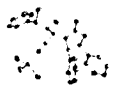

Table 1. Crystal data and structure refinement for lsh156.

Identification code	lsh156, CR 258	
Empirical formula	C_{30} H_{33} N O_3 Si	
Formula weight	483.66	
Temperature	100(2) K	
Wavelength	0.71073 Å	
Crystal system	Monoclinic	
Space group	P2(1)	
Unit cell dimensions	a = 11.699(8) Å	α= 90°.
	b = 17.054(10) Å	β= 107.790(16)°.
	c = 14.580(9) Å	γ = 90°.
Volume	2770(3) $Å^3$	
Z	4	
Density (calculated)	1.160 Mg/m^3	
Absorption coefficient	0.114 mm^{-1}	
F(000)	1032	
Crystal size	0.44 x 0.21 x 0.07 mm^3	
Theta range for data collection	1.47 to 25.11°.	
Index ranges	-13<=h<=13, -20<=k<=19, -17<=l<=17	
Reflections collected	21275	
Independent reflections	9466 [R(int) = 0.0840]	
Completeness to theta = 25.11°	98.7 %	
Absorption correction	Semi-empirical from equivalents	
Max. and min. transmission	0.9920 and 0.9514	
Refinement method	Full-matrix least-squares on F^2	
Data / restraints / parameters	9466 / 1 / 642	
Goodness-of-fit on F^2	0.977	
Final R indices [I>2sigma(I)]	R1 = 0.0525, wR2 = 0.1036	
R indices (all data)	R1 = 0.0912, wR2 = 0.1205	
Absolute structure parameter	-0.11(12)	
Extinction coefficient	0.0237(11)	
Largest diff. peak and hole	0.289 and -0.247 $e.Å^{-3}$	

Table 3. Bond lengths [Å] and angles [°] for lsh156.

Si(1)-C(13)	1.842(4)	C(17)-C(18)	1.487(5)
Si(1)-C(15)	1.846(4)	C(17)-C(24)	1.549(5)
Si(1)-C(12)	1.849(4)	C(18)-C(19)	1.388(5)
Si(1)-C(14)	1.861(4)	C(18)-C(23)	1.393(5)
Si(2)-C(42)	1.835(4)	C(19)-C(20)	1.388(5)
Si(2)-C(45)	1.855(4)	C(20)-C(21)	1.376(5)
Si(2)-C(44)	1.858(4)	C(21)-C(22)	1.378(6)
Si(2)-C(43)	1.865(4)	C(22)-C(23)	1.380(5)
O(1)-C(9)	1.416(4)	C(24)-C(25)	1.522(5)
O(2)-C(16)	1.205(4)	C(25)-C(26)	1.381(5)
O(3)-C(16)	1.368(4)	C(25)-C(30)	1.390(5)
O(3)-C(17)	1.451(4)	C(26)-C(27)	1.386(6)
O(4)-C(39)	1.403(4)	C(27)-C(28)	1.397(6)
O(5)-C(46)	1.213(4)	C(28)-C(29)	1.365(6)
O(6)-C(46)	1.370(5)	C(29)-C(30)	1.379(5)
O(6)-C(47)	1.480(4)	C(31)-C(32)	1.392(6)
N(1)-C(16)	1.353(4)	C(31)-C(36)	1.392(5)
N(1)-C(10)	1.450(4)	C(32)-C(33)	1.364(6)
N(1)-C(24)	1.473(4)	C(33)-C(34)	1.366(6)
N(2)-C(46)	1.342(4)	C(34)-C(35)	1.393(6)
N(2)-C(54)	1.458(4)	C(35)-C(36)	1.399(6)
N(2)-C(40)	1.461(5)	C(36)-C(37)	1.501(5)
C(1)-C(2)	1.385(5)	C(37)-C(39)	1.540(5)
C(1)-C(6)	1.389(5)	C(37)-C(38)	1.541(6)
C(2)-C(3)	1.383(6)	C(39)-C(40)	1.578(5)
C(3)-C(4)	1.381(6)	C(40)-C(41)	1.467(5)
C(4)-C(5)	1.386(5)	C(41)-C(42)	1.204(5)
C(5)-C(6)	1.388(5)	C(47)-C(48)	1.500(5)
C(6)-C(7)	1.509(5)	C(47)-C(54)	1.545(5)
C(7)-C(8)	1.529(5)	C(48)-C(53)	1.388(5)
C(7)-C(9)	1.538(5)	C(48)-C(49)	1.390(5)
C(9)-C(10)	1.559(5)	C(49)-C(50)	1.397(6)
C(10)-C(11)	1.477(5)	C(50)-C(51)	1.379(6)
C(11)-C(12)	1.204(5)	C(51)-C(52)	1.382(6)

C(52)-C(53)	1.389(6)	C(56)-C(57)	1.388(5)
C(54)-C(55)	1.514(5)	C(57)-C(58)	1.380(6)
C(55)-C(56)	1.383(5)	C(58)-C(59)	1.387(6)
C(55)-C(60)	1.388(5)	C(59)-C(60)	1.391(5)

C(13)-Si(1)-C(15)	112.5(2)	O(1)-C(9)-C(7)	111.8(3)
C(13)-Si(1)-C(12)	106.28(18)	O(1)-C(9)-C(10)	108.9(3)
C(15)-Si(1)-C(12)	106.90(18)	C(7)-C(9)-C(10)	110.7(3)
C(13)-Si(1)-C(14)	109.64(19)	N(1)-C(10)-C(11)	111.9(3)
C(15)-Si(1)-C(14)	111.4(2)	N(1)-C(10)-C(9)	110.3(3)
C(12)-Si(1)-C(14)	109.91(18)	C(11)-C(10)-C(9)	109.2(3)
C(42)-Si(2)-C(45)	107.83(18)	C(12)-C(11)-C(10)	174.4(4)
C(42)-Si(2)-C(44)	107.57(18)	C(11)-C(12)-Si(1)	177.6(3)
C(45)-Si(2)-C(44)	111.42(19)	O(2)-C(16)-N(1)	128.7(3)
C(42)-Si(2)-C(43)	107.58(18)	O(2)-C(16)-O(3)	122.1(3)
C(45)-Si(2)-C(43)	111.5(2)	N(1)-C(16)-O(3)	109.1(3)
C(44)-Si(2)-C(43)	110.76(19)	O(3)-C(17)-C(18)	111.9(3)
C(16)-O(3)-C(17)	107.8(3)	O(3)-C(17)-C(24)	103.4(3)
C(46)-O(6)-C(47)	107.2(3)	C(18)-C(17)-C(24)	116.4(3)
C(16)-N(1)-C(10)	121.7(3)	C(19)-C(18)-C(23)	119.8(4)
C(16)-N(1)-C(24)	111.9(3)	C(19)-C(18)-C(17)	122.4(3)
C(10)-N(1)-C(24)	124.3(3)	C(23)-C(18)-C(17)	117.7(3)
C(46)-N(2)-C(54)	112.0(3)	C(18)-C(19)-C(20)	118.9(4)
C(46)-N(2)-C(40)	122.5(3)	C(21)-C(20)-C(19)	121.5(4)
C(54)-N(2)-C(40)	125.5(3)	C(20)-C(21)-C(22)	119.1(4)
C(2)-C(1)-C(6)	122.4(4)	C(21)-C(22)-C(23)	120.7(4)
C(3)-C(2)-C(1)	119.3(4)	C(22)-C(23)-C(18)	119.9(4)
C(4)-C(3)-C(2)	119.3(4)	N(1)-C(24)-C(25)	111.6(3)
C(3)-C(4)-C(5)	120.9(4)	N(1)-C(24)-C(17)	98.5(3)
C(4)-C(5)-C(6)	120.7(4)	C(25)-C(24)-C(17)	115.8(3)
C(5)-C(6)-C(1)	117.4(4)	C(26)-C(25)-C(30)	118.2(3)
C(5)-C(6)-C(7)	119.6(3)	C(26)-C(25)-C(24)	123.2(3)
C(1)-C(6)-C(7)	123.0(3)	C(30)-C(25)-C(24)	118.6(3)
C(6)-C(7)-C(8)	111.8(3)	C(25)-C(26)-C(27)	121.0(4)
C(6)-C(7)-C(9)	110.8(3)	C(26)-C(27)-C(28)	120.2(4)
C(8)-C(7)-C(9)	111.3(3)	C(29)-C(28)-C(27)	118.5(4)

C(28)-C(29)-C(30)	121.5(4)
C(29)-C(30)-C(25)	120.6(4)
C(32)-C(31)-C(36)	121.4(4)
C(33)-C(32)-C(31)	120.9(4)
C(32)-C(33)-C(34)	119.2(4)
C(33)-C(34)-C(35)	120.7(4)
C(34)-C(35)-C(36)	121.3(4)
C(31)-C(36)-C(35)	116.5(4)
C(31)-C(36)-C(37)	123.1(4)
C(35)-C(36)-C(37)	120.4(4)
C(36)-C(37)-C(39)	110.9(3)
C(36)-C(37)-C(38)	112.5(3)
C(39)-C(37)-C(38)	111.6(3)
O(4)-C(39)-C(37)	111.2(3)
O(4)-C(39)-C(40)	110.2(3)
C(37)-C(39)-C(40)	108.8(3)
N(2)-C(40)-C(41)	111.2(3)
N(2)-C(40)-C(39)	112.0(3)
C(41)-C(40)-C(39)	106.8(3)
C(42)-C(41)-C(40)	170.7(4)
C(41)-C(42)-Si(2)	176.4(4)
O(5)-C(46)-N(2)	128.9(4)
O(5)-C(46)-O(6)	121.9(4)
N(2)-C(46)-O(6)	109.2(3)
O(6)-C(47)-C(48)	110.8(3)
O(6)-C(47)-C(54)	101.6(3)
C(48)-C(47)-C(54)	118.1(3)
C(53)-C(48)-C(49)	119.0(4)
C(53)-C(48)-C(47)	116.9(4)
C(49)-C(48)-C(47)	124.0(4)
C(48)-C(49)-C(50)	120.5(4)
C(51)-C(50)-C(49)	119.6(4)
C(50)-C(51)-C(52)	120.3(4)
C(51)-C(52)-C(53)	120.0(4)
C(48)-C(53)-C(52)	120.5(4)
N(2)-C(54)-C(55)	114.0(3)
N(2)-C(54)-C(47)	98.9(3)
C(55)-C(54)-C(47)	113.2(3)
C(56)-C(55)-C(60)	119.2(3)
C(56)-C(55)-C(54)	122.4(3)
C(60)-C(55)-C(54)	118.3(3)
C(55)-C(56)-C(57)	120.1(4)
C(58)-C(57)-C(56)	121.1(4)
C(57)-C(58)-C(59)	118.9(4)
C(58)-C(59)-C(60)	120.3(4)
C(55)-C(60)-C(59)	120.4(4)

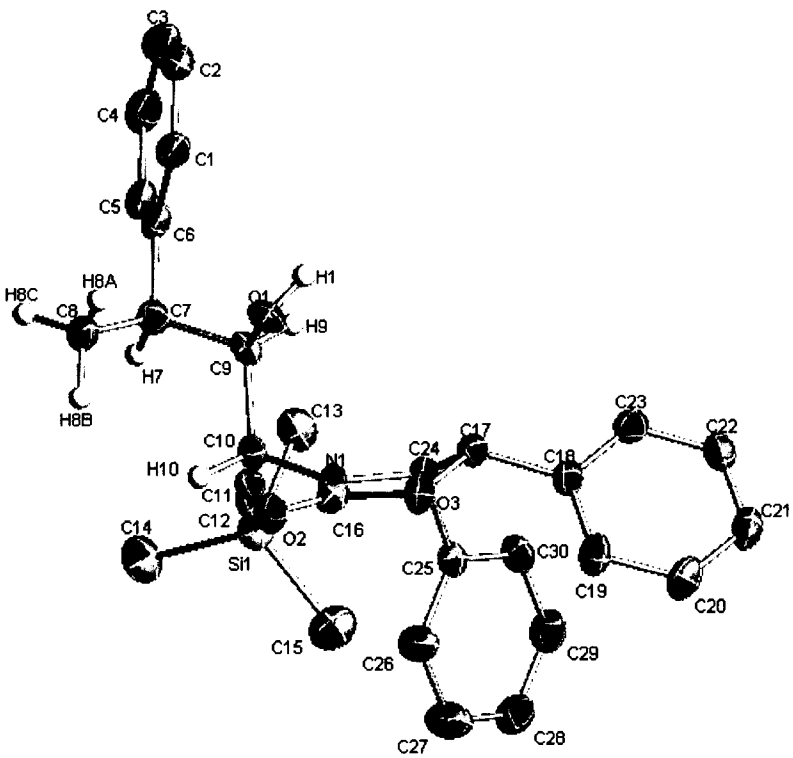

I. lsh158, Chris Hyland

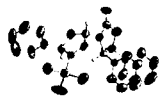

Table 1. Crystal data and structure refinement for lsh158m.

Identification code	lsh158m	
Empirical formula	$C_{28}\ H_{29}\ N\ O_3\ Si$	
Formula weight	455.61	
Temperature	273(2) K	
Wavelength	0.71073 ≈	
Crystal system	Monoclinic	
Space group	P2(1)/n	
Unit cell dimensions	a = 16.2933(19) ≈	α= 90∞.
	b = 12.0291(14) ≈	β= 99.948(2)∞.
	c = 27.005(3) ≈	γ = 90∞.
Volume	5213.3(11) ≈^{3}	
Z	8	
Density (calculated)	1.161 Mg/m^3	
Absorption coefficient	0.118 mm^{-1}	
F(000)	1936	
Crystal size	0.22 x 0.09 x 0.05 mm^3	
Theta range for data collection	1.36 to 19.78∞.	
Index ranges	-15<=h<=15, -11<=k<=11, -25<=l<=25	
Reflections collected	23519	
Independent reflections	4715 [R(int) = 0.0745]	
Completeness to theta = 19.78∞	100.0 %	
Absorption correction	SADABS	
Max. and min. transmission	0.9946 and 0.9741	
Refinement method	Full-matrix least-squares on F^2	
Data / restraints / parameters	4715 / 0 / 602	
Goodness-of-fit on F^2	0.987	
Final R indices [I>2sigma(I)]	R1 = 0.0502, wR2 = 0.1204	
R indices (all data)	R1 = 0.1145, wR2 = 0.1588	
Extinction coefficient	0.00043(19)	
Largest diff. peak and hole	0.182 and -0.203 e.≈$^{-3}$	

Table 3. Bond lengths [≈] and angles [∞] for lsh158m.

Si(1)-C(48)	1.836(7)	C(10)-C(11)	1.370(7)
Si(1)-C(49)	1.845(6)	C(11)-C(12)	1.389(7)
Si(1)-C(47)	1.845(6)	C(12)-C(13)	1.361(8)
Si(1)-C(46)	1.864(6)	C(13)-C(14)	1.360(8)
Si(2)-C(19)	1.849(6)	C(14)-C(15)	1.379(8)
Si(2)-C(21)	1.849(6)	C(16)-C(17)	1.493(7)
Si(2)-C(20)	1.853(6)	C(17)-C(18)	1.313(6)
Si(2)-C(18)	1.878(5)	C(18)-C(22)	1.513(6)
O(1)-C(1)	1.207(6)	C(22)-C(23)	1.511(7)
O(2)-C(1)	1.376(6)	C(23)-C(28)	1.347(8)
O(2)-C(2)	1.443(6)	C(23)-C(24)	1.374(8)
O(3)-C(16)	1.413(5)	C(24)-C(25)	1.387(9)
O(3)-C(22)	1.450(6)	C(25)-C(26)	1.340(12)
O(4)-C(29)	1.205(6)	C(26)-C(27)	1.366(13)
O(5)-C(29)	1.372(6)	C(27)-C(28)	1.375(12)
O(5)-C(30)	1.450(6)	C(30)-C(31)	1.488(8)
O(6)-C(44)	1.406(6)	C(30)-C(37)	1.551(7)
O(6)-C(50)	1.443(6)	C(31)-C(32)	1.369(8)
N(1)-C(1)	1.354(6)	C(31)-C(36)	1.375(8)
N(1)-C(16)	1.454(6)	C(32)-C(33)	1.395(10)
N(1)-C(9)	1.463(6)	C(33)-C(34)	1.351(12)
N(2)-C(29)	1.350(7)	C(34)-C(35)	1.356(12)
N(2)-C(44)	1.447(6)	C(35)-C(36)	1.382(9)
N(2)-C(37)	1.453(6)	C(37)-C(38)	1.513(7)
C(2)-C(3)	1.486(7)	C(38)-C(39)	1.373(7)
C(2)-C(9)	1.546(7)	C(38)-C(43)	1.379(7)
C(3)-C(4)	1.363(8)	C(39)-C(40)	1.395(7)
C(3)-C(8)	1.379(7)	C(40)-C(41)	1.363(8)
C(4)-C(5)	1.389(9)	C(41)-C(42)	1.369(8)
C(5)-C(6)	1.356(10)	C(42)-C(43)	1.375(8)
C(6)-C(7)	1.351(10)	C(44)-C(45)	1.488(7)
C(7)-C(8)	1.368(8)	C(45)-C(46)	1.318(6)
C(9)-C(10)	1.507(6)	C(46)-C(50)	1.520(7)
C(10)-C(15)	1.365(7)	C(50)-C(51)	1.503(7)

C(51)-C(52)	1.353(8)	C(53)-C(54)	1.364(11)
C(51)-C(56)	1.370(9)	C(54)-C(55)	1.348(12)
C(52)-C(53)	1.387(10)	C(55)-C(56)	1.383(10)

C(48)-Si(1)-C(49)	111.7(4)	C(6)-C(5)-C(4)	120.4(8)
C(48)-Si(1)-C(47)	109.0(4)	C(7)-C(6)-C(5)	120.1(8)
C(49)-Si(1)-C(47)	109.0(3)	C(6)-C(7)-C(8)	119.8(8)
C(48)-Si(1)-C(46)	109.0(3)	C(7)-C(8)-C(3)	121.3(7)
C(49)-Si(1)-C(46)	110.3(3)	N(1)-C(9)-C(10)	113.2(4)
C(47)-Si(1)-C(46)	107.8(3)	N(1)-C(9)-C(2)	99.4(4)
C(19)-Si(2)-C(21)	109.5(3)	C(10)-C(9)-C(2)	114.9(4)
C(19)-Si(2)-C(20)	111.2(3)	C(15)-C(10)-C(11)	119.0(5)
C(21)-Si(2)-C(20)	109.8(3)	C(15)-C(10)-C(9)	119.3(6)
C(19)-Si(2)-C(18)	107.6(3)	C(11)-C(10)-C(9)	121.7(5)
C(21)-Si(2)-C(18)	110.6(3)	C(10)-C(11)-C(12)	120.3(5)
C(20)-Si(2)-C(18)	108.2(3)	C(13)-C(12)-C(11)	120.1(6)
C(1)-O(2)-C(2)	108.4(4)	C(14)-C(13)-C(12)	119.5(6)
C(16)-O(3)-C(22)	109.7(4)	C(13)-C(14)-C(15)	120.5(7)
C(29)-O(5)-C(30)	108.6(4)	C(10)-C(15)-C(14)	120.6(6)
C(44)-O(6)-C(50)	109.5(4)	O(3)-C(16)-N(1)	110.9(4)
C(1)-N(1)-C(16)	121.5(5)	O(3)-C(16)-C(17)	103.9(4)
C(1)-N(1)-C(9)	113.1(4)	N(1)-C(16)-C(17)	112.8(4)
C(16)-N(1)-C(9)	124.0(4)	C(18)-C(17)-C(16)	112.6(5)
C(29)-N(2)-C(44)	120.8(5)	C(17)-C(18)-C(22)	107.5(5)
C(29)-N(2)-C(37)	113.0(5)	C(17)-C(18)-Si(2)	125.5(4)
C(44)-N(2)-C(37)	122.9(4)	C(22)-C(18)-Si(2)	126.8(4)
O(1)-C(1)-N(1)	129.1(6)	O(3)-C(22)-C(23)	109.7(4)
O(1)-C(1)-O(2)	122.1(6)	O(3)-C(22)-C(18)	104.9(4)
N(1)-C(1)-O(2)	108.8(5)	C(23)-C(22)-C(18)	113.6(5)
O(2)-C(2)-C(3)	111.3(5)	C(28)-C(23)-C(24)	118.6(6)
O(2)-C(2)-C(9)	104.9(4)	C(28)-C(23)-C(22)	121.2(7)
C(3)-C(2)-C(9)	117.6(5)	C(24)-C(23)-C(22)	120.2(6)
C(4)-C(3)-C(8)	118.4(6)	C(23)-C(24)-C(25)	120.8(7)
C(4)-C(3)-C(2)	123.5(6)	C(26)-C(25)-C(24)	119.0(9)
C(8)-C(3)-C(2)	118.1(6)	C(25)-C(26)-C(27)	120.9(10)
C(3)-C(4)-C(5)	120.0(7)	C(26)-C(27)-C(28)	119.4(10)

C(23)-C(28)-C(27)	121.1(9)	C(52)-C(51)-C(56)	118.5(6)
O(4)-C(29)-N(2)	129.5(6)	C(52)-C(51)-C(50)	123.5(7)
O(4)-C(29)-O(5)	121.7(6)	C(56)-C(51)-C(50)	117.9(7)
N(2)-C(29)-O(5)	108.8(6)	C(51)-C(52)-C(53)	121.2(8)
O(5)-C(30)-C(31)	112.6(5)	C(54)-C(53)-C(52)	118.4(9)
O(5)-C(30)-C(37)	103.7(4)	C(55)-C(54)-C(53)	122.0(9)
C(31)-C(30)-C(37)	116.6(5)	C(54)-C(55)-C(56)	118.2(10)
C(32)-C(31)-C(36)	119.6(6)	C(51)-C(56)-C(55)	121.6(9)
C(32)-C(31)-C(30)	122.8(7)		
C(36)-C(31)-C(30)	117.6(7)		
C(31)-C(32)-C(33)	120.1(8)		
C(34)-C(33)-C(32)	119.1(10)		
C(33)-C(34)-C(35)	121.6(10)		
C(34)-C(35)-C(36)	119.6(10)		
C(31)-C(36)-C(35)	119.9(8)		
N(2)-C(37)-C(38)	114.3(4)		
N(2)-C(37)-C(30)	100.1(4)		
C(38)-C(37)-C(30)	114.2(4)		
C(39)-C(38)-C(43)	118.7(5)		
C(39)-C(38)-C(37)	121.0(5)		
C(43)-C(38)-C(37)	120.3(6)		
C(38)-C(39)-C(40)	120.4(6)		
C(41)-C(40)-C(39)	120.0(6)		
C(40)-C(41)-C(42)	119.9(6)		
C(41)-C(42)-C(43)	120.2(6)		
C(42)-C(43)-C(38)	120.8(6)		
O(6)-C(44)-N(2)	110.6(4)		
O(6)-C(44)-C(45)	104.0(4)		
N(2)-C(44)-C(45)	112.5(4)		
C(46)-C(45)-C(44)	113.0(5)		
C(45)-C(46)-C(50)	106.3(5)		
C(45)-C(46)-Si(1)	126.0(4)		
C(50)-C(46)-Si(1)	127.4(5)		
O(6)-C(50)-C(51)	108.4(5)		
O(6)-C(50)-C(46)	105.2(4)		
C(51)-C(50)-C(46)	115.4(5)		

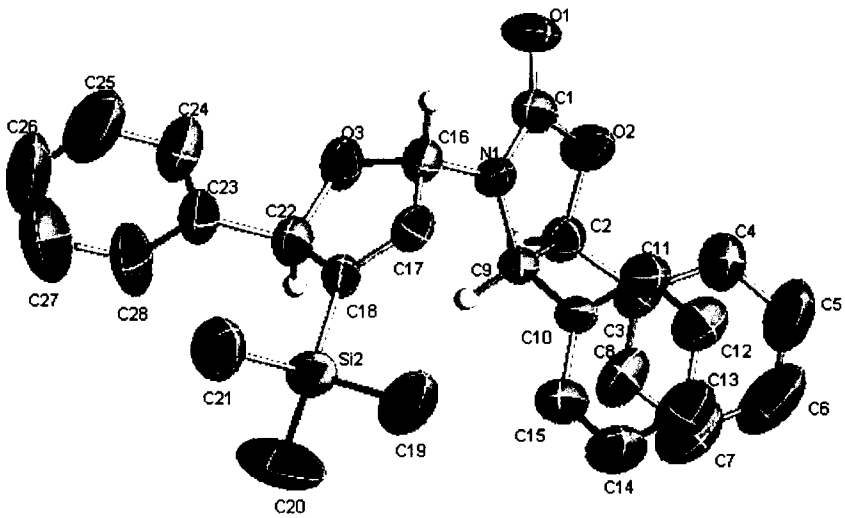

J. lsh159m, Eva Maria Garcia-Frutos

Table 1. Crystal data and structure refinement for lsh159m.

Identification code	lsh159m, EG-498	
Empirical formula	C25 H29 N O6	
Formula weight	439.49	
Temperature	100(2) K	
Wavelength	0.71073 Å	
Crystal system	Orthorhombic	
Space group	P2(1)2(1)2(1)	
Unit cell dimensions	a = 6.1812(6) Å	α= 90°.
	b = 17.4619(17) Å	β= 90°.
	c = 21.134(2) Å	γ = 90°.
Volume	2281.1(4) $Å^3$	
Z	4	
Density (calculated)	1.280 Mg/m^3	
Absorption coefficient	0.091 mm^{-1}	
F(000)	936	
Crystal size	0.38 x 0.15 x 0.03 mm^3	
Theta range for data collection	1.51 to 26.38°.	
Index ranges	-7<=h<=7, -21<=k<=21, -26<=l<=26	
Reflections collected	19597	
Independent reflections	2698 [R(int) = 0.0990]	
Completeness to theta = 26.38°	100.0 %	
Absorption correction	SADABS	
Max. and min. transmission	0.9974 and 0.9662	
Refinement method	Full-matrix least-squares on F^2	
Data / restraints / parameters	2698 / 0 / 293	
Goodness-of-fit on F^2	1.103	
Final R indices [I>2sigma(I)]	R1 = 0.0452, wR2 = 0.0859	
R indices (all data)	R1 = 0.0744, wR2 = 0.0954	
Absolute structure parameter	1(10)	
Extinction coefficient	0.0210(16)	
Largest diff. peak and hole	0.237 and -0.263 $e.Å^{-3}$	

Table 3. Bond lengths [Å] and angles [°] for lsh159m.

O(1)-C(1)	1.219(3)	C(4)-C(5)	1.383(4)
O(2)-C(1)	1.363(3)	C(5)-C(6)	1.390(4)
O(2)-C(2)	1.461(3)	C(6)-C(7)	1.380(4)
O(3)-C(18)	1.357(4)	C(7)-C(8)	1.392(4)
O(3)-C(19)	1.442(4)	C(9)-C(10)	1.511(4)
O(4)-C(22)	1.406(3)	C(10)-C(15)	1.391(4)
O(4)-C(21)	1.423(3)	C(10)-C(11)	1.392(4)
O(5)-C(22)	1.406(3)	C(11)-C(12)	1.390(4)
O(5)-C(23)	1.428(3)	C(12)-C(13)	1.378(4)
O(6)-C(24)	1.413(4)	C(13)-C(14)	1.383(4)
O(6)-C(25)	1.422(4)	C(14)-C(15)	1.374(4)
N(1)-C(1)	1.353(4)	C(16)-C(17)	1.503(4)
N(1)-C(9)	1.459(3)	C(16)-C(21)	1.524(4)
N(1)-C(16)	1.469(3)	C(17)-C(18)	1.312(4)
C(2)-C(3)	1.496(4)	C(19)-C(20)	1.513(5)
C(2)-C(9)	1.548(4)	C(19)-C(21)	1.521(4)
C(3)-C(4)	1.386(4)	C(23)-C(24)	1.503(4)
C(3)-C(8)	1.396(4)		

C(1)-O(2)-C(2)	107.8(2)	C(4)-C(3)-C(2)	122.7(3)
C(18)-O(3)-C(19)	114.1(3)	C(8)-C(3)-C(2)	117.9(3)
C(22)-O(4)-C(21)	117.1(2)	C(5)-C(4)-C(3)	120.2(3)
C(22)-O(5)-C(23)	113.2(2)	C(4)-C(5)-C(6)	120.6(3)
C(24)-O(6)-C(25)	110.4(2)	C(7)-C(6)-C(5)	119.4(3)
C(1)-N(1)-C(9)	111.6(2)	C(6)-C(7)-C(8)	120.4(3)
C(1)-N(1)-C(16)	122.9(2)	C(7)-C(8)-C(3)	120.0(3)
C(9)-N(1)-C(16)	125.3(2)	N(1)-C(9)-C(10)	113.9(2)
O(1)-C(1)-N(1)	128.7(3)	N(1)-C(9)-C(2)	99.2(2)
O(1)-C(1)-O(2)	121.9(3)	C(10)-C(9)-C(2)	113.2(2)
N(1)-C(1)-O(2)	109.4(2)	C(15)-C(10)-C(11)	117.6(3)
O(2)-C(2)-C(3)	110.8(2)	C(15)-C(10)-C(9)	120.2(3)
O(2)-C(2)-C(9)	102.4(2)	C(11)-C(10)-C(9)	122.2(3)
C(3)-C(2)-C(9)	117.0(2)	C(12)-C(11)-C(10)	120.8(3)
C(4)-C(3)-C(8)	119.4(3)	C(13)-C(12)-C(11)	120.1(3)

C(12)-C(13)-C(14)	119.9(3)	O(3)-C(19)-C(21)	110.1(2)
C(15)-C(14)-C(13)	119.6(3)	C(20)-C(19)-C(21)	112.3(3)
C(14)-C(15)-C(10)	122.0(3)	O(4)-C(21)-C(19)	107.3(2)
N(1)-C(16)-C(17)	112.7(2)	O(4)-C(21)-C(16)	110.8(2)
N(1)-C(16)-C(21)	110.6(2)	C(19)-C(21)-C(16)	110.6(2)
C(17)-C(16)-C(21)	109.2(3)	O(4)-C(22)-O(5)	112.2(2)
C(18)-C(17)-C(16)	122.2(3)	O(5)-C(23)-C(24)	106.4(2)
C(17)-C(18)-O(3)	126.1(3)	O(6)-C(24)-C(23)	108.3(2)
O(3)-C(19)-C(20)	106.4(3)		

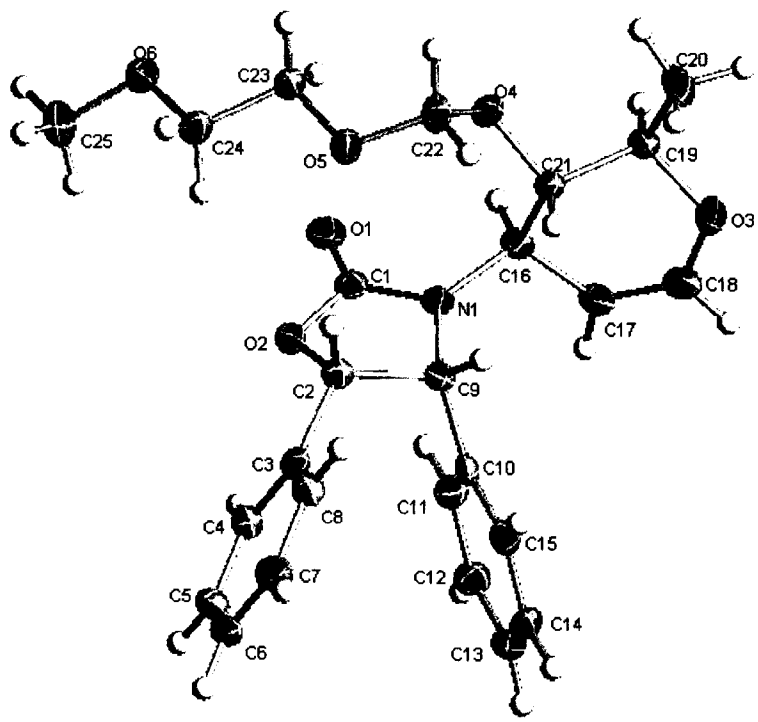

Table 1. Crystallographic Data

	5a	5b	6a	6b	7	8
Emperical Formula	$C_{31}H_{50}CoN_5O_7$	$C_{30}H_{41}CoN_6O_7$	$C_{29.5}H_{53}CoN_6O_{7.5}$	$C_{25}H_{40}CoN_7O_5$	$C_{62}H_{106}Co_2N_{12}O_{22}Rh_2$	$C_{88}H_{110}Co_2N_{20}O_{12}Ru$
fw	663.69	664.68	670.70	577.56	1695.25	1858.88
T(K)	173(2)	298(2)	173(2)	173(2)	173(3)	173(2)
wavelength (Å)	0.71073	0.71073	0.71073	0.71073	0.71073	0.71073
Cryst. syst.	monoclinic	monoclinic	orthorhombic	monoclinic	trigonal	monoclinic
space group	Cc	Cc	Pbca	$P2_1/c$	R-3	$P2_1/n$
Unit Cell dimensions						
a (Å)	10.5774(16)	10.6644(19)	14.7441(13)	16.167(4)	39.468(8)	12.0984(12)
b (Å)	20.901(3)	21.732(4)	13.4 537(12)	11.435(3)	39.468(8)	11.8549(12)
c (Å)	14.663(2)	14.189(3)	32.905(3)	15.670(4)	14.566(4)	29.740(3)
α (deg)	90	90	90	90	90	90
β (deg)	104.217	102.815(5)	90	102.626(5)	90	99.127(2)
γ (deg)	90	90	90	90	120	90
V(Å^3), Z	3142.2(8)	3206.5(11)	6527.1(10)	2826.9(12)	19650(8)	4211.5(7)
d calcd (Mg/mm^{-1})	1.403	1.360	1.353	1.352	1.277	1.463
abs coeff (mm^{-1})	0.601	0.590	0.581	0.654	0.812	0.642
GOF of F^2	1.028	0.951	1.042	1.038	1.082	1.131
Final R indices[a]	$R_1 = 0.0462$	$R_1 = 0.0672$	$R_1 = 0.0588$	$R_1 = 0.0659$	$R_1 = 0.0741$	$R_1 = 0.0814$
[I> 2σ (I)]	$wR_2 = 0.1102$	$wR_2 = 0.1069$	$wR_2 = 0.1287$	$wR_2 = 0.1562$	$wR_2 = 0.1961$	$wR_2 = 0.1869$
R indices	$R_1 = 0.0526$	$R_1 = 0.1655$	$R_1 = 0.0997$	$R_1 = 0.1235$	$R_1 = 0.1288$	$R_1 = 0.1186$
(all data)	$wR_2 = 0.1132$	$wR_2 = 0.1323$	$wR_2 = 0.1492$	$wR_2 = 0.1997$	$wR_2 = 0.2248$	$wR_2 = 0.2059$

[a] $R = \Box||F_o| - |F_c|| / \sum|F_o| \_ Rw = [\Box [w(F_o - F_c^2)^2] / \Box [w (F_o^2)]]^{1/2}$; $w = 4 F_o^2 / \sigma^2 (F_o)^2$.